



# Structure and Rheology of complex liquids and gels containing polysaccharides and proteins

Trong Bach Nguyen

## ► To cite this version:

Trong Bach Nguyen. Structure and Rheology of complex liquids and gels containing polysaccharides and proteins. Polymers. Le Mans Université, 2014. English. NNT : 2014LEMA1005 . tel-01220605

**HAL Id: tel-01220605**

**<https://theses.hal.science/tel-01220605>**

Submitted on 2 Nov 2015

**HAL** is a multi-disciplinary open access archive for the deposit and dissemination of scientific research documents, whether they are published or not. The documents may come from teaching and research institutions in France or abroad, or from public or private research centers.

L'archive ouverte pluridisciplinaire **HAL**, est destinée au dépôt et à la diffusion de documents scientifiques de niveau recherche, publiés ou non, émanant des établissements d'enseignement et de recherche français ou étrangers, des laboratoires publics ou privés.

# Thèse de Doctorat

Trong Bach NGUYEN

*Mémoire présenté en vue de l'obtention du  
**grade de Docteur de l'Université du Maine**  
sous le label de L'Université Nantes Angers Le Mans*

École doctorale: 3MPL

Discipline: Chimie et Physico-chimie des polymères  
Spécialité: Biopolymère  
Unité de Recherche: IMMM, UMR CNRS 6283

Soutenue le 16 Septembre 2014

## STRUCTURE AND RHEOLOGY OF MIXTURES OF THE PROTEIN $\beta$ -LACTOGLOBULIN AND THE POLYSACCHARIDE $\kappa$ -CARRAGEENAN

### JURY

Rapporteurs:	<b>Prof. Camille MICHON</b> , AgroParisTech, France <b>Dr. Christophe SCHMITT</b> , Nestlé Research Center, Switzerland
Examineurs:	<b>Prof. Shingo MATSUKAWA</b> , Tokyo University of Marine Science and Technology, Japan <b>Dr. Isabelle CAPRON</b> , INRA Nantes, France
Directeur de thèse:	<b>Dr. Taco NICOLAI</b> , Directeur de Recherche CNRS, Université du Maine, France
Co-directeur:	<b>Prof. Christophe CHASSENIEUX</b> , Université du Maine, France
Co-encadrant:	<b>Prof. Lazhar BENYAHIA</b> , Université du Maine, France



## ACKNOWLEDGMENT

There are many, whom I would like to acknowledge here, that have helped me during my thesis.

In the first place I would like to thank Doctor Dominique Durand, the first person I contacted and he gave me the chance to work with the ‘dream team’, my supervisors. I am grateful to Doctor Taco Nicolai, Professor Christophe Chassenieux and Professor Lazhar Benyahia for all their help and advice throughout my PhD time at University of Le Mans, I have been really lucky to be able to work with them. Especially, the daily supervision by Taco helped me to improve my research skills and to resolve difficulties. It is the main reason that I have been able to finish my thesis successfully.

I also thank to the Ministry of Education and Training of Vietnam for financial support during 3 study-years.

I am also grateful to Professor Camille Michon and Professor Sylvie Turgeon as members in my academic committee who gave a lot of useful advices.

I should not forget thank the whole staff at PCI, they always supported me and assured the best working conditions. A special thanks to Magali Martin, Jean-Luc Moneger, Frederick Niepceron, Boris Jacquette and Cyrille Dechance for helping with the analysis of SEC, TGA, FRAP and the assistance with the rheometers and the confocal microscopy, and Danielle Choplin who helped me with my official documents. Of course, I also thank all my fun friends at PCI who made my stay a pleasure.

I thank all of Vietnamese students and Vietnamese families who accompanied during my stay in France.

Finally, I am indebted to my family, especially, my mother, wife and son, who had a difficult time in my absence that they had overcome and have always fully supported me throughout my long stay in France. It is really wonderful that my wife gave me the biggest present – a new family member, my daughter.



# Table of Contents

<b>General Introduction .....</b>	<b>1</b>
<b><i>Chapter 1: Background .....</i></b>	<b>3</b>
<b>1.1. Beta lactoglobulin .....</b>	<b>3</b>
<i>Molecular structure.....</i>	3
<i>Aggregation and gelation of <math>\beta</math>-lactoglobulin .....</i>	4
<b>1.2. Kappa carrageenan .....</b>	<b>7</b>
<i>Aggregation and gelation of kappa carrageenan .....</i>	8
<b>1.3. Mixtures of <math>\beta</math>-lactoglobulin and <math>\kappa</math>-carrageenan.....</b>	<b>11</b>
<i>Mixing after heating.....</i>	13
<i>Mixing before heating .....</i>	14
<b><i>References.....</i></b>	<b>16</b>
<b><i>Chapter 2: Materials and methods.....</i></b>	<b>25</b>
<b>2.1. Materials .....</b>	<b>25</b>
<b>2.2. Methods .....</b>	<b>26</b>
2.2.1. Light scattering.....	26
2.2.2. Turbidity measurements.....	28
2.2.3. Determination of the protein concentration with UV-Visible spectroscopy.....	29
2.2.4. Confocal Laser Scanning Microscopy (CLSM).....	29
2.2.5. Rheology .....	30
2.2.6. Calcium activity measurements.....	31
<b><i>References.....</i></b>	<b>32</b>
<b><i>Chapter 3: Gelation of kappa carrageenan .....</i></b>	<b>33</b>
<b>3.1. Introduction .....</b>	<b>33</b>
<b>3.2. Results .....</b>	<b>34</b>
3.2.1. Single salt induced $\kappa$ -carrageenan gelation .....	34
3.2.1.1. <i>Gelation of <math>\kappa</math>-car induced by <math>K^+</math> .....</i>	34
3.2.1.2. <i>Gelation of <math>\kappa</math>-car induced by <math>Ca^{2+}</math> .....</i>	36
3.2.2. Influence of $Ca^{2+}$ on the $K^+$ -induced gelation of $\kappa$ -car .....	40
3.2.3. Influence of $Na^+$ on the $K^+$ -induced gelation of $\kappa$ -car.....	43
<b>3.3. Conclusions .....</b>	<b>46</b>
<b><i>References.....</i></b>	<b>47</b>

<b>Chapter 4: Mixtures of <math>\beta</math>-lactoglobulin and <math>\kappa</math>-carrageenan.....</b>	<b>49</b>
<b>4.1. Introduction .....</b>	<b>49</b>
<b>4.2. Mixtures of <math>\kappa</math>-carrageenan with native <math>\beta</math>-lactoglobulin .....</b>	<b>50</b>
<i>Conclusion.....</i>	53
<b>4.3. Mixtures of <math>\kappa</math>-carrageenan with <math>\beta</math>-lactoglobulin strands .....</b>	<b>54</b>
4.3.1. Mixtures with $\kappa$ -car coils.....	54
4.3.2. Effect of $\kappa$ -carrageenan gelation on phase separation.....	56
4.3.3. Conclusion .....	57
<b>4.4. Mixtures of <math>\kappa</math>-carrageenan with <math>\beta</math>-lactoglobulin microgels .....</b>	<b>58</b>
4.4.1. Mixtures of $\beta$ -lg microgels with $\kappa$ -car coils.....	58
4.4.1.1. <i>Effect of the concentration of <math>\kappa</math>-car and <math>\beta</math>-lg microgels .....</i>	58
4.4.1.2. <i>Effect of the size and morphology of the <math>\beta</math>-lg aggregates.....</i>	58
4.4.2. Effect of $\kappa$ -carrageenan gelation on the structure .....	60
4.4.3. Effect of $\kappa$ -carrageenan gelation on the rheology .....	64
4.4.4. Conclusion.....	66
<b>4.5. Heated mixtures of <math>\kappa</math>-carrageenan and native <math>\beta</math>-lactoglobulin.....</b>	<b>67</b>
4.5.1. Mixtures of $\beta$ -lg and $\kappa$ -car coils.....	67
4.5.2. Effect of $\kappa$ -car gelation on the structure and the rheology .....	71
4.5.3. Conclusion.....	75
<b><i>References.....</i></b>	<b>77</b>
<b><i>General conclusion and outlook .....</i></b>	<b>79</b>
<b><i>The list of publications.....</i></b>	<b>83</b>

## General Introduction

The main ingredients of foods are proteins, polysaccharides and lipids, which procure both nutrition and texture. The relatively recent recognition that processed foods need to be healthier, has led to an increasing need to develop novel products that contain less fat and salt. In addition, there is a tendency to add other functional ingredients in a way that retains their functionality during storage and digestion. Finally, there is a drive to replace relatively expensive proteins by less expensive polysaccharides. Obviously, for a rational development of such food products it is essential to understand the physical chemical properties of aqueous solutions and gels containing proteins and polysaccharides by themselves and in mixtures. This explains why these systems are currently intensively investigated.

Carrageenans are an important class of hydrophilic sulfated polysaccharides widely used as thickening, gelling and stabilizing agents in food products such as sauces, meats and dairy products. Especially, in frozen foods its high stability to freeze-thawing cycles is very important. They are also helpful for the smoothness, creaminess, and body of the products to which they are added. In combination with proteins such as  $\beta$ -lactoglobulin ( $\beta$ -lg), casein, etc... their presence allows different textures to be obtained and to reduce the fat content of food.

Many food formulations yield complex microstructures composed of water, proteins, carbohydrates, fats, lipids and minor components. Protein-polysaccharide interactions are of outmost importance in these structures, and play an essential role in the stability and the rheological behavior of the final product. Understanding of the interactions between these macromolecules will therefore facilitate development of new products.

An example is the use of kappa carrageenan ( $\kappa$ -car) in dairy products (Trius et al., 1996). Milk protein/ $\kappa$ -car interaction improves the functional properties of dairy products under controlled conditions of pH, ionic strength,  $\kappa$ -car concentration,  $\beta$ -lg/ $\kappa$ -car ratio, temperature, and processing. In industrial applications,  $\kappa$ -car is used to stabilize and prevent whey separation in processing of dairy products such as milk shakes, ice cream, chocolate milk, and creams.  $\kappa$ -car interacts with dairy proteins to form a weak stabilizing network that is able to keep chocolate particles in suspension in chocolate milks. The network also prevents protein-protein interactions and aggregation during storage, inhibits whey separation in fluid products and decreases shrinkage in ice cream.

The texture of many food products is a consequence of gelation of either the proteins or the polysaccharides, or both. Gelation of one type of macromolecules will be influenced by the presence of the other type, when both are present. When both the polysaccharides and the proteins gel, synergy between the two interpenetrating networks may be a useful property that can be exploited in product development.

## ***Objectives***

The objective of the present investigation was to study the influence of aggregation and gelation of  $\beta$ -lg on the structure and the rheology of  $\kappa$ -car solutions and gels. Protein particles were formed by heating native  $\beta$ -lg, which caused their denaturation and aggregation. For this study, protein particles were either formed separately and subsequently mixed with  $\kappa$ -car or formed directly in mixtures of  $\kappa$ -car and native  $\beta$ -lg. Systems with the same composition prepared by these two different methods, were compared. Heating mixtures can also lead to gelation of the proteins. In this case interpenetrated networks may be formed by subsequent gelation of the polysaccharides. The research presented in this thesis is essentially experimental using scattering techniques and confocal laser scanning microscopy (CLSM) to study the structure and shear rheology to study the dynamic mechanical properties.

The thesis consists of four chapters and a general conclusion:

**Chapter 1** gives a review of the literature on the biopolymers used in this study separately and in mixtures

**Chapter 2** presents the materials and methods used in the research

**Chapter 3** describes the investigation of  $\kappa$ -carrageenan gelation in the presence of single or mixed salts

**Chapter 4** describes the investigation of the structure and rheology of mixtures of  $\kappa$ -car and  $\beta$ -lg aggregates or gels

The research has resulted in 4 publications in scientific journals in which more details can be found. They are included as an appendix to the thesis.

## Chapter 1:

# BACKGROUND

### 1.1. Beta lactoglobulin

$\beta$ -lactoglobulin ( $\beta$ -lg) is the major whey protein (~50%) in the milk of ruminants and its properties have been regularly reviewed (Tilley, 1960; Lyster, 1972; Kinsella and Whitehead, 1987; Hambling et al., 1992; Sawyer, 2003). 10 different genetic variants of  $\beta$ -lg have been identified. The most important genetic variants A and B differ at positions 64 (Asp/Gly) and 118 (Val/Ala).  $\beta$ -lg has been the subject of a wide range of biophysical studies because of its abundance and ease of isolation from milk. Its biological function is not clear, but it is a member of the lipocalin family of proteins (Banaszak et al., 1994; Flower, 1996) known for its ability to bind small hydrophobic molecules into a hydrophobic cavity. This led to the proposal that  $\beta$ -lg functions as a transport protein for retinoid species, such as vitamin A (Papiz et al., 1986). However, according to Flower et al. (2000)  $\beta$ -lg has a wide range of functions, which explains the significant quantities of  $\beta$ -lg found in milk.

#### *Molecular structure*

$\beta$ -lactoglobulin is a small globular protein that is soluble in water over broad range of the pH (2-9). Its isoelectric point (pI) is about 5.2. The primary structure consists of 162 amino acid residues with a molecular weight  $M_w \sim 18.4$  kg/mol. The secondary structure of  $\beta$ -lg was found to contain 15%  $\alpha$ -helix, 50%  $\beta$ -sheet and 15-20% reversed turn –  $\beta$ -strands (Creamer et al., 1983).  $\beta$ -lg contains two disulphide bridges and one free cysteine group (McKenzie and Sawyer, 1967; Hambling et al., 1992).

The 3D tertiary structure of native  $\beta$ -lg is shown in figure 1.1. It shows an eight-stranded  $\beta$ -barrel (calyx) formed by  $\beta$ -sheets, flanked by a three-turn  $\alpha$ -helix. In aqueous solution the proteins can associate into dimers and oligomers depending on the pH, temperature and ionic strength, with the dimer being the prevalent form under physiological conditions (Kumosinski & Timasheff, 1966; McKenzie et al., 1967; Gottschalk et al., 2003). A ninth  $\beta$ -sheet strand forms the greater part of dimer interface at neutral pH (Papiz et al., 1986; Bewley et al., 1997).

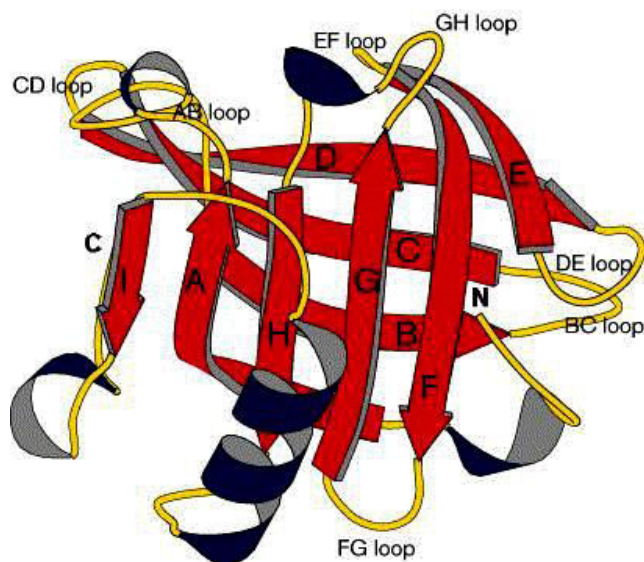


**Figure 1.1.** Schematic drawing of the structure of  $\beta$ -lactoglobulin (Brownlow et al., 1997)

### ***Aggregation and gelation of $\beta$ -lactoglobulin***

The well-defined structure of  $\beta$ -lg can be perturbed by heating leading to denaturation of the native proteins, which generally causes their aggregation. Different types of interaction are involved in this process such as hydrogen bonding, Van de Waals and hydrophobic interactions. Close to and above pI, disulfide bonds are exchanged leading to the formation of covalent disulfide bridges between different proteins (Bauer et al., 1998; Carrota et al., 2003; Croguennec et al., 2003; Surroca et al., 2002; Otte et al., 2000).

The aggregation process and the resulting structures depend strongly on the temperature, pH, type and concentration of salt and the protein concentration (Foegeding et al., 1992; Iametti et al., 1995; Foegeding, 2006; Mehalebi et al., 2008; Ako et al., 2009; Ako et al., 2010; Schmitt et al., 2010; Nicolai et al., 2011; Ryan et al., 2012; Leksrisompong et al., 2012; Ruhs et al., 2012; Phan-Xuan et al., 2013; Phan-Xuan et al., 2014). Scattering and microscopy techniques have been used to study the effect of these parameters on the size, mass, and density of the aggregates. In salt free solutions aggregates with three different morphologies are formed during heating, depending on the pH, see figure 1.2: spherical particles around pI in the pH range 4.0-6.1, short curved strands at higher and lower pH, and long rigid strands at low pH (1.5-2.5). The rigid strands can be very long, but are formed only when the proteins are partially hydrolyzed into shorter peptides. The hydrodynamic radius ( $R_h$ ) of the short curved strands formed above pI was found to increase with decreasing pH from about 12nm at pH 8.0 to about 20nm at pH 6.1 (Mehalebi et al., 2008).

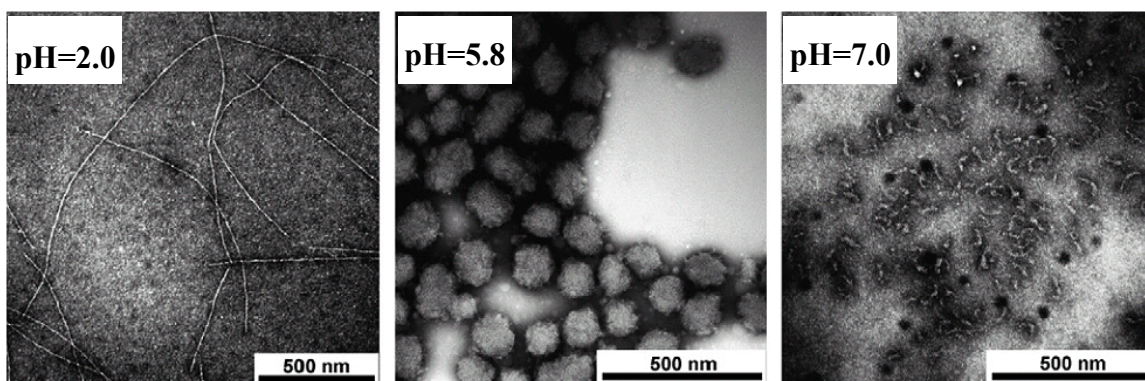


**Figure 1.2.** Negative-staining TEM images of  $\beta$ -lg aggregates formed at different pH: long rigid strands at pH 2.0, spheres at pH 5.8 and small curved strands at pH 7.0. Scale bars are 500 nm (Jung et al., 2008).

During heating the concentration of aggregates increases progressively until all native proteins are transformed and steady state is reached. However, at higher protein concentrations the strands or spheres have a tendency to associate randomly into larger aggregates. The size of the secondary aggregates at steady state increases with increasing protein concentration until above a critical value ( $C_{gel}$ ) a gel is formed or macroscopic flocs that precipitate.

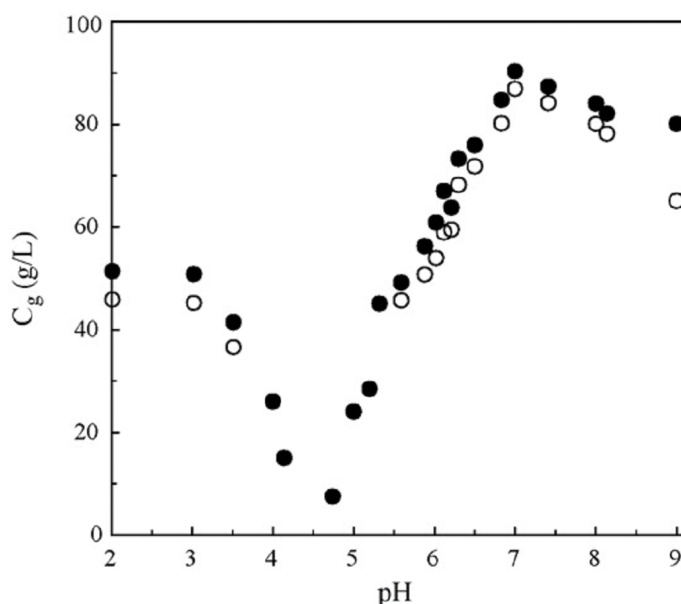


**Figure 1.3.** Sol-gel state diagram of  $\beta$ -lg solutions at steady state. The closed and open symbols indicate, respectively, the critical concentration beyond which the systems no longer flow when tilted or beyond which insoluble material is observed after dilution (Mehalebi et al., 2008).

Mehalebi et al. (2008) have reported the sol-gel/precipitate state diagram of  $\beta$ -lg in salt free water at steady state as a function of the protein concentration and the pH between 2 and 9, see figure 1.3.  $C_{gel}$  is low close to pI and increases with increasing or decreasing pH to reach about 90g/L for  $pH \geq 7$ . In a very narrow range around pI secondary aggregation of the spherical particles leading to precipitation occurs at all concentrations. For this reason stable suspensions of spherical particles were found only in very narrow pH range (5.75-6.1) (Phan-Xuan et al., 2011). In this range the hydrodynamic radius increased with decreasing pH from about 45nm to about 200nm. The spherical particles consist of a network of crosslinked proteins with a density of about 0.2 g/mL and are therefore called microgels.

The presence of salt influences significantly the aggregation process. At neutral pH, addition of NaCl induces secondary aggregation of the short strands at lower protein concentrations (Baussay et al., 2004). As a consequence  $C_{gel}$  decreases with increasing NaCl concentration. However, the overall structure of the aggregates is independent of the NaCl concentration. Addition of salt also leads to an increase of the aggregation rate.

The effect of adding  $CaCl_2$  is more dramatic as it influences not only the secondary aggregation, but can also drive a change in the morphology from small strands to microgels. In the presence of calcium ions, stable suspensions of microgels can also form at  $pH > 6.1$  (Phan-Xuan et al., 2013). The effect is not determined by the total amount of salt, but by the ratio (R) between the molar concentration of  $CaCl_2$  and  $\beta$ -lg (Phan-Xuan et al., 2014). The critical ratio at which the transition between the formation of strands and microgels occurs increases with increasing pH from  $R = 0$  at  $pH < 6.2$  to  $R \approx 2.5$  at  $pH = 7.5$  via  $R \approx 1.5$  at  $pH = 7.0$ . At a given pH, the size and the density of the microgels increases with increasing R. Stable suspensions of microgels with sizes between 100 to 400 nm and densities between 0.2 – 0.4 g/ml can be formed in a narrow range of R. At  $R > 3$  or at  $\beta$ -lg concentrations above 60g/L, the microgels associate.

The aggregation rate increases sharply with increasing temperature as it is controlled by the protein denaturizing step (Durand et al., 2002; Baussay et al., 2004; Nicolai et al., 2011; Phan-Xuan et al., 2013). The structure and size of aggregates formed at  $pH > 6.2$  in the absence of  $CaCl_2$  were not influenced significantly by the heating temperature (Phan-Xuan et al., 2013). The structure and size of the microgels was not influenced either by the heating temperature when aggregation was fast, i.e. between 75 and 85<sup>0</sup>C (Phan-Xuan et al., 2013). However, at lower heating temperatures when aggregation is slow an influence of the heating



temperature on the microgel formation was reported (Bromley et al., 2006; Phan-Xuan et al., 2013).

The aggregation and gelation process is schematically represented in figure 1.4. In aqueous solution, when native  $\beta$ -lg is heated the monomer-dimer equilibrium is shifted towards the monomers (step 1). The protein structure is modified and becomes more mobile. Irreversible bonds are formed leading to the formation of strand-like or spherical aggregates (step 2, 3) depending on the pH and the type and concentration of added salt (Mehalebi et al., 2008; Ako et al., 2009; Phan-Xuan et al., 2013 and 2014). These primary aggregates can further assemble into larger aggregates (step 4) or even a gel at higher protein or salt concentrations.

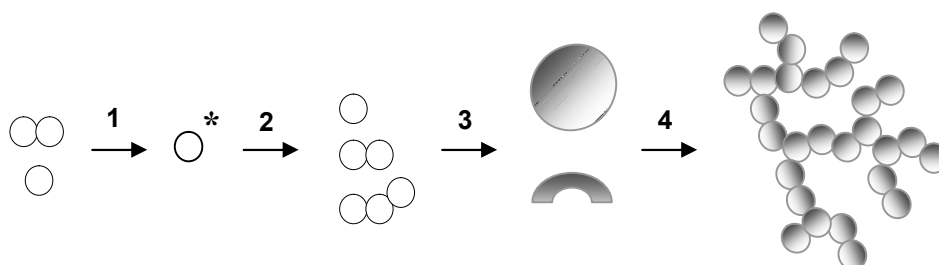


**Figure 1.4.** Schematic representation of the aggregation process of  $\beta$ -lactoglobulin

## 1.2. Kappa carrageenan

Carrageenans are sulfated linear polysaccharides of D-galactose and 3,6-anhydro-D-galactose extracted from certain genera of red seaweeds. There are different types of carrageenan that differ from one to another in their content of 3,6-anhydro-D-galactose and the number and position of ester sulfate groups (Trius et al., 1996). Kappa carrageenan ( $\kappa$ -car) is the most commonly type used in applications (figure 1.5), because it can form thermo-reversible gels in the presence of specific monovalent cations like  $K^+$ . For this reason, it is frequently employed as a thickener and gelling agent in the food industry, often in milk products.

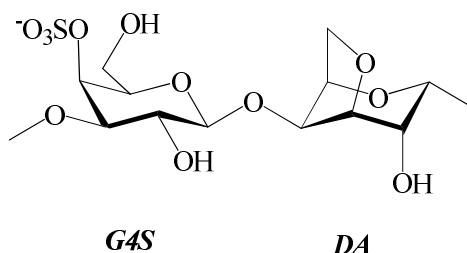


**Figure 1.5.** Idealized repeating unit of  $\kappa$ -carrageenan

In aqueous solution,  $\kappa$ -car has a random coil conformation above a critical temperature ( $T_c$ ) and a helical conformation below this temperature (Rees et al., 1969, McKinnon et al., 1969). The coil-helix transition temperature depends sensitively on the type and the concentration of the cations that are present in the solution (Morris et al., 1980; Rochas & Rinaudo, 1980; Viebke et al., 1994; Kara et al., 2003; Piculell, 2006), see figure 1.6. It is important to consider also the activity of the counterions in the calculation of the total ion concentration. For instance, in the case of potassium counterions the effective potassium concentration in salt free  $\kappa$ -car solutions is equal to  $0.55 \cdot C_p / M_m$  where  $C_p$  is the  $\kappa$ -car concentration and  $M_m$  is the molar mass of the monomer ( $M_m = 383 \text{ g/mol}$ ).

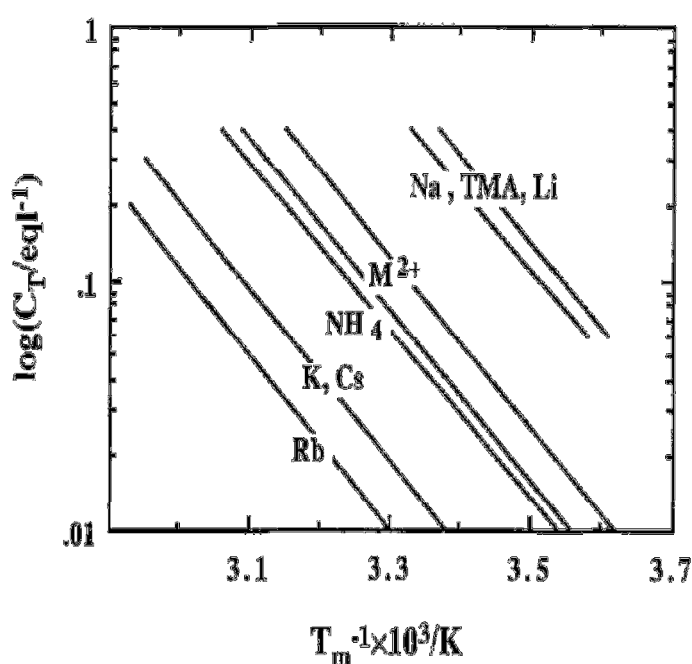


**Figure 1.6.** Dependence of the transition midpoint temperature ( $T_m$ ) of kappa-carrageenan on the total concentration ( $C_T$ ) of various cations in the systems. (Rochas & Rinaudo, 1980).

$\kappa$ -car is particularly sensitive to potassium and a concentration of 0.01M is enough to induce the transition at room temperature, whereas 0.2M sodium would be needed. Often the transition temperature is higher on heating ( $T_m$ ) than on cooling.

#### ***Aggregation and gelation of kappa carrageenan***

$\kappa$ -car chains with the helical conformation aggregate and if their concentration is sufficiently high they form a percolating network, see figure 1.7.

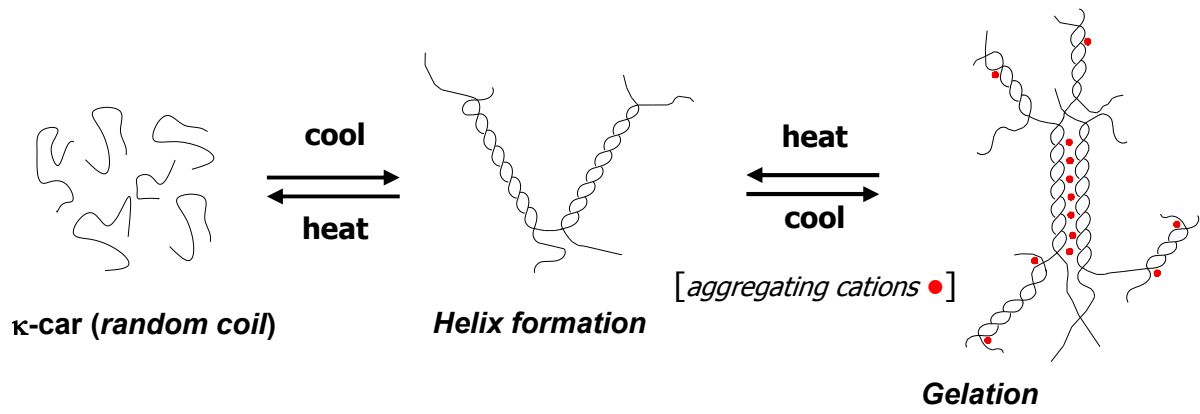


**Figure 1.7.** Schematic representation of the aggregation and gelation of  $\kappa$ -carrageenan

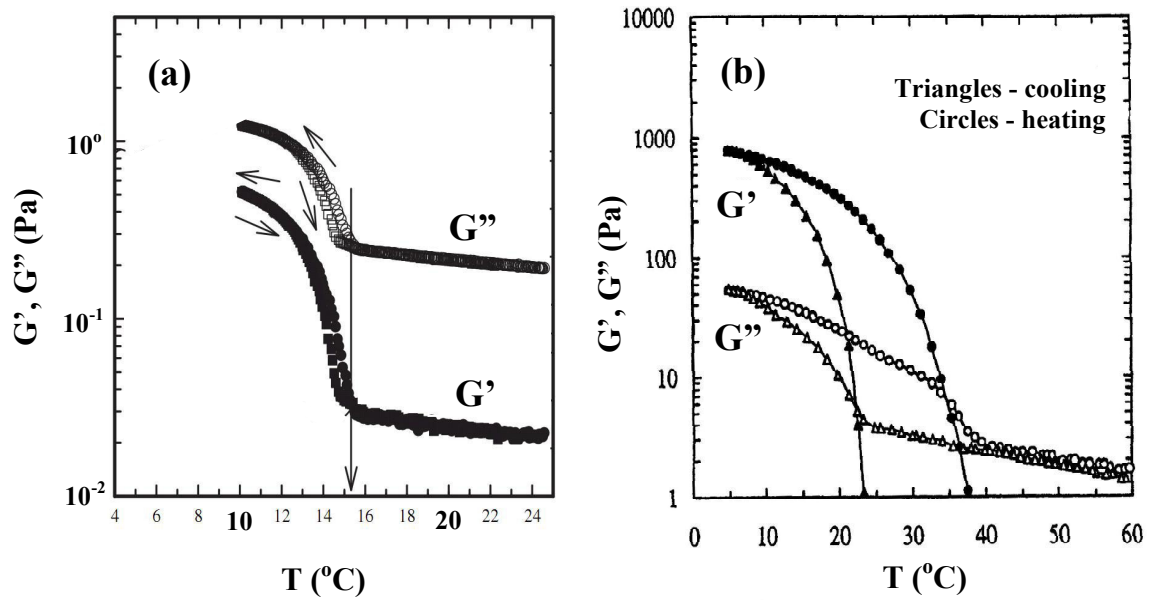


**Figure 1.8.** (a) Evolution of  $G'$  (closed symbols) and  $G''$  (open symbols) as a function of temperature for 4g/L  $\kappa$ -car without KCl added, on cooling (circles) and heating (squares). Measurements were made at a frequency of 1 rad.s<sup>-1</sup> and 50% strain (Núñez-Santiago et al., 2011).

(b) Changes in  $G'$  (closed symbols) and  $G''$  (open symbols) on cooling and heating at 1°C/min for 10g/L  $\kappa$ -car with 5mM added KCl. Measurements were made at a frequency of 10 rad.s<sup>-1</sup> and 2% strain (Doyle et al., 2002).

As a consequence  $\kappa$ -car solutions form a self supporting gel below  $T_c$  if the polymer concentration is not too low (Hermansson, 1989; Piculell, 1991; Hermansson et al., 1991; Borgström et al., 1996; Meunier et al., 1999; Chronakis et al., 2000; Doyle et al., 2002). Gelation is very slow close to  $T_c$ , but the gelation rate increases with decreasing temperature (Meunier et al., 1999). Since the coil-helix transition is reversible,  $\kappa$ -car gelation can be reversed by heating, but the melting temperature is often higher than the gelling temperature, see figure 1.8.

The coil-helix temperature and thus the gelling temperature depend on the concentration and type of salt. Gelation also depends on the polymer concentration via the counterion concentration if the latter are effective in inducing the coil-helix transition. Meunier et al. (1999) showed that in the range of 0.2 to 2g/L of sodium  $\kappa$ -car, gels were formed at the same temperature in the presence of 0.01M KCl and 0.1M NaCl, see figure 1.9. However, the gelation rate increased with increasing polymer concentration.

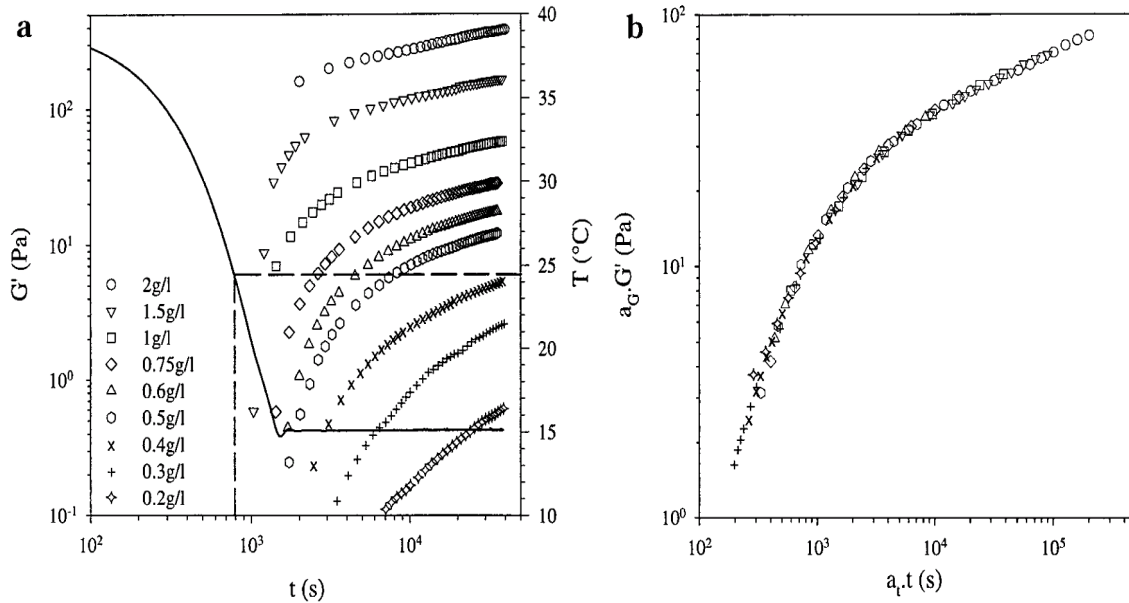


**Figure 1.9.** (a) Time dependence of the storage shear modulus on cooling at different concentrations of  $\kappa$ -car. The solid line indicates the time dependence of the temperature. The dashed lines indicate the position of the temperature where the coil helix transition occurs.

(b) Master curve of the data shown in figure (a) obtained by vertical and horizontal shifts with  $C_{ref} = 1.0$  g/L (Meunier et al., 1999).

The effect of the salt concentration on the elastic modulus of  $\kappa$ -car gels has been studied in some detail for potassium and calcium that are most commonly used to induce

gelation. Generally, it is found that the elastic modulus increases with increasing potassium concentration (Doyle et al., 2002), while it reaches a maximum when the calcium concentration is increased (Doyle et al., 2002; MacArtain et al., 2003; Thrimawithana et al., 2010). Another difference between gels induced by potassium and those induced by calcium is that the latter are increasingly turbid with increasing ion concentration (Doyle et al., 2002; MacArtain et al., 2003), while the former remain transparent.

The effect of mixed salts on the gelation of  $\kappa$ -car has been studied relatively little even though in applications often more than one type of salt is present. The most extensive study was reported by Hermansson et al. who found that adding NaCl to a  $\kappa$ -car solution containing 20mM potassium led to an increase of the elastic modulus, whereas in the absence of potassium these solutions did not gel (Hermansson et al., 1991). An even stronger synergistic effect was found when  $\text{CaCl}_2$  was added. Addition of as little as 2mM  $\text{CaCl}_2$  was found to increase the elastic modulus significantly. Mangione et al. reported that addition of 100mM NaCl to a  $\kappa$ -car solution containing 20mM KCl did not influence  $T_c$ , but led to a significant increase of the elastic shear modulus (Mangione et al., 2005). These results clearly show that gelation of  $\kappa$ -car in mixed salt solutions cannot be deduced from that of the pure salt solutions.

### **1.3. Mixtures of $\beta$ -lactoglobulin and $\kappa$ -carrageenan**

In general, mixtures of two different polymers in solution show three types of behaviour: co-solubility, segregative phase separation, and complex coacervation, see figure 1.10. When interaction between the polymers is weak or when the system is very dilute, mixing entropy dominates and homogeneous mixtures are formed. When the interaction is attractive soluble or insoluble complexes may be formed depending on the strength of the interactions, the molecular weight and flexibility of the polymers, and the distribution of negative and positive charges on the polymer. When the interaction is repulsive, contact between the same polymers is more favorable than contact between different polymers. In this case, phase separation occurs into two phases each enriched with one of the two polymers.

The behavior of polymer mixtures may depend on the conditions used such as pH, ionic strength, and temperature. For instance, in mixtures of anionic polysaccharides and proteins, complex coacervation is generally observed below the isoelectric point of the proteins (Tolstoguzov, 1991 & 2003), while homogeneous mixing or segregative phase

separation is often observed above the isoelectric point (Grinberg & Tolstoguzov, 1997; Benichou et al., 2002). In the case of charged polysaccharides mixing is favored by the contribution of counterions to the mixing entropy.

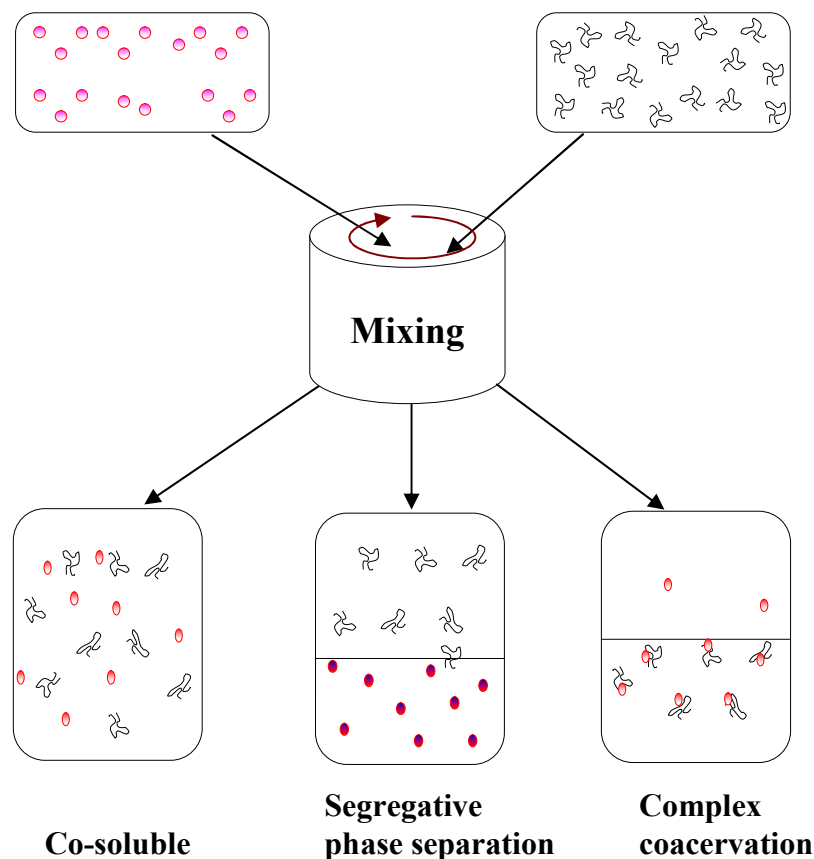


**Figure 1.10.** Behaviour of binary polymer solutions.

For the investigation reported in this thesis we only studied mixtures at pH 7 where both  $\kappa$ -car and  $\beta$ -lg are negatively charged. Therefore we limit our review of the literature on  $\kappa$ -car/ $\beta$ -lg mixtures to this situation. Native  $\beta$ -lg and  $\kappa$ -car form homogeneous mixtures in aqueous solution at least in the range of  $\beta$ -lg (up to  $C_b = 100$  g/L) and  $\kappa$ -car (up to  $C_k = 20$  g/L) covered in the investigation. However,  $\beta$ -lg aggregates can be incompatible with  $\kappa$ -car depending on the concentration and the size of the aggregates. The effect of phase separation has been studied for mixtures with separately formed  $\beta$ -lg aggregates and for mixtures in which the  $\beta$ -lg aggregates were formed in-situ by heating.

Mixtures of  $\beta$ -lg aggregates and  $\kappa$ -car have been studied extensively in the past. The effect of the pH on the behavior of mixtures was studied by a number of authors (Mleko et al., 1997; Turgeon & Beaulieu, 2001; Gustaw & Mleko, 2003; de Jong et al., 2009; Stone &

Nickerson, 2012; Çakır et al., 2012; Hosseini et al., 2013; Ould Eleya et al. 2000b). However, as mentioned above, here we focus on the situation at neutral pH. We will distinguish two situations: heated mixtures of native  $\beta$ -lg and  $\kappa$ -car (mixing before heating), and mixtures of preheated  $\beta$ -lg and  $\kappa$ -car (mixing after heating). In both cases the mixtures contain  $\beta$ -lg aggregates and  $\kappa$ -car, but the aggregates were formed in different circumstances. Of course, only mixing before heating allows the formation of  $\beta$ -lg gels mixed with  $\kappa$ -car.

### ***Mixing after heating***

A number of authors studied mixtures of  $\kappa$ -car with protein aggregates prepared separately by heating native protein in the absence or presence of salt (Tziboula & Horne, 1999; Croguennoc et al., 2001a; Baussay et al., 2006a,b; Gaaloul et al., 2010; Ako et al., 2011). The mixtures were found to phase separate above a critical  $\kappa$ -car concentration leading to the formation of spherical protein rich micro-domains that tend to cluster and slowly precipitate under gravity. The critical  $\kappa$ -car concentration decreased with increasing aggregate size from more than above 10g/L if the radius of gyration was  $R_g = 20\text{nm}$  to less than 2g/L when  $R_g > 300\text{nm}$  (Baussay et al., 2006a). The extent of phase separation increased with increasing  $\kappa$ -car concentration, and in the case of polydisperse  $\beta$ -lg aggregates the larger aggregates phase separate preferentially (Croguennoc et al., 2001a).

The effect of  $\kappa$ -car gelation on phase separation in mixtures at neutral pH in the presence of salt was reported by Baussay et al. (2006a) and Ako et al. (2011). Salt induced gelation of  $\kappa$ -car, coil-helix transition occurred at its critical concentration that depends on concentration of polymers. The turbidity induced by micro phase separation was found to drop dramatically during cooling below  $T_c$  when the  $\kappa$ -car gelled and to increase again when the gel melted at a higher temperature (Baussay et al., 2006b). It was shown that the protein aggregates were expelled from the protein rich domains, which explained the reduction of the turbidity, but the domains remained visible in microscopy. In another study, microphase separation was observed during cooling a mixture of  $\beta$ -lg aggregates and  $\kappa$ -car in the presence of 0.2M NaCl after heating at 60°C, but the domains dispersed again below  $T_c$  when  $\kappa$ -car gelled (Ako et al., 2011). Inducing only the coil-helix transition in the presence of 0.2M NaI, without gelation, did not lead to dispersion of the domains. The strength of  $\beta$ -lg network will increase at low concentration of  $\kappa$ -car (0-1.7g/L) but drop at higher  $\kappa$ -car concentration (2.55 and 3.4g/L).

## Mixing before heating

The behavior of heated mixtures of native  $\beta$ -lg and  $\kappa$ -car has been studied more often. The presence of  $\kappa$ -car coils in the mixtures does not influence the denaturation of  $\beta$ -lg and the aggregate structure, but it accelerates the aggregate growth (Capron et al., 1999a). Micro phase separation of the mixtures was observed when above a critical polymer concentration (Croguennoc et al., 2001b; Zhang & Foegeding, 2003; Gustaw & Mleko, 2003; de la Fuente et al., 2004; Gaaloul et al., 2009b; Flett & Corredig, 2009; Gaaloul et al., 2010; Ako et al., 2011). At lower  $\beta$ -lg concentrations the protein rich domains form clusters that precipitate, but at higher  $\beta$ -lg concentrations they can form a space spanning network that can support its own weight (Croguennoc et al., 2001b; Zhang & Foegeding, 2003). The structure also depends on the heating time, because more and larger aggregates are formed with increasing heating time. de la Fuente et al., 2004 found that mixtures containing 2wt % WPI and 0.1wt%  $\kappa$ -car at 0.1M NaCl were homogeneous after heating at 75°C for 5 min, but showed micro phase separation when heated longer (15min).

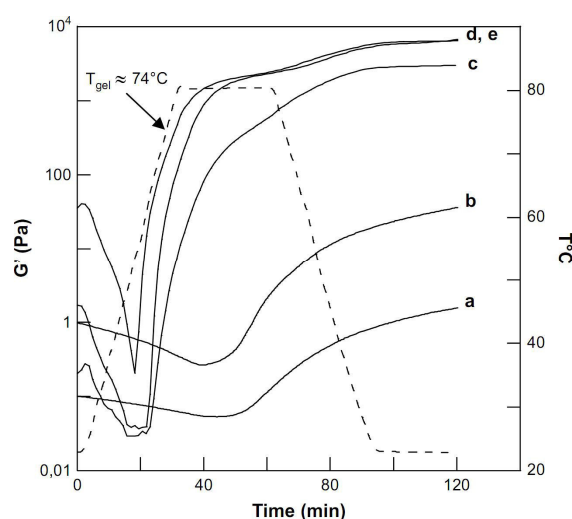


**Figure 1.11.** Evolution of shear modulus ( $G'$ ) during heating for mixtures containing 8% WPI and without  $\kappa$ -car (a), 0.2% (b), 0.4% (c), 0.6% (d) and 0.8%  $\kappa$ -car (e). Dashed line shows temperature of mixtures (Gaaloul et al., 2009a).

Gelation of  $\beta$ -lg in heated mixtures containing  $\kappa$ -car coils was studied at high concentration of protein either in the absence or presence of NaCl (Mleko et al., 1997; Capron et al., 1999a,b; Gustaw et al., 2003; Gaaloul et al., 2009a; Cakir et al., 2011). Gelation is faster if more  $\kappa$ -car is added (Capron et al., 1999a; Gaaloul et al., 2009a). Gaaloul et al.



(2009a) found that the elastic modulus of 8% WPI heated at 80°C increased with increasing  $\kappa$ -car up to 0.6% (figure 1.11), while Cakir et al. (2011) reported a maximum around 0.2%  $\kappa$ -car for 13% WPI heated at 80°C. Capron et al. (1999a) also reported a maximum at about 0.1%  $\kappa$ -car for 5%  $\beta$ -lg heated at 75°C.

In the presence of salt,  $\kappa$ -car can gel after cooling in the heated mixtures leading to an increase of the elastic modulus (Capron et al., 1999b; Ould Eleya et al., 2000a,b; Turgeon & Beaulieu, 2001; Harrington et al., 2009; Gaaloul et al., 2009a; Çakır & Foegeding, 2011; Ako et al., 2011). Ako et al. (2011) found that at 250mM NaCl the  $\kappa$ -car formed in the WPI gel was stronger than without the proteins. However, Harrington et al. (2009) found that in 8mM CaCl<sub>2</sub> the  $\kappa$ -car gels was weaker in the WPI gel. They attributed this to competition for Ca<sup>2+</sup> between the proteins and the  $\kappa$ -car. At higher  $\kappa$ -car concentrations the gel properties are dominated by those of the polysaccharide (Turgeon & Beaulieu, 2001, Ako et al., 2011).

## References

- Ako, K., Durand, D., & Nicolai, T. (2011). Phase separation driven by aggregation can be reversed by elasticity in gelling mixtures of polysaccharides and proteins. *Soft Matter*, 7, 2507-2516.
- Ako, K., Nicolai, T., & Durand, D. (2010). Salt-Induced Gelation of Globular Protein Aggregates: Structure and Kinetics. *Biomacromolecules*, 11(4), 864-871.
- Ako, K., Nicolai, T., Durand, D., & Brotons, G. (2009). Micro-phase separation explains the abrupt structural change of denatured globular protein gels on varying the ionic strength or the pH. *Soft Matter*, 5, 4033-4041.
- Banaszak, L., Winter, N., Xu, Z., Bernlohr, D. A., Cowan, S., & Jones, T. A. (1994). Lipid-binding Proteins: A family of fatty acid and retinoid transport proteins. *Advances in Protein Chemistry*, 45, 90-151.
- Bauer, R., Hansen, S., & Øgendal, L. (1998). Detection of Intermediate Oligomers, Important for the Formation of Heat Aggregates of  $\beta$ -Lactoglobulin. *International Dairy Journal*, 8(2), 105-112.
- Baussay, K., Durand, D., & Nicolai, T. (2006b). Coupling between polysaccharide gelation and micro-phase separation of globular protein clusters. *Journal of Colloid and Interface Science*, 304(2), 335-341.
- Baussay, K., Le Bon, C., Nicolai, T., Durand, D., & Busnel, J. P. (2004). Influence of the ionic strength on the heat-induced aggregation of the globular protein  $\beta$ -lactoglobulin at pH 7. *International Journal of Biological Macromolecules*, 34(1-2), 21-28.
- Baussay, K., Nicolai, T., & Durand, D. (2006a). Effect of the Cluster Size on the Micro Phase Separation in Mixtures of  $\beta$ -Lactoglobulin Clusters and  $\kappa$ -Carrageenan. *Biomacromolecules*, 7(1), 304-309.
- Benichou, A., Aserin, A., & Gart, N. (2002). Protein-Polysaccharide Interactions for Stabilization of Food Emulsions. *Journal of Dispersion Science and Technology*, 23(1-3), 93-123.
- Bewley, M. C., Qin, B. Y., Jameson, G. B., Sawyer, L., & Baker, E. N. (1997). III.1 - Bovine  $\beta$ -lactoglobulin and its variants : A three-dimensional structural perspective. *International Dairy Federation special issue*, 100-109.

- Borgström, J., Piculell, L., Viebke, C., & Talmon, Y. (1996). On the structure of aggregated kappa-carrageenan helices. A study by cryo-TEM, optical rotation and viscometry. *International Journal of Biological Macromolecules*, 18, 223-229.
- Bromley, E. H. C., Krebs, M. R. H., & Donald, A. M. (2006). Mechanisms of structure formation in particulate gels of  $\beta$ -lactoglobulin formed near the isoelectric point. *The European Physical Journal E*, 21(2), 145-152.
- Çakır, E., Daubert, C. R., Drake, M. A., Vinyard, C. J., Essick, G., & Foegeding, E. A. (2012). The effect of microstructure on the sensory perception and textural characteristics of whey protein/ $\kappa$ -carrageenan mixed gels. *Food Hydrocolloids*, 26(1), 33-43.
- Çakır, E., & Foegeding, E. A. (2011). Combining protein micro-phase separation and protein-polysaccharide segregative phase separation to produce gel structures. *Food Hydrocolloids*, 25(6), 1538–1546.
- Capron, I., Nicolai, T., & Durand, D. (1999a). Heat induced aggregation and gelation of  $\beta$ -lactoglobulin in the presence of  $\kappa$ -carrageenan. *Food Hydrocolloids*, 13(1), 1-5.
- Capron, I., Nicolai, T., & Smith, C. (1999b). Effect of addition of  $\kappa$ -carrageenan on the mechanical and structural properties of  $\beta$ -lactoglobulin gels. *Carbohydrate Polymers*, 40(3), 233–238.
- Carrotta, R., Arleth, L., Pedersen, J. S., & Bauer, R. (2003). Small-angle X-ray scattering studies of metastable intermediates of  $\beta$ -lactoglobulin isolated after heat-induced aggregation. *Biopolymers*, 70(3), 377-390.
- Chronakis, I. S., Doublier, J. L., & Piculell, L. (2000). Viscoelastic properties for kappa- and iota-carrageenan in aqueous NaI from the liquid-like to the solid-like behaviour. *International Journal of Biological Macromolecules*, 28(1), 1-14.
- Creamer, L. K., Parry, D. A. D., & Malcolm, G. N. (1983). Secondary structure of bovine  $\beta$ -lactoglobulin B. *Archives of Biochemistry and Biophysics*, 227(1), 98-105.
- Croguennec, T., Bouhallab, S., Mollé, D., O’Kennedy, B. T., & Mehra, R. (2003). Stable monomeric intermediate with exposed Cys-119 is formed during heat denaturation of  $\beta$ -lactoglobulin. *Biochemical and Biophysical Research Communications*, 301(2), 465-471.
- Croguennoc, P., Durand, D., & Nicolai, T. (2001a). Phase Separation and Association of Globular Protein Aggregates in the Presence of Polysaccharides: 1. Mixtures of Preheated  $\beta$ -Lactoglobulin and  $\kappa$ -Carrageenan at Room Temperature. *Langmuir*, 17(14), 4372–4379.

- Croguennoc, P., Nicolai, T., & Durand, D. (2001b). Phase separation and association of globular protein aggregates in the presence of polysaccharides: 2. Heated mixtures of native  $\beta$ -lactoglobulin and  $\kappa$ -carrageenan. *Langmuir*, 17(14), 4380-4385.
- de Jong, S., Klok, H. J., & van de Velde, F. (2009). The mechanism behind microstructure formation in mixed whey protein-polysaccharide cold-set gels. *Food Hydrocolloids*, 23(3), 755-764.
- de la Fuente, M. A., Hemar, Y., & Singh, H. (2004). Influence of  $\kappa$ -carrageenan on the aggregation behaviour of proteins in heated whey protein isolate solutions. *Food Chemistry*, 86(1), 1-9.
- Doyle, J., Giannouli, P., Philp, K., & Morris, E. R. (2002). Effect of  $K^+$  and  $Ca^{2+}$  cations on gelation of  $\kappa$ -carrageenan. *Gums and Stabilisers for the Food Industry*, 11, 158-164.
- Durand, D., Gimel, J. C., & Nicolai, T. (2002). Aggregation, gelation and phase separation of heat denatured globular proteins. *Physica A: Statistical Mechanics and its Applications*, 304(1-2), 253-265.
- Flett, K. L., & Corredig, M. (2009). Whey protein aggregate formation during heating in the presence of  $\kappa$ -carrageenan. *Food Chemistry*, 115(4), 1479–1485.
- Flower, D. R. (1996). The lipocalin protein family: structure and function. *Biochemical Journal*, 318, 1-14.
- Flower, D. R., North, A. C. T., & Sansom, C. E. (2000). The lipocalin protein family: structural and sequence overview. *Biochimica et Biophysica Acta (BBA) - Protein Structure and Molecular Enzymology*, 1482(1-2), 9-24.
- Foegeding, E. A. (2006). Food biophysics of protein gels: A challenge of nano and macroscopic proportions. *Food Biophysics*, 1(1), 41-50.
- Foegeding, E. A., Kuhn, P. R., & Hardin, C. C. (1992). Specific divalent cation-induced changes during gelation of  $\beta$ -lactoglobulin. *J. Agric. Food Chem.*, 40(11), 2092–2097.
- Gaaloul, S., Corredig, M., & Turgeon, S. L. (2009b). Rheological study of the effect of shearing process and  $\kappa$ -carrageenan concentration on the formation of whey protein microgels at pH 7. *Journal of Food Engineering*, 95(2), 254–263.

- Gaaloul, S., Turgeon, S. L., & Corredig, M. (2009a). Influence of shearing on the physical characteristics and rheological behaviour of an aqueous whey protein isolate–kappa-carrageenan mixture. *Food Hydrocolloids*, 23(5), 1243–1252.
- Gaaloul, S., Turgeon, S. L., & Corredig, M. (2010). Phase Behavior of Whey Protein Aggregates/ $\kappa$ -Carrageenan Mixtures: Experiment and Theory. *Food Biophysics*, 5(2), 103–113.
- Gottschalk, M., Nilsson, H., Roos, H., & Halle, B. (2003). Protein self-association in solution: The bovine  $\beta$ -lactoglobulin dimer and octamer. *Protein Science*, 12(11), 2404–2411.
- Grinberg, V. Y., & Tolstoguzov, V. B. (1997). Thermodynamic incompatibility of proteins and polysaccharides in solutions. *Food Hydrocolloids*, 11(2), 145–158.
- Gustaw, W., & Mleko, S. (2003). The effect of pH and carrageenan concentration on the rheological properties of whey protein gels. *Polish Journal of Food and Nutrition Sciences*, 12(4), 39–44.
- Hambling, S. G., McAlpine, A. S., & Sawyer, L. (1992).  $\beta$ -Lactoglobulin. *Advanced dairy chemistry-1: Proteins*(Book), 141–190.
- Harrington, J. C., Foegeding, E. A., Mulvihill, D. M., & Morris, E. R. (2009). Segregative interactions and competitive binding of  $\text{Ca}^{2+}$  in gelling mixtures of whey protein isolate with  $\text{Na}^+$   $\kappa$ -carrageenan. *Food Hydrocolloids*, 23(2), 468–489.
- Hermansson, A. M. (1989). Rheological and Microstructural Evidence for Transient States During Gelation of Kappa-Carrageenan in the Presence of Potassium. *Carbohydrate Polymers*, 10, 163–181.
- Hermansson, A. M., Eriksson, E., & Jordansson, E. (1991). Effects of Potassium, Sodium and Calcium on the Microstructure and Rheological Behaviour of Kappa-Carrageenan Gels. *Carbohydrate Polymers*, 16(3), 297–320.
- Hosseini, S. M. H., Djomeh, Z. E., Razavi, S. H., Movahedi, A. A. M., Saboury, A. A., Mohammadifar, M. A., Farahnaky, A., Atri, M. S., & der Meeren, P. V. (2013). Complex coacervation of  $\beta$ -lactoglobulin –  $\kappa$ -Carrageenan aqueous mixtures as affected by polysaccharide sonication. *Food Chemistry*, 141(1), 215–222.
- Iametti, S., Cairoli, S., De Gregori, B., & Bonomi, F. (1995). Modifications of High-Order Structures upon Heating of  $\beta$ -Lactoglobulin: Dependence on the Protein Concentration. *J. Agric. Food Chem.*, 43(1), 53–58.

- Jung, J. M., Savin, G., Pouzot, M., Schmitt, C., & Mezzenga, R. (2008). Structure of Heat-Induced  $\beta$ -Lactoglobulin Aggregates and their Complexes with Sodium-Dodecyl Sulfate. *Biomacromolecules*, 9(9), 2477–2486.
- Kara, S., Tamerler, C., Bermek, H., & Pekcan, Ö. (2003). Cation effects on sol–gel and gel–sol phase transitions of  $\kappa$ -carrageenan–water system. *International Journal of Biological Macromolecules*, 31(4-5), 177–185.
- Kinsella, J. E., & Whitehead, D. M. (1987). Proteins in Whey: Chemical, Physical, and Functional Properties. *Advances in Food and Nutrition Research*, 33, 343–438.
- Kumosinski, T. F., & Timasheff, S. N. (1966). Molecular Interactions in  $\beta$ -Lactoglobulin. X. The Stoichiometry of the  $\beta$ -Lactoglobulin Mixed Tetramerization. *Journal of the American Chemical Society*, 88(23), 5635–5642.
- Leksrisonpong, P. N., Lanier, T. C., & Foegeding, E. A. (2012). Effects of Heating Rate and pH on Fracture and Water-Holding Properties of Globular Protein Gels as Explained by Micro-Phase Separation. *Journal of Food Science*, 77(2), E60–E67.
- Lyster, R. L. J. (1972). Reviews of the progress of dairy science. Section C. Chemistry of milk proteins. *Journal of Dairy Research*, 39(2), 279–318.
- MacArtain, P., Jacquier, J. C., & Dawson, K. A. (2003). Physical characteristics of calcium induced  $\kappa$ -carrageenan networks. *Carbohydrate Polymers*, 53(4), 395–400.
- Mangione, M. R., Giacomazza, D., Bulone, D., Martorana, V., Cavallaro, G., & San Biagio, P. L. (2005).  $K^+$  and  $Na^+$  effects on the gelation properties of  $\kappa$ -Carrageenan. *Biophysical Chemistry*, 113(2), 129–135.
- McKenzie, H. A., Sawyer, W. H., & Smith, M. B. (1967). Optical rotatory dispersion and sedimentation in the study of association-dissociation: Bovine  $\beta$ -lactoglobulins near pH5. *Biochimica et Biophysica Acta (BBA) - Protein Structure and Molecular Enzymology*, 147(1), 73–92.
- McKinnon, A. A., Rees, D. A., & Williamson, F. B. (1969). Coil to double helix transition for a polysaccharide. *J. Chem. Soc. D*, 13, 701–702.
- Mehalebi, S., Nicolai, T., & Durand, D. (2008). Light scattering study of heat-denatured globular protein aggregates. *International Journal of Biological Macromolecules*, 43(2), 129–135.

- Meunier, V., Nicolai, T., Durand, D., & Parker, A. (1999). Light Scattering and Viscoelasticity of Aggregating and Gelling  $\kappa$ -Carrageenan. *Macromolecules*, 32, 2610-2616.
- Mleko, S., Li-Chan, E. C. Y., & Pikus, S. (1997). Interactions of  $\kappa$ -carrageenan with whey proteins in gels formed at different pH. *Food Research International*, 30(6), 427-433.
- Morris, E. R., Rees, D. A., & Robinson, G. (1980). Cation-specific aggregation of carrageenan helices: Domain model of polymer gel structure. *Journal of Molecular Biology*, 138(2), 349-362.
- Nicolai, T., Britten, M., & Schmitt, C. (2011).  $\beta$ -Lactoglobulin and WPI aggregates: Formation, structure and applications. *Food Hydrocolloids*, 25(8), 1945-1962.
- Núñez-Santiago, M. C., Tecante, A., Garnier, C., & Doublier, J. L. (2011). Rheology and microstructure of  $\kappa$ -carrageenan under different conformations induced by several concentrations of potassium ion. *Food Hydrocolloids*, 25(1), 32-41.
- Otte, J., Zakora, M., & Qvist, K. B. (2000). Involvement of Disulfide Bonds in Bovine  $\beta$ -Lactoglobulin B Gels Set Thermally at Various pH. *Journal of Food Science*, 65(3), 384-389.
- Ould Eleya, M. M., & Turgeon, S. L. (2000a). Rheology of  $\kappa$ -carrageenan and  $\beta$ -lactoglobulin mixed gels. *Food Hydrocolloids*, 14(1), 29-40.
- Ould Eleya, M. M., & Turgeon, S. L. (2000b). The effects of pH on the rheology of  $\beta$ -lactoglobulin/ $\kappa$ -carrageenan mixed gels. *Food Hydrocolloids*, 14(3), 245-251.
- Papiz, M. Z., Sawyer, L., Eliopoulos, E. E., North, A. C. T., Findlay, J. B. C., Sivaprasadarao, R., Jones, T. A., Newcomer, M. E., & Kraulis, P. J. (1986). The structure of  $\beta$ -lactoglobulin and its similarity to plasma retinol-binding protein. *Nature\_letters to nature*, 324, 383-385.
- Phan-Xuan, T., Durand, D., Nicolai, T., Donato, L., Schmitt, C., & Bovetto, L. (2011). On the crucial importance of the pH for the formation and self-stabilization of protein microgels and strands. *Langmuir*, 27, 15092-15101.
- Phan-Xuan, T., Durand, D., Nicolai, T., Donato, L., Schmitt, C., & Bovetto, L. (2013). Tuning the Structure of Protein Particles and Gels with Calcium or Sodium Ions. *Biomacromolecules*, 14(6), 1980-1989.
- Phan-Xuan, T., Durand, D., Nicolai, T., Donato, L., Schmitt, C., & Bovetto, L. (2014). Heat induced formation of beta-lactoglobulin microgels driven by addition of calcium ions. *Food Hydrocolloids*, 34, 227-235.

Piculell, L. (1991). Effects of ions on the disorder-order transitions of gel-forming polysaccharides. *Food Hydrocolloids*, 5, 57-69.

Piculell, L. (2006). Gelling Carrageenans. In A. M. Stephen, G. O. Philips & P. A. Williams *Food Polysaccharides and their Applications*, 239, Boca Raton: CRC Press.

Rees, D. A., Steele, I. W., & Williamson, F. B. (1969). Conformational analysis of polysaccharides. III. The relation between stereochemistry and properties of some natural polysaccharide sulfates (1). *Journal of Polymer Science Part C: Polymer Symposia*, 28(1), 261–276.

Rochas, C., & Rinaudo, M. (1980). Activity coefficients of counterions and conformation in kappa-carrageenan systems. *Biopolymers*, 19(9), 1675–1687.

Rühs, P. A., Scheuble, N., Windhab, E. J., Mezzenga, R., & Fischer, P. (2012). Simultaneous Control of pH and Ionic Strength during Interfacial Rheology of  $\beta$ -Lactoglobulin Fibrils Adsorbed at Liquid/Liquid Interfaces. *Langmuir*, 28(34), 12536–12543.

Ryan, K. N., Vardhanabhuti, B., Jaramillo, D. P., van Zanten, J. H., Coupland, J. N., & Foegeding, E. A. (2012). Stability and mechanism of whey protein soluble aggregates thermally treated with salts. *Food Hydrocolloids*, 27(2), 411-420.

Sawyer, L. (2003).  $\beta$ -Lactoglobulin. *Advanced Dairy Chemistry-1 Proteins*((Book)), 319-386

Schmitt, C., Moitzi, C., Bovay, C., Rouvet, M., Bovetto, L., Donato, L., Leser, M. E., Schurtenberger, P., & Stradner, A. (2010). Internal structure and colloidal behaviour of covalent whey protein microgels obtained by heat treatment. *Soft Matter*, 6, 4876–4884.

Stone, A. K., & Nickerson, M. T. (2012). Formation and functionality of whey protein isolate–(kappa-, iota-, and lambda-type) carrageenan electrostatic complexes. *Food Hydrocolloids*, 27(2), 271-277.

Surroca, Y., Haverkamp, J., & Heck, A. J. R. (2002). Towards the understanding of molecular mechanisms in the early stages of heat-induced aggregation of  $\beta$ -lactoglobulin AB. *Journal of Chromatography A*, 970(1-2), 275-285.

Thrimawithana, T. R., Young, S., Dunstan, D. E., & Alany, R. G. (2010). Texture and rheological characterization of kappa and iota carrageenan in the presence of counter ions. *Carbohydrate Polymers*, 82(1), 69-77.



- Tilley, J. M. A. (1960). The chemical and physical properties of bovine  $\beta$ -lactoglobulin. *Dairy. Sci. Abstr.*, 22, 11-25.
- Tolstoguzov, V. B. (1991). Functional properties of food proteins and role of protein-polysaccharide interaction. *Food Hydrocolloids*, 4(6), 429-468.
- Tolstoguzov, V. B. (2003). Some thermodynamic considerations in food formulation. *Food Hydrocolloids*, 17(1), 1-23.
- Trius, A., Sebranek, J. G., & Lanier, D. T. (1996). Carrageenans and their use in meat products. *Critical Reviews in Food Science and Nutrition*, 36(1-2), 69-85.
- Turgeon, S. L., & Beaulieu, M. (2001). Improvement and modification of whey protein gel texture using polysaccharides. *Food Hydrocolloids*, 15(4-6), 583-591.
- Tziboula, A., & Horne, D. S. (1999). Influence of whey protein denaturation on  $\kappa$ -carrageenan gelation. *Colloids and Surfaces B: Biointerfaces*, 12(3-6), 299-308.
- Viebke, C., Piculell, L., & Nilsson, S. (1994). On the Mechanism of Gelation of Helix-Forming Biopolymers. *Macromolecules*, 27, 4160-4166
- Zhang, G., & Foegeding, E. A. (2003). Heat-induced phase behavior of  $\beta$ -lactoglobulin/polysaccharide mixtures. *Food Hydrocolloids*, 17(6), 785-792.



## Chapter 2:

# MATERIALS AND METHODS

### 2.1. Materials

For the research presented in this thesis I used mainly  $\beta$ -lactoglobulin (Chapter 4) and sodium  $\kappa$ -carrageenan (Chapter 3 and 4).

The *sodium  $\kappa$ -carrageenan* ( **$\kappa$ -car**) used for this study is an alkali treated extract from *Eucheuma cottonii* and was a gift from Cargill (Baupre, France). Using NMR it was found that the sample contained less than 5%  $\iota$ -carrageenan. A freeze-dried sample of  $\kappa$ -car was dissolved by stirring for a few hours in Milli-Q water (70°C) with 200 ppm sodium azide added as a bacteriostatic agent. The solution was extensively dialysed against Milli-Q water at pH= 7 and subsequently filtered through 0.45  $\mu$ m pore size Anotop filters. The pH of the solution was adjusted to 7 by adding small amounts of HCl 0.1 M. The required amounts of KCl, CaCl<sub>2</sub> or NaCl were added in the form of concentrated salt solutions. The  $\kappa$ -car concentration ( $C_k$ ) was determined by measuring the refractive index using refractive index increment 0.145 ml/g. The molar mass ( $M_w$ ) and radius of gyration ( $R_g$ ) were determined by light scattering as described elsewhere (Meunier et al., 1999) with  $M_w = 2.1 \times 10^5$  g/mol and  $R_g = 52$ nm.

$\kappa$ -car was fluorescently labelled by *fluorescein isothiocyanate* (FITC) to investigate the distribution on mixtures with  $\beta$ -lg. The protocol was prepared following the procedure from Heilig et al., 2009. 1g  $\kappa$ -car powder was dissolved in 80ml of *dimethyl sulfoxide* (DMSO) containing 80 $\mu$ l of pyridine and stirred for 1 hour before adding 0.1g FITC and 40 $\mu$ l *dibutyltin dilaurate*. The solution was stirred for 30 min and subsequently heated at 95°C for 3 hours. After cooling to room temperature, the excess FITC was removed by washing in isopropanol and centrifugation at 9600g for 45min. The washing step was repeated until FITC could no longer be detected in the *isopropanol*. Finally, the modified  $\kappa$ -car was freeze dried and kept in the dark. No effect of labeling on rheology and on the structure of the mixtures was observed.

The  *$\beta$ -lactoglobulin* ( **$\beta$ -lg**) (Biopure, lot JE 001-8-415) used in this study was purchased from Davisco Foods International, Inc. (Le Sueur, MN, USA) and consisted of

approximately equal quantities of variants A and B. The powder was dissolved in Milli-Q water which contained 200 ppm NaN<sub>3</sub> to prevent bacterial growth. Solutions were dialysed extensively against Milli-Q water with 200 ppm sodium azide and subsequently filtered through 0.2 µm pore size Anotop filters. The pH of the solution was adjusted to 7 by adding small amounts of NaOH 0.1 M. The protein concentration was determined by UV absorption at 278 nm using extinction coefficient 0.96 Lg<sup>-1</sup>cm<sup>-1</sup>.

Stable suspensions of protein particles were prepared by heating aqueous solutions of β-Ig at different concentrations (10 to 80) g/L in pure water at pH= 7 and (20 and 40) g/L in pure water at pH= 7 with different amounts of CaCl<sub>2</sub>. The solutions were heated in airtight vials in a water bath at 85°C until steady state was reached (overnight) and the residual fraction of native proteins was negligible. The z-average hydrodynamic radius (R<sub>h</sub>) of the particles was determined by dynamic light scattering (Nicolai, 2007) and was found to range from 17 to 320nm, depending on the concentrations of β-Ig and CaCl<sub>2</sub> and the pH. In the absence of added salt, small strand-like β-Ig aggregates were formed, while larger spherical particles were produced after adding controlled amounts of CaCl<sub>2</sub>. A detailed description of the formation of the protein particles and their characterization using light scattering can be found in refs (Phan-Xuan et al., 2013 & 2014). The specific concentrations used to prepare β-Ig aggregates will be presented in the results section.

## 2.2. Methods

### 2.2.1. Light scattering

Light scattering is a common useful technique to measure the average molecular weight (M<sub>w</sub>), the z-average size (radius of gyration (R<sub>g</sub>) and hydrodynamic radius (R<sub>h</sub>)) and the size distribution. Depending on the purpose of study, two distinct methods are used: static light scattering and dynamic light scattering. Static Light Scattering (SLS) is a technique in which the average intensity of the scattered light of the sample is measured as a function of the scattering wave vector (q) that depends on the scattering angle (θ):  $q = 4\pi n \sin(\theta) / \lambda$ , where  $n$  is the refractive index of the solution and  $\lambda$  is the wavelength of the incident light. In dilute solution the radius of gyration (R<sub>g</sub>) can be calculated from the initial dependence of the intensity on q in the range between 20 and 100 nm.

$$I_r / (KC) = M_w / (1 + (q \cdot R_g)^2 / 3) \quad (2.1)$$

where  $I_r$  is the scattering intensity of the sample minus that of the solvent divided by that of a standard (toluene).  $K$  is an optical constant that depends on the refractive index increment of the solute ( $\partial n / \partial c$ ) and the Raleigh factor of the standard ( $R_{st}$ ):

$$K = \frac{4\pi^2 n_s^2}{\lambda^4 N_a} \left( \frac{\partial n}{\partial c} \right)^2 \left( \frac{n_{tol}}{n_s} \right)^2 \frac{1}{R_{tol}} \quad (2.2)$$

with  $N_a$  Avogadro's number.  $(n_{tol}/n_s)^2$  corrects for the difference in refractive index between the sample and the toluene standard. We have used  $(\partial n / \partial c) = 0.189 \text{ mL/g}$ ;  $R_{tol} = 1.495 \times 10^{-5} \text{ cm}^{-1}$  at  $20^\circ\text{C}$  and  $\lambda = 632 \text{ nm}$ .

Dynamic light scattering (DLS) is a technique in which the autocorrelation function of the scattered light intensity fluctuation is measured. It can be used to determine the distribution of hydrodynamic radii in the range between about 1 and 500 nm. The normalized electric field autocorrelation functions ( $g_1(t)$ ) obtained from the dynamic light scattering measurements (Berne & Pecora, 1976) were analyzed in terms of a distribution of relaxation times ( $\tau$ ):

$$g_1(t) = \int A(\tau) \exp(-t / \tau) d(\tau) \quad (2.3)$$

In dilute solutions, the relaxation is caused by translational diffusion of the particles and the z-average diffusion coefficient ( $D$ ) can be calculated from the average relaxation time:

$$D = \langle \tau^{-1} \rangle / q^2 \quad (2.4)$$

The z-average hydrodynamic radius of the solute can be calculated using the Stokes-Einstein equation:

$$R_h = \frac{kT}{6\pi\eta D} \quad (2.5)$$

with  $\eta$  the viscosity of the solvent,  $k$  Boltzman's constant, and  $T$  the absolute temperature. For polydisperse samples a distribution of the hydrodynamic radii can be obtained in this way from the distribution of relaxation times. If  $q \cdot R_h > 1$  one has to consider the effects of internal dynamics and polydispersity. Therefore measurements were done at different angles to ensure that the limiting regime of  $q \cdot R_h < 1$  was reached.

For this study light scattering measurements were done with a commercial apparatus (ALV-CGS3, ALV-Langen) operating with a vertically polarized He-Ne laser with wavelength  $\lambda=632\text{nm}$ . The sample is inserted in a temperature controlled vat and is illuminated by a laser. The fluctuations of the scattered light intensity are detected at different scattering angle by a fast photon diode on a rotating arm (figure 2.1). The range of scattering angles was 12-150 degrees. The temperature was controlled at  $20^{\circ}\text{C}$  with a thermostat bath to within  $\pm 0.2^{\circ}\text{C}$ .

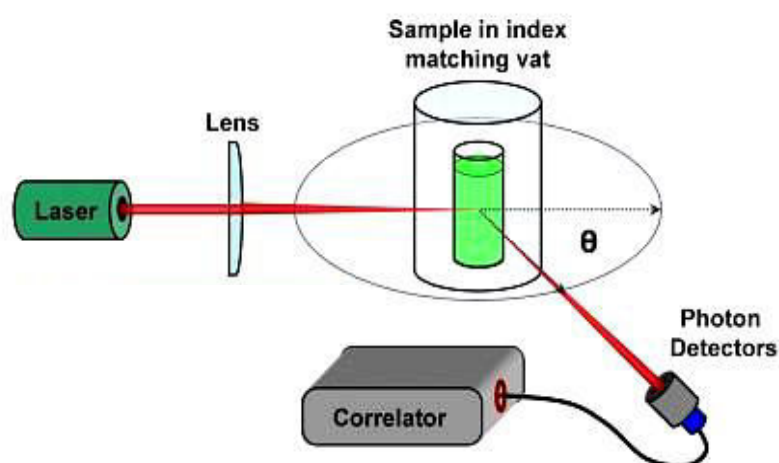


**Figure 2.1.** Schematic diagram of a light scattering apparatus.

### 2.2.2. Turbidity measurements

Turbidity is a measure of the loss of transparency due to very strong scattering of light by the solute:

$$\tau = \left[ \ln \left( \frac{I_0}{I} \right) \right] \frac{1}{l} \quad (2.6)$$

where  $I$  is the intensity of the light transmitted through the sample with path length ( $l$ ) and  $I_0$  is that for the pure solvent.

Here, turbidity measurements were done in rectangular air tight cells using a UV-Visible spectrometer Varian Cary-50 Bio (Les Ulis, France). Different path lengths were used depending on the turbidity of the samples in order to avoid saturation. Measurements were done at different wavelengths (300; 400; 500; 600; 680; 750 and 800nm) and different temperatures that were controlled within  $0.2^{\circ}\text{C}$  using a thermostat bath.

### 2.2.3. Determination of the protein concentration with UV-Visible spectroscopy

Protein concentrations (C) were determined by ultraviolet spectroscopy by measuring the absorbance (A) at the maximum situated at a wavelength of 278 nm using the Beer-Lambert's law:  $A = \epsilon.l.C$ , with a molar extinction coefficient  $\epsilon = 0.96 \text{ Lg}^{-1}\text{cm}^{-1}$ . In order to avoid effects of turbidity and interactions, the samples were diluted to a concentration of about 1g/L.

### 2.2.4. Confocal Laser Scanning Microscopy (CLSM)

Confocal laser scanning microscopy (CLSM) is a useful method to study the structure of systems that are heterogeneous on microscopic length scales. Contrary to standard optical microscopy the image of a single focal plane is obtained, which necessitates the use of fluorescent probes in order to gather sufficient light. Different components can be distinguished by using different fluorescent labeling.

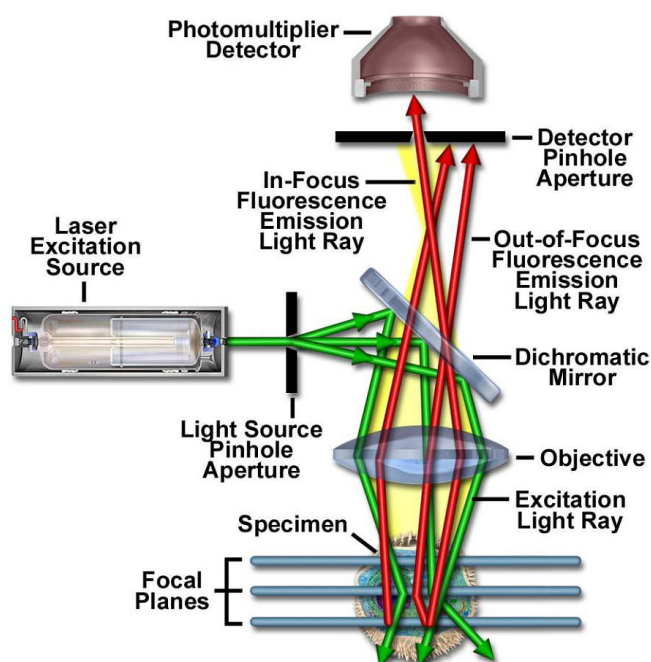


**Figure 2.2.** Schematic diagram of the optical pathway and principal components in a modern confocal laser scanning microscope.

A schematic drawing of a CLSM apparatus is given in figure 2.2. A laser beam is reflected by a dichromatic mirror toward to specimen after through the pinhole. The light emitted by the probes passes through the same dichotic mirror and is detected by a

photomultiplier detector after passing through a pinhole that stops out-of-focus light. The objective is to concentrate the energy of light ray to specimen.

In this study, observations were made with a Leica TCS-SP2 (Leica Microsystems Heidelberg, Germany). Images of 512x512 pixels were produced at different magnifications with two different water immersion objectives lenses: HCx PL APO 63x NA=1.2 and 20x NA=0.7.  $\beta$ -lg was labelled with the fluorochrome rhodamine B isothiocyanate (Rho. B), by adding a small amount of a concentrated rhodamine solution to reach a final concentration of 5 ppm.  $\kappa$ -car was covalently labeled with fluorescein isothiocyanate isomer I (FITC) as described in ref. (Heilig et al., 2009). The incident light was emitted by a laser beam at 543 nm and/or at 488 nm. The fluorescence intensity was recorded between 560 and 700 nm.

In most cases the solutions were inserted between a concave slide and a cover slip and hermetically sealed, which allowed heating in a thermostat bath. In a few cases the samples were inserted in a Chambered Coverglass which allowed rapid observation.

### 2.2.5. Rheology

Rheology is the study of the flow or deformation of materials under mechanical stress. Here we use oscillatory shear measurements to characterize the mechanical properties of the materials as a function of the shear stress ( $\sigma$ ) and the oscillation. A sinusoidal shear stress is imposed at a frequency ( $\omega$ ):  $\sigma = \sigma_0 \sin(\omega.t)$ , and resulting deformation ( $\gamma$ ) of the material is measured:  $\gamma = \gamma_0 \sin(\omega.t + \delta)$ , where  $\delta$  is the phase shift. At low stresses in the so-called linear response regime  $\gamma_0 \propto \sigma_0$  and the in phase and out of phase deformation are characterized by the storage ( $G'$ ) and the loss modulus ( $G''$ ), respectively:

$$G'(\omega) = \frac{\sigma_0}{\gamma_0} \sin \delta \quad (2.7)$$

$$G''(\omega) = \frac{\sigma_0}{\gamma_0} \cos \delta \quad (2.8)$$

For elastic solids  $G'$  is larger than  $G''$  and independent of the frequency, while for Newtonian liquids  $G'$  is smaller than  $G''$  and both moduli depend on the frequency:  $G' \propto \omega^{-2}$  and  $G'' \propto \omega^{-1}$ . Viscoelastic liquid (solid) materials show solid-like behavior at high frequencies and liquid (solid) like behavior at low frequencies.



A schematic drawing of the instrument used for the present study (AR2000, TA Instruments) is given in figure 2.4. A plate - plate geometry was used with a diameter of 40 mm. The gap was in most cases set at 700  $\mu\text{m}$ , but the effect of varying the gap width was tested. The temperature was controlled by a Peltier system on a wide range of value (5 to 85°C) and the geometry was covered with paraffin oil to prevent water evaporation. For some systems the gel partially slipped leading to a strong decrease of the shear modulus. In this case sandpaper was glued onto the two surfaces of the geometry and plate. In all cases the dynamic measurements were done in the linear response regime.

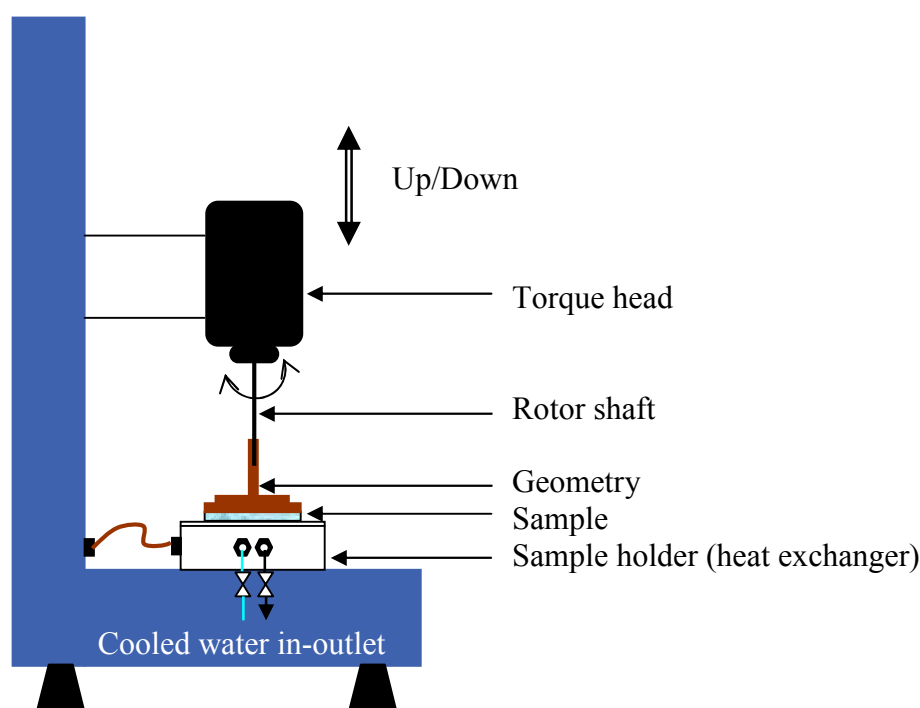


**Figure 2.3.** Schematic drawing of the rheometer used in this study.

### 2.2.6. Calcium activity measurements

The calcium ion activity in solution was determined by a calcium-specific electrode (Fisher Scientific, USA). A calibration curve was obtained by measuring  $\text{CaCl}_2$  solutions in water at concentrations ranging from 0 to 25 mM. The concentration of free calcium ions was calculated by assuming that the activity of bound  $\text{Ca}^{2+}$  was zero and the activity of free  $\text{Ca}^{2+}$  was the same as in pure water.

## References

- Berne, B. J., & Pecora, R. (1976). Dynamic Light Scattering with applications to Chemistry, Biology, and Physics. *Wiley: New York, (Book)*.
- Heilig, A., Göggerle, A., & Hinrichs, J. (2009). Multiphase visualisation of fat containing  $\beta$ -lactoglobulin- $\kappa$ -carrageenan gels by confocal scanning laser microscopy, using a novel dye, V03-01136, for fat staining. *LWT - Food Science and Technology*, 42(2), 646–653.
- Meunier, V., Nicolai, T., Durand, D., & Parker, A. (1999). Light Scattering and Viscoelasticity of Aggregating and Gelling  $\kappa$ -Carrageenan. *Macromolecules*, 32, 2610-2616.
- Nicolai, T. (2007). Food characterisation using scattering methods. *In Understanding and controlling the microstructure of complex foods*, McClements, D. J., Ed. Woodhead: Cambridge, 288-310
- Phan-Xuan, T., Durand, D., & Nicolai, T. (2013). Tuning the Structure of Protein Particles and Gels with Calcium or Sodium Ions. *Biomacromolecules*, 14(6), 1980–1989.
- Phan-Xuan, T., Durand, D., Nicolai, T., Donato, L., Schmitt, C., & Bovetto, L. (2014). Heat induced formation of beta-lactoglobulin microgels driven by addition of calcium ions. *Food Hydrocolloids*, 34, 227–235.

## Chapter 3:

# GELATION OF KAPPA CARRAGEENAN

### 3.1. Introduction

As mentioned in the chapter 1, in aqueous solution,  $\kappa$ -carrageenan has a random coil conformation above a critical temperature ( $T_c$ ) and a helical conformation below this temperature (Rees et al., 1969, McKinnon et al., 1969). Most often  $\kappa$ -car in the helical conformation will aggregate and can form a gel if the concentration is sufficiently high. The critical gelation temperature ( $T_g$ ) is close to  $T_c$ , which depends on the concentration and the type of cations that are present (Rochas & Rinaudo, 1980; Michel et al., 1997).

The effect of both the concentration and type of cation on the elastic modulus of  $\kappa$ -car gels has been studied in some detail for potassium and calcium that are most commonly used to induce gelation. Generally, it is found that the elastic modulus increases with increasing potassium concentration (Doyle et al., 2002; Nguyen et al., 2014; Nono et al., 2011; Núñez-Santiago & Tecante; 2007; Thrimawithana et al., 2010), while it reaches a maximum when the calcium concentration is increased (Doyle et al., 2002; MacArtain et al., 2003; Thrimawithana et al., 2010). Another difference between gels induced by potassium and those induced by calcium is that the latter are increasingly turbid with increasing ion concentration (Doyle et al., 2002; MacArtain et al., 2003), while the former remain transparent.

In most applications of  $\kappa$ -car in food products more than one type of salt is present. As was mentioned in chapter 1,  $\kappa$ -car in mixed salts was studied by Hermansson et al. (1991) and Mangione et al. (2005) who found that either adding NaCl or CaCl<sub>2</sub> led to an increase of the elastic modulus of the potassium induced  $\kappa$ -car gel. However, the critical temperature was not influenced.

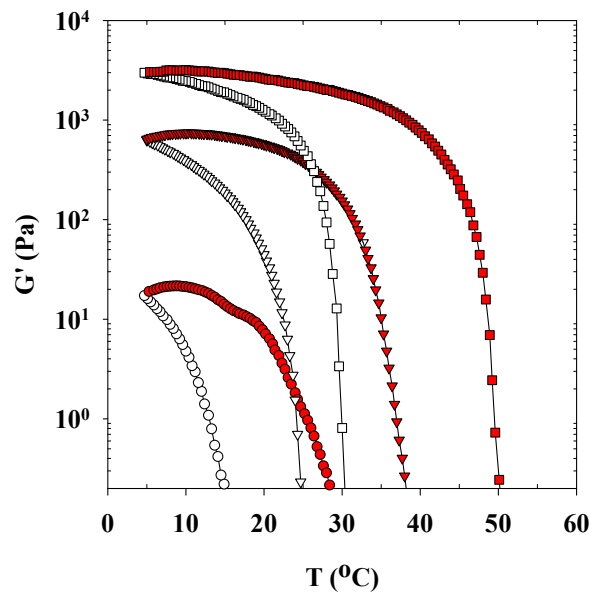
In this chapter, we present a systematic investigation of the influence of adding CaCl<sub>2</sub> or NaCl on  $\kappa$ -car gelation at pH 7 induced by potassium and compare it with gelation induced by pure CaCl<sub>2</sub> and pure KCl on the elastic modulus at steady state, on the gelation kinetics and the turbidity. The results have been published in Carbohydrate Polymer to which we refer for further details, see paper 1 of the Appendix.

## 3.2. Results

### 3.2.1. Single salt induced $\kappa$ -carrageenan gelation

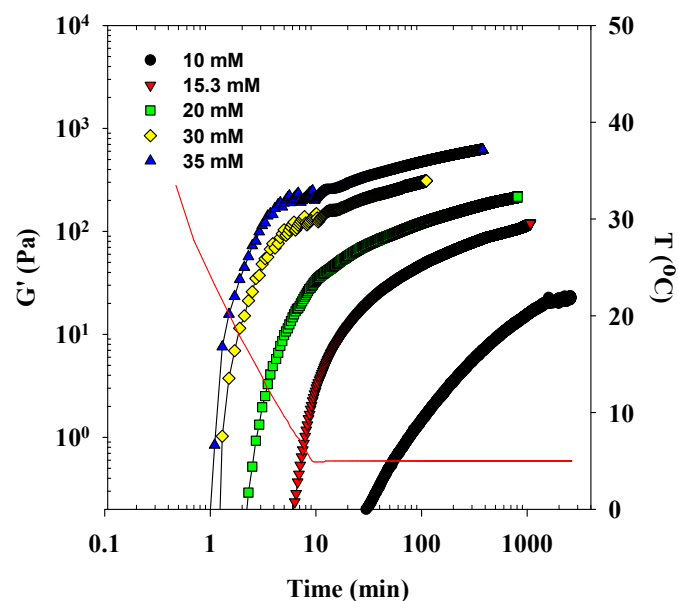
#### 3.2.1.1. Gelation of $\kappa$ -car induced by $K^+$

$\kappa$ -car solutions at concentrations between 0.5 to 16g/L were investigated at 10, 20 or 30mM KCl. Figure 3.1 shows the storage shear moduli at 0.1Hz of  $\kappa$ -car solutions as a function of temperature during a cooling and subsequent heating ramp for  $C_k = 8\text{g/L}$  at different KCl concentrations.  $G'$  increases steeply at the critical gel temperature ( $T_g$ ) and decreases steeply at the critical melting temperature ( $T_m$ ).



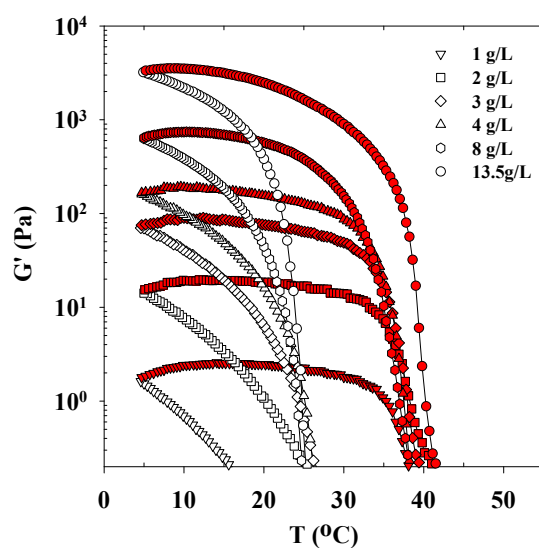
**Figure 3.1.** Storage shear modulus at 0.1 Hz during cooling (open symbols) and subsequent heating (filled symbols) ramps at a rate of  $2^\circ\text{C}/\text{min}$  at  $C_k = 8\text{g/L}$  in the presence of 10mM (circles), 20mM (triangles) and 30mM KCl (squares)

The gel and melting temperatures increased with increasing KCl concentration in agreement with results reported in the literature (Doyle et al., 2002). At a given temperature below  $T_g$ , the gelation rate increased with increasing KCl concentration as is illustrated in figure 3.2 where the evolution of  $G'$  at 0.1Hz is shown for  $C_k = 2\text{g/L}$  after quickly cooling down to  $5^\circ\text{C}$  from the liquid state at  $50^\circ\text{C}$ . Notice that the shear modulus did not reach a stable value, but continued to increase logarithmically at long times indicating that  $\kappa$ -car gels slowly restructure. The frequency dependence of  $G'$  was weak so that the value obtained at 0.1Hz can be considered characteristic for the elastic modulus of the  $\kappa$ -car gel.



**Figure 3.2.** Evolution of the storage shear modulus at 0.1Hz for 2g/L  $\kappa$ -car at different concentrations of KCl during and after rapid cooling to 5°C. The solid line indicates the temperature of the sample.

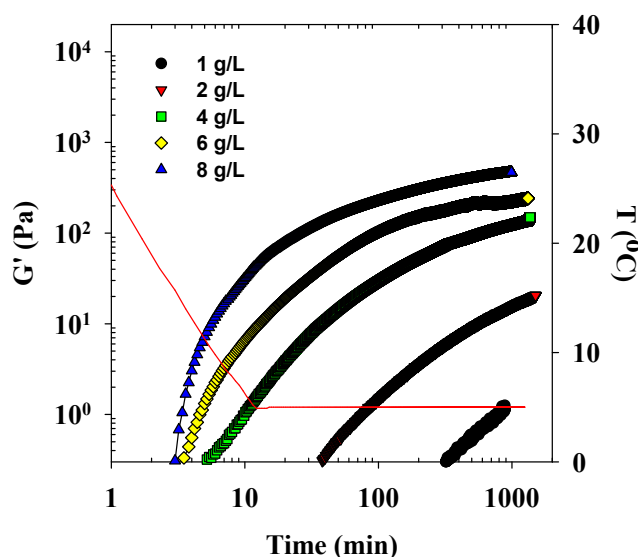
The effect of the  $\kappa$ -car concentration at 20mM KCl on the evolution of  $G'$  during cooling and heating ramps is shown in figure 3.3.



**Figure 3.3.** Storage shear modulus at 0.1 Hz during cooling (open symbols) and subsequent heating (filled symbols) ramps at a rate of 2°C/min of aqueous solutions of  $\kappa$ -car containing 20mM KCl and different  $\kappa$ -car concentrations.

Figure 3.3 shows that the gel ( $T_g \approx 24^\circ\text{C}$ ) and melting temperature ( $T_m \approx 39^\circ\text{C}$ ) did not depend significantly on the  $\kappa$ -car concentration in agreement with literature results (Kara et al., 2003). However, at  $C_k = 1\text{g/L}$  gelation was very slow and the rise of  $G'$  is only observed at lower temperatures. At  $C_k = 0.5\text{g/L}$  the concentration was too low to allow gelation. Similar results were seen at 10mM KCl (paper 1) and 30mM KCl (results not shown).

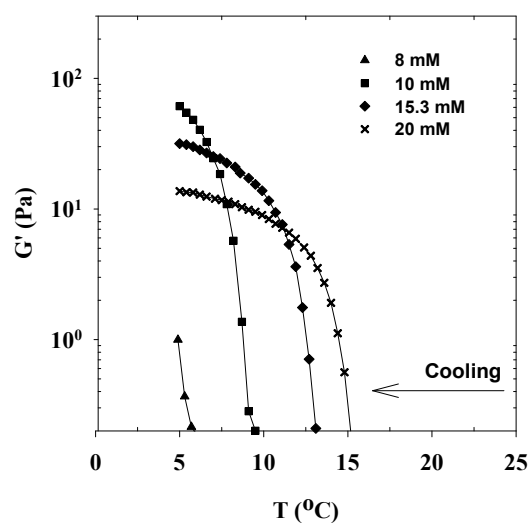
Though  $T_g$  is independent of the  $\kappa$ -car concentration, the gelation rate and final gel strength at a given temperature increases with the  $\kappa$ -car concentrations as was already discussed in some detail by Meunier et al. (1999). This is demonstrated in figure 3.4 where the evolution of  $G'$  at  $5^\circ\text{C}$  is shown as a function of time.



**Figure 3.4.** Evolution of the storage shear modulus at 0.1Hz for different concentrations of  $\kappa$ -car at 10mM KCl during and after rapid cooling to  $5^\circ\text{C}$ . The solid line indicates the temperature of the sample.

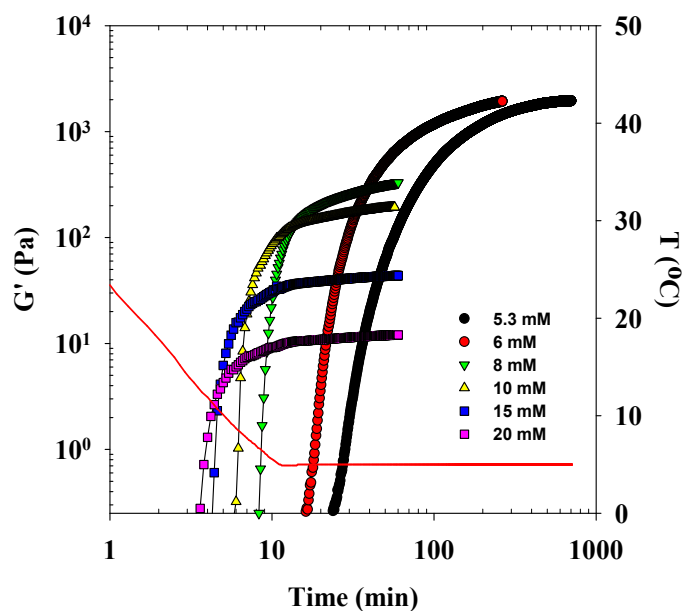
### 3.2.1.2. Gelation of $\kappa$ -car induced by $\text{Ca}^{2+}$

Figure 3.5 shows the storage shear moduli at 0.1Hz of  $\kappa$ -car solutions as a function of the temperature during a cooling ramp for  $C_k = 2\text{g/L}$  at different  $\text{CaCl}_2$  concentrations ( $[\text{CaCl}_2]$ ). The critical gelation temperatures increased with increasing  $\text{CaCl}_2$  concentration.



**Figure 3.5.** Storage shear modulus at 0.1 Hz during cooling ramps at a rate of 2 °C/min for aqueous solutions of 2g/L  $\kappa$ -car containing different  $\text{CaCl}_2$  concentrations.

The gelation rate of  $\kappa$ -car after rapid cooling to 5°C is shown in figure 3.6. Remarkably, in the presence of  $\text{CaCl}_2$ , gelation was much faster than in the presence of KCl at the same low concentration of  $\kappa$ -car used in this experiment even at  $\text{Ca}^{2+}$  concentrations at which  $T_g$  was lower.



**Figure 3.6.** Evolution of the storage shear modulus at 0.1Hz for 2g/L  $\kappa$ -car at different concentrations of  $\text{CaCl}_2$  during and after rapid cooling to 5°C. The solid line indicates the temperature of the sample.

At  $[\text{CaCl}_2] \leq 4.7\text{mM}$ , no gelation was observed at  $5^\circ\text{C}$  for at least 24h. At  $5.3\text{mM}$   $\text{CaCl}_2$ , gelation was slowest but the gel reached the highest value of  $G'$ . As mentioned in the introduction, this is also similar when authors observed that the elastic modulus of  $\kappa$ -car gel increased with increasing potassium concentration (Doyle et al., 2002), while Young's modulus solution containing  $10\text{g/L}$   $\kappa$ -car reached a maximum when the calcium concentration was increased (Doyle et al., 2002; Harrington et al., 2009).

Figure 3.7 shows the effect of the  $\kappa$ -car concentration on gelation during and after rapid cooling to  $50^\circ\text{C}$  for  $[\text{CaCl}_2] = 10\text{mM}$ . Interestingly, the rate of gelation induced by calcium did not depend on the  $\kappa$ -car concentration at least in the range investigated between 1 and  $8\text{g/L}$ , but the elastic moduli of the gels increased with increasing  $\kappa$ -car concentration.

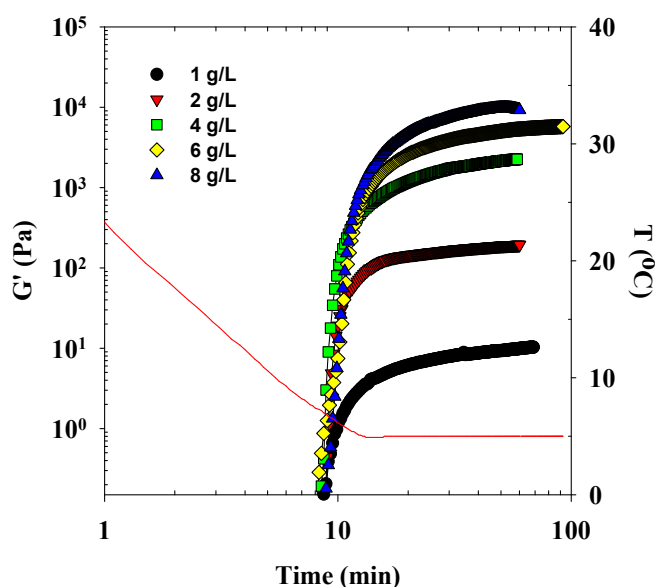


**Figure 3.7.** Evolution of the storage shear modulus at  $0.1\text{Hz}$  for different concentrations of  $\kappa$ -car at  $10\text{mM}$   $\text{CaCl}_2$  during and after rapid cooling to  $5^\circ\text{C}$ . The solid line indicates the temperature of the sample.

Figure 3.8 compares the elastic modulus at the quasi-plateau where the increase of  $G'$  becomes logarithmic as a function of the salt concentration for  $\text{CaCl}_2$  and  $\text{KCl}$  at  $C_k = 2\text{g/L}$ . Below  $5\text{mM}$   $\text{CaCl}_2$  and below  $10\text{mM}$   $\text{KCl}$ , gelation was not observed at  $5^\circ\text{C}$ . The elastic modulus increased with increasing  $\text{KCl}$  concentration, but it decreased with increasing  $\text{CaCl}_2$  concentration. A possible reason for this behavior is that the gels became increasingly heterogeneous (MacArtain et al., 2003) when more  $\text{CaCl}_2$  was added, see paper 1 in the appendix.



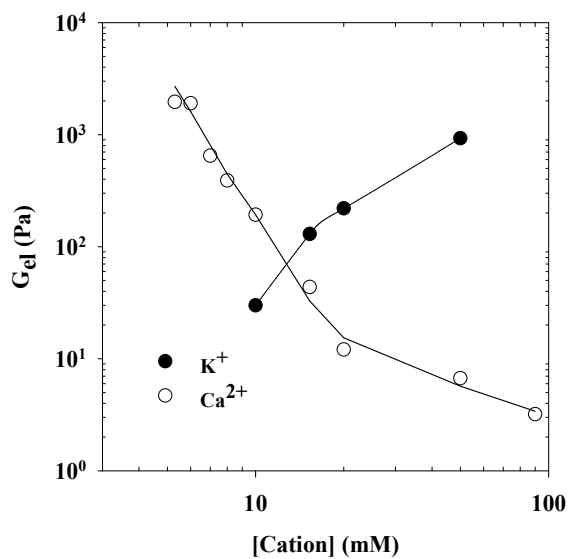


**Figure 3.8.** Elastic modulus of  $\kappa$ -car gels at  $C_k = 2\text{g/L}$  as a function of the cation concentration at  $5^\circ\text{C}$  in the presence of KCl (closed symbols) or  $\text{CaCl}_2$  (open symbols). The solid lines are guides to the eye.

The different kinetics of  $K^+$ -induced and  $\text{Ca}^{2+}$ -induced  $\kappa$ -car gelation is illustrated in figure 3.9. The initial increase of  $G'$  was much steeper in the presence of  $\text{Ca}^{2+}$  than in the presence of  $K^+$ .

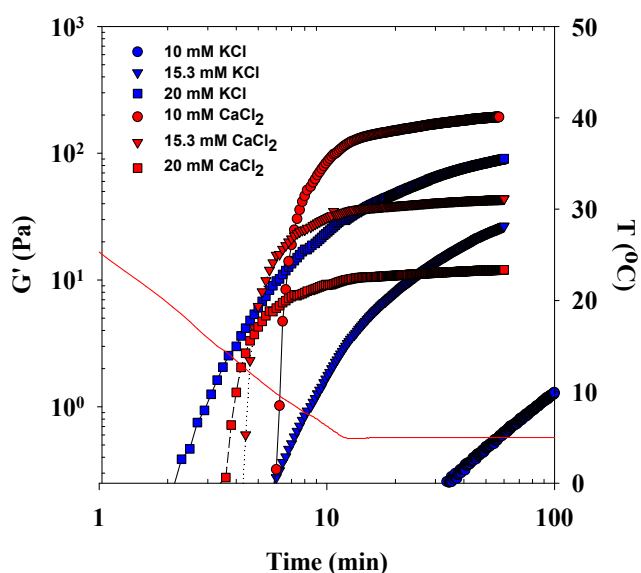


**Figure 3.9.** Comparison of the evolution of the storage shear modulus of  $2\text{g/L}$   $\kappa$ -car at different concentrations of KCl and  $\text{CaCl}_2$  during and after rapid cooling to  $5^\circ\text{C}$ . The solid line indicates the temperature of the sample.

### 3.2.2. Influence of $\text{Ca}^{2+}$ on the $\text{K}^{+}$ -induced gelation of $\kappa$ -car

We have seen that both potassium and calcium ions can induce  $\kappa$ -car to form a gel, but in a different manner. We will in the following consider the synergic effects of adding both ions. Figure 3.10 compares cooling and subsequent heating ramps of 2g/L  $\kappa$ -car at 10mM KCl and different amounts of  $\text{CaCl}_2$ . Addition of  $\text{CaCl}_2$  did not influence the gelation temperature ( $T_g \approx 22^\circ\text{C}$ ). The apparently lower value at the lowest  $\text{CaCl}_2$  concentration was caused by the slow kinetics at low  $\text{CaCl}_2$  concentrations (paper 1). No significant gelation was observed during the cooling ramp in the absence of  $\text{CaCl}_2$ . However, the melting temperature significantly increased with increasing  $\text{CaCl}_2$  concentration. Notice that with pure  $\text{CaCl}_2$  at 5.3mM or less, no gelation was observed during the cooling ramps and that at 10mM  $\text{CaCl}_2$  it was observed only below  $10^\circ\text{C}$ , see figure 3.5. This means that the coil-helix transition was in all cases induced by  $\text{K}^{+}$ . In pure KCl aggregation and gelation of the helices is very slow. The effect of adding  $\text{CaCl}_2$  is not to induce the coil-helix transition at a higher temperature, but to reduce electrostatic repulsion between the chains so that gelation can occur rapidly. Remarkably, gels became stiffer when more  $\text{CaCl}_2$  was added while in pure  $\text{CaCl}_2$  they became weaker. This is consistent with the observation that these gels were more homogeneous than pure  $\text{CaCl}_2$  gels (paper 1).

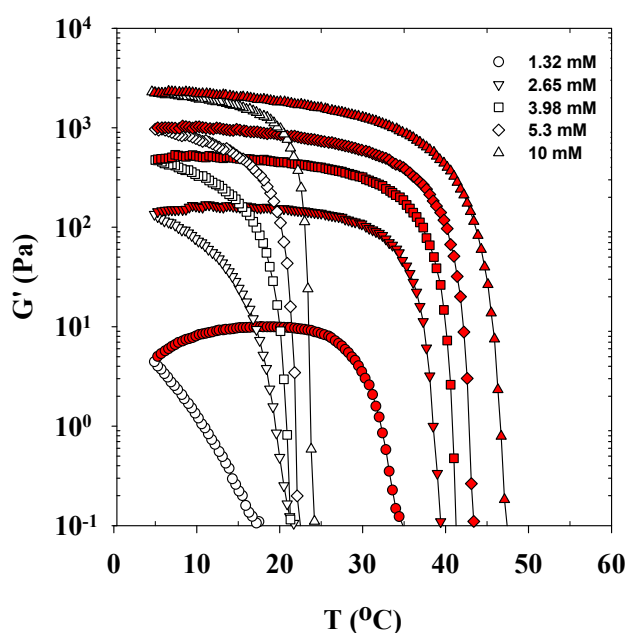


**Figure 3.10.** Storage shear modulus at 0.1 Hz during cooling (open symbols) and subsequent heating (filled symbols) ramps at a rate of  $2^\circ\text{C}/\text{min}$  of aqueous solutions of 2g/L  $\kappa$ -car containing 10mM KCl and different concentrations of  $\text{CaCl}_2$ .

Figure 3.11 compares cooling and subsequent heating ramp of  $\kappa$ -car in mixed salt at different  $\kappa$ -car concentrations. As in the pure salts, the critical temperature was independent of the concentration, and the elastic modulus increased with increasing  $\kappa$ -car concentration.

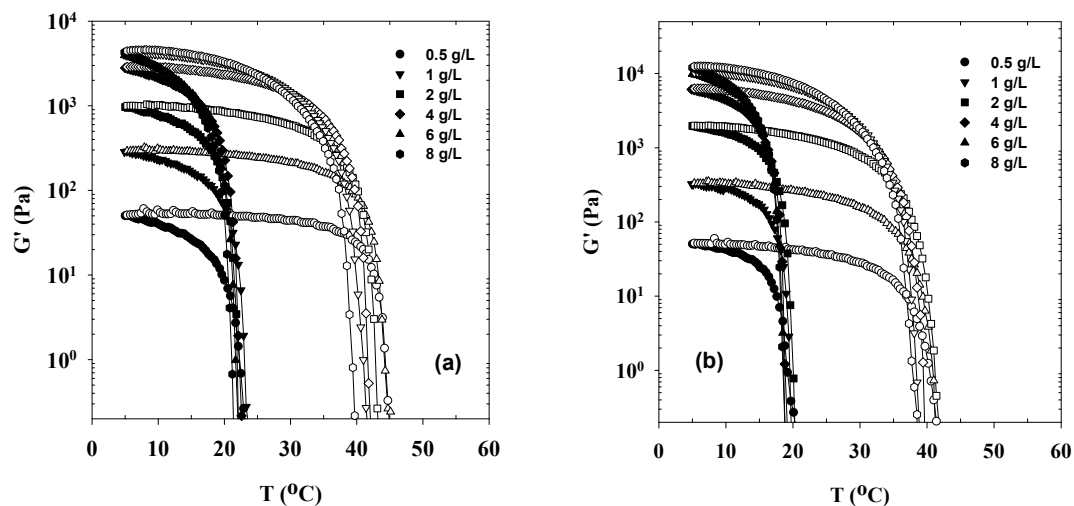


**Figure 3.11.** Storage shear modulus at 0.1 Hz during cooling (closed symbols) and subsequent heating (open symbols) ramps at a rate of  $2^{\circ}\text{C}/\text{min}$  of  $\kappa$ -car solutions containing 10mM KCl and 5.3mM  $\text{CaCl}_2$  (a) or 5.3mM KCl and 10mM  $\text{CaCl}_2$  (b) at different  $\kappa$ -car concentrations.

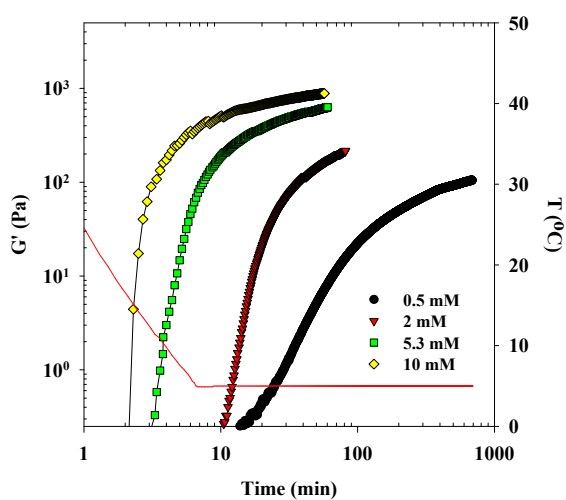


**Figure 3.12.** Evolution of the storage shear modulus at 0.1Hz of aqueous solutions of 2g/L  $\kappa$ -car containing 4mM  $\text{CaCl}_2$  and different concentrations of KCl during and after rapid cooling to  $5^{\circ}\text{C}$ . The solid line indicates the temperature of the sample.

The effect of adding KCl up to 10mM on  $\kappa$ -car gelation was investigated at different  $\text{CaCl}_2$  concentrations (4, 5.3, 10, 15.3mM). At 4mM  $\text{CaCl}_2$  no gelation was observed at 5°C without KCl, but with increasing KCl concentration gelation was faster and led to stiffer gels (figure 3.12). We stress that in the absence of  $\text{CaCl}_2$ , gelation of  $\kappa$ -car was extremely slow at these low KCl concentrations. At 10mM and 15.3mM  $\text{CaCl}_2$  gelation was already observed in the absence of KCl (figure 3.5), but again addition of KCl led to faster gelation and stiffer gels. The effect of KCl on the elastic modulus was especially important at low KCl concentrations ( $[\text{KCl}] < 2\text{mM}$ , see figure 3.13).

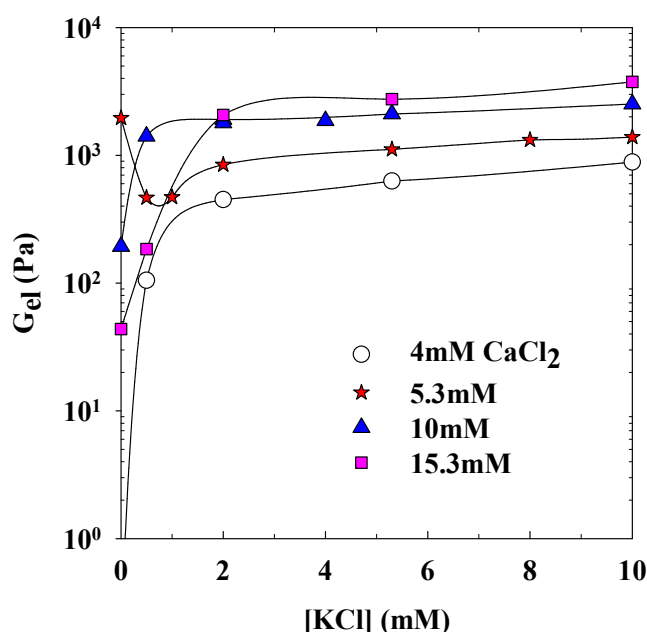


**Figure 3.13.** Elastic modulus of  $\kappa$ -car gels at  $C_k = 2\text{g/L}$  as a function of the KCl concentration at 5°C in the presence of different  $\text{CaCl}_2$  concentrations

A remarkable behavior was observed at 5.3mM  $\text{CaCl}_2$ . As for the other  $\text{CaCl}_2$  concentrations, gelation was faster and the elastic modulus of the gels increased with increasing KCl concentration. Surprisingly, however, the quasi-plateau value of  $G'$  was significantly higher in pure 5.3mM  $\text{CaCl}_2$  than when KCl was added especially at 0.5 or 1mM even though gelation was faster (figure 3.14).

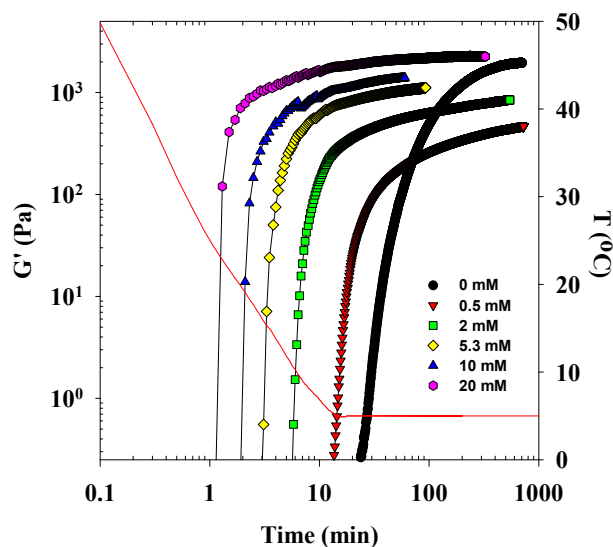


**Figure 3.14.** Evolution of the storage shear modulus at 0.1Hz of aqueous solutions of 2g/L  $\kappa$ -car containing 5.3mM  $\text{CaCl}_2$  and different concentrations of KCl during and after rapid cooling to 5°C. The solid line indicates the temperature of the sample.

The observed effects of adding KCl can be explained as follows. In the absence of KCl, the coil-helix transition needs to be induced by  $\text{CaCl}_2$ , which does not occur at 5°C below 5mM  $\text{CaCl}_2$ . The modulus of  $\text{Ca}^{2+}$ -induced gels decreases with increasing  $\text{CaCl}_2$  concentration. When KCl is added, the transition is induced by  $\text{K}^+$  leading to a different type of gel that is more homogeneous than  $\text{Ca}^{2+}$ -induced gels. The  $\text{K}^+$ -induced gels were stronger than the  $\text{Ca}^{2+}$ -induced gels even at very low KCl concentrations except at 5.3mM  $\text{CaCl}_2$ , which explains why in this case  $G'$  dropped when KCl was added even though gelation was faster.  $G'$  subsequently increased as more KCl was added, because the  $\text{K}^+$ -induced gel became stiffer.

### 3.2.3. Influence of $\text{Na}^+$ on the $\text{K}^+$ -induced gelation of $\kappa$ -car

The strong influence of  $\text{CaCl}_2$  on  $\text{K}^+$ -induced gelation of  $\kappa$ -car is caused by effective screening of the electrostatic interactions between the helices. The effect of adding a monovalent cation was studied by adding up to 200mM NaCl to  $\kappa$ -car solution at  $C_k = 2\text{g/L}$  containing 10mM KCl. As was found for  $\text{CaCl}_2$ , the gelation rate and the elastic modulus increased with increasing NaCl concentration (figure 3.15).

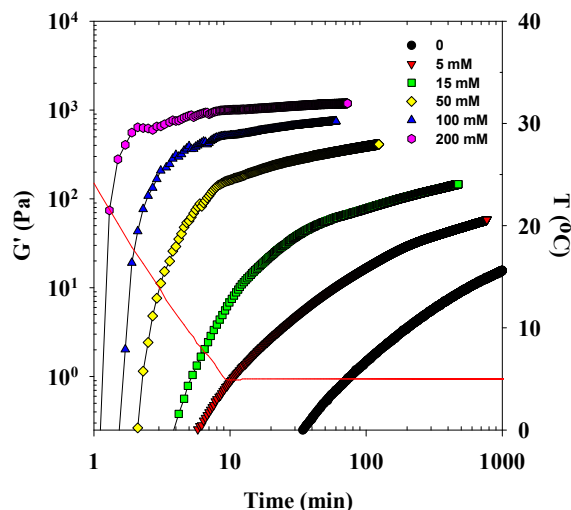


**Figure 3.15.** Evolution of the storage shear modulus at 0.1Hz of 2g/L  $\kappa$ -car with 10mM KCl at different NaCl concentrations during and after rapid cooling to 5°C. The solid line indicates the temperature of the sample.

In the absence of KCl weak turbid gels were formed only for  $[\text{NaCl}] \geq 100\text{mM}$ . Similar results were also reported by Mangione et al. (2005) who showed that the modulus of 4g/L  $\kappa$ -car at 20mM KCl was much higher after addition of 100mM NaCl.

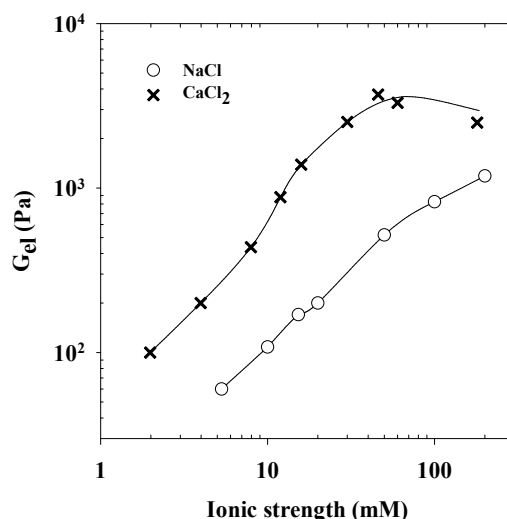


**Figure 3.16.** Elastic modulus of 2g/L  $\kappa$ -car with 10mM KCl at 5°C as a function of the ionic strength of added  $\text{CaCl}_2$  (crosses) or added NaCl (circles). The solid lines are guides to the eye.

The dependence of the elastic modulus on the ionic strength of the added NaCl or CaCl<sub>2</sub> ( $I = [\text{NaCl}]$  and  $I = 3 \cdot [\text{CaCl}_2]$ ) is compared in figure 3.16. If the effect of adding CaCl<sub>2</sub> or NaCl is simply screening of the electrostatic interaction, it should be the same at the same ionic strength. However, quantitative comparison of the elastic modulus at the same ionic strength shows that the influence of CaCl<sub>2</sub> was much stronger, which suggest that Ca<sup>2+</sup> binds specifically to  $\kappa$ -car. Indeed, measurement of the Ca<sup>2+</sup> activity showed a significant reduction in the presence of  $\kappa$ -car (figure 3.17).

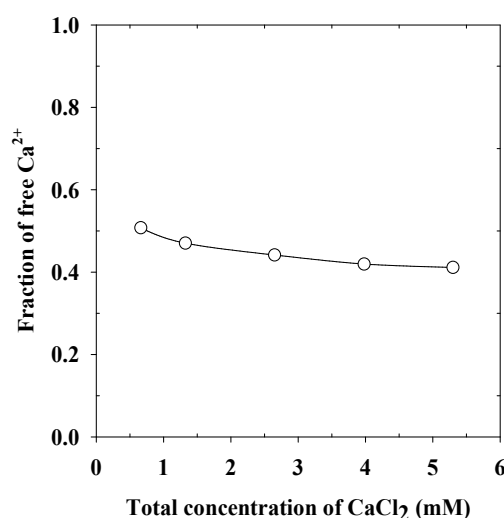


**Figure 3.17.** Fraction of free calcium ion concentration as a function of the total calcium ion concentration in 2g/L  $\kappa$ -car.

The turbidity of 2g/L  $\kappa$ -car solutions and gels at 5°C in the absence of KCl is shown as a function of the total ionic strength of (NaCl/CaCl<sub>2</sub>) or (NaCl/CaCl<sub>2</sub> and 10mM KCl) in figure 3.18a. The ionic strength of the added NaCl or CaCl<sub>2</sub> ( $I = [\text{NaCl}]$  and  $I = 3 \cdot [\text{CaCl}_2]$ ) or NaCl/CaCl<sub>2</sub> with 10mM KCl ( $I = [\text{NaCl}] + 10$  and  $I = 3 \cdot [\text{CaCl}_2] + 10$ ). The systems were transparent when they were in the liquid state ( $[\text{NaCl}] < 100\text{mM}$ ,  $[\text{CaCl}_2] < 5\text{mM}$ ) or weak gels, but the gels became increasingly turbid when more salt was added. We note that the gels formed in pure KCl remained transparent up to at least 50mM. When NaCl or CaCl<sub>2</sub> was added the turbidity of K<sup>+</sup>-induced gels remained much lower than in the absence of KCl (figure 3.18a), but a small increase of the turbidity with increasing NaCl or CaCl<sub>2</sub> was seen here as well. It is clear that the structure of K<sup>+</sup>-induced gels is different from that induced by Ca<sup>2+</sup> and Na<sup>+</sup>. The latter are more heterogeneous probably because they form thicker strands of parallel packed helices.

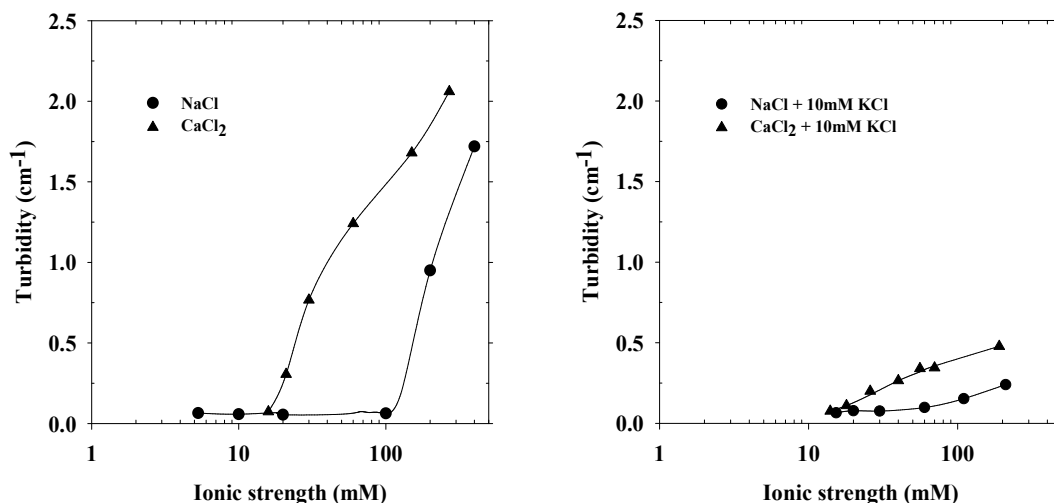


**Figure 3.18.** (a) Turbidity of 2g/L  $\kappa$ -car as a function of the total ionic strength at 5°C in the presence of NaCl (circles) or CaCl<sub>2</sub> (triangles).

(b) Turbidity of 2g/L  $\kappa$ -car containing 10mM KCl as a function of the total ionic strength at 5°C in the presence of NaCl (circles) or CaCl<sub>2</sub> (triangles).

### 3.3. Conclusions

$\kappa$ -car gels are formed below the coil-helix transition temperature in the presence of KCl or CaCl<sub>2</sub>, but with different structures. The gel stiffness increases with increasing KCl concentration and the gels remain transparent, while the gel stiffness decreases with increasing CaCl<sub>2</sub> concentration and they become increasingly turbid.

Addition of NaCl reduces the electrostatic repulsion between the helices which facilitates their association for K<sup>+</sup> induced gelation. As a consequence the gel stiffness and the gelation rate increase with increasing NaCl concentration. A similar effect on K<sup>+</sup> induced  $\kappa$ -car gelation was observed when CaCl<sub>2</sub> was added. However, the effect was much stronger than for NaCl at the same ionic strength indicating specific binding of Ca<sup>2+</sup> to  $\kappa$ -car.

The presence of a small amount of KCl strongly modified the Ca<sup>2+</sup> induced gelation of  $\kappa$ -car. Especially at higher CaCl<sub>2</sub> concentrations, it led to a strong increase of the elastic modulus and a reduction of the turbidity. The synergy between Ca<sup>2+</sup> and K<sup>+</sup> was most striking when the gels were weak in the pure salts.



## References

- Doyle, J., Giannouli, P., Philp, K., & Morris, E. R. (2002). Effect of  $K^+$  and  $Ca^{2+}$  cations on gelation of  $\kappa$ -carrageenan. *Gums and Stabilisers for the Food Industry*, 11, 158-164.
- Harrington, J. C., Foegeding, E. A., Mulvihill, D. M., & Morris, E. R. (2009). Segregative interactions and competitive binding of  $Ca^{2+}$  in gelling mixtures of whey protein isolate with  $Na^+$   $\kappa$ -carrageenan. *Food Hydrocolloids*, 23(2), 468-489.
- Hermansson, A. M., Eriksson, E., & Jordansson, E. (1991). Effects of Potassium, Sodium and Calcium on the Microstructure and Rheological Behaviour of Kappa-Carrageenan Gels. *Carbohydrate Polymers*, 16(3), 297-320.
- Kara, S., Tamerler, C., Bermek, H., & Pekcan, Ö. (2003). Cation effects on sol-gel and gel-sol phase transitions of  $\kappa$ -carrageenan-water system. *International Journal of Biological Macromolecules*, 31(4-5), 177-185.
- MacArtain, P., Jacquier, J. C., & Dawson, K. A. (2003). Physical characteristics of calcium induced  $\kappa$ -carrageenan networks. *Carbohydrate Polymers*, 53(4), 395-400.
- Mangione, M. R., Giacomazza, D., Bulone, D., Martorana, V., Cavallaro, G., & San Biagio, P. L. (2005).  $K^+$  and  $Na^+$  effects on the gelation properties of  $\kappa$ -Carrageenan. *Biophysical Chemistry*, 113(2), 129-135.
- McKinnon, A. A., Rees, D. A., & Williamson, F. B. (1969). Coil to double helix transition for a polysaccharide. *J. Chem. Soc. D*, 13, 701-702.
- Meunier, V., Nicolai, T., Durand, D., & Parker, A. (1999). Light Scattering and Viscoelasticity of Aggregating and Gelling  $\kappa$ -Carrageenan. *Macromolecules*, 32, 2610-2616.
- Michel, A. S., Mestdagh, M. M., & Axelos, M. A. V. (1997). Physico-chemical properties of carrageenan gels in the presence of various cations. *International Journal of Biological Macromolecules*, 21, 195-200.
- Nguyen, T. B., Phan-Xuan, T., Benyahia, L., & Nicolai, T. (2014). Combined effects of temperature and elasticity on phase separation in mixtures of  $\kappa$ -carrageenan and  $\beta$ -lactoglobulin aggregates. *Food Hydrocolloids*, 34, 138-144.
- Nono, M., Nicolai, T., & Durand, D. (2011). Gel formation of mixtures of  $\kappa$ -carrageenan and sodium caseinate. *Food Hydrocolloids*, 25(4), 750-757.

- Núñez-Santiago, M. C., & Tecante, A. (2007). Rheological and calorimetric study of the sol–gel transition of  $\kappa$ -carrageenan. *Carbohydrate Polymers*, 69(4), 763–773.
- Rees, D. A., Steele, I. W., & Williamson, F. B. (1969). Conformational analysis of polysaccharides. III. The relation between stereochemistry and properties of some natural polysaccharide sulfates (1). *Journal of Polymer Science Part C: Polymer Symposia*, 28(1), 261–276.
- Rochas, C., & Rinaudo, M. (1980). Activity coefficients of counterions and conformation in kappa-carrageenan systems. *Biopolymers*, 19(9), 1675–1687.
- Thrimawithana, T. R., Young, S., Dunstan, D. E., & Alany, R. G. (2010). Texture and rheological characterization of kappa and iota carrageenan in the presence of counter ions. *Carbohydrate Polymers*, 82(1), 69–77.

## Chapter 4:

# MIXTURES OF $\beta$ -LACTOGLOBULIN AND $\kappa$ -CARRAGEENAN

### 4.1. Introduction

Food products often contain aqueous mixtures of proteins and polysaccharides and understanding the behavior such mixtures is important for the use of existing food products or the development of new ones. Complex coacervation, phase separation and gelation can give rise to a wide range of phenomena that are, as yet, far from being fully understood (Tolstoguzov, 2003; Turgeon et al., 2003; Turgeon et al., 2007).

As mentioned in the introduction of chapter 1, when  $\beta$ -lg is heated in aqueous solution it denatures leading to irreversible aggregation and at high concentrations to gelation (Clark, 1999; Foegeding, 2006; Nicolai, 2007). The structure and size of the aggregates depend on the protein concentration, the pH, the type and concentration of added salt (Nicolai et al., 2011). When  $\beta$ -lg is heated at a pH above its isoelectric point ( $pI = 5.2$ ) in the presence of anionic polysaccharides, usually heterogeneous gels with a variety of different structures are formed (Ako et al., 2011; Cakir & Foegeding, 2011; de Jong et al., 2009).  $\kappa$ -car is an anionic polysaccharide isolated from algae and is used as thickening or gelling agent in food products (Piculell, 2006). In aqueous solution it has a random coil conformation at high temperatures, but in the presence of salt it takes a helical conformation below a critical temperature ( $T_c$ ) that depends on the type and concentration of the cations.  $\kappa$ -car helices have a tendency to aggregate which can lead to the formation of a percolating network. Gelation of  $\kappa$ -car can be reversed by heating above another critical temperature that is generally higher than the gelling temperature ( $T_g$ ). The effect of adding single or mixed salt on  $\kappa$ -car gelation was discussed in the chapter 3 and is important for the understanding of the gelation of  $\kappa$ -car in the presence of  $\beta$ -lg that will be discussed in this chapter.

Here we report on an investigation of aqueous mixtures of the protein  $\beta$ -lg and  $\kappa$ -car at pH 7, where both biopolymers are negatively charged and do not associate. At this pH native  $\beta$ -lg is compatible with  $\kappa$ -car up to high concentrations of both components. However, as was discussed in chapter 1 microphase separation has been observed to occur in mixtures of  $\kappa$ -car and  $\beta$ -lg aggregates. The objective of the investigation was to elucidate the effect of  $Ca^{2+}$

ions on the structure and the rheological properties presence of the mixtures, which important as  $\text{Ca}^{2+}$  ions are present in most food application containing  $\kappa$ -car and milk proteins.

Mixtures of native  $\beta$ -lg and  $\kappa$ -car are considered in section 4.2. In section 4.3 we look at mixtures of  $\kappa$ -car and  $\beta$ -lg strands that are formed by heating native  $\beta$ -lg in pure water. The effect of the size and morphology of  $\beta$ -lg aggregates formed in the presence of different amounts of  $\text{CaCl}_2$  on the structure and rheology of the mixtures will be investigated in section 4.4. Finally, we will compare the properties of these systems with those of heated mixtures of native  $\beta$ -lg and  $\kappa$ -car in section 4.5. The results are published in the form of 3 articles (Food Hydrocolloids-34, 2014; Condensed Matter (in press); Colloids and Surfaces A, submitted) to which we refer for further details, see papers 2, 3 and 4.

## 4.2. Mixtures of $\kappa$ -carrageenan with native $\beta$ -lactoglobulin

We studied the effect of adding native  $\beta$ -lg up to  $C_b = 60\text{g/L}$  on gelation of  $\kappa$ -car at  $C_k = 2\text{g/L}$  in the presence of  $10\text{mM}$  KCl. All mixtures were transparent and showed no sign of phase separation. The storage shear modulus of the solutions was measured during and after rapidly cooling to  $5^\circ\text{C}$  for  $100\text{min}$ , see figure 4.1. Remarkably, adding  $\beta$ -lg led to a significant increase of  $G'$  already before  $\kappa$ -car gelled even at very low protein concentrations. A similar modulus was also observed in pure  $\beta$ -lg solutions ( $5\text{g/L}$ ), see figure 4.1a. Most likely this effect is an artifact due to the adsorption of protein at the water-oil interface.

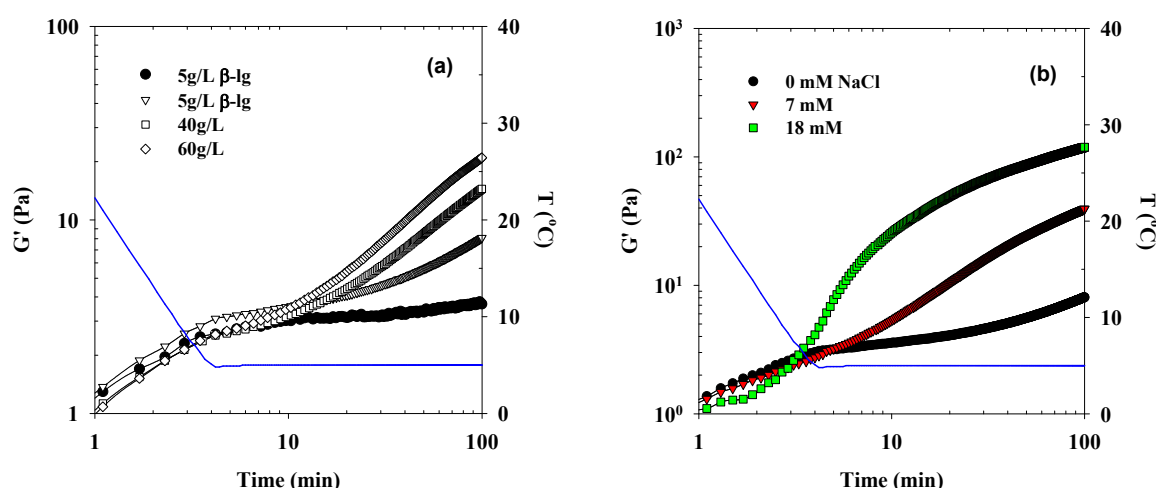


**Figure 4.1.** Evolution of  $G'$  at  $0.1\text{Hz}$  during and after rapid cooling from  $50^\circ\text{C}$  to  $5^\circ\text{C}$  for pure  $\beta$ -lg (closed symbols) or mixtures with  $2\text{g/L}$   $\kappa$ -car at  $10\text{mM}$  KCl (open symbols), containing different concentrations of native  $\beta$ -lg (a). In figure (b) we show the effect of

adding NaCl to mixtures containing 5g/L  $\beta$ -lg and 2 g/L  $\kappa$ -car at 10mM KCl. The solid lines indicate the temperature as a function of time.

In the absence of  $\beta$ -lg,  $\kappa$ -car gelation was very slow, but the rate increased with increasing native  $\beta$ -lg concentration. The elastic modulus obtained after 100 min at 5°C increased weakly with increasing protein concentration between 5 and 60g/L, see figure 4.1a. The effect may be explained by the presence of sodium counterions that are added together with  $\beta$ -lg in the mixtures. Indeed if a small amount of NaCl (7mM) was added to the mixture containing 5g/L  $\beta$ -lg a similar acceleration of  $\kappa$ -car gelation was found, see figure 4.1b.

It was shown in chapter 3 that addition of  $\text{CaCl}_2$  increases the elastic modulus of  $\text{K}^+$ -induced  $\kappa$ -car gels. The effect of adding  $\text{CaCl}_2$  on the elastic modulus of  $\kappa$ -car gels at  $C = 2\text{g/L}$  in the presence of 40g/L native  $\beta$ -lg is shown in figure 4.2. It is clear that the presence of native  $\beta$ -lg strongly reduces the stiffening by  $\text{Ca}^{2+}$ . The reason is that  $\beta$ -lg competes with  $\kappa$ -car for  $\text{Ca}^{2+}$  as was already noted by Harrington et al. (2009) for calcium induced gelation of  $\kappa$ -car in the presence of native WPI.

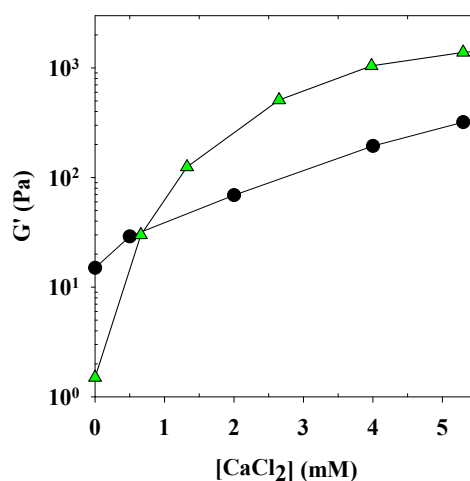


**Figure 4.2.** Elastic shear modulus of  $\kappa$ -car gels at 2 g/L after 100 min at 5°C in the presence of 10mM KCl as a function of the concentration of  $\text{Ca}^{2+}$ . The results for pure  $\kappa$ -car (triangles) are compared with mixtures containing 40 g/L native  $\beta$ -lg (circles).

The effect can clearly be seen when an increasing amount of native  $\beta$ -lg is added to  $\kappa$ -car solution with a given  $\text{CaCl}_2$  concentration. Figure 4.3a shows the evolution of  $G'$  during and after rapid cooling to 5°C for 2g/L  $\kappa$ -car with 2.65mM  $\text{CaCl}_2$  and 10mM KCl in the

presence of different concentrations of native  $\beta$ -lg. With increasing concentration of native protein elastic modulus of the  $\kappa$ -car gel decreased (figure 4.3b), because the fraction of  $\text{Ca}^{2+}$  bound by the proteins increased (figure 4.3c).

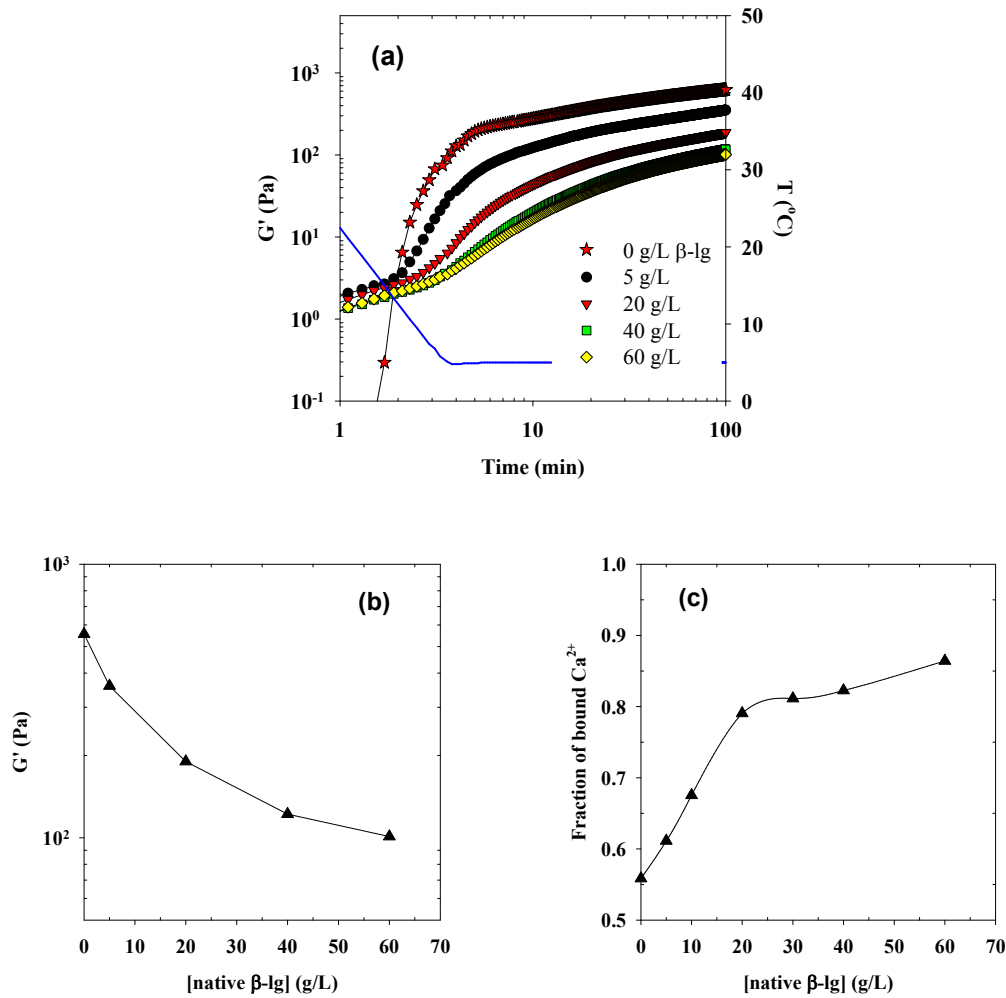


**Figure 4.3.** (a) Evolution of  $G'$  at 0.1Hz during and after rapid cooling from 50°C to 5°C for mixtures of 2 g/L  $\kappa$ -car at 10 mM KCl and 2.65 mM  $\text{CaCl}_2$ , containing different concentrations of native  $\beta$ -lg. The solid line indicates the temperature as a function of time. (b) Dependence of the elastic shear modulus of  $\kappa$ -car gels after 100 min at 5°C on the concentration of native  $\beta$ -lg. The systems contained 2 g/L  $\kappa$ -car, 10 mM KCl and 2.65 mM  $\text{CaCl}_2$ . (c) Fraction of bound  $\text{Ca}^{2+}$  ions in the mixtures for which the elastic shear modulus is shown in figure a.

This competition for  $\text{Ca}^{2+}$  was also observed in the absence of KCl when gelation was induced by  $\text{Ca}^{2+}$ . Pure  $\kappa$ -car solutions formed a gel within 3 days in the fridge ( $4^\circ\text{C}$ ) for  $[\text{CaCl}_2] > 5\text{mM}$  as was discussed in (chapter 3). However, in the presence of 40g/L native protein no gels were formed even at  $[\text{CaCl}_2] = 10\text{mM}$ , the gels were only observed at 12-17mM  $\text{CaCl}_2$  but they became weaker with increasing concentration of  $\text{CaCl}_2$  (figure 4.4a).

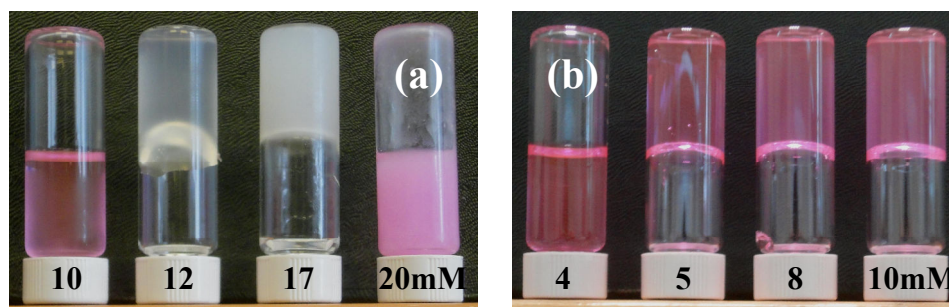


**Figure 4.4.** Mixtures of 2g/L  $\kappa$ -car in the presence (a) and absence (b) of 40g/L native  $\beta$ -lg at different concentrations of  $\text{CaCl}_2$  after keeping in the fridge for 3 days.

Besides, in the presence of  $\text{Ca}^{2+}$  up to 10mM the mixtures containing 40g/L  $\kappa$ -car that was transparent became turbid and more heterogeneous with increasing concentration of  $\text{CaCl}_2$ , see figure 4.4a. Aggregation of  $\kappa$ -car or protein was induced by high  $[\text{CaCl}_2]$  that caused micro phase separation and precipitation of mixtures, micro structures of mixtures were observed with CLSM (results not shown).

## Conclusion

Native  $\beta$ -lg is compatible with  $\kappa$ -car and mixtures with 2g/L  $\kappa$ -car remain transparent at least up to  $C_b = 100\text{g/L}$ . In mixtures containing  $\text{CaCl}_2$ ,  $\beta$ -lg competes with  $\kappa$ -car for  $\text{Ca}^{2+}$  leading to a decrease of the effect of stiffening  $\kappa$ -car gels induced by  $\text{Ca}^{2+}$ .

### 4.3. Mixtures of $\kappa$ -carrageenan with $\beta$ -lactoglobulin strands

#### 4.3.1. Mixtures with $\kappa$ -car coils

$\beta$ -lg strands were prepared by heating 50g/L native  $\beta$ -lg in pure water at pH = 7 overnight at 85°C. Using light scattering we found that the strands had a z-average hydrodynamic radius  $R_h = 17\text{nm}$  and a weight average molar mass  $M_w = 1.5 \times 10^6 \text{ g/mol}$ . In mixtures with  $\kappa$ -car coils, micro phase separation occurred above a critical concentration of  $\kappa$ -car, see figure 4.5. Dense protein domains with a radius of a few microns were observed with CLSM at  $C_k > 8\text{g/L}$   $\kappa$ -car for  $C_b \leq 15\text{g/L}$ , but at higher protein concentrations the critical  $\kappa$ -car concentration decreased with increasing  $C_b$ .

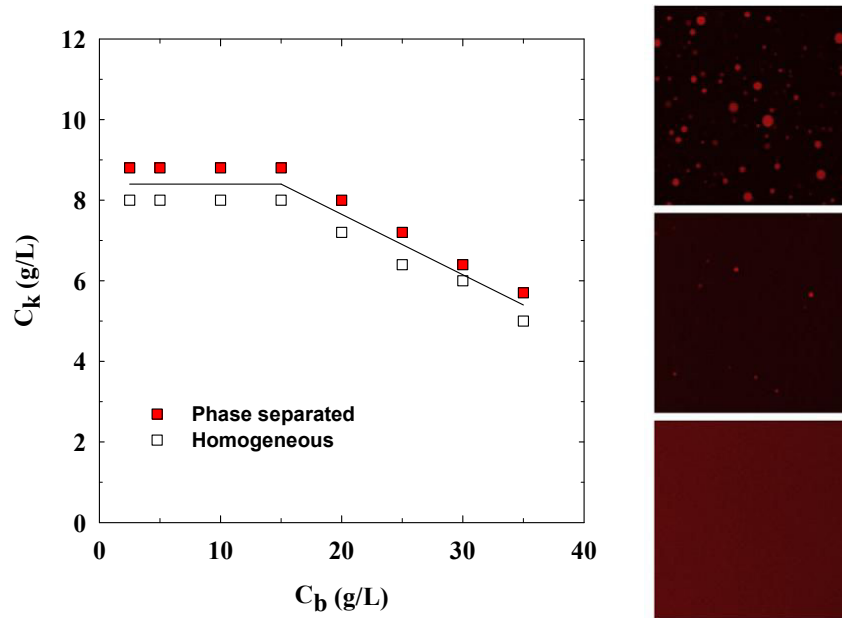


**Figure 4.5.** Phase diagram of mixtures of  $\beta$ -lg strands ( $R_h = 17\text{nm}$ ) and  $\kappa$ -car coils. The open and closed symbols correspond to homogeneous and micro phase separated mixtures, respectively. The solid line indicates the phase boundary. CLSM images representing  $150 \times 150 \mu\text{m}$  are shown for mixtures containing 20 g/L  $\beta$ -lg and different  $\kappa$ -car concentrations: 10, 8 and 7.5 g/L, top to bottom.

The distributions of the proteins in the mixtures was observed with CLSM, at different concentrations of strands (10, 20 and 30 g/L) and  $\kappa$ -car coils (2-12g/L). Mixtures were homogeneous at 2g/L  $\kappa$ -car, but at higher  $\kappa$ -car concentration spherical dense protein micro domains were formed (figure 4.6).



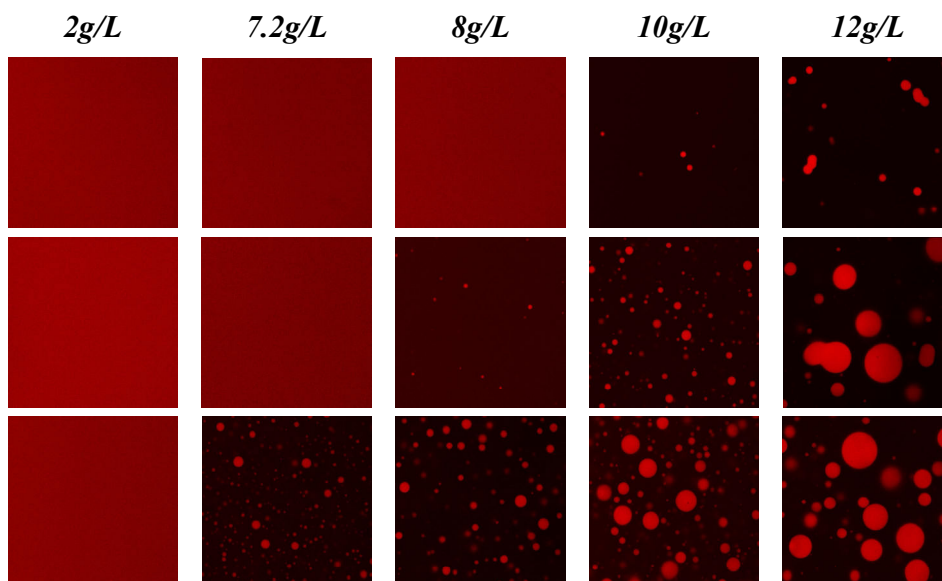


**Figure 4.6.** CLSM images (160x160 $\mu$ m) of mixtures containing 10 (top), 20 (middle) and 30g/L  $\beta$ -lg strands at different concentrations of  $\kappa$ -car. The  $\beta$ -lg strands were labeled (red).

The turbidity is a useful qualitative measure of the extent of phase separation for the mixtures. Figure 4.7a shows the evolution of turbidity for a mixture containing 20g/L  $\beta$ -lg strands and 8g/L  $\kappa$ -car during stepwise cooling from 80°C to 20°C and subsequently heating back to 80°C. The turbidity increased for  $T < 35^\circ\text{C}$ , due to micro phase separation. Results obtained at other concentrations of  $\kappa$ -car are shown in figure 4.7b. For  $C_k \leq 7\text{g/L}$  no phase separation was observed even at the lowest temperature tested (10°C), while at  $C_k > 8\text{g/L}$ , phase separation occurred already at the highest temperature tested (50°C).

If phase separation is caused by thermodynamic incompatibility of polymers of different chemistry, an increase of the compatibility with increasing temperature is expected, because the contribution of the mixing entropy to the free energy increases. Another potential driving force for phase separation is depletion of  $\kappa$ -car chains from between the protein aggregates (Gaaloul et al., 2010; Tuinier et al., 2003). However, the depletion interaction is itself an entropic effect and therefore no effect of the temperature is expected. Therefore we may conclude that depletion was not the main driving force of phase separation in these mixtures.

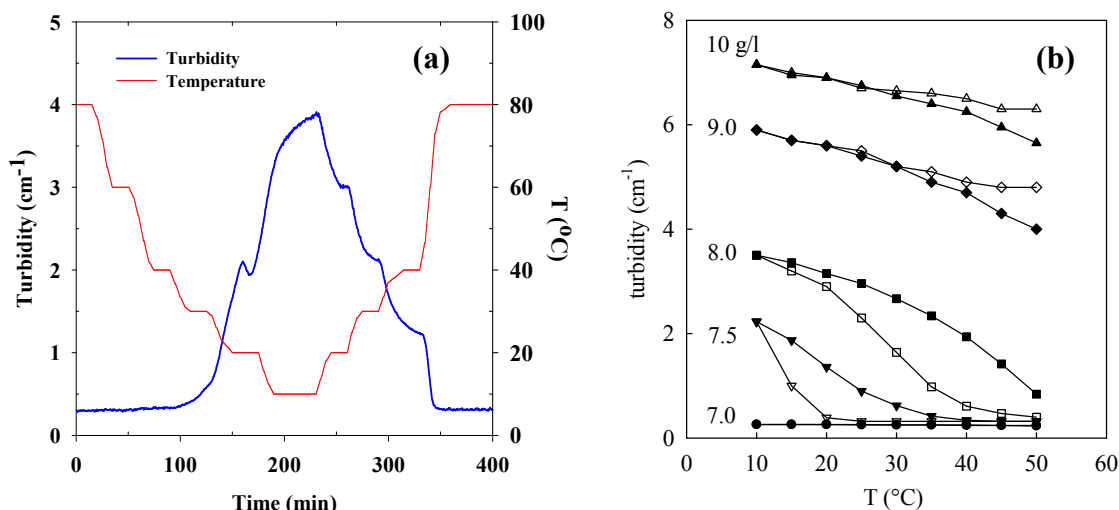


**Figure 4.7.** (a) Evolution of turbidity for 20g/L strands and 8g/L  $\kappa$ -car on cooling and heating. (b) Temperature dependence of the turbidity of aqueous mixtures of 20 g/L  $\beta$ -lg strands and different  $\kappa$ -car concentrations indicated in the figure after cooling (open symbols) and subsequent heating (closed symbols) in steps of 5 °C.

### 4.3.2. Effect of $\kappa$ -carrageenan gelation on phase separation

The effect of  $\kappa$ -car gelation on phase separation was studied by cooling mixtures in the presence of KCl. Figure 4.8a, shows the turbidity of a mixture containing 20g/L  $\beta$ -lg strands and 8g/L  $\kappa$ -car during stepwise cooling. The turbidity increased with decreasing temperature until 20°C as was observed in the absence of KCl, but then it fell sharply when  $\kappa$ -car formed a gel. During subsequent heating the turbidity increased first sharply when the  $\kappa$ -car gel melted and then decreased when the temperature was further increased similarly to what was observed in the absence of KCl. It appears that micro phase separation can be reverted, at least partially, by gelation of  $\kappa$ -car. Figure 4.8b shows the turbidities related to storage moduli ( $G'$ ) of mixtures containing 20g/L aggregates, 10g/L  $\kappa$ -car and different concentrations of KCl (10 and 20mM). The dependence of the turbidity, i.e. the extent of phase separation, correlates well with the elastic modulus of the  $\kappa$ -car gels.

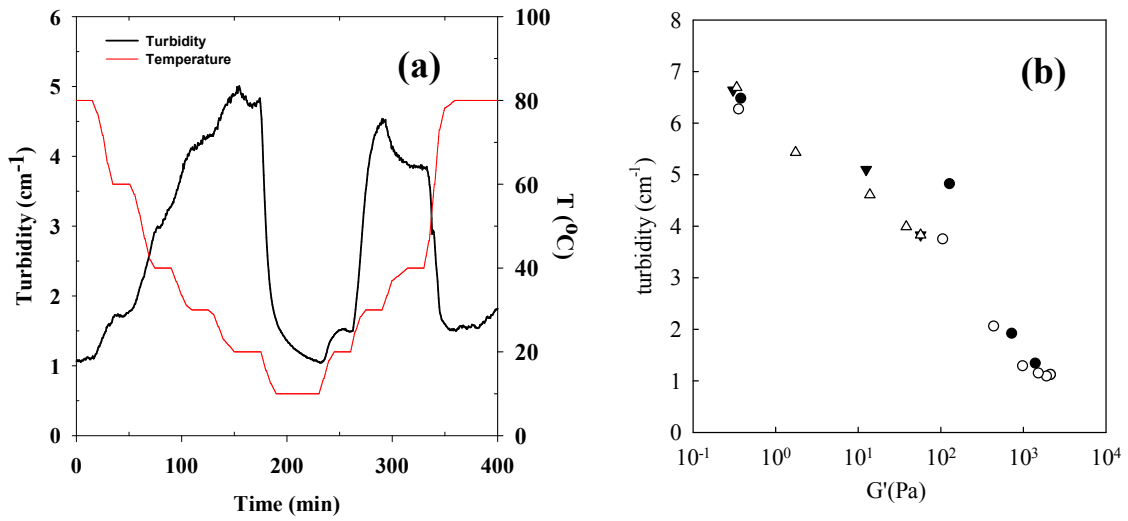


**Figure 4.8.** (a) Evolution of turbidity for 20g/L strands and 8g/L  $\kappa$ -car at 20mM KCl on cooling and heating. (b) Correlation between the turbidity and the elastic modulus of  $\kappa$ -car gels in mixtures of 20g/L  $\beta$ -lg strands and 10g/L  $\kappa$ -car obtained during cooling (open symbols) and heating (closed symbols) at either 10mM (circles) or 20mM KCl (triangles).

The effect of gelation on phase separation was less important at higher  $\kappa$ -car concentrations even though the gels were stiffer. The reason is that the incompatibility increased and this effect dominated the effect of increased elasticity. The effect of  $\kappa$ -car gelation on phase separation is significant only close to the phase boundary.

#### 4.3.3. Conclusion

Segregative phase separation between  $\beta$ -lg aggregates and  $\kappa$ -car led to the formation of spherical protein rich domains with a diameter of a few microns. Microphase separation is favored by a reduction of the temperature close to the binodal implying that depletion is not the main driving force for phase separation.

Gelation of the  $\kappa$ -car can reverse phase separation close to the phase boundary. The extent of reversibility is directly correlated to the elastic shear modulus of the polysaccharide gel. Close to the binodal, transient phase separation occurs during cooling and heating caused by the combined effects of temperature and elasticity on the phase separation.

## 4.4. Mixtures of $\kappa$ -carrageenan with $\beta$ -lactoglobulin microgels

### 4.4.1. Mixtures of $\beta$ -lg microgels with $\kappa$ -car coils

#### 4.4.1.1. Effect of the concentration of $\kappa$ -car and $\beta$ -lg microgels

In first instance, we investigated mixtures of  $\kappa$ -car (0.5-8g/L) and  $\beta$ -lg microgels with  $R_h = 240\text{nm}$  (2-40g/L) in pure water. The  $\beta$ -lg microgels were prepared by heating 40g/L native  $\beta$ -lg in the presence of 5.3mM  $\text{CaCl}_2$  overnight at  $85^\circ\text{C}$ . Micro phase separation was observed with CLSM at all protein concentrations for  $C_k \geq 1\text{g/L}$ , see figure 4.9. The amount of protein dense domains increased with increasing protein and polysaccharide concentration. The protein rich domains associated into large flocks that slowly precipitated, see figure 4.14.

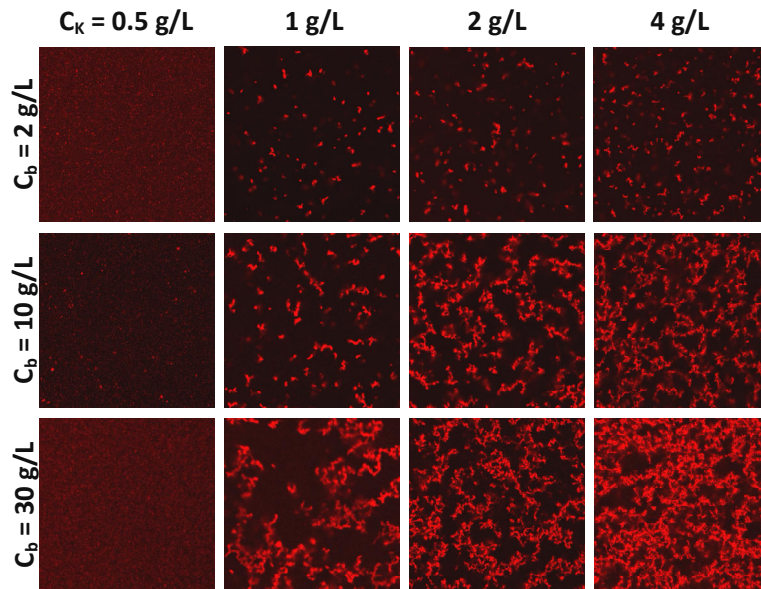


**Figure 4.9.** CLSM images ( $160 \times 160 \mu\text{m}$ ) of mixtures containing 2 (top), 10 (middle) and 30g/L (bottom)  $\beta$ -lg microgels with  $R_h = 240\text{nm}$  at different concentrations of  $\kappa$ -car

#### 4.4.1.2. Effect of the size and morphology of the $\beta$ -lg aggregates

$\beta$ -lg aggregates with different size and morphology were prepared by heating native protein overnight at  $85^\circ\text{C}$  with different amounts of  $\text{CaCl}_2$ . Figure 4.10 shows the hydrodynamic radius of the aggregates formed at  $C_b = 20\text{g/L}$  (a) and  $C_b = 40\text{g/L}$  (b) as a function of  $\text{CaCl}_2$  concentration. The average radius increases sharply above a certain  $\text{CaCl}_2$  concentration, because the morphology of the aggregates changes from strands to microgels. More  $\text{CaCl}_2$  is needed to induce the transition when the protein concentration is higher, but the results superimpose when they are plotted as function of the molar ratio of  $\text{CaCl}_2$  to  $\beta$ -lg

( $R = [\text{CaCl}_2]/[\beta\text{-lg}]$ ) showing that the transition occurs between 1 and 2 calcium ions are added per protein (figure 4.10a,b).

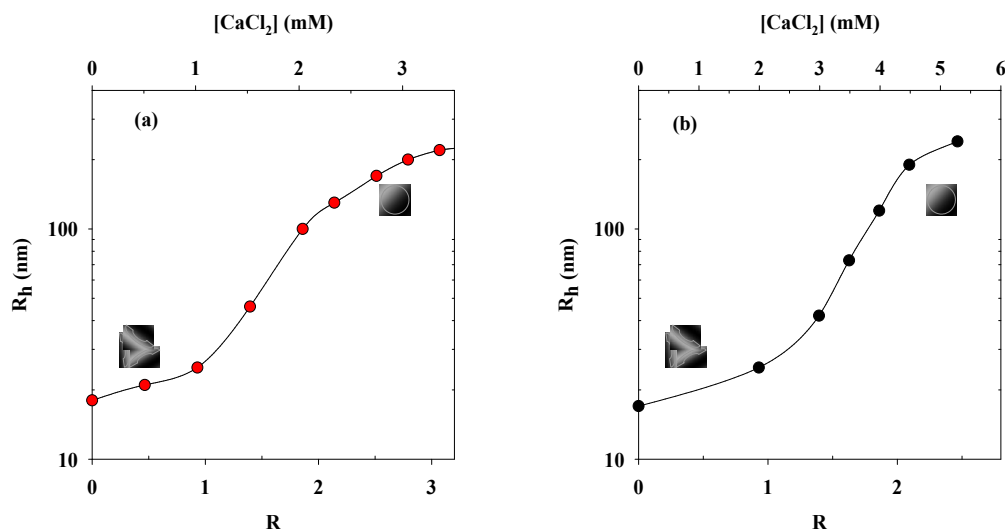


**Figure 4.10.** Hydrodynamic radii of  $\beta\text{-lg}$  aggregates of 20 (a) and 40g/L (b) formed as a function of  $\text{Ca}^{2+}$  to protein ratio.

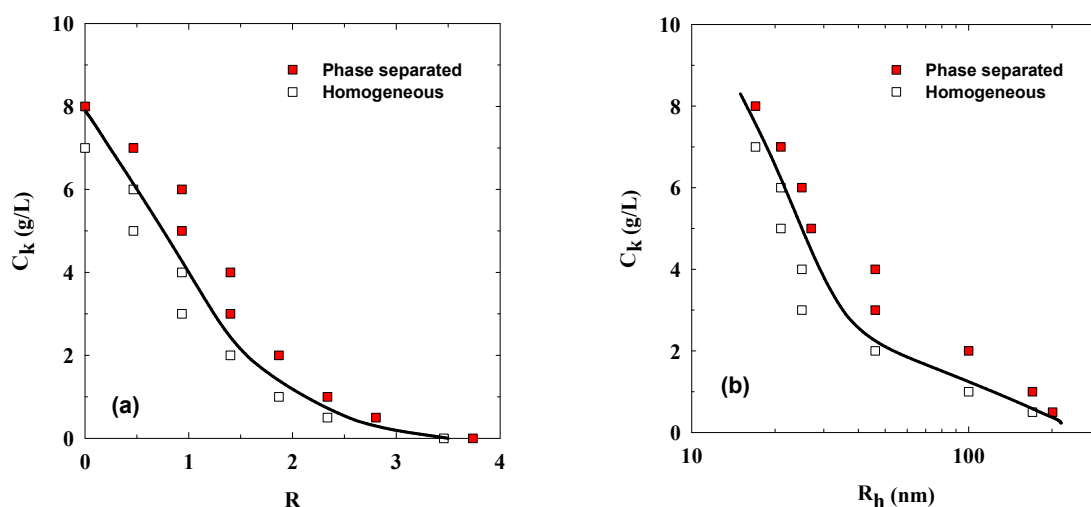


**Figure 4.11.** Critical  $\kappa$ -car concentration as a function of the molar ratio of  $\text{CaCl}_2$  to proteins (a) and of the  $\beta\text{-lg}$  aggregate size (b) in mixtures with 20g/L  $\beta\text{-lg}$  microgels induced by  $\text{CaCl}_2$ . The open and closed symbols correspond to homogeneous and phase separated mixtures, respectively. The solid line indicates the phase boundary.

Mixtures containing different concentrations of  $\kappa$ -car and 20g/L  $\beta\text{-lg}$  aggregates prepared at different  $\text{CaCl}_2$  concentrations were investigated with CLSM. The critical  $\kappa$ -car concentration at which micro phase separation occurred, decreased with increasing  $R$  (figure

4.11a) and the corresponding aggregate size (figure 4.11b). At lower  $\kappa$ -car concentrations mixtures with  $\beta$ -lg strands are homogeneous, while mixtures with  $\beta$ -lg microgels phase separate.

The extent of phase separation was determined after the dense domains had precipitated by measuring the concentration of residual  $\beta$ -lg in the supernatant, see figure 4.12a. It was verified that no dense domains remained in the supernatant. As might be expected the fraction of protein in the supernatant decreased with increasing  $R$ . It was only weakly dependent on the  $\kappa$ -car concentration in the range 2-5g/L, because in this range most microgels phase separated and most strands remained compatible. In fact, the fraction of phase separated protein corresponds approximately to the fraction of microgels. At  $C_k = 1$ g/L smaller microgels remained compatible, so that more  $\text{CaCl}_2$  was needed to induce phase separation. At  $C_k = 0.5$ g/L even the larger microgels remained compatible. The size of the aggregates in the supernatant as determined with dynamic light scattering was close to that in the pure aggregate solutions (figure 4.12b).

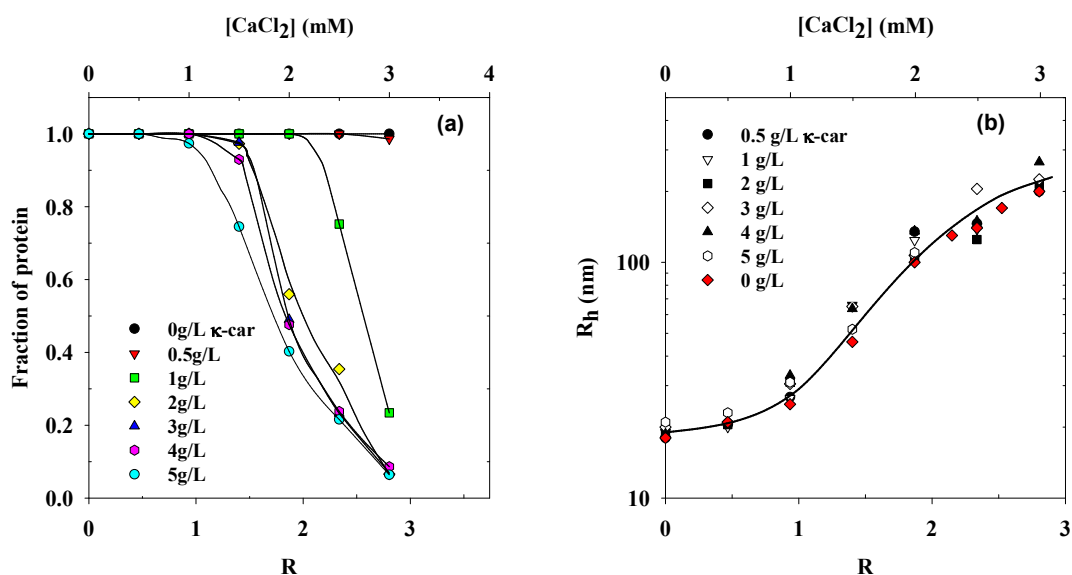


**Figure 4.12.** Fraction (a) and hydrodynamic radius (b) of  $\beta$ -lg aggregates in the supernatant of mixtures containing 20g/L  $\beta$ -lg aggregates and different concentrations of  $\kappa$ -car and  $\text{CaCl}_2$ .

#### 4.4.2. Effect of $\kappa$ -carrageenan gelation on the structure

Figure 4.13 shows CLSM images of mixtures of  $\kappa$ -car and 10 g/L  $\beta$ -lg microgels with  $R_h = 240$ nm in pure water, with 10mM KCl and with 20mM KCl at 20°C. In the presence of

KCl, micro phase separation was observed even at 0.5g/L  $\kappa$ -car. Similar behavior was observed at other microgel concentrations.

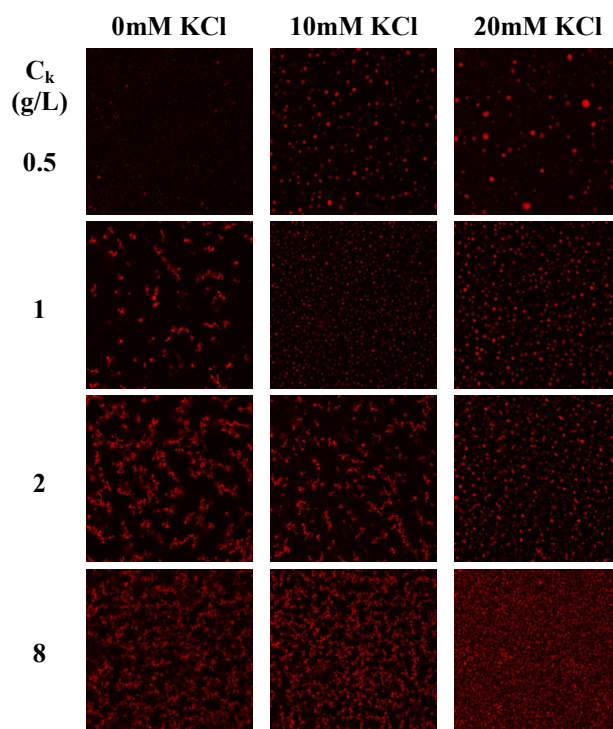


**Figure 4.13.** CLSM images (160x160 $\mu$ m) of mixtures containing 10g/L microgels ( $R_h=240$ nm) at different concentrations of KCl and  $\kappa$ -car.

In the absence of KCl the protein rich domains flocculated and precipitated (figure 4.14). The amount of precipitate increased with increasing  $\kappa$ -car concentration as more proteins entered the dense domains until for  $C_k=8$ g/L it occupied the whole volume. In the presence of 20mM KCl gels were formed quickly at 20°C which trapped the protein domains.

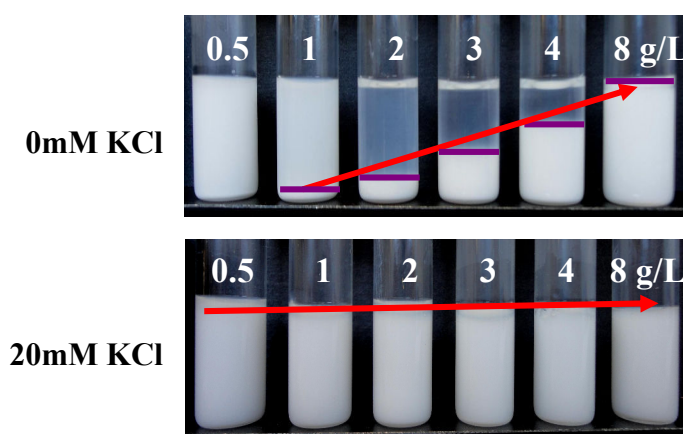


**Figure 4.14.** Mixtures of 10g/L microgels ( $R_h = 240$ nm) in the absence and presence of 20mM KCl at different  $\kappa$ -car concentrations. The samples were photographed after 3 days.



Gelation of  $\kappa$ -car inhibited clustering of the protein domains. This effect was stronger at 20mM KCl than at 10mM KCl, because gelation at 20°C was slow in the latter case. However, when mixtures containing 20mM KCl were heated to 50°C for 15 min in order to melt the gel, the protein domains flocculated in a manner similar to mixtures in the absence of KCl (figure 4.15). At low  $\kappa$ -car concentration fusion of domains was observed rather than clustering.

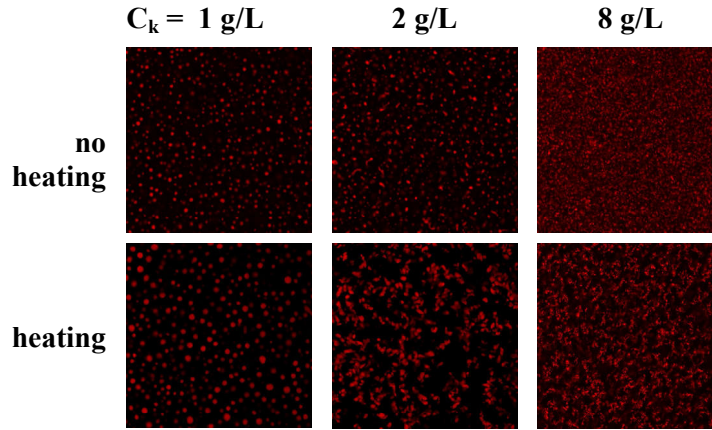


**Figure 4.15.** CLSM images ( $160 \times 160 \mu\text{m}$ ) of mixtures containing 10g/L  $\beta$ -lg microgels ( $R_h=240\text{nm}$ ) and 20mM KCl at different concentrations of  $\kappa$ -car after preparation (top row) and heating at 50°C for 15min (bottom row).

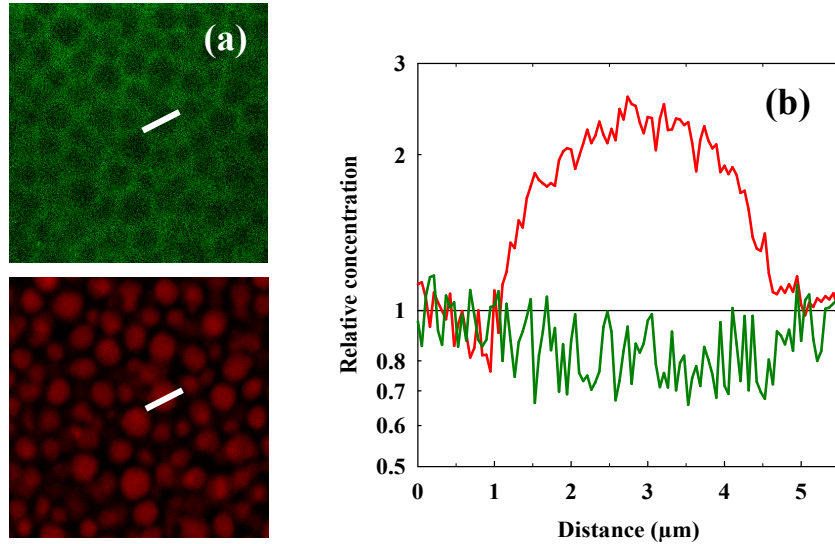


**Figure 4.16.** (a) CLMS images ( $40 \times 40 \mu\text{m}$ ) visualizing  $\beta$ -lg (red) and  $\kappa$ -car (green) for a mixture containing 40 g/L  $\beta$ -lg microgels and 2 g/L  $\kappa$ -car at 15mM KCl.

(b) Relative variation of the  $\beta$ -lg concentration (red) and the  $\kappa$ -car concentration (green) along the white lines in the CLMS images.



The distribution of  $\kappa$ -car in the micro phase separated mixtures is shown in figure 4.16 for a mixtures containing 40g/L  $\beta$ -lg microgels ( $R_h = 110\text{nm}$ ) and 2g/L  $\kappa$ -car covalently labeled with FITC at 15mM KCl. At the conditions of the experiment the fluorescence intensity was proportional to the polymer concentration. The profile of  $\beta$ -lg and  $\kappa$ -car fluorescence intensities showed that the protein concentration was more than a factor 2 higher in the domains, but that the  $\kappa$ -car concentration was reduced by less than 30% in the protein rich domains. This means that  $\kappa$ -car distribution was not much influenced by micro phase separation.

As was shown above, cooling renders mixtures of  $\kappa$ -car and  $\beta$ -lg aggregates more compatible. In a few cases we observed that homogeneous mixtures at 20°C became inhomogeneous at 5°C. This is illustrated in figure 4.17 for mixtures of 2g/L  $\kappa$ -car and 40g/L  $\beta$ -lg aggregates in 10mM KCl.

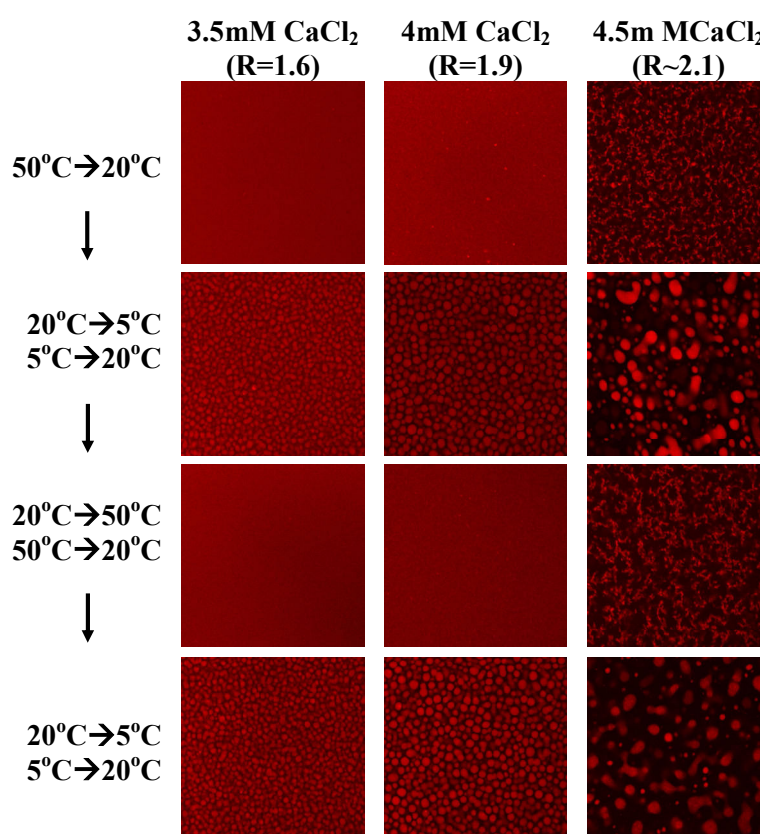


**Figure 4.17.** CLSM images ( $160\times 160\mu\text{m}$ ) of mixtures containing 2g/L  $\kappa$ -car, 40g/L  $\beta$ -lg microgels and 10mM KCl at different concentrations of  $\text{CaCl}_2$  and with different temperature histories.

Figure 4.17 shows that the stronger phase separation at 5°C was preserved at 20°C at which temperature the images were taken, because  $\kappa$ -car gelation inhibited dispersion of the micro domains. This appears in contradiction with the observation discussed above that gelation inverses phase separation. We believe that the  $\kappa$ -car gels formed at these low polymer and KCl concentrations are too weak to drive dispersion. However, when the solutions were heated to 50°C so that the  $\kappa$ -car gel melted, the protein domains dispersed rapidly. Even when phase separation already occurred at 20°C it could be reinforced by further cooling to 5°C. However, the effect of cooling to 5°C was only significant close to the phase boundary.

#### 4.4.3. Effect of $\kappa$ -carrageenan gelation on the rheology

The shear modulus of pure  $\kappa$ -car and mixtures containing either 10 or 40g/L microgels ( $R_h = 240\text{nm}$ ) at 10mM KCl were investigated at different concentrations of  $\kappa$ -car while cooling from 50 to 10°C in steps of 5°C maintaining the temperature for 20min at each step. The storage shear moduli at 10°C are shown as a function of  $C_k$  in figure 4.18. In each case  $G'$  increased with increasing  $C_k$ , but the increase was stronger when more microgels were present. We believe that the increase of  $G'$  is caused by the fact that the microgels were formed in the presence of  $\text{CaCl}_2$  and that together with the microgels  $\text{Ca}^{2+}$  is added to  $\kappa$ -car solution. We showed in chapter 3 that a small amount of  $\text{Ca}^{2+}$  reinforces  $\text{K}^+$ -induced  $\kappa$ -car gels.

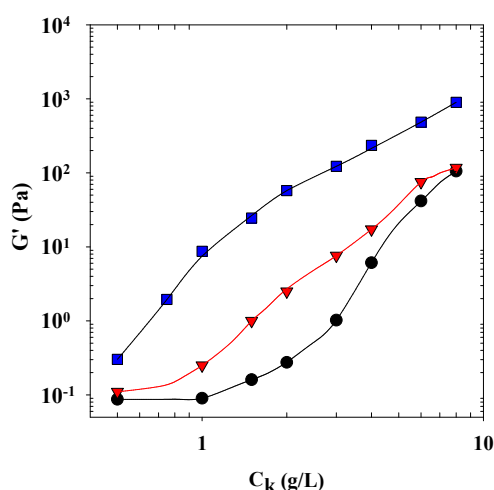


**Figure 4.18.** Dependence of the shear modulus on the  $\kappa$ -car concentration and 10mM KCl without protein (circles), with 10g/L  $\beta$ -lg microgels (triangles) and with 40g/L  $\beta$ -lg microgels (squares).

The effect of adding microgels was largest at about 2g/L  $\kappa$ -car. Therefore, we investigated gelation of mixtures with this  $\kappa$ -car concentration during and after rapid cooling from 50 to 5°C with different concentrations of microgels (figure 4.19a). The rate of  $\kappa$ -car gelation increased with increasing microgel concentration, because more calcium ions were added together with the microgels. As was mentioned above,  $G'$  was already significantly higher than for pure  $\kappa$ -car before gelation due to the adsorption of protein at the water-oil interface.

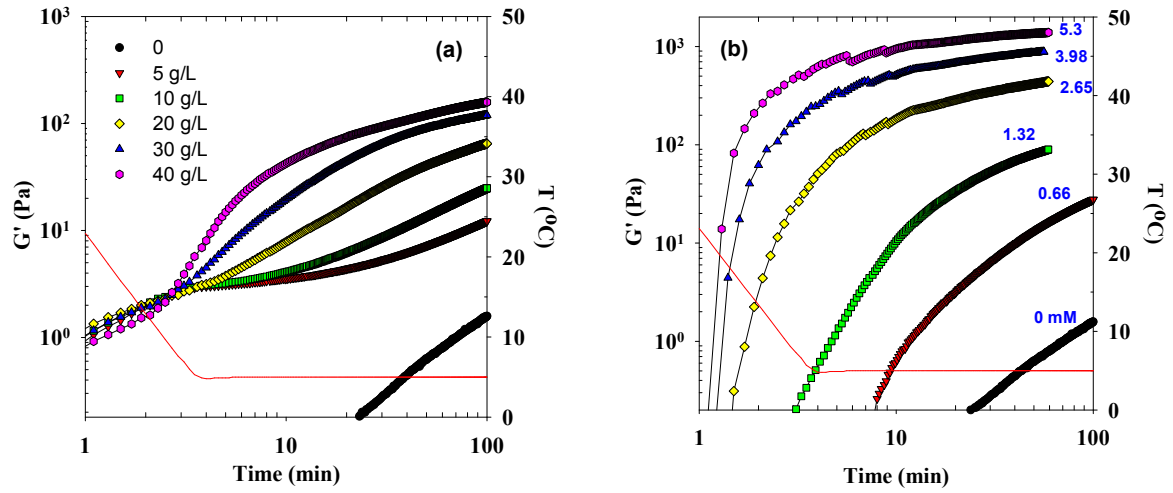


**Figure 4.19.** (a) Evolution of  $G'$  at 0.1Hz for mixtures of 2 g/L  $\kappa$ -car and different concentrations of  $\beta$ -lg microgels with  $R_h = 240\text{nm}$  in 10 mM KCl during and after rapid cooling from 50°C to 5°C. The microgels contained 2.5 calcium ions per protein ( $R=2.5$ ). (b) Evolution of  $G'$  at 0.1Hz for solutions of 2 g/L  $\kappa$ -car in the presence of 10mM KCl at different concentrations of  $\text{CaCl}_2$  during and after rapid cooling from 50°C to 5°C. The solid lines indicate the temperature as a function of time for both (a) and (b).

When we compare the evolution of  $G'$  in figure 4.19a with that of pure  $\kappa$ -car containing the same amount of calcium ions (figure 4.19b), we find that the gels in the presence of microgels are much weaker. The reason is that the proteins strongly bind  $\text{Ca}^{2+}$  so that less  $\text{Ca}^{2+}$  is available to reinforce the  $\kappa$ -car gel as we discussed in section 4.2 for the case of mixtures with native  $\beta$ -lg. Figure 4.20a compares the dependence of  $G'$  on the concentration of calcium ions for  $\kappa$ -car gels formed at 5°C without protein, with native proteins, with strands and with microgels. Addition of native  $\beta$ -lg or strands strongly reduces the elastic modulus, but the addition of microgels reduces it further. The reason is that microgels bind  $\text{Ca}^{2+}$  more strongly as is shown in figure 4.20b in which the fraction of free

$\text{Ca}^{2+}$  is plotted as a function of the total calcium concentration in pure  $\kappa$ -car and in the presence of native or aggregated  $\beta$ -lg.

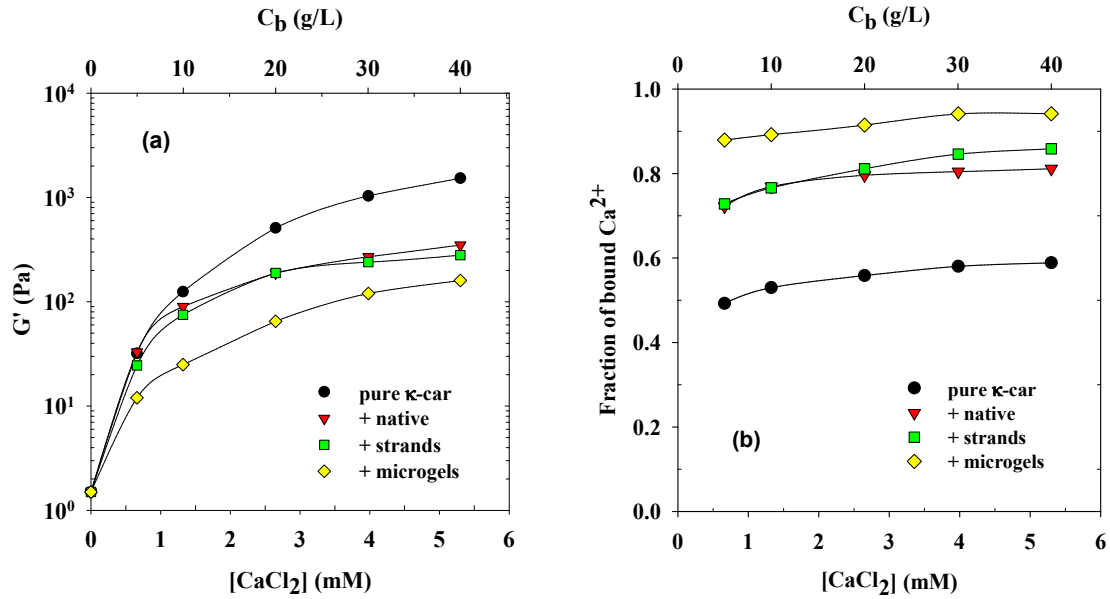


**Figure 4.20.** (a) Elastic shear modulus of  $\kappa$ -car gels ( $C_k = 2$  g/L) after 100 min at  $5^\circ\text{C}$  in the presence of 10mM KCl as a function of the concentration of  $\text{Ca}^{2+}$ . The results for pure  $\kappa$ -car are compared with mixtures containing native  $\beta$ -lg, strands or microgels. The molar ratio of calcium ions to  $\beta$ -lg was  $R = 2.5$ .

(b) Fraction of bound  $\text{Ca}^{2+}$  in mixtures containing 2g/L  $\kappa$ -car and different concentration of native, strands, microgels or pure  $\kappa$ -car solutions as a function of  $\text{CaCl}_2$  concentrations.

#### 4.4.4. Conclusion

In mixtures with  $\kappa$ -car,  $\beta$ -lg microgels formed by heating in the presence of  $\text{CaCl}_2$  phase separated at much lower  $\kappa$ -car concentrations than small  $\beta$ -lg strands formed by heating in pure water. At lower  $\kappa$ -car concentrations the effect of  $\text{CaCl}_2$  on the structure of the mixtures is directly related to the transition between the formation of  $\beta$ -lg strands and microgels. Phase separation led to the formation of spherical protein rich domains with a diameter of a few microns. The concentration of  $\kappa$ -car was decreased by only about 30% within the protein rich domains. The protein rich domains cluster into large flocks that slowly sediment, but the precipitate can be easily dispersed by shaking.

In the mixtures  $\beta$ -lg microgels competes with  $\kappa$ -car more strongly for  $\text{Ca}^{2+}$  than native  $\beta$ -lg or  $\beta$ -lg strands. As a consequence the effect of stiffening  $\kappa$ -car by addition of  $\text{CaCl}_2$  is less important in mixtures with  $\beta$ -lg microgels.

#### 4.5. Heated mixtures of $\kappa$ -carrageenan and native $\beta$ -lactoglobulin

In sections 4.3 and 4.4 we investigated systems for which  $\beta$ -lg was first heated separately and subsequently mixed with  $\kappa$ -car, i.e. mixing after heating (MAH). In this section we will discuss the situation where  $\kappa$ -car was first mixed with native  $\beta$ -lg and subsequently heated, i.e. mixing before heating (MBH). The two procedures are schematized in figure 4.21.

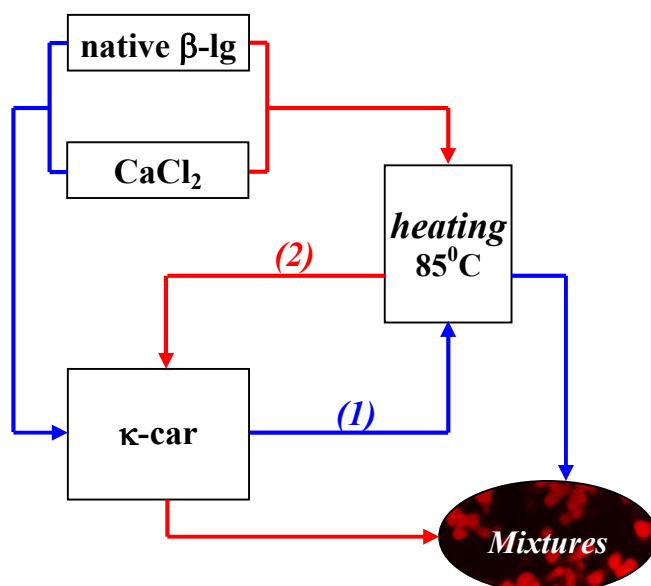


**Figure 4.21.** Scheme of the two different procedures to prepare mixtures of  $\kappa$ -car and aggregated  $\beta$ -lg: (1) mixing before heating (MBH) and (2) mixing after heating (MAH)

##### 4.5.1. Mixtures of $\beta$ -lg and $\kappa$ -car coils

The effect of heating after mixing or before mixing on the structure of the mixtures is illustrated in figure 4.22 for mixtures containing 40g/L  $\beta$ -lg and 2g/L  $\kappa$ -car at different concentrations of  $\text{CaCl}_2$ . The microgels were formed by heating native  $\beta$ -lg separately (MAH) and when they were formed by heating the mixtures (MBH), see figure 4.22.

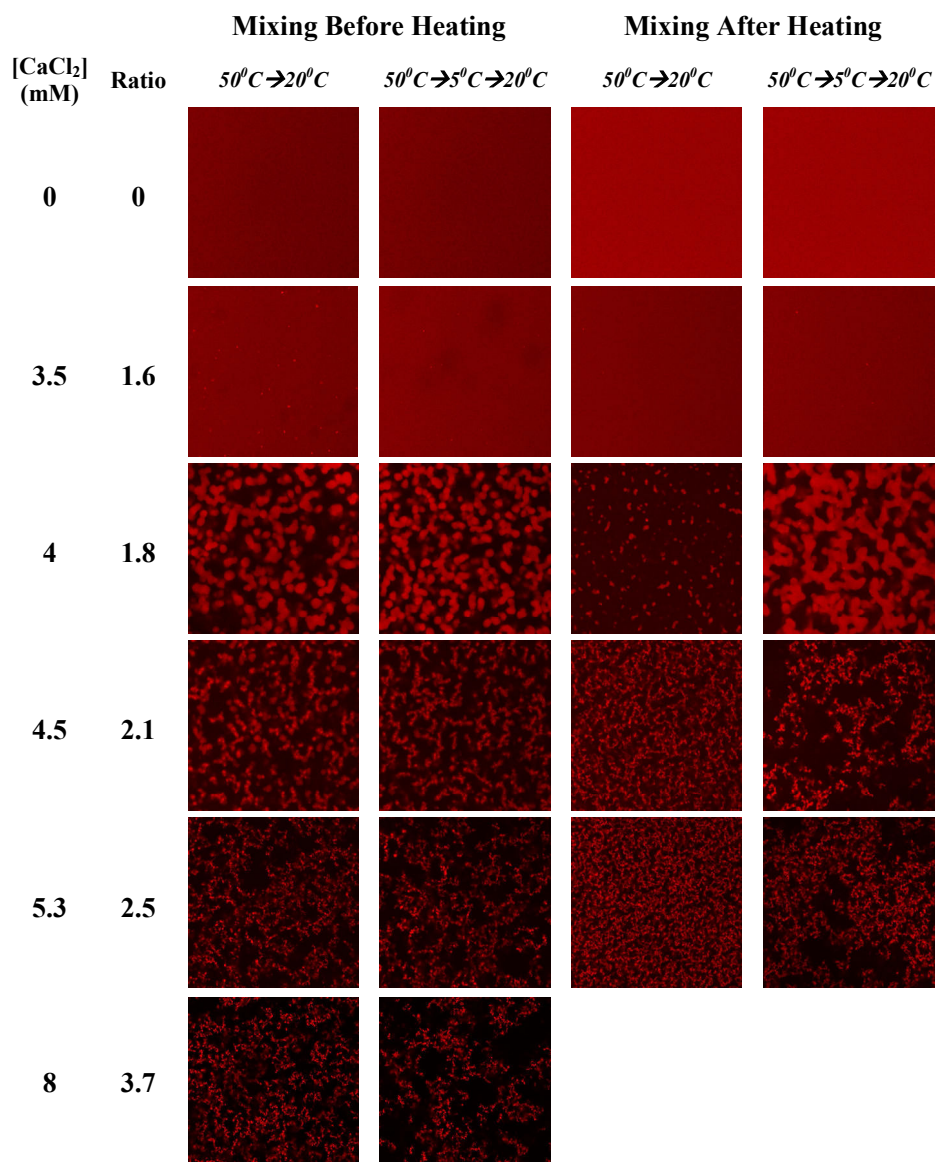


**Figure 4.22.** CLSM images (160x160μm) of mixtures containing 40g/L β-lg and 2g/L κ-car at different concentrations of CaCl<sub>2</sub>.

The microstructures of mixtures prepared by the two different methods were very similar and in both cases protein rich domains were formed at [CaCl<sub>2</sub>] ≥ 4mM of R ≥ 1.8. This similarity is remarkable, because the β-lg gelled in heated mixtures for [CaCl<sub>2</sub>] ≥ 4mM, see below. The effect of further cooling to 5°C was small for mixtures prepared by MBH. Similar observations were done for mixtures containing 20g/L β-lg and 2g/L κ-car that did not form gels. Phase separation started in this case at a lower CaCl<sub>2</sub> concentration, but at approximately the same value of R.

The phase diagram of mixtures containing 20g/L  $\beta$ -lg as a function of the  $\kappa$ -car and  $\text{CaCl}_2$  concentrations prepared by MBH or MAH is shown in figure 4.23. In both cases the critical  $\text{CaCl}_2$  concentration to induce phase separation decreased with increasing  $\kappa$ -car concentration. For  $C_k < 4\text{g/L}$ , micro phase separation started at a slightly lower  $\text{CaCl}_2$  concentration for MAH than for MBH. However, mixtures prepared by MBH phase separated for  $C_k \geq 5\text{g/L}$  already in the absence of  $\text{CaCl}_2$ , whereas this required  $C_k \geq 8\text{g/L}$  for the case of MAH.

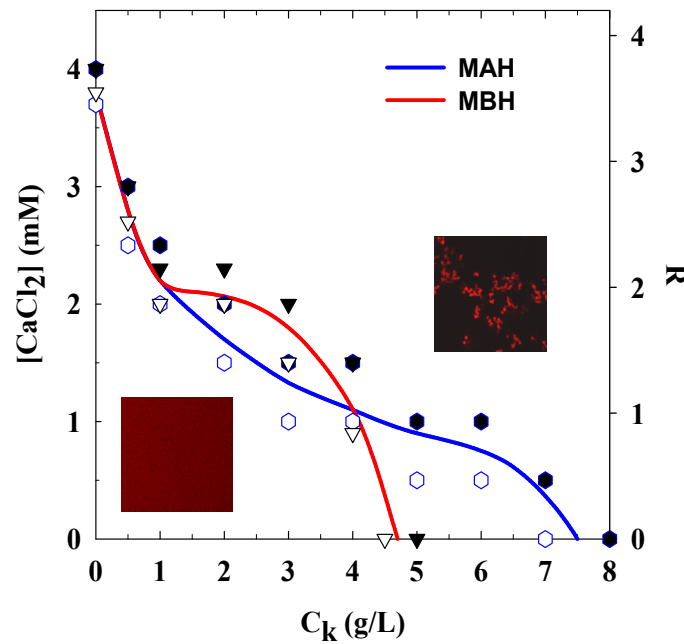


**Figure 4.23.** Phase diagram of mixtures containing 20g/L  $\beta$ -lg as a function of the  $\kappa$ -car and  $\text{CaCl}_2$  concentrations prepared by mixing before heating (MBH) or mixing after heating (MAH). The open and closed symbols correspond to homogeneous and phase separated mixtures, respectively. The solid lines indicate the phase boundary.

Similarly to MAH,  $\beta$ -lg rich domains that were formed during heating the mixtures agglomerated into large flocks that slowly precipitated. The concentration of residual protein in the supernatant sharply decreased with increasing concentration of  $\text{CaCl}_2$  above a critical value that increased with increasing  $\kappa$ -car concentration, see figure 4.24a.

The latter can be explained by the fact that larger strands formed when native  $\beta$ -lg is heated in the presence of  $\kappa$ -car (MBH) phase separated slower than of MAH, because the depletion interaction caused micro phase separation for MBH case, while weak compatibility



between small aggregates and a low concentrations of  $\kappa$ -car chains was a cause to inhibit phase separation, thus it was necessary to phase separate at high  $C_k$ .

At  $C_k = 1\text{-}3\text{g/L}$ , the fraction of protein in the supernatant reduced sharply when protein started forming a microgel ( $R \sim 2$ ), they were still about 60% and around 10% when large microgels were completely formed. However, at  $C_k \geq 4\text{g/L}$  the fraction of protein in the supernatant decreased immediately when protein formed small microgels or even strands ( $C_k = 5\text{g/L}$ ). The reason was the mixtures phase separated by thermodynamic incompatibility and could form a gel for mixtures containing  $20\text{g/L}$   $\beta$ -lg and  $5\text{g/L}$   $\kappa$ -car at  $[\text{CaCl}_2] > 2\text{mM}$ .

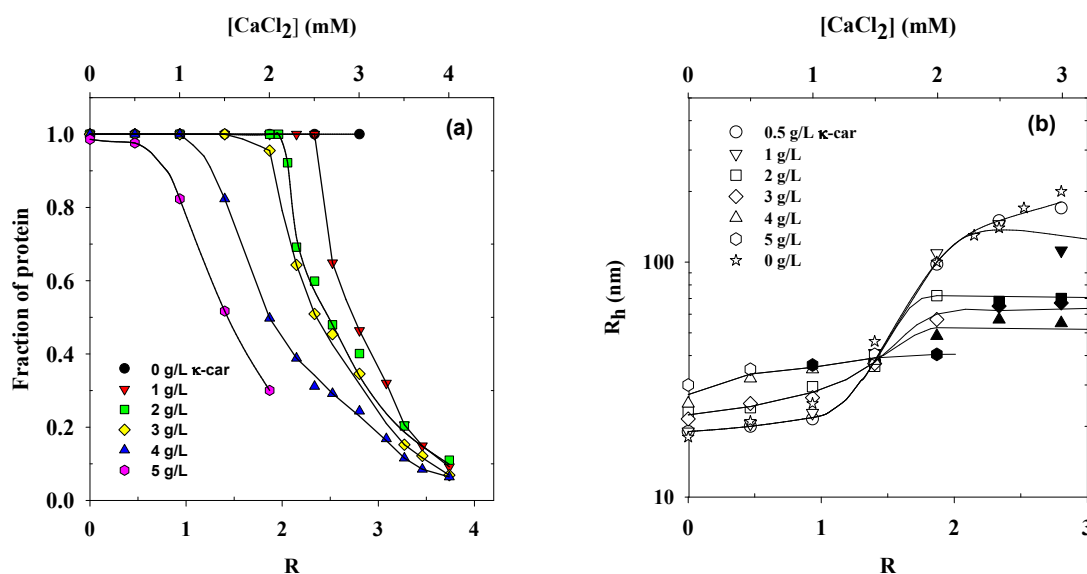


**Figure 4.24.** Fraction (a) and evolution size (b) of  $\beta$ -lg aggregates in the supernatant of mixtures containing  $20\text{g/L}$  native  $\beta$ -lg and different concentrations of  $\kappa$ -car and  $\text{CaCl}_2$  after heating. In figure (b) the filled symbols indicate system phase separated above 10%.

The hydrodynamic radius of the residual aggregates in the supernatant is plotted in figure 4.24b. It appears that larger  $\beta$ -lg strands are formed when native  $\beta$ -lg is heated in the presence of  $\kappa$ -car, which may explain why phase separation is observed at a lower critical  $\kappa$ -car concentration for  $[\text{CaCl}_2] \leq 1\text{mM}$ . On the other hand, smaller microgels are formed in the presence of  $\kappa$ -car as can be clearly seen at  $C_k = 2$  or  $3\text{g/L}$  and  $[\text{CaCl}_2] = 2\text{mM}$ . At these conditions phase separation was still negligible, but the aggregates were clearly smaller than in the absence of  $\text{CaCl}_2$ . This may be due to the competition for  $\text{Ca}^{2+}$  with  $\kappa$ -car and can explain why more  $\text{CaCl}_2$  was needed to induce phase separation at these  $\kappa$ -car concentrations. For phase separated samples the size of the residual aggregates in the supernatant is most



likely smaller than those that precipitated as larger aggregates will preferentially enter the dense domains.

A major difference between the two methods is that during heating the mixtures protein aggregates become covalently linked within the phase separated structure, while for mixtures prepared by MAH the dense domains disperse rapidly upon dilution. Figure 4.25 compares the effect of dilution for mixtures prepared by mixing before heating and mixing after heating. In the case of MAH, dilution by a factor two was sufficient to render the system homogeneous at  $[\text{CaCl}_2] = 1.5\text{mM}$ , while at  $[\text{CaCl}_2] = 3\text{mM}$  dilution by a factor 20 was needed. In the case of MBH no amount of dilution led to dispersion of the flocculated domains.

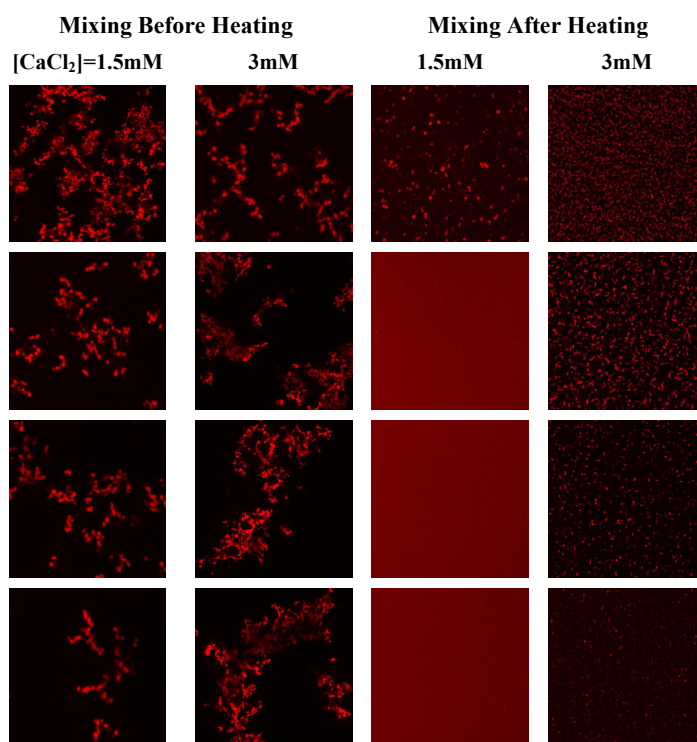


**Figure 4.25.** Effect of dilution on the structure of mixtures of  $\kappa$ -car and partially labeled  $\beta$ -Ig ( $C_k = 5\text{g/L}$ ,  $C_b = 20\text{g/L}$ ) in the presence of  $1.5\text{mM}$  and  $3\text{mM}$   $\text{CaCl}_2$  prepared by heating after mixing or heating before mixing. Dilution factors are from top to bottom: undiluted, x2, x5, x20. The images represent  $160 \times 160 \mu\text{m}$ .

#### 4.5.2. Effect of $\kappa$ -car gelation on the structure and the rheology

The effect of  $\kappa$ -car gelation was studied by heating the mixtures in the presence of  $10\text{mM}$  KCl and subsequently cooling. Figure 4.26 compares heated mixtures containing

40g/L native protein, 2g/L  $\kappa$ -car and different amounts of  $\text{CaCl}_2$ , with mixtures prepared by MAH with the same composition.

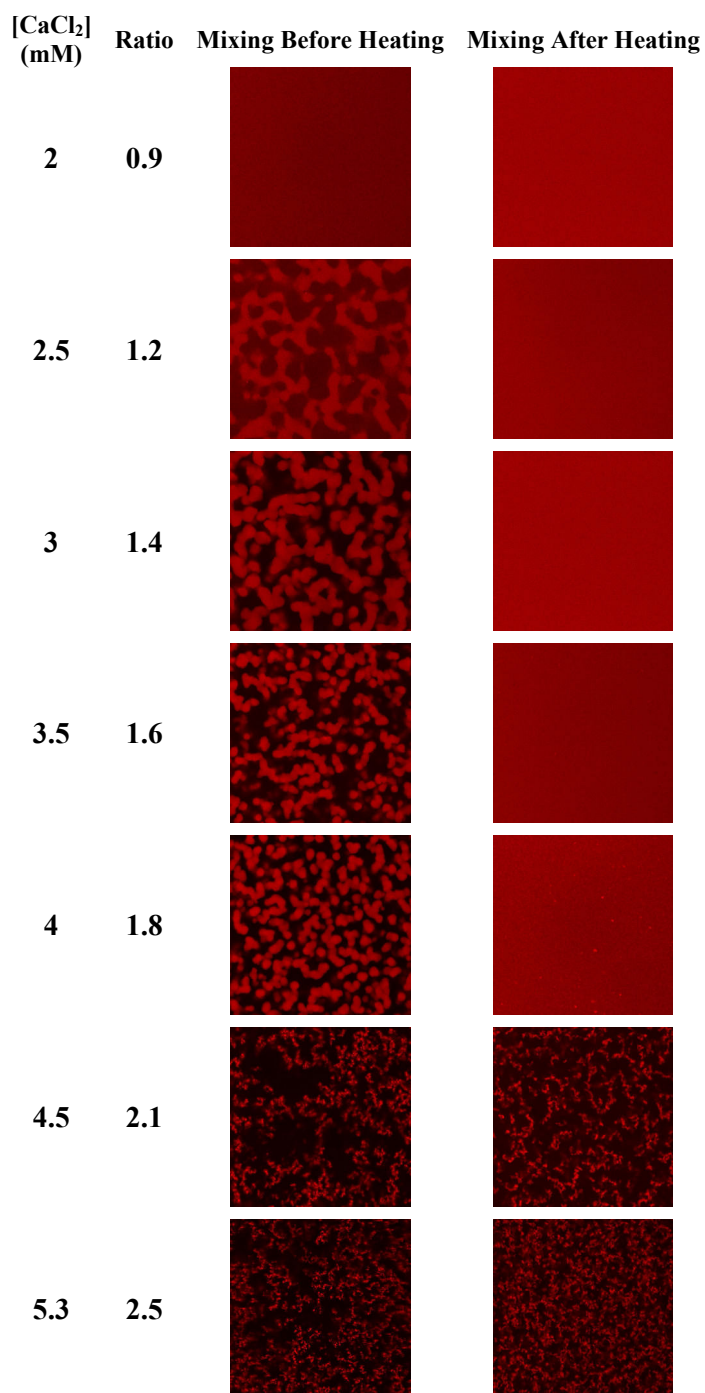


**Figure 4.26.** CLSM images (160x160 $\mu\text{m}$ ) of mixtures containing 40g/L  $\beta$ -lg and 2g/L  $\kappa$ -car at 10mM KCl and different concentrations of  $\text{CaCl}_2$ .

We find that the heated mixtures phase separated at significantly lower  $\text{CaCl}_2$  concentrations ( $[\text{CaCl}_2] \geq 2.5\text{mM}$ ) than the mixtures prepared by MAH ( $[\text{CaCl}_2] \geq 4.5\text{mM}$ ). In the absence of KCl, we found that the critical  $\text{CaCl}_2$  concentrations were the same ( $[\text{CaCl}_2] \geq 4\text{mM}$ ) (figure 4.22). We believe that the addition of 10mM KCl favored aggregation of the proteins, which in turn favored phase separation. At higher  $\text{CaCl}_2$  concentrations the morphology of the systems is similar whether or not the proteins and/or the polysaccharide have gelled.

As was mentioned in chapter 1, in pure water heating 40g/L  $\beta$ -lg leads to gelation for  $[\text{CaCl}_2] \geq 7\text{mM}$ . Figure 4.27 shows the evolution of  $G'$  at 0.1 Hz during and after heating to 85°C for mixtures of 40g/L native  $\beta$ -lg and 2g/L  $\kappa$ -car in the presence (a) and absence (b) of 10mM KCl at different concentrations of  $\text{CaCl}_2$ . In the presence of 2g/L  $\kappa$ -car the heated mixture gelled for  $[\text{CaCl}_2] \geq 4\text{mM}$  and for  $[\text{CaCl}_2] \geq 2\text{mM}$  when 10mM KCl was added (figure 4.27). Most likely, gelation is induced at lower  $\text{CaCl}_2$  concentrations in the mixtures by the incompatibility between  $\kappa$ -car and the growing  $\beta$ -lg aggregates. The lower critical  $\text{CaCl}_2$  concentration in the presence of 10mM KCl confirms that adding KCl favors protein aggregation. For  $[\text{CaCl}_2] \geq 7\text{mM}$ , gelation of the proteins was the same as in pure water.

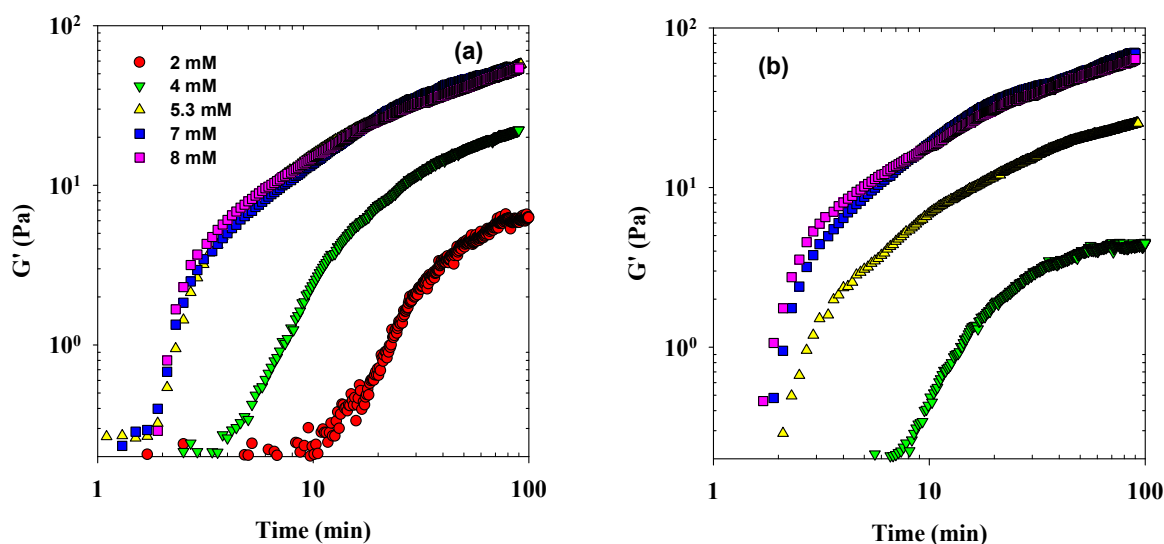


**Figure 4.27.** Evolution of  $G'$  at 0.1 Hz during and after heating to 85°C for solutions of 40 g/L  $\beta$ -lg and 2g/L  $\kappa$ -car at different concentrations of  $\text{CaCl}_2$  with (a) and without (b) 10 mM KCl. Symbols of figure (b) for the different  $\text{CaCl}_2$  concentrations are the same in figure (a).

Figure 4.28 shows the elastic modulus of the gels during cooling to 5°C and subsequent heating back to 85°C at a rate of 2°C per minute. In the absence of KCl, we observed the weak progressive increased of  $G'$  with decreasing temperature that is well-known for protein gels. However, in the presence of 10mM KCl  $G'$  increased sharply below a critical temperature of about 20°C caused by gelation of  $\kappa$ -car within the  $\beta$ -lg gel. The shear modulus decreased again during heating when the  $\kappa$ -car gel melted, but at a higher critical temperature than at which it was formed during cooling.

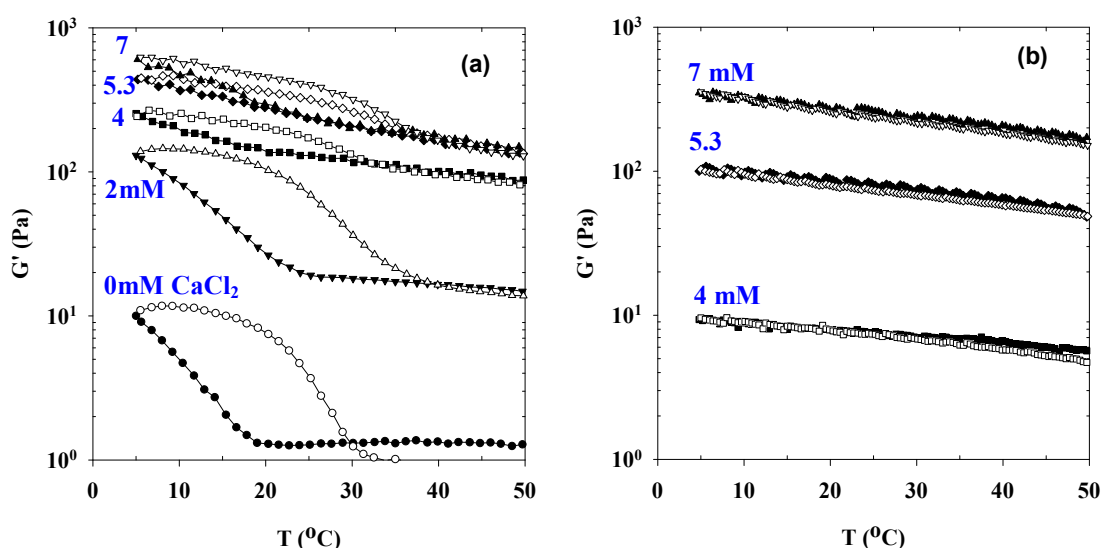


**Figure 4.28.** Temperature dependence of  $G'$  at 0.1Hz during cooling (closed symbols) and subsequent heating (open symbols) of  $\beta$ -lg gels (40g/L) containing 2g/L  $\kappa$ -car. The gels were formed at different concentrations of  $\text{CaCl}_2$  with (a) and without (b) 10mM KCl.

Figure 4.29 shows the elastic moduli of the interpenetrated networks of  $\kappa$ -car and  $\beta$ -lg measured 100min after cooling quickly from 50°C to 5°C. The contribution of the  $\beta$ -lg gels was determined by extrapolation of the linear temperature dependence of  $G'$  at  $T > T_c$  to 5°C. The difference corresponds to the contribution of the  $\kappa$ -car gel. If use for the latter the values found for the mixtures with native  $\beta$ -lg before heating, we find that the mixed gels were somewhat stiffer than the sum of the two individual networks up to  $[\text{CaCl}_2] < 5.3\text{mM}$  (figure 4.29). This means that either a stronger  $\kappa$ -car gel was formed within the gelled  $\beta$ -lg than with native  $\beta$ -lg or that the two interpenetrated networks did not deform independently. At  $[\text{CaCl}_2] > 5.3\text{mM}$ , the sum is not shown because there was syneresis of strong  $\kappa$ -car gels in the mixtures with 40g/L native  $\beta$ -lg. The synergic effect was largest at  $[\text{CaCl}_2] \geq 2\text{mM}$  where the

heated mixtures were homogeneous, which implies that it was not caused by microphase separation.

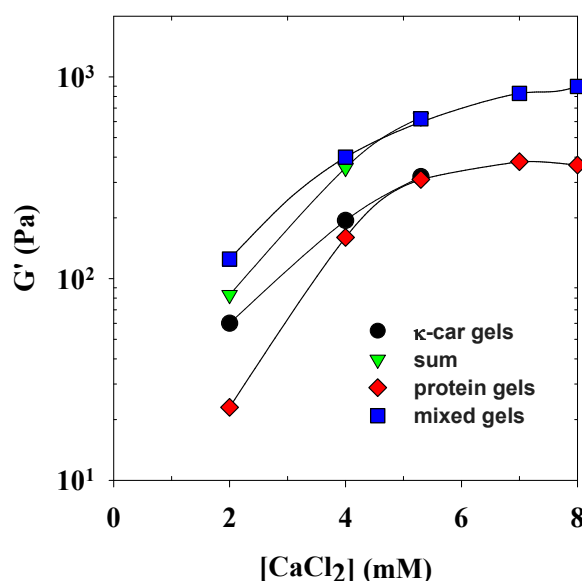


**Figure 4.29.** Dependence on the  $\text{CaCl}_2$  concentration of the elastic modulus of interpenetrated  $\kappa$ -car (2 g/L) and  $\beta$ -lg gels (40 g/L) gels at  $5^\circ\text{C}$  (squares) in the presence of 10mM KCl. For comparison we also show the elastic modulus of  $\kappa$ -car gels formed in the presence of native  $\beta$ -lg before heating (circles), the contribution to  $G'$  of the  $\beta$ -lg gel in mixed gels (diamonds) and the sum (triangles).

### 4.5.3. Conclusion

The presence of  $\kappa$ -car led to the formation of larger  $\beta$ -lg strands when heated in pure water or with less than one calcium ion per protein. At higher  $\text{CaCl}_2$  concentrations competition for  $\text{Ca}^{2+}$  with  $\kappa$ -car led to formation of smaller microgels than in the absence of  $\kappa$ -car.

The structure of mixtures of  $\beta$ -lg aggregates and  $\kappa$ -car coils with the same composition are similar whether prepared by mixing after heating or mixing before heating. However, in the former case phase separation can be reversed by dilution, while in the latter case the proteins become strongly bound within the domains and persist after dilution.

Addition of 10mM KCl to the mixtures favors  $\beta$ -lg aggregation during heating, which led to micro phase separation at lower  $\text{CaCl}_2$  concentrations than mixtures prepared by mixing after heating.

Heat-induced gelation of native  $\beta$ -lg was facilitated by the presence of  $\kappa$ -car, probably because it favored contact between the growing  $\beta$ -lg aggregates that are incompatible with  $\kappa$ -car. Above a critical amount of added  $\text{CaCl}_2$  micro phase separation occurs during heating and heterogeneous gels are formed. When the solution contains 10mM KCl,  $\kappa$ -car gels within the  $\beta$ -lg gel upon cooling at a temperature close to that of the equivalent pure  $\kappa$ -car solutions. The  $\kappa$ -car gels melted again when heated, but the  $\beta$ -lg gel remained intact during cooling and reheating. The mixed gel was somewhat stiffer than the sum of the  $\kappa$ -car gel in the presence of uncrosslinked native  $\beta$ -lg and the  $\beta$ -lg gel in the presence of uncrosslinked  $\kappa$ -car coils, indicating that the structure of the  $\kappa$ -car network that was formed within the  $\beta$ -lg gel was different from that formed in the presence of  $\beta$ -lg aggregates.

## References

- Ako, K., Durand, D., & Nicolai, T. (2011). Phase separation driven by aggregation can be reversed by elasticity in gelling mixtures of polysaccharides and proteins. *Soft Matter*, 7, 2507-2516.
- Çakır, E., & Foegeding, E. A. (2011). Combining protein micro-phase separation and protein-polysaccharide segregative phase separation to produce gel structures. *Food Hydrocolloids*, 25(6), 1538–1546.
- Clark, A. H. (1999). Gelation of globular proteins. In S. E. Hill, D. A. Ledward & J. R. Mitchell *Functional Properties of Food Macromolecules* (2nd edition, Gaithersburg: Aspen Publishers), 77-142.
- de Jong, S., Klok, H. J., & van de Velde, F. (2009). The mechanism behind microstructure formation in mixed whey protein-polysaccharide cold-set gels. *Food Hydrocolloids*, 23(3), 755-764.
- Foegeding, E. A. (2006). Food biophysics of protein gels: A challenge of nano and macroscopic proportions. *Food Biophysics*, 1(1), 41-50.
- Gaaloul, S., Turgeon, S. L., & Corredig, M. (2010). Phase Behavior of Whey Protein Aggregates/ $\kappa$ -Carrageenan Mixtures: Experiment and Theory. *Food Biophysics*, 5(2), 103-113.
- Harrington, J. C., Foegeding, E. A., Mulvihill, D. M., & Morris, E. R. (2009). Segregative interactions and competitive binding of  $\text{Ca}^{2+}$  in gelling mixtures of whey protein isolate with  $\text{Na}^+$  $\kappa$ -carrageenan. *Food Hydrocolloids*, 23(2), 468-489.
- Nicolai, T. (2007). Structure of self-assembled globular proteins. In E. Dickinson & M. E. Leser *Food Colloids: Self-Assembly and Material Science*, 302, 35-56.
- Nicolai, T., Britten, M., & Schmitt, C. (2011).  $\beta$ -Lactoglobulin and WPI aggregates: Formation, structure and applications. *Food Hydrocolloids*, 25(8), 1945–1962.
- Piculell, L. (2006). Gelling Carrageenans. In A. M. Stephen, G. O. Philips & P. A. Williams *Food Polysaccharides and their Applications*, 239, Boca Raton: CRC Press.
- Tolstoguzov, V. B. (2003). Some thermodynamic considerations in food formulation. *Food Hydrocolloids*, 17(1), 1-23.
- Tuinier, R., Rieger, J., & de Kruif, C. G. (2003). Depletion-induced phase separation in colloid-polymer mixtures. *Adv Colloid Interface Sci*, 103(1), 1-31.

Turgeon, S. L., Beaulieu, M., Schmitt, C., & Sanchez, C. (2003). Protein-polysaccharide interactions: phase-ordering kinetics, thermodynamic and structural aspects. *Current Opinion in Colloid & Interface Science*, 8(4-5), 401-414.

Turgeon, S. L., Schmitt, C., & Sanchez, C. (2007). Protein-polysaccharide complexes and coacervates. *Current Opinion in Colloid & Interface Science*, 12(4-5), 166-178.



## GENERAL CONCLUSION AND OUTLOOK

### Conclusion

The objective of this thesis was to study the structure and the rheology of mixtures of  $\beta$ -lg aggregates or gels with  $\kappa$ -car solutions or gels and in particular the effect of calcium ions. In first instance, we investigated gelation of pure  $\kappa$ -car solutions. Addition of KCl induces the formation of homogeneous gels with a stiffness that increases with increasing salt concentration. A larger amount of  $\text{CaCl}_2$  is needed to induce gelation and the gels are more heterogeneous. In addition, the stiffness of  $\text{Ca}^{2+}$ -induced gels decreases with increasing concentrations. An important finding is that the presence of even small quantities of NaCl or  $\text{CaCl}_2$  in addition to KCl accelerates  $\text{K}^+$ -induced  $\kappa$ -car gelation and leads to stronger gels, without influencing the critical gelation temperature. It is clear, that the type of ion that induces the coil-helix transition is a crucial factor that determines the structure and the elasticity of the gels in mixed salts.

Native  $\beta$ -lg and  $\kappa$ -car are compatible in aqueous solution up to high polymer concentrations. Addition of large amounts (60 g/L) of native  $\beta$ -lg leads to weak acceleration of  $\text{K}^+$ -induced gelation of  $\kappa$ -car, which can be explained by the effect of the sodium counterions that are added together with the proteins. In the presence of native  $\beta$ -lg the effect of  $\text{CaCl}_2$  on  $\text{K}^+$ -induced gelation of  $\kappa$ -car is less important than for pure  $\kappa$ -car solutions. The reason is that  $\beta$ -lg specifically binds  $\text{Ca}^{2+}$  and competes with  $\kappa$ -car for the calcium ions. The same effect of competition was observed in mixtures with  $\beta$ -lg strands formed by heating the proteins in pure water.

Mixtures of  $\kappa$ -car coils and  $\beta$ -lg aggregates phase separated above a critical  $\kappa$ -car concentration that decreased with increasing sizes of the aggregates, but was little dependent on the  $\beta$ -lg concentration. Phase separation led to the formation of micron sized protein enriched domains that stick together, but do not easily fuse.  $\kappa$ -car chains are only weakly depleted from the protein rich domains. The domains redisperse when the system is diluted. Close to the critical concentration the extent of phase separation decreased with increasing temperature and gelation of  $\kappa$ -car drives a fraction of the  $\beta$ -lg aggregates back into the continuous phase.

The size and morphology of aggregates formed by heating  $\beta$ -lg in the presence of  $\text{CaCl}_2$  changed from relatively small strands to larger spherical microgels when the number of

calcium ions per protein was increased from 1 to 2. As a consequence, micro phase separation was observed at much lower  $\kappa$ -car concentrations when the aggregates were prepared in presence of  $\text{CaCl}_2$ . The rate of  $\text{K}^+$ -induced gelation of  $\kappa$ -car increased with increasing protein concentration in mixtures with microgels. This effect was caused by the increase of the concentration of  $\text{Ca}^{2+}$  counterions together with the microgels. The effect was less than for equivalent pure  $\kappa$ -car solutions because of the competition for the calcium ions with the microgels. Microgels bind  $\text{Ca}^{2+}$  more strongly than native  $\beta$ -lg or  $\beta$ -lg strands so that at the same composition of  $\beta$ -lg,  $\kappa$ -car and  $\text{Ca}^{2+}$ ,  $\kappa$ -car gels are weaker in the presence of microgels than in the presence of native  $\beta$ -lg.

Similar effects on the structure are observed when native  $\beta$ -lg is mixed with  $\kappa$ -car before heating at different  $\text{CaCl}_2$  concentrations. However, in this case the protein rich domains are covalently crosslinked and remain stable upon dilution. Another important difference is that heated  $\beta$ -lg gels at lower  $\text{CaCl}_2$  concentrations in the presence of  $\kappa$ -car than in pure solutions. In the presence of KCl,  $\kappa$ -car forms a gel within the heat-set  $\beta$ -lg gel. The elastic modulus of the mixed gel is close to the sum of the  $\kappa$ -car gel mixed with native  $\beta$ -lg and the  $\beta$ -lg gel formed with  $\kappa$ -car coils at the same polymer and salt composition.

Calcium ions bind specifically to both  $\beta$ -lg and  $\kappa$ -car which strongly modifies their aggregation and gelation. The structure and mechanical properties of mixed  $\beta$ -lg and  $\kappa$ -car solutions and gels is determined by the competition of the two polymers for the calcium ions.

## Perspective

In this thesis we have studied only mixtures at neutral pH. In many food applications the pH is lower, which will no doubt have a significant effect on the properties of the mixtures. For instance, the strand-microgel transition occurs at lower  $\text{CaCl}_2$  concentrations, when the pH is decreased. Therefore, the present investigation of the effect of calcium on the properties of the mixtures needs to be extended to mixtures at lower pH.

We have tested on for a few mixtures the effect of adding  $\text{Mg}^{2+}$  and found that it was similar to the effect of  $\text{Ca}^{2+}$ . Nevertheless, generalisation of the present investigation on the effect of  $\text{Ca}^{2+}$  to other divalent ions will be valuable for food applications using  $\kappa$ -car as a textural additive. In addition, the effect of combining both mono- and divalent salt should be investigated.

Here we have studied only the linear rheological properties of gels formed at static conditions. However, it would be interesting to study also the non-linear rheological properties and the effect of shearing during the gelation process. An investigation by Gaaloul et al. (2009a,b) in the absence of salt showed that interesting textures can be obtained by shearing during gelation of WPI and  $\kappa$ -car, but the effect of  $\text{Ca}^{2+}$  was not investigated.

## References

Gaaloul, S., Corredig, M., & Turgeon, S. L. (2009b). Rheological study of the effect of shearing process and  $\kappa$ -carrageenan concentration on the formation of whey protein microgels at pH 7. *Journal of Food Engineering*, 95(2), 254–263.

Gaaloul, S., Turgeon, S. L., & Corredig, M. (2009a). Influence of shearing on the physical characteristics and rheological behaviour of an aqueous whey protein isolate–kappa-carrageenan mixture. *Food Hydrocolloids*, 23(5), 1243–1252.

## THE LIST OF PUBLICATIONS

***This thesis is based on the work contained in the following papers:***

1. Synergistic effects of mixed salt on the gelation of  $\kappa$ -carrageenan. (*Carbohydrate Polymers* 2014, 112, 10-15)
2. Combined effects of temperature and elasticity on phase separation in mixtures of  $\kappa$ -carrageenan and  $\beta$ -lactoglobulin aggregates. (*Food Hydrocolloids* 2014, 34, 138-144)
3. The effect of the protein aggregate morphology on phase separation in mixtures with polysaccharides. (*Journal of Physics: Condensed Matter* 2014, 26, 464102)
4. The effect of the competition for calcium ions between  $\kappa$ -carrageenan and  $\beta$ -lactoglobulin on the rheology and the structure in mixed gels. (*Journal of Colloids and Surfaces A: Physicochemical and Engineering Aspects*, In press)

***Related publications not included in the thesis:***

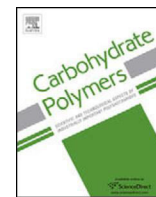
5. Stabilization of water-in-water emulsions by addition of protein particles. (*Langmuir* 2013, 29, 10658-10664)



## **PAPER 1**







# Synergistic effects of mixed salt on the gelation of $\kappa$ -carrageenan



Bach T. Nguyen, Taco Nicolai\*, Lazhar Benyahia, Christophe Chassenieux

LUNAM, Université du Maine, IMMM UMR CNRS 6283, PCI, 72085 Le Mans cedex 9, France

## ARTICLE INFO

### Article history:

Received 16 December 2013  
Received in revised form 12 May 2014  
Accepted 14 May 2014  
Available online 27 May 2014

### Keywords:

Carrageenan  
Gel  
Rheology  
Polysaccharide  
Turbidity

## ABSTRACT

The effect of the addition of calcium or sodium ions on the potassium induced gelation of  $\kappa$ -carrageenan ( $\kappa$ -car) is investigated using oscillatory shear rheology and turbidimetry. Both the gelation kinetics and the steady state shear moduli are investigated. Gelation in mixed salt solutions is compared with that in pure potassium and calcium solutions. It is shown that the elastic shear modulus increases with increasing pure KCl concentration, but decreases with increasing pure  $\text{CaCl}_2$  concentration. In mixed salts, gelation of  $\kappa$ -car is induced by potassium and addition of  $\text{CaCl}_2$  leads to an increase of the elastic modulus with increasing  $\text{CaCl}_2$  concentration.  $\kappa$ -Car gelled at low mixed salt concentrations for which it remained liquid in pure salt. At equivalent ionic strengths, the effect of adding NaCl on potassium induced gelation is much weaker. In pure KCl solutions,  $\kappa$ -car gels are transparent, but in pure  $\text{CaCl}_2$  they become increasingly turbid with increasing  $\text{CaCl}_2$  concentration. The turbidity of gels formed in mixed salts is intermediate.

© 2014 Elsevier Ltd. All rights reserved.

## 1. Introduction

$\kappa$ -Carrageenan ( $\kappa$ -car) is an anionic polysaccharide extracted from red algae and is used extensively for its capacity to form a gel in aqueous solutions (Piculell, 2006). Gelation of  $\kappa$ -car occurs upon cooling below a critical temperature ( $T_c$ ) that depends on the concentration and the type of cations that are present (Rochas & Rinaudo, 1980). Gelation is induced by a conformational transition of the  $\kappa$ -car chains from a random coil to a helix. The transition occurs over a relatively narrow range of temperatures and the fraction of helices increases with decreasing temperature in this range. Chains with the helical conformation aggregate and if their concentration is sufficiently high they form a percolating network.  $T_c$  corresponds to the temperature where the concentration of helices is sufficient to form a percolating network. A particularly effective cation to induce the coil-helix transition of  $\kappa$ -car is potassium. The presence of only 10 mM potassium can induce gelation at room temperature, while a more than ten times larger amount is needed for sodium (Hermansson, Eriksson, & Jordansson, 1991; Mangione et al., 2005; Michel, Mestdagh, & Axelos, 1997; Nono, Durand, & Nicolai, 2012; Nono, Nicolai, & Durand, 2011). Gelation can be reversed by heating, but the melting temperature is often higher than the gelling temperature.

The effect of both the concentration and type of cation on the elastic modulus of  $\kappa$ -car gels has been studied in some detail for potassium and calcium, which are most commonly used to induce

gelation. It is found that when considering the effect of the ion concentration one also needs to take into account the activity of the counterions. Generally, it is found that the elastic modulus increases with increasing potassium concentration (Doyle, Giannouli, Philp, & Morris, 2002; Nguyen, Phan-Xuan, Benyahia, & Nicolai, 2012; Nono et al., 2011; Núñez-Santiago & Tecante, 2007; Thrimawithana, Young, Dunstan, & Alany, 2010), while it reaches a maximum when the calcium concentration is increased (Doyle et al., 2002; MacArtain, Jacquier, & Dawson, 2003; Thrimawithana et al., 2010). Another difference between gels induced by potassium and those induced by calcium is that the latter are increasingly turbid with increasing ion concentration (Doyle et al., 2002; MacArtain et al., 2003), while the former remain transparent.

The effect of mixed salts on the gelation of  $\kappa$ -car has been studied relatively little even though in applications often more than one type of salt is present. The most extensive study was reported by Hermansson et al. (1991) who found that adding NaCl to a  $\kappa$ -car solution containing 20 mM potassium led to an increase of the elastic modulus, whereas in the absence of potassium these solutions did not gel. An even stronger synergistic effect was found when  $\text{CaCl}_2$  was added. Addition of as little as 2 mM  $\text{CaCl}_2$  was found to increase the elastic modulus significantly. Mangione et al. (2005) reported that addition of 100 mM NaCl to a  $\kappa$ -car solution containing 20 mM KCl did not influence  $T_c$ , but led to a significant increase of the elastic shear modulus. These results clearly show that gelation of  $\kappa$ -car in mixed salt solutions cannot be deduced from that of the pure salt solutions.

Here we present a systematic investigation of the influence of adding  $\text{CaCl}_2$  or NaCl on  $\kappa$ -car gelation induced by potassium and compare it with gelation induced by pure  $\text{CaCl}_2$  and pure KCl. We

\* Corresponding author. Tel.: +33 043833139.

E-mail address: [Taco.Nicolai@univ-lemans.fr](mailto:Taco.Nicolai@univ-lemans.fr) (T. Nicolai).

have studied not only the effect on the elastic modulus at steady state, but also on the gelation kinetics and the turbidity.

## 2. Materials and methods

### 2.1. Materials

The sodium  $\kappa$ -carrageenan used for this study is an alkali treated extract from *Eucheuma cottonii* and was a gift from Cargill (Baupre, France). Using NMR it was found that the sample contained less than 5%  $\iota$ -carrageenan. A freeze-dried sample of  $\kappa$ -car was dissolved by stirring for a few hours in Milli-Q water (70 °C) with 200 ppm sodium azide added as a bacteriostatic agent. The solution was extensively dialysed against Milli-Q water at pH 7 and subsequently filtered through 0.45  $\mu$ m pore size Anotop filters. The pH of the solution was adjusted to 7 by adding small amounts of HCl 0.1 M. The  $\kappa$ -car concentration ( $C_K$ ) was determined by measuring the refractive index using refractive index increment 0.145 mL/g. The molar mass ( $M_w$ ) and radius of gyration ( $R_g$ ) were determined by light scattering as described elsewhere (Meunier, Nicolai, Durand, & Parker, 1999):  $M_w = 2.1 \times 10^5$  g/mol,  $R_g = 52$  nm. The sample contained 5500 mg/100 g Na, 56 mg/100 g Ca and 300 mg/100 g K.

### 2.2. Methods

The shear moduli were determined as a function of the frequency and the temperature using a stress imposed rheometer (AR2000, TA Instruments) with plate – plate geometry (diameter 40 mm, gap 700  $\mu$ m). The temperature was controlled by a Peltier system and the geometry was covered with paraffin oil to prevent water evaporation. In all cases the measurements were done in the linear response regime. For some systems we observed a decrease of the shear modulus during gelation, which is caused by partial detaching of the gels from the geometry. Here we only show results of measurements where this did not occur and the results were quantitatively reproducible.

Turbidity measurements were done as a function of the wavelength in rectangular air tight cells using a UV–visible spectrometer Varian Cary-50 Bio. Different path lengths were used depending on the turbidity of the samples in order to avoid saturation. Measurements were done at different temperatures that were controlled within 0.2 °C using a thermostated bath.

## 3. Results

### 3.1. Pure potassium induced gelation

Fig. 1 shows the evolution of the storage shear modulus ( $G'$ ) at 0.1 Hz during a cooling and subsequent heating ramp (2 °C/min) for aqueous solutions of  $\kappa$ -car in 10 mM KCl at various  $\kappa$ -car concentrations between 2 and 13.5 g/L. For  $C > 4$  g/L,  $G'$  increased steeply at a critical temperature  $T_c \approx 18$  °C. At lower concentrations, weaker gels are formed and the initial steep increase of  $G'$  is below the sensitivity of the apparatus. Therefore we observe for these solutions only the slower increase at lower temperatures. At lower concentrations no significant increase of  $G'$  was observed during the cooling ramp.

During subsequent heating,  $G'$  first increased weakly followed by a decrease at significantly higher temperatures than  $T_c$  caused by melting of the gel. The initial increase can be explained by the slow gelation kinetics that initially dominates the effect of decreasing gel strength with increasing temperature. As was reported elsewhere (Meunier et al., 1999), the kinetics of gelation can be very slow,

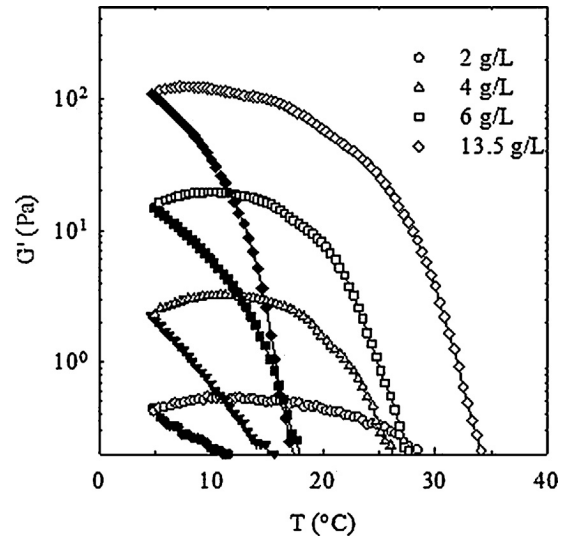


Fig. 1. Storage shear modulus at 0.1 Hz of different concentrations of  $\kappa$ -car at 10 mM KCl during a cooling (filled symbols) and subsequent heating (open symbols) ramp at a rate of 2 °C/min.

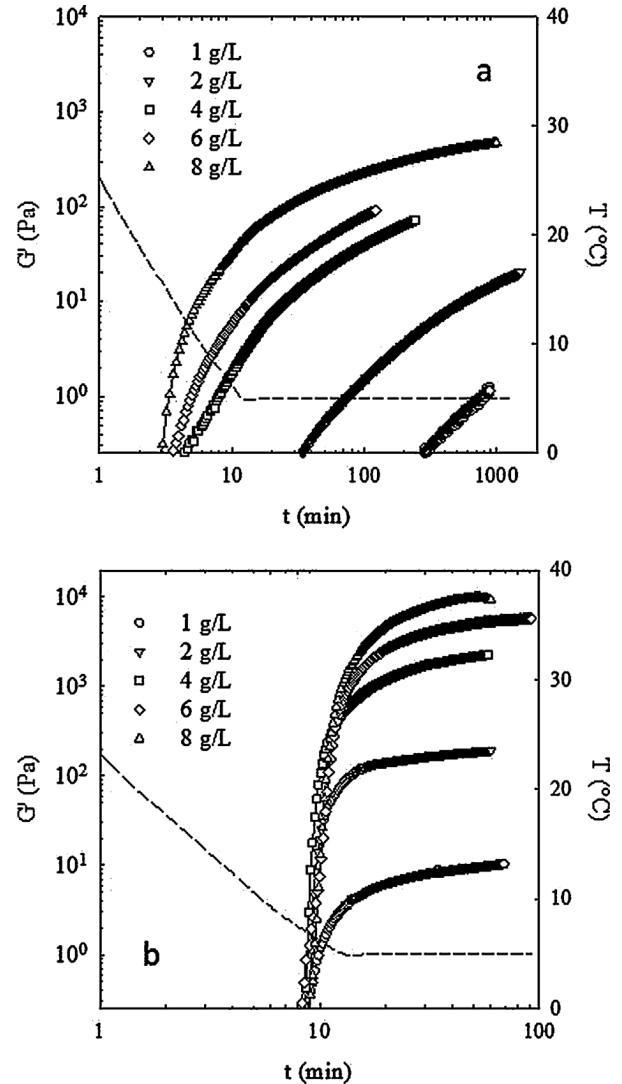
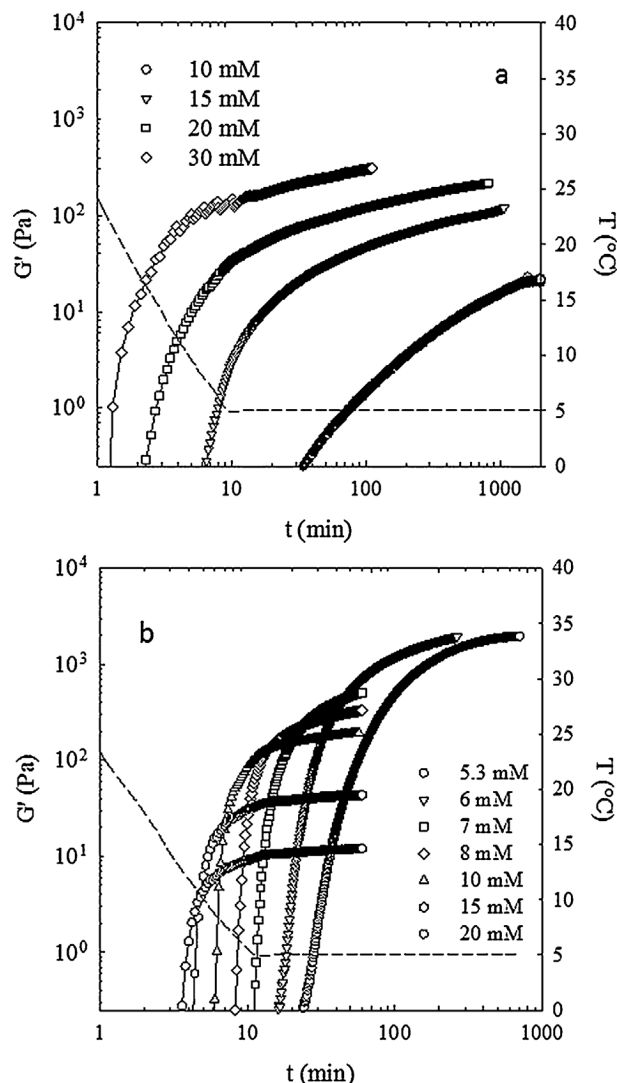


Fig. 2. Evolution of the storage shear modulus at 0.1 Hz for different concentrations of  $\kappa$ -car at 10 mM KCl (a) or 10 mM  $\text{CaCl}_2$  (b) during and after rapid cooling to 5 °C. The dashed lines indicate the temperature of the sample.



**Fig. 3.** Evolution of the storage shear modulus at 0.1 Hz of 2 g/L  $\kappa$ -car at different KCl concentrations (a) or different  $\text{CaCl}_2$  concentrations (b) during and after rapid cooling to 5 °C. The dashed lines indicate the temperature of the sample.

which is illustrated in Fig. 2a where the evolution of  $G'$  is shown after rapid cooling to 5 °C from the liquid state at 50 °C.

The effect of the KCl concentration on the evolution of the shear modulus after rapid cooling to 5 °C at  $C=2$  g/L  $\kappa$ -car is shown in Fig. 3a. At low KCl concentrations gelation is extremely slow, but with increasing KCl concentration gelation becomes faster and the shear modulus becomes larger.

### 3.2. Pure calcium induced gelation

Fig. 2b shows that in the presence of 10 mM  $\text{CaCl}_2$  gelation was fast even at low  $\kappa$ -car concentrations and the gel moduli were much higher than at 10 mM KCl even though the critical gelation temperature was lower ( $T_c \approx 10$  °C). The evolution after rapidly cooling to 5 °C is shown for  $C=2$  g/L  $\kappa$ -car at different  $\text{CaCl}_2$  concentrations in Fig. 3b. Clearly gelation induced by calcium ions is much faster than gelation induced by potassium ions except at 5.3 mM  $\text{CaCl}_2$  where it took several hours to approach steady state. We did not observe gelation at  $[\text{CaCl}_2]=4$  mM in the fridge at 4 °C even after several weeks. Samples with higher  $\kappa$ -car concentrations up to 8 g/L did not show gelation at 4 mM  $\text{CaCl}_2$  either. Trials with intermediate

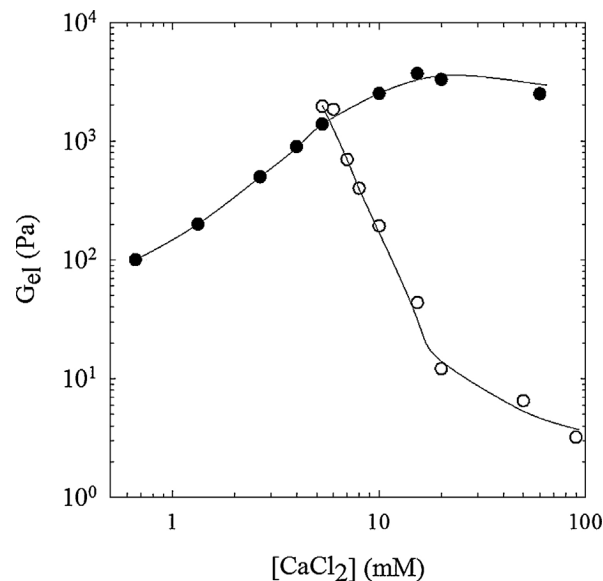


**Fig. 4.** Elastic modulus of  $\kappa$ -car gels at  $C=2$  g/L as a function of the  $\text{CaCl}_2$  concentration at 5 °C in the absence (open symbols) and presence of 10 mM KCl (closed symbols).

$\text{CaCl}_2$  concentration showed that a gel was formed at 5.0 mM after 2 days, but no gels were formed at 4.7 mM.

The frequency dependence of the shear moduli was measured after the system was allowed to evolve at 5 °C. For all systems discussed here  $G'$  was larger than  $G''$  and was almost independent of the frequency at lower frequencies where  $G'$  is equal to the elastic modulus ( $G_{el}$ ) of the gels. The dependence of  $G_{el}$  near steady state on the  $\text{CaCl}_2$  concentration is shown in Fig. 4. Remarkably, the gel modulus decreased with increasing  $\text{CaCl}_2$  concentration, whereas it increased with increasing KCl concentration, see Fig. 3a. Another notable difference between gels induced by KCl and  $\text{CaCl}_2$  was that the latter became increasingly turbid with increasing  $[\text{CaCl}_2]$ , whereas the former remained transparent, see Fig. 5.

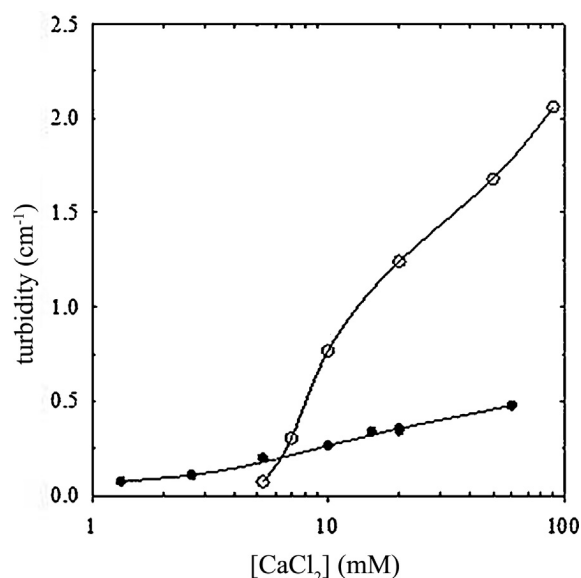


**Fig. 5.** Turbidity of  $\kappa$ -car gels at  $C=2$  g/L as a function of the  $\text{CaCl}_2$  concentration at 5 °C in the absence (open symbols) and presence of 10 mM KCl (closed symbols).

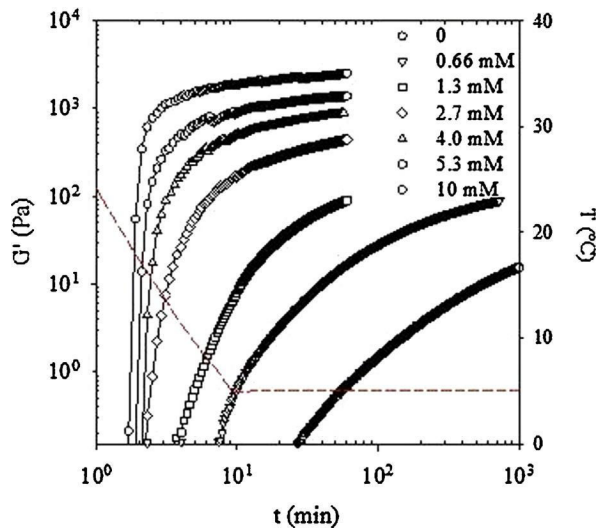


**Fig. 6.** Evolution of the storage shear modulus at 0.1 Hz of 2 g/L  $\kappa$ -car with 10 mM KCl at different  $\text{CaCl}_2$  concentrations during and after rapid cooling to 5 °C. The dashed line indicates the temperature of the sample.

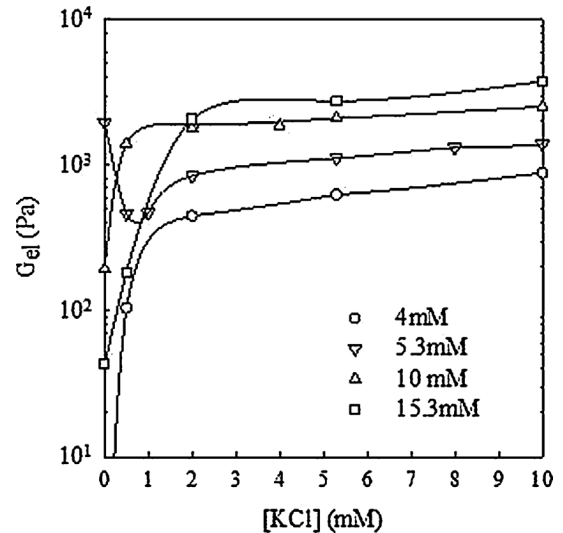
### 3.3. Influence of $\text{CaCl}_2$ on potassium induced gelation

Fig. 6 shows the evolution of  $G'$  after rapid cooling to 5 °C for  $\kappa$ -car solutions at  $C = 2$  g/L in the presence of 10 mM KCl and various concentrations of  $\text{CaCl}_2$ . The critical gelation temperature of  $\kappa$ -car in 10 mM KCl is higher than that in pure  $\text{CaCl}_2$  in the range used here. In fact, temperature ramps showed that addition of  $\text{CaCl}_2$  did not increase  $T_c$  significantly. Therefore we may assume that for all systems gelation is induced by KCl. However, gelation was found to be much faster in the presence of  $\text{CaCl}_2$  even if it was in very small amounts. In addition, the gel modulus at steady state increased with increasing  $\text{CaCl}_2$  concentration in contrast to pure  $\text{CaCl}_2$  solutions for which it decreased, see Fig. 3b.

In Fig. 4 the elastic modulus near steady state is shown as a function of the  $\text{CaCl}_2$  concentration and compared to that in the absence of KCl. In the latter case,  $G_{el}$  decreased rapidly with increasing  $\text{CaCl}_2$  concentration starting from about 2 kPa at 5.3 mM  $\text{CaCl}_2$ . In the presence of 10 mM KCl the elastic modulus increased with increasing  $\text{CaCl}_2$  concentration until about 15 mM where it reached a value of 4 kPa. The presence of 10 mM KCl also led to a decrease of the turbidity of the gels, implying that they were more homogeneous, see Fig. 5.

The effect of the KCl concentration on the elastic modulus in the presence of different amounts of  $\text{CaCl}_2$  is shown in Fig. 7. It appears that addition of as little as 0.5 mM KCl has a strong effect on  $\kappa$ -car gelation in the presence of  $\text{CaCl}_2$ . The presence of a small amount of KCl induced gelation at  $[\text{CaCl}_2] = 4$  mM when in pure salts no gelation was observed. Adding more than 2 mM KCl does not further strengthen the gel significantly even though it led to an increase of  $T_c$ . A peculiar phenomenon was observed at 5.3 mM  $\text{CaCl}_2$ . In this case the gel in pure  $\text{CaCl}_2$  was slightly stronger than when KCl was added. However, addition of KCl strongly increased the gelation rate, which was very slow in the absence of KCl, see Fig. 3b.

Fig. 8 shows the dependence of the gel modulus at 5 °C on the  $\kappa$ -car concentration in the presence of 10 mM  $\text{CaCl}_2$  and 5.3 mM KCl. The results in the mixed salt are compared to that in pure 10 mM  $\text{CaCl}_2$ . We note that in pure 5.3 mM KCl gelation was very slow and the elastic modulus was very small. As might be expected, in both cases  $G_{el}$  increased with increasing  $\kappa$ -car concentration. However, the increase is weaker in the mixed salt and the effect of adding KCl decreased with increasing  $\kappa$ -car concentration.



**Fig. 7.** Elastic modulus of  $\kappa$ -car gels at  $C = 2$  g/L as a function of the KCl concentration at 5 °C in the presence of different  $\text{CaCl}_2$  concentrations.

Clearly, the synergistic effect of mixing the two types of salt is less important when the gels are strong.

### 3.4. Influence of NaCl on potassium induced gelation

A possible origin of the strong influence of  $\text{CaCl}_2$  on the potassium induced gelation of  $\kappa$ -car is screening of the electrostatic interactions between the chains. In this case addition of NaCl would have the same effect at the same ionic strength ( $I$ ). Fig. 9 shows the effect of adding NaCl on the gelation of 2 g/L  $\kappa$ -car at 5 °C induced by the presence of 10 mM KCl. Qualitatively the effect of adding NaCl was the same as that of adding  $\text{CaCl}_2$ , i.e. acceleration of the gelation process and increase of the elastic modulus. However, quantitative comparison of the elastic modulus at the same ionic strength ( $I = [\text{NaCl}]$  and  $I = 3[\text{CaCl}_2]$ ) shows that the influence of  $\text{CaCl}_2$  was much stronger, see Fig. 10. Nevertheless, the presence of  $\text{Na}^+$  was significant even at concentrations as low as 5 mM. This means that the contribution of the sodium counterions of the  $\kappa$ -car cannot be completely neglected, because we add roughly 2 mM  $\text{Na}^+$  counterions per gram of  $\kappa$ -car.

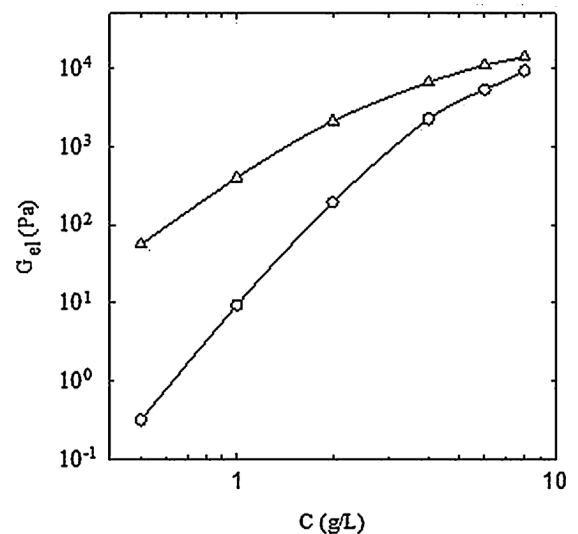


**Fig. 8.** Dependence of the elastic modulus at 5 °C on the  $\kappa$ -car concentration at  $[\text{CaCl}_2] = 10$  mM with ( $\Delta$ ) and without 5.3 mM KCl ( $\circ$ ).



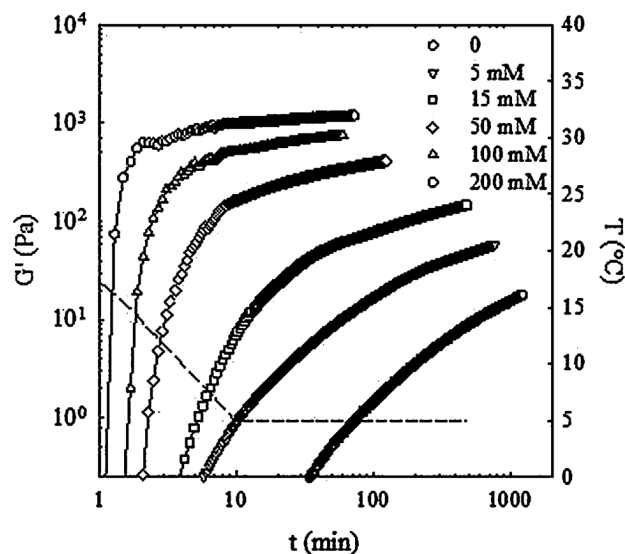


**Fig. 9.** Evolution of the storage shear modulus at 0.1 Hz of 2 g/L  $\kappa$ -car with 10 mM KCl at different NaCl concentrations during and after rapid cooling to 5 °C. The dashed line indicates the temperature of the sample.

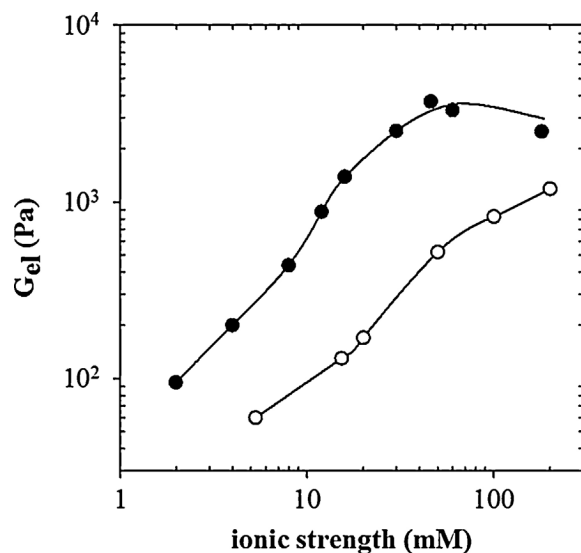


**Fig. 10.** Elastic modulus of 2 g/L  $\kappa$ -car with 10 mM KCl at 5 °C as a function of the ionic strength of added  $\text{CaCl}_2$  (closed symbols) or added NaCl (open symbols). Solid lines are guides to the eye.

#### 4. Discussion

$\kappa$ -Carrageenan gels because helices from different chains associate laterally. Therefore a necessary condition to form a gel is to induce the coil–helix transition. This transition occurs below a critical temperature that is strongly dependent on the type and concentration of ions that are present including the counterions. However, the critical temperature is independent of the polysaccharide concentration as long as the contribution of the counterions can be neglected. The association of helices accelerates with increasing concentration and for a given concentration with decreasing temperature, as was reported in more detail elsewhere (Meunier et al., 1999).

It is remarkable that the gel stiffness increased with increasing the cation concentration in the case of pure  $\text{K}^+$ , at least up to 100 mM, but the elastic modulus decreased in the case of pure  $\text{Ca}^{2+}$ . As was mentioned in the introduction, it has been reported that  $G_{el}$  increases at low  $\text{Ca}^{2+}$  and decreases only at higher  $\text{Ca}^{2+}$

concentrations, while here we only observe a decrease. However, the initial increase may have been observed for samples for which  $G'$  had not yet reached its steady state value, because the gelation kinetics can be very slow at lower salt concentrations. Another remarkable difference between gels induced by pure  $\text{K}^+$  and by pure  $\text{Ca}^{2+}$  is that the latter become increasingly turbid when more ions are present, while the former remain transparent. The most likely cause for the difference between gelation induced by pure  $\text{K}^+$  and pure  $\text{Ca}^{2+}$  is that in the presence of higher  $\text{Ca}^{2+}$  concentrations the helices stack into thicker strands that form more heterogeneous gels.

In the presence of pure  $\text{K}^+$  the association of the helices was very slow at low polymer concentrations even 15 degrees below  $T_c$ . Most likely the association was inhibited by electrostatic repulsion between the helices, which explains why adding NaCl strongly sped up this process. NaCl did not modify the coil–helix transition induced by 10 mM KCl, at least below 0.2 M, but it screened the electrostatic repulsion. By itself NaCl induced the formation of weak turbid gels only above 0.1 M.

The synergistic effect on gelation of adding  $\text{K}^+$  and  $\text{Ca}^{2+}$  together was very strong and cannot be explained only in terms of the ionic strength. Especially at low ionic strengths the effect of adding  $\text{Ca}^{2+}$  on  $\text{K}^+$  induced gelation was much stronger than that of  $\text{Na}^+$  even though neither of the ions influenced the coil–helix transition at these lower ionic strengths. This observation indicates that specific binding of  $\text{Ca}^{2+}$  to  $\kappa$ -car occurred as was already suggested by Doyle et al. (2002), which reduced the charge density of the chains much more effectively than merely screening.

Inversely, addition of as little as 2 mM KCl completely modified  $\text{Ca}^{2+}$  induced gelation. Instead of decreasing with increasing  $\text{Ca}^{2+}$  concentration in pure  $\text{CaCl}_2$ , the elastic modulus increased with increasing  $\text{Ca}^{2+}$  concentration when KCl was present. We note that by itself 2 mM KCl did not give rise to a significant increase of the shear modulus. Clearly, such small amounts of  $\text{K}^+$  do not influence the electrostatic interactions significantly, so the effect must be attributed to the influence on the helix formation. The much lower turbidity in the presence of  $\text{K}^+$  even at high  $\text{Ca}^{2+}$  concentrations also indicates that different types of gels are formed that are much more homogeneous. Remarkably, gels were formed rapidly in 2 mM KCl even for  $[\text{CaCl}_2] < 5 \text{ mM}$ , i.e. under conditions where pure salts did not cause a significant increase of the shear modulus.

The case of 5.3 mM  $\text{CaCl}_2$  is peculiar in that addition of KCl led to a decrease of  $G_{el}$  up to 1 mM. At higher KCl concentrations  $G_{el}$  increased again, but remained slightly lower than without KCl. However, the gels with added KCl were formed much more rapidly, compare Figs. 3b and 6. The minimum of  $G_{el}$  as a function of the KCl concentration at 5.3 mM  $\text{CaCl}_2$  can be understood from the fact that when KCl is added the gel is no longer induced by  $\text{Ca}^{2+}$ , but by  $\text{K}^+$ . At higher  $\text{CaCl}_2$  concentrations the  $\text{K}^+$  induced gel is stronger than the  $\text{Ca}^{2+}$  induced gel, but in the presence of 5.3 mM  $\text{CaCl}_2$  it is slightly weaker.

The increase of the stiffness of  $\text{K}^+$  induced gels by the reduction of electrostatic repulsion should also apply to screening by KCl at temperatures significantly below  $T_c$ . The origin for the increase of the elastic modulus with increasing KCl concentration could therefore be, at least in part, the effect of screening rather than the effect of increasing  $T_c$ . In fact, if we consider the further addition of KCl in excess of 10 mM in the same way as that of NaCl and  $\text{CaCl}_2$ , we find that the increase of the  $G_{el}$  with increasing ionic strength by adding more KCl shown in Fig. 2a is intermediate between that by adding NaCl and by adding  $\text{CaCl}_2$ .

#### 5. Conclusion

$\kappa$ -Car gels are formed below the coil–helix transition temperature in the presence of KCl or  $\text{CaCl}_2$ , but with different structures.

In KCl the gel stiffness increases with increasing salt concentration and the gels remain transparent, while in  $\text{CaCl}_2$  the gel stiffness decreases with increasing salt concentration and they become increasingly turbid.

Addition of NaCl reduces the electrostatic repulsion between the helices which facilitates their association for  $\text{K}^+$  induced gelation. As a consequence the gel stiffness and the gelation rate increase with increasing NaCl concentration. A similar effect on  $\text{K}^+$  induced  $\kappa$ -car gelation is observed when  $\text{CaCl}_2$  is added. However, the effect is much stronger than for NaCl at the same ionic strength indicating specific binding of  $\text{Ca}^{2+}$  to  $\kappa$ -car.

The presence of a small amount of KCl strongly modifies the  $\text{Ca}^{2+}$  induced gelation of  $\kappa$ -car. Especially at higher  $\text{CaCl}_2$  concentrations it leads to a strong increase of the elastic modulus and a reduction of the turbidity. The synergistic between  $\text{Ca}^{2+}$  and  $\text{K}^+$  is most striking when the gels are weak in the pure salts.

### Acknowledgement

BTN thanks the Ministry of Education and Training of Vietnam for financial support.

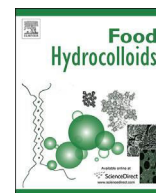
### References

- Doyle, J., Giannouli, P., Philp, K., & Morris, E. (2002). Effect of  $\text{K}^+$  and  $\text{Ca}^{2+}$  cations on gelation of  $\kappa$ -carrageenan. *Gums and Stabilisers for the Food Industry*, 11, 158–164.
- Hermansson, A.-M., Eriksson, E., & Jordansson, E. (1991). Effects of potassium, sodium and calcium on the microstructure and rheological behaviour of kappa-carrageenan gels. *Carbohydrate Polymers*, 16(3), 297–320.
- MacArtain, P., Jacquier, J., & Dawson, K. (2003). Physical characteristics of calcium induced  $\kappa$ -carrageenan networks. *Carbohydrate Polymers*, 53(4), 395–400.
- Mangione, M. R., Giacomazza, D., Bulone, D., Martorana, V., Cavallaro, G., & San Biagio, P. L. (2005).  $\text{K}^+$  and  $\text{Na}^+$  effects on the gelation properties of  $\kappa$ -carrageenan. *Biophysical Chemistry*, 113, 129–135.
- Meunier, V., Nicolai, T., Durand, D., & Parker, A. (1999). Light scattering and viscoelasticity of aggregating and gelling  $\kappa$ -carrageenan. *Macromolecules*, 32, 2610–2616.
- Michel, A., Mestdagh, M., & Axelos, M. (1997). Physico-chemical properties of carrageenan gels in presence of various cations. *International Journal of Biological Macromolecules*, 21(1), 195–200.
- Nguyen, B. T., Phan-Xuan, T., Benyahia, L., & Nicolai, T. (2012). Combined effects of temperature and elasticity on phase separation in mixtures of  $\kappa$ -carrageenan and  $\beta$ -lg aggregates. *Food Hydrocolloids*, 138–144.
- Nono, M., Durand, D., & Nicolai, T. (2012). Rheology and structure of mixtures of  $\iota$ -carrageenan and sodium caseinate. *Food Hydrocolloids*, 27(1), 235–241.
- Nono, M., Nicolai, T., & Durand, D. (2011).  $G_{el}$  formation of mixtures of  $\kappa$ -carrageenan and sodium caseinate. *Food Hydrocolloids*, 25(4), 750–757.
- Núñez-Santiago, M. d. C., & Tecante, A. (2007). Rheological and calorimetric study of the sol–gel transition of  $\kappa$ -carrageenan. *Carbohydrate Polymers*, 69(4), 763–773.
- Picullell, L. (2006). Gelling carrageenans. In A. M. Stephen, G. O. Philips, & P. A. Williams (Eds.), *Food polysaccharides and their applications* (p. 239). Boca Raton: CRC Press.
- Rochas, C., & Rinaudo, M. (1980). Activity coefficients of counterions and conformation in kappa-carrageenan systems. *Biopolymers*, 19, 1675–1687.
- Thrimawithana, T., Young, S., Dunstan, D., & Alany, R. (2010). Texture and rheological characterization of kappa and iota carrageenan in the presence of counter ions. *Carbohydrate Polymers*, 82(1), 69–77.

## **PAPER 2**







# Combined effects of temperature and elasticity on phase separation in mixtures of $\kappa$ -carrageenan and $\beta$ -lactoglobulin aggregates



Nguyen Trong Bach, Tuan Phan-Xuan, Lazhar Benyahia, Taco Nicolai\*

LUNAM, Université du Maine, IMMM UMR CNRS 6283, PCI, 72085 Le Mans cedex 9, France

## ARTICLE INFO

### Article history:

Received 23 May 2012

Accepted 12 November 2012

### Keywords:

Protein  
Polysaccharide  
Phase separation  
Gelation

## ABSTRACT

Aqueous mixtures of small aggregates of the globular whey protein ( $\beta$ -lactoglobulin) and the anionic polysaccharide ( $\kappa$ -carrageenan) were studied at neutral pH. The effect of the temperature on the phase separation was investigated by measuring the turbidity during cooling and heating. Gelation of  $\kappa$ -carrageenan was induced by adding small quantities of KCl. It is shown that gelation partially reverts phase separation. The dependence of phase separation on the elastic modulus was quantified. Phase separation could be rendered irreversible by ageing in the presence of calcium ions.

© 2012 Elsevier Ltd. All rights reserved.

## 1. Introduction

Food products often contain aqueous mixtures of proteins and polysaccharides and understanding the behaviour of such mixtures is important for the use of existing food products or the development of new ones. Complex coacervation, phase separation and gelation can give rise to a wide range of phenomena that are, as yet, far from being fully understood (Tolstoguzov, 2003; Turgeon, Beaulieu, Schmitt, & Sanchez, 2003; Turgeon, Schmitt, & Sanchez, 2007). Here we report on an investigation of aqueous mixtures of the globular protein  $\beta$ -lactoglobulin ( $\beta$ -lg) and the polysaccharide  $\kappa$ -carrageenan ( $\kappa$ -car) at pH 7, where both are negatively charged and do not associate.

$\beta$ -lg is the main protein component of whey. When heated in aqueous solution it denatures leading to irreversible aggregation and at high concentrations to gelation (Clark, 1999; Foegeding, 2006; Nicolai, 2007b). The structure and size of the aggregates depend on the protein concentration, the pH, the type and concentration of added salt (Nicolai, Britten, & Schmitt, 2011). When  $\beta$ -lg is heated at a pH above its isoelectric point ( $pI = 5.2$ ) in the presence of anionic polysaccharides, usually heterogeneous gels with a variety of different structures are formed (Ako, Durand, & Nicolai, 2011; Cakir & Foegeding, 2011; de Jong, Klok, & van de Velde, 2009). The origin of these structures is micro-phase separation between  $\beta$ -lg aggregates and the polysaccharides that is frozen-in by gel formation.

One of the polysaccharides that has been most intensively investigated in this context is  $\kappa$ -carrageenan.  $\kappa$ -car is an anionic

polysaccharide isolated from green algae that gels in aqueous solutions when cooled below a critical temperature ( $T_g$ ) in the presence of specific cations (Piculell, 2006). Notably, potassium can induce gelation at room temperature at low concentrations. The gelation of  $\kappa$ -car is preceded by a coil–helix transition and is probably caused by parallel association of the helices. Gelation of  $\kappa$ -car is reversible, but the melting temperature ( $T_m$ ) is usually significantly higher than  $T_g$ .

$\kappa$ -car is fully compatible with native  $\beta$ -lg up to very high concentrations, but mixed gels formed by heating  $\kappa$ -car/ $\beta$ -lg mixtures show clear signs of phase separation initiated by the formation of  $\beta$ -lg aggregates (Cakir et al., 2011; Capron, Nicolai, & Smith, 1999; Croguennoc, Durand, & Nicolai, 2001a). In order to better understand the process of phase separation, studies have been made of mixtures of stable  $\beta$ -lg aggregates suspensions and  $\kappa$ -car at room temperature (Baussay, Nicolai, & Durand, 2006b; Croguennoc, Durand, & Nicolai, 2001b). These investigations have shown that phase separation occurs above a critical  $\kappa$ -car concentration that decreases with increasing size of the  $\beta$ -lg aggregates, but is only weakly dependent on the  $\beta$ -lg concentration. Phase separation was found to lead to the formation of relatively stable micron sized protein rich domains that stick, but do not spontaneously fuse. Initially, the domains are liquid and the phase separation can be fully reversed by dilution. However, in the presence of salt the aggregates within the domains slowly form permanent bonds and convert into microgels. This phenomenon is called cold gelation, because it does not require heat induced denaturation of native proteins (Ako, Nicolai, & Durand, 2010; Barbut & Foegeding, 1993; Bryant & McClements, 2000).

As far as we are aware, the effect of the temperature on phase separation between globular protein aggregates and polysaccharides

\* Corresponding author.

E-mail address: [Taco.Nicolai@univ-lemans.fr](mailto:Taco.Nicolai@univ-lemans.fr) (T. Nicolai).

has not yet been investigated. An increase of the critical  $\kappa$ -car concentration with increasing temperature might be expected because the contribution of the mixing entropy to the free energy increases. However, it has been suggested that the main origin for phase separation is depletion of polysaccharide chains from between neighbouring protein aggregates (Gaaloul, Turgeon, & Corredig, 2010; Tuinier, Rieger, & Kruif, 2003). Depletion causes an effective attraction between the aggregates and can lead to phase separation. However, if depletion is the main driving force for phase separation, no effect of the temperature is expected as the origin of the depletion interaction is entropic and therefore has the same temperature dependence as the mixing entropy.

Remarkably, gelation of  $\kappa$ -car chains can lead to reversal of the phase separation as long as the domains are liquid (Baussay, Nicolai, & Durand, 2006a). Most often, the reversal is only partial, i.e., the domains persist, but a large fraction of the aggregates exits the domains and disperse into the continuous polysaccharide rich phase. The ejected aggregates reenter the domains as soon as the  $\kappa$ -car gel is melted by raising the temperature above  $T_m$ . So far, the relationship between the elasticity and the extent of phase separation has not yet been quantified.

One of the objectives of the present work was to investigate the effect of temperature on the phase separation between  $\beta$ -lg aggregates and  $\kappa$ -car. The second objective was to quantify the relationship between the elastic modulus of the  $\kappa$ -car gel and the extent of phase separation. We will show that the combined effects of temperature and elasticity can explain the curious phenomenon of transient phase separation during cooling of these mixtures that was reported recently (Ako et al., 2011). Finally, the effect of ageing due to crosslinking of the aggregates in the protein dense domains will be discussed.

## 2. Materials and methods

### 2.1. Materials

The sodium  $\kappa$ -carrageenan used for this study is an alkali treated extract from *Eucheuma cottonii* and was a gift from Cargill (Baupre, France). Using NMR it was found that the sample contained less than 5%  $\kappa$ -carrageenan. A freeze-dried sample of  $\kappa$ -car was dissolved by stirring for a few hours in Milli-Q water (70 °C) with 200 ppm sodium azide added as a bacteriostatic agent. The solution was extensively dialysed against Milli-Q water at pH7 and subsequently filtered through 0.45  $\mu$ m pore size Anotop filters. The pH of the solution was adjusted to 7 by adding small amounts of HCl 0.1 M. The  $\kappa$ -car concentration ( $C_k$ ) was determined by measuring the refractive index using refractive index increment 0.145 g/ml. The molar mass ( $M_w$ ) and radius of gyration ( $R_g$ ) were determined by light scattering as described elsewhere (Meunier, Nicolai, Durand, & Parker, 1999):  $M_w = 2.1 \times 10^5$  g/mol,  $R_g = 52$  nm.

The  $\beta$ -lactoglobulin (Biopure, lot JE 001-8-415) used in this study was purchased from Davisco Foods International, Inc. (Le Sueur, MN, USA) and consisted of approximately equal quantities of variants A and B. The powder was dissolved in Milli-Q water which contained 200 ppm NaN<sub>3</sub> to prevent bacterial growth. Solutions were dialysed extensively against Milli-Q water with 200 ppm sodium azide and subsequently filtered through 0.2  $\mu$ m pore size Anotop filters. The pH of the solution was adjusted to 7 by adding small amounts of NaOH 0.1 M. The protein concentration was determined by UV absorption at 278 nm using extinction coefficient  $0.96 \text{ Lg}^{-1}\text{cm}^{-1}$ .

$\beta$ -lg aggregates were prepared by heating a solution containing 50 g/L native  $\beta$ -lg at 85 °C until steady state was reached (overnight) and the residual fraction of native proteins was negligible. The hydrodynamic radius of the aggregates was determined using dynamic light scattering (Nicolai, 2007a) and was found to be

$17 \pm 2$  nm. Mixtures with the required composition were prepared by first mixing the  $\beta$ -lg aggregate solution with a KCl solution and subsequently adding the  $\kappa$ -car solution. The mixtures were kept while stirring at 50 °C for 15 min.

### 2.2. Methods

The shear moduli were determined as a function of the frequency and the temperature using a stress imposed rheometer (AR2000, TA Instruments) using a plate – plate geometry (diameter 40 mm, gap 700  $\mu$ m). The temperature was controlled by a Peltier system and the geometry was covered with paraffin oil to prevent water evaporation. For some systems the gel partially slipped leading to a strong decrease of the shear modulus. In this case sandpaper was glued onto the two surfaces of the geometry. In all cases the measurements were done in the linear response regime.

Turbidity measurements were done as a function of the wavelength in rectangular air tight cells using a UV–Visible spectrometer Varian Cary-50 Bio (Les Ulis, France). Different path lengths were used depending on the turbidity of the samples in order to avoid saturation. Measurements were done at different temperatures that were controlled within 0.2 °C using a thermostat bath.

Confocal Laser Scanning Microscopy (CLSM) was used in the fluorescence mode. Observations were made with a Leica TCS-SP2 (Leica Microsystems Heidelberg, Germany). A water immersion objective lens was used HCxPL APO 63x NA = 1.2 with theoretical resolution of 0.3  $\mu$ m in the  $x$ – $y$  plane.  $\beta$ -lg was labelled with the fluorochrome rhodamine B isothiocyanate, by adding a small amount of a concentrated rhodamine solution (5 ppm) to the  $\beta$ -lg solutions before heat treatment. No effect of labelling on the phase separation was observed. The fluorescence of the probe was not influenced by heating.

## 3. Results

### 3.1. Phase behaviour

Mixtures of  $\kappa$ -car and small  $\beta$ -lg aggregates ( $R_h = 17 \pm 2$  nm) with a range of  $\kappa$ -car ( $C_k$ ) and  $\beta$ -lg ( $C_b$ ) concentrations were checked for signs of phase separation. Phase separation was easily detected by a strong increase of the turbidity. The phase diagram is shown in Fig. 1. Phase separation led to the formation of dense spherical

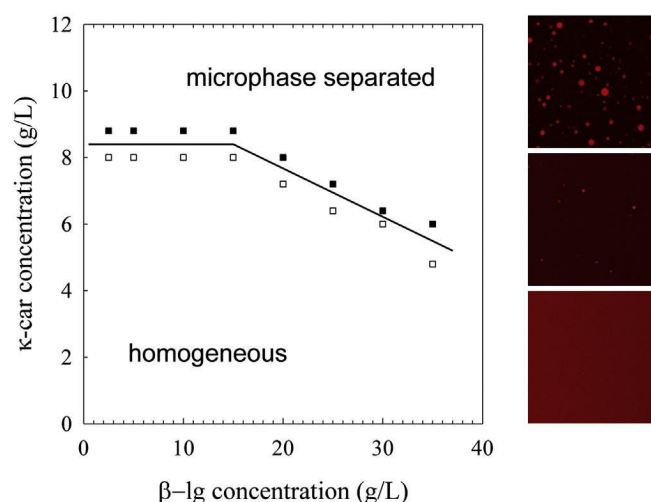


**Fig. 1.** Phase diagram of aqueous mixtures of  $\beta$ -lg aggregates and  $\kappa$ -car chains at 20 °C. The open and filled symbols correspond to homogeneous and phase separated mixtures, respectively. The solid line indicates the phase boundary. CLSM images representing  $150 \times 150 \mu\text{m}$  are shown of mixtures containing 20 g/L  $\beta$ -lg and different  $\kappa$ -car concentrations: 10, 8 and 7.5 g/L, top to bottom.

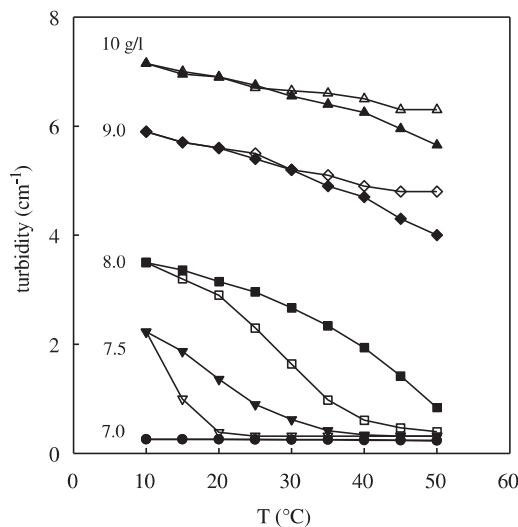


**Fig. 2.** Temperature dependence of the turbidity of aqueous mixtures of 20 g/L  $\beta$ -Ig aggregates and different  $\kappa$ -car concentrations indicated in the figure after cooling (open symbols) and subsequent heating (closed symbols) in steps of 5 °C following the protocol described in the text.

domains enriched in proteins that can be visualized using CLSM. The number of domains increased with increasing  $\kappa$ -car and  $\beta$ -Ig concentration. The protein concentration in the domains was determined by measuring the fluorescence intensity that is proportional to  $C_b$  at the conditions used for this study.  $C_b$  increased from about 70 g/L to about 150 g/L. The domains merged and precipitated slowly, but could be easily redispersed by shaking.

The turbidity is a useful qualitative measure of the extent of phase separation for these mixtures, because, at least initially, more phase separation expressed itself in the formation of more and denser domains with about the same size. This means that the turbidity was approximately proportional to the amount of phase separated proteins. However, over a period of hours the turbidity decreased due to merging and precipitation of the domains.

### 3.2. The effect of temperature on phase separation

The effect of heating on the phase separation was studied by measuring the turbidity as a function of the temperature for mixtures containing 20 g/L protein aggregates and various amounts of  $\kappa$ -car, see Fig. 2. The temperature was decreased from 50 °C to

10 °C in steps of 5 °C and subsequently increased again to 50 °C. The turbidity was monitored during 20 min at each temperature. This allowed the system to reach steady state in most situations except very close to the phase boundary, where the turbidity kept increasing significantly for a longer time. However, as mentioned above, only a quasi steady state is reached, because on time scales of hours the protein rich domains slowly fused and precipitated.

At  $C_k = 7$  g/L and lower, the system remained homogeneous at all temperatures, but at  $C_k = 7.5$  g/L the turbidity increased sharply when the temperature was decreased below 20 °C. When the temperature was subsequently increased, the turbidity decreased again and the system became homogeneous at 35 °C. The difference between the behaviour at the same temperatures after cooling and after heating can be explained by the fact that close to the phase boundary phase separation was slow and it took longer than 20 min to reach steady state. At  $C_k = 8$  g/L, a similar increase of the turbidity was observed during cooling, but it started at higher temperatures. At  $C_k = 9$  g/L and higher, the effect of the temperature became relatively small. At these higher concentrations, the turbidity is lower at higher temperatures during heating, which is caused by partial sedimentation of the protein rich domains.

The effect of heating on the onset of phase separation was investigated also at other protein concentrations and in each case we found a small increase of the critical  $\kappa$ -car concentration ( $C_k^*$ ) by between 1 and 2 g per litre when the temperature was increased to 80 °C.

### 3.3. The effect of elasticity on phase separation

As was mentioned in the introduction,  $\kappa$ -car solutions gel when cooled in the presence of a small amount of potassium ions. Fig. 3 shows the storage shear modulus ( $G'$ ) at 0.1 Hz as a function of the temperature during a cooling and heating ramp at a rate of 2 °C/min for  $\kappa$ -car solutions containing 0.02 M KCl. Gels were formed below a critical gelation temperature ( $T_g$ ) and melted when subsequently heated above a somewhat higher critical melting temperature ( $T_m$ ). Varying the heating and cooling rates shifts the critical temperatures, but the effect becomes very small below 2 °C/min.  $T_g$  and  $T_m$  depended little on the  $\kappa$ -car concentration in this range, but  $G'$  increased with increasing  $C_k$  (Fig. 3a). Increasing the KCl concentration led to an increase of both the critical temperatures and the shear modulus (Fig. 3b). These results were not significantly influenced by the addition of  $\beta$ -Ig at least up to 20 g/L.

The effect of gelation on phase separation was investigated by measuring the turbidity as a function of the temperature. We note

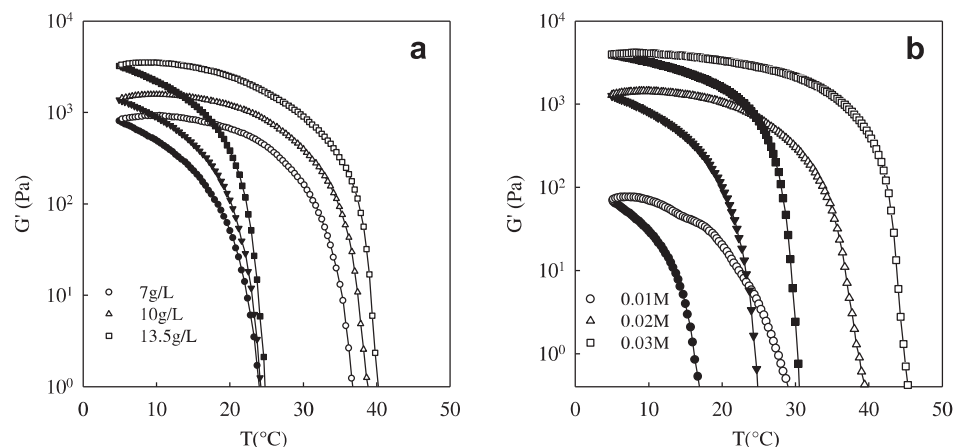


**Fig. 3.** Storage shear modulus at 0.1 Hz during cooling (closed symbols) and subsequent heating (open symbols) ramps at a rate of 2 °C/min of aqueous solutions of  $\kappa$ -car containing 0.02 M KCl and different  $\kappa$ -car concentrations (a) or  $C_k = 10$  g/L and different KCl concentrations (b).

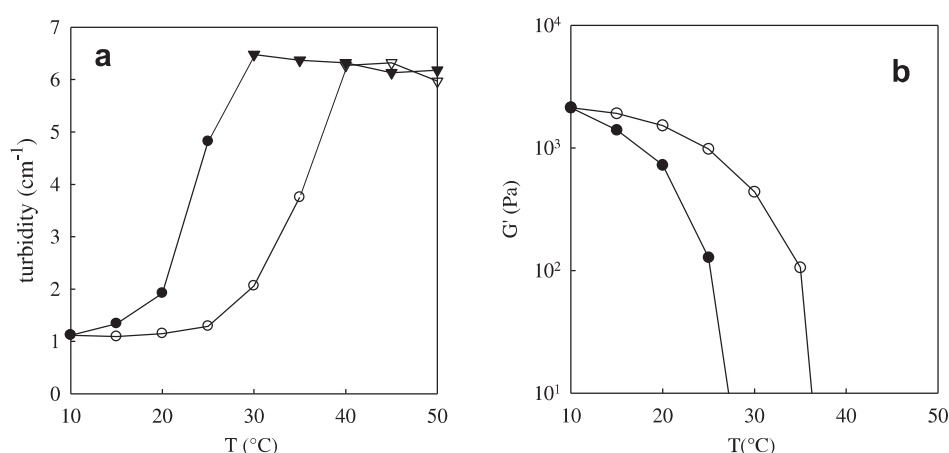


**Fig. 4.** Temperature dependence of the turbidity (a) and the elastic modulus (b) of an aqueous mixture containing 20 g/L  $\beta$ -lg aggregates, 10 g/L  $\kappa$ -car and 0.02 M KCl after cooling (closed symbols) and subsequent heating (open symbols) in steps of 5 °C following the protocol described in the text. The triangles in Fig. 4a indicate liquid samples.

that pure  $\kappa$ -car solutions and gels were transparent at the conditions studied here. Fig. 4a shows the temperature dependence of the turbidity for a mixture with  $C_b = 20$  g/L and  $C_k = 10$  g/L containing 0.02 M KCl. At this  $\kappa$ -car concentration the effect of the temperature on phase separation was negligible, see Fig. 2. It is clear that gelling had an effect on the phase separation as it caused a strong reduction of the turbidity.

In order to correlate directly the elasticity of the  $\kappa$ -car gel with the turbidity, we have measured the storage shear modulus at 0.1 Hz in steps of 5 °C using the same heating and cooling protocol as for the turbidity measurements, see Fig. 4b. We note that the values of  $G'$  obtained in this way are somewhat higher than those obtained during the heating and cooling ramps shown in Fig. 2 especially close to  $T_g$ , where gel formation was slow. The frequency dependence of  $G'$  was very weak for the gels so that the value of  $G'$  can be equated with the elastic modulus. The values of  $G'$  for the liquids ( $G'(0.1 \text{ Hz}) < 1 \text{ Pa}$ ) depended on the frequency and are not representatives of the elasticity of the system.

Fig. 5a shows the dependence of the turbidity on the elastic modulus obtained during heating and cooling in the presence of 0.01 and 0.02 M KCl. Stronger gels were formed when more KCl was added, but within the experimental uncertainty we found the same correlation between the elastic modulus and the turbidity. The same measurements were done for mixtures containing less (9 g/L)

and more (13.5 g/L)  $\kappa$ -car. The turbidity was normalized by that in the liquid state to compensate for the stronger phase separation at higher  $\kappa$ -car concentrations. Fig. 5b shows that the effect of the elasticity on the turbidity decreased with increasing  $\kappa$ -car concentration. As might be expected, larger elasticity was necessary to reverse the stronger phase separation at higher  $\kappa$ -car concentrations. It is clear, however, that the effect of increased incompatibility with increasing  $\kappa$ -car concentration dominates the effect of increased elasticity.

### 3.4. Combined effects of temperature and elasticity

We have seen that at lower  $\kappa$ -car concentrations (8 and 7.5 g/L) the extent of phase separation depends strongly on the temperature. When 0.01 M or more KCl was added to these mixtures the combined effects of temperature and gelation led to the disappearance of phase separation at  $C_k = 7.5$  g/L. The reason is that phase separation occurred for this mixture only below the gelation temperature.

At  $C_k = 8$  g/L the combined effects of temperature and elasticity caused transient phase separation during cooling. Fig. 6a shows a mixture containing 0.03 M KCl that was cooled slowly from 50 °C to 10 °C. The extent of phase separation increased during cooling leading to a progressive increase of the turbidity until at about

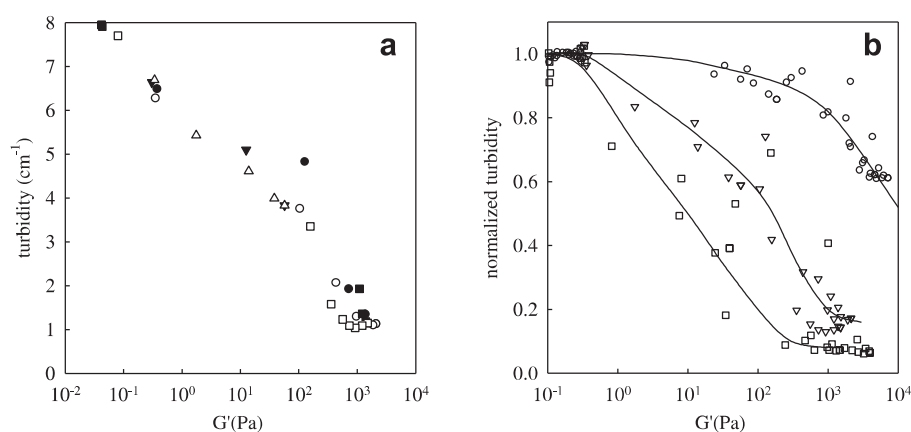


**Fig. 5.** (a) Dependence of the turbidity on the elasticity of the  $\kappa$ -car gels in aqueous mixtures of 20 g/L  $\beta$ -lg aggregates and 10 g/L  $\kappa$ -car obtained during cooling (open symbols) and subsequent heating (closed symbols) following the protocol described in the text. Samples containing either 0.01 M (circles) or 0.02 M (triangles) KCl are indicated by different symbols. (b) Turbidity normalized by the turbidity in the liquid state at  $C_k = 9$  g/L (squares),  $C_k = 10$  g/L (triangles) and  $C_k = 13.5$  g/L (circles). The solid lines are guides to the eye.



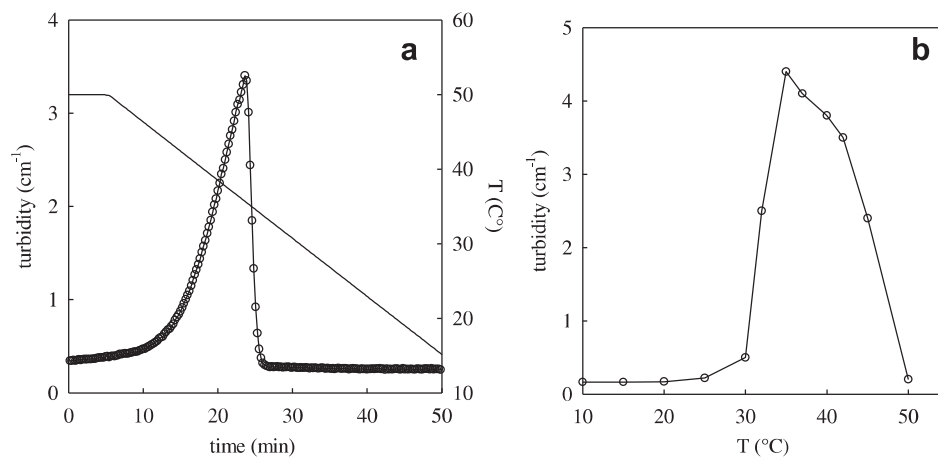


**Fig. 6.** (a) Turbidity of an aqueous mixture of 20 g/L  $\beta$ -lg aggregates and 8 g/L  $\kappa$ -car containing 0.03 M KCl while cooling from 50 °C to 10 °C. The solid line in Fig. 6a indicates the temperature of the mixture. (b) Temperature dependence of the turbidity of the same mixture as in Fig. 6a while cooling in small temperature steps.

35 °C it suddenly dropped to a low value. The drop occurred when the  $\kappa$ -car gelled and shows that phase separation was reversed by the elasticity of the  $\kappa$ -car network. The elastic modulus of the gel reached about  $3 \times 10^3$  Pa. The same system was also cooled in small temperature steps monitoring the turbidity for 20 min at each temperature. Fig. 6b clearly shows the increased effect of phase separation when lowering the temperature below 50 °C and the reversal when  $\kappa$ -car gels below 35 °C. Note that the maximum turbidity was higher in this case because more time was given to phase separate.

The combined effects of temperature and elasticity during heating cannot easily be shown for this system, because at 0.03 M KCl  $\kappa$ -car melts above 45 °C where phase separation is very slow. However, it is very clear at 0.01 M KCl where the system gels during cooling at 20 °C and melts during heating at 30 °C, see Fig. 7. Note that the turbidity during heating was larger than during cooling. We will speculate about the origin of this difference below.

### 3.5. The effect of ageing

In an earlier study it was found that the extent to which phase separation is reversed by gelation decreased with waiting time in the liquid state and became very small after an hour (Baussay et al.,

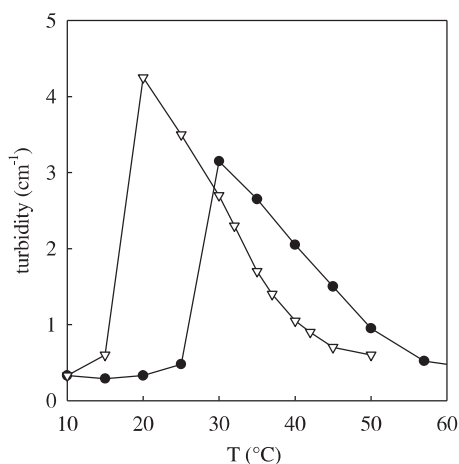


**Fig. 7.** Temperature dependence of the turbidity of a mixture of 20 g/L  $\beta$ -lg aggregates and 8 g/L  $\kappa$ -car containing 0.01 M KCl while cooling (open symbols) and heating (closed symbols) in small temperature steps.

2006a). This phenomenon was attributed to the slow formation of permanent bonds. The latter also explains why when the system was strongly diluted in water it dispersed increasingly slowly with increasing waiting time until after one or two days the domains had converted into stable microgels.

No effect of ageing was observed for the mixtures used here. The effect of gelation on the turbidity was identical even after keeping the mixtures for days in the liquid state. The difference can be explained by the fact that in the earlier study the mixtures contained 0.1 M NaCl. As was mentioned in the introduction, addition of salt can lead to aggregation and gelation of globular protein aggregates. The rate of cold gelation increases with increasing temperature and increasing ionic strength. It also depends on the type of salt. Notably, calcium can induce cold gelation even at very low concentrations. We investigated whether the protein rich domains that were formed in the mixtures studied here could be stabilized by adding small amounts of CaCl<sub>2</sub>. The degree of reversibility of phase separation by gelation was determined by measuring the relative decrease of the turbidity:  $(\tau_{\text{liq}} - \tau_{\text{gel}}) / (\tau_{\text{liq}} - \tau_{\text{gel}})_{t=0}$ , as a function of ageing time in the liquid state at 45 °C and 80 °C. Fig. 8 shows that at 80 °C full stabilization is fast at 3 mM CaCl<sub>2</sub>, but it is important even when as little as 1 mM CaCl<sub>2</sub> is added. As expected, stabilization was slower at 45 °C, results not shown. We note that adding CaCl<sub>2</sub> at these low concentrations does not influence the gelation of  $\kappa$ -car induced by KCl.

## 4. Discussion

Native  $\beta$ -lg is compatible with  $\kappa$ -car up to at least  $C_k = 20$  g/L, but  $\beta$ -lg aggregates are incompatible with  $\kappa$ -car above a critical  $\kappa$ -car concentration ( $C_k^*$ ). It was shown elsewhere that  $C_k^*$  depends little on the protein concentration, but decreases with increasing size of the aggregates (Baussay et al., 2006b). The phase diagram of the mixtures of  $\kappa$ -car and small aggregates shown in Fig. 1 is consistent with this earlier more detailed investigation. Phase separation in solutions containing two different polymers is due to thermodynamic incompatibility and is quite common. The extent of phase separation increases with increasing size of the aggregates, because the mixing entropy decreases.

The effect of the temperature on the phase separation of protein aggregates and polysaccharides had, as far as we are aware, not yet been investigated. The effect is quite subtle as heating up to 80 °C leads only to a small decrease of  $C_k^*$ . It can be explained by the increase of the mixing entropy with increasing temperature that

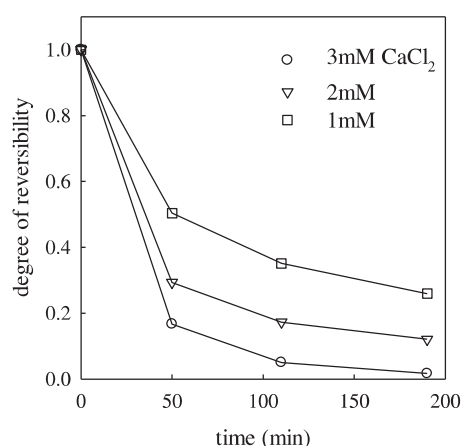


**Fig. 8.** Degree of reversibility of the phase separation by gelation defined as the relative change of the turbidity between the liquid and the gelled state:  $(\tau_{\text{liq}} - \tau_{\text{gel}})/(\tau_{\text{liq}} - \tau_{\text{gel}})_{t=0}$ , as a function of ageing time in the liquid state at 80 °C in the presence of different concentrations of  $\text{CaCl}_2$ . The mixture contained 20 g/L  $\beta$ -lg aggregates, 10 g/L  $\kappa$ -car and 0.03 M KCl.

offsets the enthalpy. However, as was mentioned in the introduction, it has been suggested that in the case of mixtures of protein aggregates and polysaccharide chains the observed phase separation was mainly driven by depletion (Gaaloul et al., 2010; Tuinier et al., 2003). When polymers are depleted from between neighbouring particles the osmotic pressure will push the particles together. The effective attraction due to depletion is thus caused by an increase of the entropy and has the same temperature dependence as the mixing entropy. The increase of the depletion interaction with increasing temperature compensates the increase of the mixing entropy. It follows that phase separation driven by depletion does not depend on the temperature. Here we find that increasing the temperature favours mixing implying that depletion is not the sole driving force for phase separation for the mixtures studied here. In fact, we observed no phase separation in mixtures of the same protein aggregates and poly (ethylene oxide) even at much higher concentrations of the latter, which shows that depletion by itself does not cause phase separation.

The explanation of the effect of gelation of the  $\kappa$ -car chains on phase separation is less straightforward. As mentioned in the introduction, reducing the temperature below a critical temperature causes a change in the conformation of  $\kappa$ -car chains from a random coil to a helix. Kappa carrageenan helices have a tendency to associate side by side. These associations can act as crosslinks and if enough crosslinks are formed, the chains percolate into a space filling network. The elastic modulus of the network increased with decreasing temperature because more crosslinks were formed. It appears from the present investigation that the elastic modulus drives, together with the osmotic modulus, a more homogeneous distribution of the carrageenan chains and thereby reduces the tendency to phase separate. It should be realized that when a gel is formed, the system is no longer in thermodynamic equilibrium and the kinetics of gelation may play a role. More detailed investigations are needed to elucidate the mechanism by which the phase separation is inversed.

The transient phase separation observed in the mixture containing 8 g/L  $\kappa$ -car is caused by the interplay of three factors: (1) the mixing entropy which causes the system to be homogeneous at high temperatures; (2) the thermodynamic incompatibility which drives the phase separation at intermediate temperatures; and (3) the elastic modulus which reverses the phase separation below  $T_g$ . With increasing  $\kappa$ -car concentration the effect of thermodynamic incompatibility increased and already at  $C_k = 9$  g/L increasing the

temperature was no longer sufficient to inhibit phase separation. At higher  $\kappa$ -car concentrations also the effect of the elasticity diminished even though the elastic modulus increased with increasing  $\kappa$ -car concentration.

As was mentioned in the introduction, in most cases the reversal of phase separation by gelation is not complete and often the protein rich domains persist in the gel, but contain much less proteins. This means that when the  $\kappa$ -car melts again after heating, phase separation occurs much faster taking advantage of the residual protein domains as nuclei. This explains why in the liquid state the turbidity was higher during heating than during cooling, see Fig. 7.

The results obtained in this study allow us to explain more fully the complex behaviour of mixtures of  $\kappa$ -car and small protein aggregates (Ako et al., 2011). For that study the  $\kappa$ -car concentration was chosen sufficiently low so that the mixtures were initially compatible at 20 °C. They were subsequently heated to 60 °C in the presence of 0.2 M NaCl leading to a growth of the aggregates by the process of cold gelation. When the aggregate size exceeded a critical value the aggregates were no longer compatible with the  $\kappa$ -car chains and phase separation occurred at 60 °C. If the solutions were kept at 60 °C the mixtures finally gelled through aggregation of the protein rich domains. However, if the mixtures were cooled to 20 °C just before they phase separated at 60 °C, transient phase separation was observed with CLSM. The present study shows that the phase separation was caused by the decrease of the compatibility between  $\kappa$ -car and protein aggregates with decreasing temperature and the subsequent reversal by the slow formation of a strong  $\kappa$ -car network.

## 5. Conclusions

Segregative phase separation between protein aggregates and polysaccharides is favoured by a reduction of the temperature close to the binodal implying that depletion is not the sole driving force for phase separation. Gelation of the polysaccharide can revert phase separation. The extent of reversal is directly correlated to the elastic shear modulus of the polysaccharide gel. Close to the binodal, transient phase separation occurs during cooling and heating caused by the combined effects of temperature and elasticity on the phase separation. Phase separation can be rendered irreversible by ageing in the presence of small amounts of calcium ions.

## References

- Ako, K., Durand, D., & Nicolai, T. (2011). Phase separation driven by aggregation can be reversed by elasticity in gelling mixtures of polysaccharides and proteins. *Soft Matter*, 7, 2507–2516.
- Ako, K., Nicolai, T., & Durand, D. (2010). Salt-induced gelation of globular protein aggregates: structure and kinetics. *Biomacromolecules*, 11, 864–871.
- Barbut, S., & Foegeding, E. A. (1993).  $\text{Ca}^{2+}$  induced gelation of pre-heated whey protein isolate. *Journal of Food Science*, 58, 867–871.
- Baussay, K., Nicolai, T., & Durand, D. (2006a). Coupling between polysaccharide gelation and micro-phase separation of globular protein clusters. *Journal of Colloid and Interface Science*, 304, 335–341.
- Baussay, K., Nicolai, T., & Durand, D. (2006b). Effect of the cluster size on the micro phase separation in mixtures of  $\beta$ -lactoglobulin clusters and  $\kappa$ -carrageenan. *Biomacromolecules*, 7, 304–309.
- Bryant, M. C., & McClements, D. J. (2000). Influence of NaCl and  $\text{CaCl}_2$  on cold-set gelation of heat-denatured whey protein. *Journal of Food Science*, 65, 802–804.
- Cakir, E., & Foegeding, E. A. (2011). Combining protein micro-phase separation and protein-polysaccharide segregative phase separation to produce gel structures. *Food Hydrocolloids*.
- Capron, I., Nicolai, T., & Smith, C. (1999). Effect of addition of kappa-carrageenan on the mechanical and structural properties of beta-lactoglobulin gels. *Carbohydrate Polymers*, 40, 233–238.
- Clark, A. H. (1999). Gelation of globular proteins. In S. E. Hill, D. A. Ledward, & J. R. Mitchell (Eds.), *Functional properties of food macromolecules* (2nd ed.). (pp. 77–142) Gaithersburg: Aspen Publishers.
- Croguennoc, P., Durand, D., & Nicolai, T. (2001a). Phase Separation and association of globular protein aggregates in the presence of polysaccharides: 1. Mixtures of

- preheated  $\beta$ -lactoglobulin and  $\kappa$ -carrageenan at room temperature. *Langmuir*, 17, 4372–4379.
- Croguennoc, P., Durand, D., & Nicolai, T. (2001b). Phase separation and association of globular protein aggregates in the presence of polysaccharides: 2. Heated mixtures of native  $\beta$ -lactoglobulin and  $\kappa$ -carrageenan. *Langmuir*, 17, 4380–4385.
- de Jong, S., Klok, H. J., & van de Velde, F. (2009). The mechanism behind microstructure formation in mixed whey protein-polysaccharide cold-set gels. *Food Hydrocolloids*, 23, 755–764.
- Foegeding, E. A. (2006). Food biophysics of protein gels: a challenge of nano and macroscopic proportions. *FOBI*, 1, 41–50.
- Gaaloul, S., Turgeon, S. L., & Corredig, M. (2010). Phase behavior of whey protein aggregates/kappa-carrageenan mixtures: experiment and theory. *Food Biophysics*, 5, 103–113.
- Meunier, V., Nicolai, T., Durand, D., & Parker, A. (1999). Light scattering and viscoelasticity of aggregating and gelling  $\kappa$ -carrageenan. *Macromolecules*, 32, 2610–2616.
- Nicolai, T. (2007a). Food structure characterisation using scattering methods. In D. J. Mc Clements (Ed.), *Understanding and controlling the microstructure of complex foods* (pp. 288–310). Cambridge: Woodhead.
- Nicolai, T. (2007b). Structure of self-assembled globular proteins. In E. Dickinson, & M. E. Leser (Eds.), *Food colloids: Self-assembly and material science*, Vol. 302 (pp. 35–56).
- Nicolai, T., Britten, M., & Schmitt, C. (2011).  $\beta$ -lactoglobulin and WPI aggregates: formation, structure and applications. *Food Hydrocolloids*, 25, 1945.
- Piculell, L. (2006). Gelling carrageenans. In A. M. Stephen, G. O. Philips, & P. A. Williams (Eds.), *Food polysaccharides and their applications* (pp. 239). Boca Raton: CRC Press.
- Tolstoguzov, V. (2003). Some thermodynamic considerations in food formulation. *Food Hydrocolloids*, 17, 1–23.
- Tuinier, R., Rieger, J., & Kruif, C. G. d. (2003). Depletion-induced phase separation in colloid–polymer mixtures. *Advances in Colloid and Interface Science*, 103, 1–31.
- Turgeon, S. L., Beaulieu, M., Schmitt, C., & Sanchez, C. (2003). Protein polysaccharide interactions: phase-ordering kinetics, thermodynamic and structural aspects. *Current Opinion in Colloid & Interface Science*, 8, 401–414.
- Turgeon, S. L., Schmitt, C., & Sanchez, C. (2007). Protein polysaccharide complexes and coacervates. *Current Opinion in Colloid & Interface Science*, 12, 166–178.





## **PAPER 3**



# The effect of protein aggregate morphology on phase separation in mixtures with polysaccharides

Bach T Nguyen, Taco Nicolai, Christophe Chassenieux and Lazhar Benyahia

LUNAM Université, IMMM, UMR CNRS 6283 - Université du Maine, 72085 Le Mans cedex 9, France

E-mail: [Taco.Nicolai@univ-lemans.fr](mailto:Taco.Nicolai@univ-lemans.fr)

Received 18 February 2014, revised 15 May 2014

Accepted for publication 30 May 2014

Published 27 October 2014

## Abstract

The morphology of aggregates formed by heating the globular protein  $\beta$ -lactoglobulin ( $\beta$ -lg) changes with the addition of a small amount of  $\text{CaCl}_2$ , from small strands to larger spherical aggregates (microgels). We investigated the effect of this morphological transition on the structure of mixtures of  $\beta$ -lg aggregates with the polysaccharide  $\kappa$ -carrageenan ( $\kappa$ -car), using confocal laser scanning microscopy and dynamic light scattering. The change in the morphology of the  $\beta$ -lg aggregates strongly reduced the  $\kappa$ -car concentration at which the system phase separated. As a consequence a dramatic change in the structure of the mixtures occurred over a narrow range of the  $\text{CaCl}_2$  concentration. Phase separation leads to the formation of micron-sized protein rich domains that have a tendency to stick together in large flocs. There is a big difference between the protein concentrations in the two phases, but the  $\kappa$ -car concentration is only weakly lower in the protein rich phase. A comparison is made between mixtures prepared at room temperature, after separately heating  $\beta$ -lg, and heated mixtures of native  $\beta$ -lg and  $\kappa$ -car. The micro-phase separated structure of the two systems is similar, but the aggregates disperse upon dilution in the former case, while they are covalently bound within the domains in the latter case. Other, more subtle, differences were also observed. The results explain the very high sensitivity of the structure of  $\beta$ -lg/ $\kappa$ -car mixtures to calcium ions.

Keywords: protein, polysaccharide, phase separation,  $\beta$ -lactoglobulin, carrageenan, aggregate

 Online supplementary data available from [stacks.iop.org/JPhysCM/26/464102/mmedia](http://stacks.iop.org/JPhysCM/26/464102/mmedia)

(Some figures may appear in colour only in the online journal)

## 1. Introduction

The texture of many food products is determined by the combined presence of proteins and polysaccharides. Thorough understanding of the structures formed by these biopolymers in aqueous solution is a prerequisite for rational design and development of novel food products. For this reason, protein/polysaccharide mixtures have been studied extensively in the past and remain an active area of research. There exists a range of proteins and polysaccharides that are suitable for use in food products, which means that a large

number of combinations can be of potential interest. They can be roughly classified into three categories, depending on the type of interaction (Semenova *et al* 2010, Turgeon *et al* 2003): no/weak interaction, so the properties of the mixture are essentially equal to the sum of the individual components; strong attractive interaction, leading to complex coacervation; and strong repulsive interaction, resulting in segregative phase separation. Complex coacervation leads to an enrichment of one phase in both components, while segregative phase separation means that each phase is enriched in one of the components.

Here, we report on an investigation of aqueous mixtures of  $\beta$ -lactoglobulin ( $\beta$ -lg) and  $\kappa$ -carrageenan ( $\kappa$ -car) at pH 7, in which both biopolymers are negatively charged.  $\beta$ -lg is a globular protein and is the major protein component of whey (Brownlow *et al* 1997, De Wit 1998, Fox 2003, Kinsella and Whitehead 1989).  $\kappa$ -car is an anionic polysaccharide isolated from algae (Morris 2007, Piculell 2006). Both biopolymers are widely used in the food industry and their aggregation and gelling properties have been investigated extensively in the past both individually (Bryant and McClements 1998, Clark 1999, De la Fuente *et al* 2002, Gosal and Ross-Murphy 2000, Morris 2007, Piculell 2006, Totosaus *et al* 2002) and in mixtures (De Kruif and Tuinier 2001, Morris and Wilde 1997, Nishinari *et al* 2000, Turgeon *et al* 2003). At pH 7, native  $\beta$ -lg is compatible with  $\kappa$ -car up to high concentrations of both components (Croguennoc *et al* 2001a).

$\beta$ -lg denatures and aggregates irreversibly when heated above about 60 °C. Depending on the environmental conditions, aggregates with different morphologies are formed, as was recently reviewed (Nicolai and Durand 2013, Nicolai *et al* 2011, Mezzenga and Fischer 2013). For pH > 6.2 small strand-like aggregates are formed, with a hydrodynamic radius of about 15 nm (Durand *et al* 2002), while closer to the iso-electric point (pI = 5.2) mainly spherical particles are formed, with hydrodynamic radii ranging between 40 and 200 nm depending on the pH (Donato *et al* 2009, Schmitt *et al* 2009, 2010). Around pH 6.0 a significant fraction of both strands and microgels is formed within the same sample (Phan-Xuan *et al* 2011). Stable suspensions of the spherical particles, also called microgels, can only be formed in a very narrow range of the pH (5.75–6.1). Closer to the iso-electric point secondary aggregation leads to precipitation. Secondary aggregation of the strands and the microgels into larger self-similar aggregates occurs at higher protein concentrations and leads to gelation.

Interestingly, the discontinuous change of the morphology can also be induced at higher pH by adding bivalent cations before heating, but not by adding monovalent salt (Phan-Xuan *et al* 2014, 2013). The transition is driven by the reduction of the net protein charge due to specific adsorption of  $\text{Ca}^{2+}$  and is controlled by the molar ratio of calcium to protein ( $R$ ). At pH 7 the fraction of microgels increases rapidly from less than 20% at  $R < 1$  to more than 80% at  $R > 2$ . At  $R = 1.5$ , the solution contains an almost equal weight fraction of strands and microgels that can be clearly distinguished in transmission electron microscope images (Phan-Xuan *et al* 2013). The transition occurs between  $R = 1$  and  $R = 2$  independent of the protein concentration and heating temperature, but a stable suspension of individual microgels can only be formed in a narrow range of  $R$  and for protein concentrations less than  $60 \text{ g L}^{-1}$  (Phan-Xuan *et al* 2014).

When  $\kappa$ -car chains are added to a stable suspension of  $\beta$ -lg aggregates at room temperature, the two components phase separate above a critical concentration of  $\kappa$ -car. This phenomenon has been studied in some detail for mixtures of  $\kappa$ -car with small strand-like  $\beta$ -lg aggregates and with larger self-similar aggregates formed by secondary aggregation of the strands (Baussay *et al* 2006, Croguennoc *et al* 2001a, de Jong *et al*

2009, Gaaloul *et al* 2010, Nguyen *et al* 2014). It was shown that the critical concentration of  $\kappa$ -car to induce phase separation is about  $8 \text{ g L}^{-1}$  for the strands (Nguyen *et al* 2014) and it decreases strongly with increasing aggregate size (Baussay *et al* 2006). The critical  $\kappa$ -car concentration decreased weakly with increasing protein concentration. It has been suggested that depletion of the  $\kappa$ -car chains is the origin of the formation of dense domains of protein aggregates (Tuinier *et al* 2003). However, we have shown that, very close to the critical concentration, microphase separation can be reverted by increasing the temperature (Nguyen *et al* 2014). Since the depletion interaction is entropic no temperature dependence would be expected if it was the main driving force.

For reasons that are not yet fully elucidated, phase separation was found to halt when the protein rich domains had grown to a diameter of a few microns. In pure water these domains are liquid and fully disperse when diluted. However, in the presence of salt the protein aggregates within the domains irreversibly crosslink at a rate that depends on the amount and valence of the added salt. In either case, the protein rich domains stick to each other and form larger clusters that precipitate, but the bonds between the domains are relatively weak and can be easily broken by shaking the sample.

Micro-phase separation also occurs when mixtures of native  $\beta$ -lg or whey proteins and  $\kappa$ -car are heated (Cakir and Foegeding 2011, Capron *et al* 1999, Croguennoc *et al* 2001b, Eleya and Turgeon 2000, Gaaloul *et al* 2009, Harrington *et al* 2009, Roesch *et al* 2004). In this case, phase separation is induced *in situ* by the growth of the aggregates. If the protein concentration is sufficiently high, heating of the mixtures leads to the formation of heterogeneous gels, consisting of a network of covalently bound protein rich domains.

In view of the sensitivity of the mixtures to the  $\beta$ -lg aggregate size, one expects that the transition of the aggregate morphology induced by adding a small amount of  $\text{CaCl}_2$ , will have a dramatic effect on the structure of heated mixtures. We investigated the effect of the transition on the structure: by mixing at room temperature  $\kappa$ -car with  $\beta$ -lg aggregates formed separately at different  $\text{CaCl}_2$  concentrations; or by heating mixtures of native  $\beta$ -lg and  $\kappa$ -car at different  $\text{CaCl}_2$  concentrations. We will show that adding small amounts of  $\text{CaCl}_2$  has indeed a dramatic effect on the structure of the mixtures that can be explained by the transition in the morphology of the  $\beta$ -lg aggregates. For this study we used sodium  $\kappa$ -car that had in all mixtures the random coil conformation. It is well known that, in solution, a conformational transition of  $\kappa$ -car between a random coil and a helix can be induced by cooling in the presence of specific salts, which leads to aggregation or gelation (Piculell 2006). The effect of gelling the  $\kappa$ -car chains on the structure and the rheology of the mixtures will be reported elsewhere.

## 2. Materials and methods

### 2.1. Materials

The  $\beta$ -lactoglobulin (Biopure, lot JE 001-8-415) used in this study was purchased from Davisco Foods International, Inc.

(Le Sueur, MN, USA) and consisted of approximately equal quantities of variants A and B. The powder was dissolved in Milli-Q water, which contained 200 ppm  $\text{NaN}_3$  to prevent bacterial growth. Solutions were dialyzed extensively against Milli-Q water with 200 ppm sodium azide and subsequently filtered through  $0.2\mu\text{m}$  pore size Anotop filters. The pH of the solution was adjusted to seven by adding small amounts of NaOH 0.1 N under vigorous stirring. The protein concentration was determined by UV absorption at 278 nm with a UV-Visible spectrometer Varian Cary-50 Bio (Les Ulis, France) using extinction coefficient  $0.96\text{Lg}^{-1}\text{cm}^{-1}$ . The protein concentration in the supernatant of the mixtures was determined in the same manner, taking into consideration the effect of the turbidity.

The sodium  $\kappa$ -carrageenan is an alkali treated extract from *Eucheuma cottonii* and was a gift from Cargill (Baupre, France). Using NMR it was found that the sample contained less than 5%  $\iota$ -carrageenan. A freeze-dried sample of  $\kappa$ -car was dissolved by stirring for a few hours in Milli-Q water ( $70^\circ\text{C}$ ) with 200 ppm sodium azide added as a bacteriostatic agent. The solution was extensively dialyzed against Milli-Q water at pH 7 with 200 ppm sodium azide and subsequently filtered through  $0.45\mu\text{m}$  pore size Anotop filters. The pH of the solution was adjusted to seven by adding small amounts of HCl 0.1 N under vigorous stirring. The  $\kappa$ -car concentration ( $C_K$ ) was determined by measuring the refractive index using refractive index increment  $0.145\text{g ml}^{-1}$ . The molar mass ( $M_w$ ) and radius of gyration ( $R_g$ ) were determined by light scattering, as described elsewhere (Meunier *et al* 1999), with  $M_w = 2.1 \times 10^5\text{g mol}^{-1}$  and  $R_g = 52\text{nm}$ .

## 2.2. Preparation of the mixtures

Mixtures of  $\beta$ -lg aggregates and  $\kappa$ -car, with identical compositions, were prepared by two methods. The first method, called mixing after heating (MAH), consisted of heating  $\beta$ -lg solutions at  $85^\circ\text{C}$  during 10 h at different concentrations of  $\text{CaCl}_2$  and subsequently mixing with the  $\kappa$ -car solution at room temperature. The second method, called mixing before heating (MBH), consisted of mixing native  $\beta$ -lg and  $\kappa$ -car at different  $\text{CaCl}_2$  concentrations at room temperature and subsequently heating at  $85^\circ\text{C}$  for 10 h. The protein concentration during heating was the same in both methods. After the heat treatment, all proteins were aggregated and a steady state was reached. In order to avoid dilution with method MAH, the concentration of the aggregate solution was increased by slow evaporation of some of the water. Care was taken that the final concentrations of the biopolymers and the  $\text{CaCl}_2$  were the same. The pH was set at 7.0 before heating by adding small amounts of a 0.1 M NaOH solution.

## 2.3. Methods

Confocal Laser Scanning Microscopy (CLSM) was used in the fluorescence mode. Observations were made with a Leica TCS-SP2 (Leica Microsystems Heidelberg, Germany). A water immersion objective lens was used HCxPL APO 63x NA = 1.2 with theoretical resolution of  $0.3\mu\text{m}$  in the x-y

plane.  $\beta$ -lg was physically labelled with the fluorochrome rhodamine B isothiocyanate, by adding a small amount of a concentrated rhodamine solution (5 ppm) to the  $\beta$ -lg solutions. No effect of labelling on the phase separation was observed.  $\kappa$ -car was covalently labelled with fluorescein isothiocyanate (FITC) following Heilig *et al* (2009).

Light scattering measurements were done with a commercial apparatus (ALV-CGS3, ALV-Langen) operating with a vertically polarized He-Ne laser with wavelength  $\lambda = 632\text{nm}$ . The temperature was controlled at  $20^\circ\text{C}$  with a thermostat bath to within  $\pm 0.2^\circ\text{C}$ . The normalized electric field autocorrelation functions ( $g_1(t)$ ) obtained from dynamic light scattering (DLS) measurements (Berne and Pecora 1976) were analyzed in terms of a distribution of relaxation times ( $\tau$ ):

$$g_1(t) = \int A(\tau) \exp(-t/\tau) d(\tau).$$

In dilute solutions, the relaxation was caused by translational diffusion of the particles. The diffusion coefficient ( $D$ ) was calculated from the average relaxation rate:

$$D = \langle \tau^{-1} \rangle / q^2$$

with  $q$  the scattering wave vector. The z-average hydrodynamic radius ( $R_h$ ) of solute was calculated using the Stokes-Einstein equation:

$$R_h = \frac{kT}{6\pi\eta D}$$

with  $\eta$  the viscosity of the solvent,  $k$  Boltzman's constant, and  $T$  the absolute temperature.

## 3. Results

We investigated the effect of the size and the morphology of  $\beta$ -lg aggregates formed at different  $\text{CaCl}_2$  concentrations on the structure of mixtures with  $\kappa$ -car. We distinguish between situations in which the aggregates were formed: in the presence of  $\kappa$ -car (MBH); separately, and subsequently mixed with  $\kappa$ -car (MAH). We fix, in the first instance, the  $\beta$ -lg concentration at  $20\text{g L}^{-1}$  and discuss the effect of varying the protein concentration later.

### 3.1. $\beta$ -lg aggregation without $\kappa$ -car

For the case of MAH,  $\beta$ -lg aggregates with different sizes and morphologies were formed separately by heating during 10 h at  $85^\circ\text{C}$  aqueous solutions containing  $C_b = 20\text{g L}^{-1}$   $\beta$ -lg at pH 7 in the presence of different  $\text{CaCl}_2$  concentrations ( $[\text{CaCl}_2]$ ). The z-average hydrodynamic radius of the aggregates was determined using dynamic light scattering, as described in the material and methods section.  $R_h$  increased initially weakly with increasing  $[\text{CaCl}_2]$  from 18 to 24 nm, but above 1 mM it increased sharply, due to the transition from the formation of strands to microgels, see figure 1. We note that the z-average value of  $R_h$  is strongly weighted towards the largest aggregates in the solution, implying that in mixtures of strands and microgels one measures essentially the size of the latter. It also means that the contribution of  $\kappa$ -car to the scattering

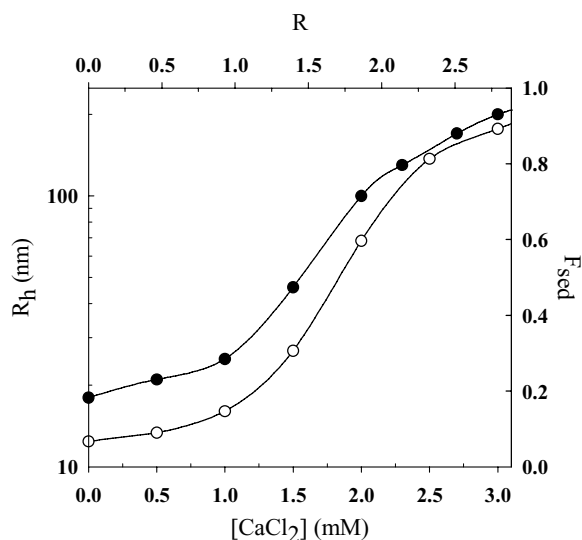


**Figure 1.** z-average hydrodynamic radius of the  $\beta$ -lg aggregates (closed symbols) and the fraction of proteins that sedimented at  $5 \times 10^4$  g (open symbols) as a function of the  $\text{CaCl}_2$  concentration or the molar ratio ( $R$ ) between  $\text{Ca}^{2+}$  and  $\beta$ -lg. The aggregates were formed by heating aqueous solutions of  $\beta$ -lg at  $20 \text{ g L}^{-1}$ .

intensity can be neglected when it is present in mixtures with protein aggregates.

The fraction of microgels can be estimated by measuring the fraction of proteins that sediment ( $F_{\text{sed}}$ ) after centrifugation at  $5 \times 10^4$  g (Phan-Xuan *et al* 2011). The latter increased rapidly for  $[\text{CaCl}_2] > 1 \text{ mM}$ , see figure 1. A small fraction of aggregates sediment also for  $[\text{CaCl}_2] < 1 \text{ mM}$ , even though no microgels are observed by TEM or light scattering in that case, indicating that a small fraction of the strands is large enough to sediment at  $5 \times 10^4$  g, as was discussed elsewhere (Phan-Xuan *et al* 2013). For  $[\text{CaCl}_2] > 3 \text{ mM}$  secondary aggregation of the microgels occurred, leading eventually to precipitation.

### 3.2. Structure of the mixtures

$20 \text{ g L}^{-1}$   $\beta$ -lg was mixed with different concentrations of  $\kappa$ -car ( $C_K$ ) either before (MBH) or after heating (MAH). In both cases the microstructure of the mixtures was investigated at room temperature with CLSM. As an example, figure 2 shows the effect of the  $\text{CaCl}_2$  concentration on the protein distribution in mixtures containing  $5 \text{ g L}^{-1}$   $\kappa$ -car. In both situations, phase separation was observed when  $\text{CaCl}_2$  was present that caused the formation of spherical protein rich domains. The first signs of phase separation were seen for heated mixtures (MBH) for  $[\text{CaCl}_2] = 0.5 \text{ M}$ , while for mixing after heating it was observed first at  $1.0 \text{ mM}$   $\text{CaCl}_2$ . The fraction of proteins involved in the formation of the domains ( $F_{\text{ps}}$ ) increased with increasing  $[\text{CaCl}_2]$ , see below.

The size of the protein rich domains decreased with increasing  $\text{CaCl}_2$  concentration and they had a tendency to stick together into large clusters or even a space filling network. In some cases partially fused domains can be seen. Similar structures were obtained with either method, though

in the case of MAH the domains appeared smaller and less clustered. An important difference between mixing before and after heating was, however, that phase separation was reversible for MAH even a week after preparation, while the protein rich domains that formed by heating the mixture resisted dilution (see supplementary information). The reason that the aggregates within the domains become irreversibly cross-linked during heating is that as long as native proteins are present that can denature, the aggregates continue to grow and form a gel. Growth of the aggregates only stops when all native proteins have been consumed or the temperature is dropped to far below the denaturation temperature. In the heated mixtures, micro-phase separation occurred when the aggregates reached a critical size, but at this point native proteins were still present, which allowed the aggregates in the domains to cross-link irreversibly. The aggregates that were formed separately no longer contained native proteins. In addition, they were mixed with  $\kappa$ -car far below the denaturation temperature. Therefore, no cross-linking of the aggregates occurred within the domains formed by MAH.

When left standing, we observed slow sedimentation of the clusters at a rate that decreased with increasing  $\kappa$ -car concentration, see figure 3. The precipitate could be easily dispersed by shaking but small clusters could not be broken into individual domains in this way. Therefore, sedimentation was significantly faster after manual dispersion of the precipitate. Similar results were obtained at other  $\kappa$ -car concentrations between 1 and  $5 \text{ g L}^{-1}$ . At lower  $\kappa$ -car concentrations the mixtures remained homogeneous up to  $3.0 \text{ mM}$   $\text{CaCl}_2$ , while at higher concentrations phase separation was observed even in the absence of  $\text{CaCl}_2$ .

### 3.3. Partitioning of $\beta$ -lg and $\kappa$ -car

The partition of the  $\beta$ -lg aggregates and the  $\kappa$ -car chains between the two phases could be quantified by measuring the fluorescence intensity of  $\beta$ -lg and  $\kappa$ -car labelled with different fluorescent probes. Figure 4 compares an image taken with fluorescence from  $\kappa$ -car with that from  $\beta$ -lg for a mixture with  $C_b = 20 \text{ g L}^{-1}$  and  $C_K = 5 \text{ g L}^{-1}$  at  $[\text{CaCl}_2] = 1.5 \text{ mM}$  that was mixed before heating. After heating this mixture, about 50% of the proteins entered the dense domains. Individual protein rich domains can be clearly seen with the protein signal. The concentration of  $\kappa$ -car is less in the protein rich domains, but the individual domains cannot be seen clearly with the  $\kappa$ -car signal, as it appears to also be lower in the space between neighbouring protein domains.

We have quantified the partitioning of  $\beta$ -lg and  $\kappa$ -car by tracing the fluorescence intensity profile along the white lines shown in the images, see figure 5. At the conditions of the experiment, the fluorescence intensity is proportional to the polymer concentration. It is clear that phase separation is much more important for the proteins than for the polysaccharides. Quantitative measurements on this and other images confirmed the visual impression that  $\kappa$ -car is also depleted from between the aggregated protein micro-domains. Similar results were obtained when the  $\kappa$ -car was mixed with  $\beta$ -lg after heating and at other  $\kappa$ -car concentrations.



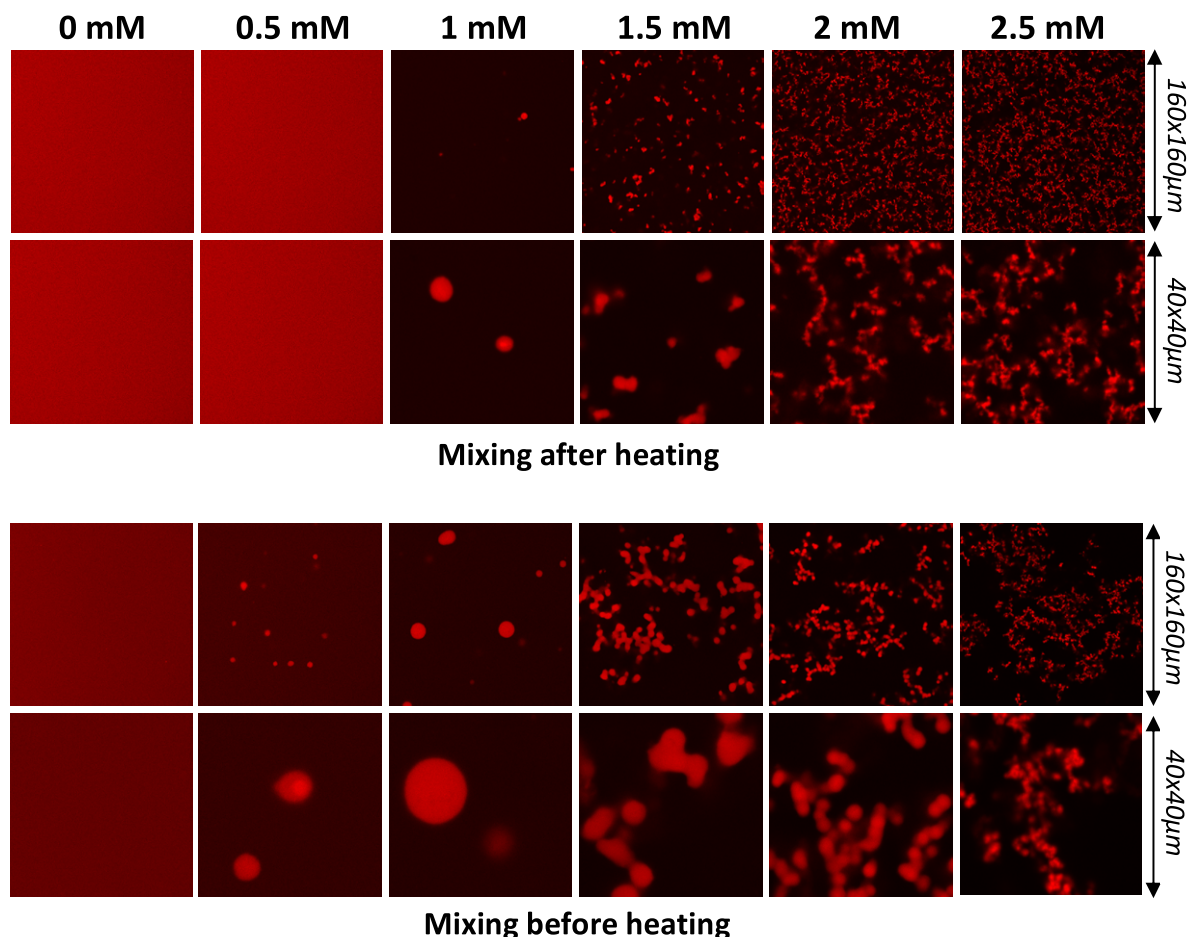


**Figure 2.** CLSM images of mixtures containing  $20 \text{ g L}^{-1}$  partially labelled  $\beta$ -Ig aggregates (red) and  $5 \text{ g L}^{-1}$   $\kappa$ -car at different  $\text{CaCl}_2$  concentrations. The protein aggregates were formed by heating either after mixing (MAH) or before mixing (MBH). For each system images are shown at two different scales.

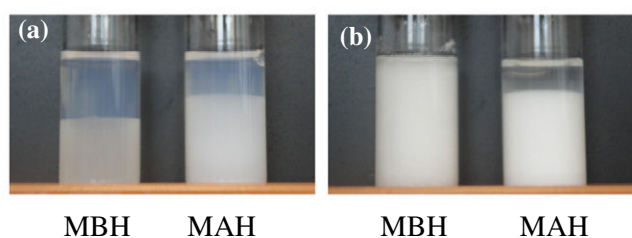


**Figure 3.** Mixtures prepared by MBH or MAH containing  $5 \text{ g L}^{-1}$   $\kappa$ -car and  $20 \text{ g L}^{-1}$   $\beta$ -Ig aggregates formed in the presence of  $1.5 \text{ mM}$  (a) or  $3.0 \text{ mM}$   $\text{CaCl}_2$  (b). The photographs were taken 5 days after preparation of the samples.

### 3.4. Extent of phase separation

The fraction of proteins that entered the dense domains ( $F_{ps}$ ) was determined by measuring the protein concentration of the supernatant after allowing the flocculated domains to settle, see figure 6. With  $0.5 \text{ g L}^{-1}$  or less  $\kappa$ -car,  $F_{ps}$  was negligible up to  $[\text{CaCl}_2] = 3 \text{ mM}$ , but at higher  $\kappa$ -car concentrations it increased rapidly with increasing  $\text{CaCl}_2$ . For systems prepared by MAH the increase of  $F_{ps}$  with increasing  $[\text{CaCl}_2]$  was almost the same between  $2$  and  $5 \text{ g L}^{-1}$   $\kappa$ -car and correlated well with the fraction of microgels, indicated

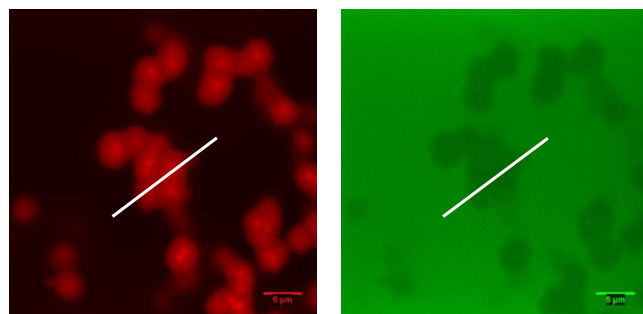


**Figure 4.** CLMS images visualizing  $\beta$ -Ig (red) and  $\kappa$ -car (green) for a mixture containing  $20 \text{ g L}^{-1}$   $\beta$ -Ig, and  $5 \text{ g L}^{-1}$   $\kappa$ -car at  $[\text{CaCl}_2] = 1.5 \text{ mM}$  prepared by mixing before heating. Relative fluorescence intensities were measured along the white lines and are shown in figure 5. The images represent  $40 \times 40 \mu\text{m}^2$ .

by the dashed line in figure 6(a). Notice that the dashed line was derived from the fraction of sedimented proteins shown in figure 1 by correcting for the small fraction of the larger strands that also sedimented during centrifugation. At  $C_K = 1 \text{ g L}^{-1}$  the increase of  $F_{ps}$  started at somewhat higher  $[\text{CaCl}_2]$ . On the other hand, for heated mixtures (MBH) the increase of  $F_{ps}$  started at lower  $[\text{CaCl}_2]$  for  $C_K = 5 \text{ g L}^{-1}$  and

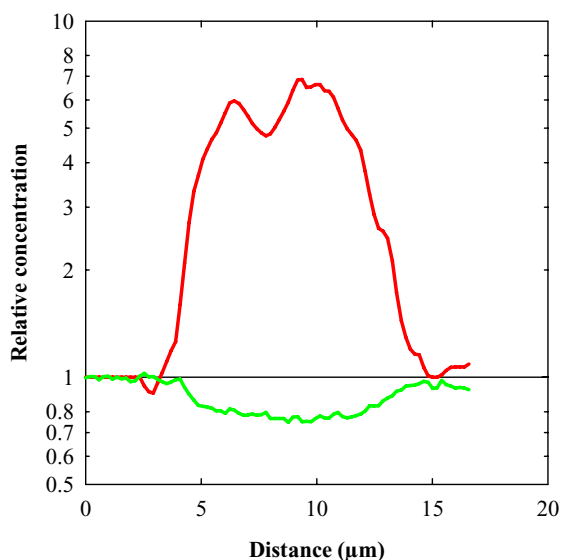


**Figure 5.** Relative variation of the  $\beta$ -lg concentration (red) and the  $\kappa$ -car concentration (green) along the white lines in the CLMS images of mixtures formed at 1.5 mM  $\text{CaCl}_2$  shown in figure 4.

shifted progressively to larger values with decreasing  $\kappa$ -car concentrations. We will discuss the origin of this behaviour below. Interestingly, at  $C_K < 4 \text{ g L}^{-1}$  phase separation was less extensive in heated mixtures.

The critical  $\kappa$ -car concentration needed to induce phase separation depended only weakly on the protein concentration as was already reported for  $\beta$ -lg strands (Nguyen *et al* 2014) and fractal aggregates (Baussay *et al* 2006, Croguennoc *et al* 2001a). A systematic investigation with microgels of different sizes ( $R_h = 130\text{--}350 \text{ nm}$ ) confirmed this observation (data not shown). For instance, for microgels with  $R_h = 240 \text{ nm}$ , the onset of phase separation occurred between 0.5 and  $1.0 \text{ g L}^{-1}$   $\kappa$ -car over the whole range of protein concentrations investigated ( $C_b = 0.5\text{--}40 \text{ g L}^{-1}$ ), see supplementary information.

### 3.5. Size of the soluble $\beta$ -lg aggregates in heated mixtures

After association of the protein rich domains into larger flocs and their precipitation under gravity, no domains remained in the supernatant. The size of the  $\beta$ -lg aggregates that did not phase separate, and therefore remained in the supernatant, was determined using dynamic light scattering. In figure 7 the size of the aggregates in the supernatant is plotted as function of the  $\text{CaCl}_2$  concentration at different  $\kappa$ -car concentrations. We distinguish between solutions for which the fraction of phase separated protein aggregates was negligible (open symbols) and those where it was significant ( $F_{ps} > 0.1$ , filled symbols). The presence of up to  $1 \text{ g L}^{-1}$   $\kappa$ -car did not significantly influence the size of the aggregates, but at higher  $\kappa$ -car concentrations we observed an increase of the size of the strands formed at lower  $\text{CaCl}_2$  concentrations. This explains why weak phase separation was observed in the heated mixtures at  $C_K = 5 \text{ g L}^{-1}$ , but not in MAH, see figure 2.

At higher  $\text{CaCl}_2$  concentrations, where in the absence of  $\kappa$ -car microgels were formed, we found that the aggregates in

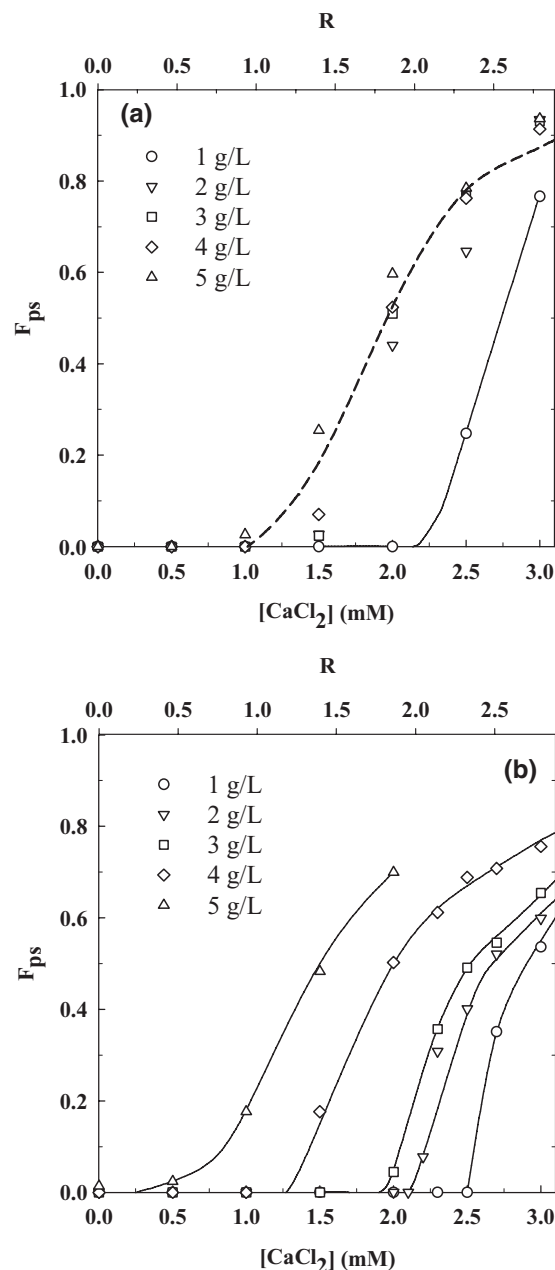


**Figure 6.** Dependence of the fraction of phase separated proteins on the  $\text{CaCl}_2$  concentration or  $R$  for mixtures containing  $20 \text{ g L}^{-1}$   $\beta$ -lg and different concentrations of  $\kappa$ -car prepared by mixing after heating (a) and mixing before heating (b). The solid lines are guides to the eye while the dashed line indicates the estimated fraction of microgels.

the supernatant were smaller than those formed in the absence of  $\kappa$ -car. This may be due to the competition between  $\kappa$ -car and  $\beta$ -lg for  $\text{Ca}^{2+}$  (Harrington *et al* 2009). If less  $\text{Ca}^{2+}$  is available for the proteins they will form smaller microgels. Notice, however, that when a fraction of the microgels has entered the dense domains the residual aggregates in the supernatant will be smaller since preferentially the larger aggregates will enter the dense protein domains. This explains why the average size of the residual aggregates in the supernatant remains small even at high  $\text{CaCl}_2$  concentrations.



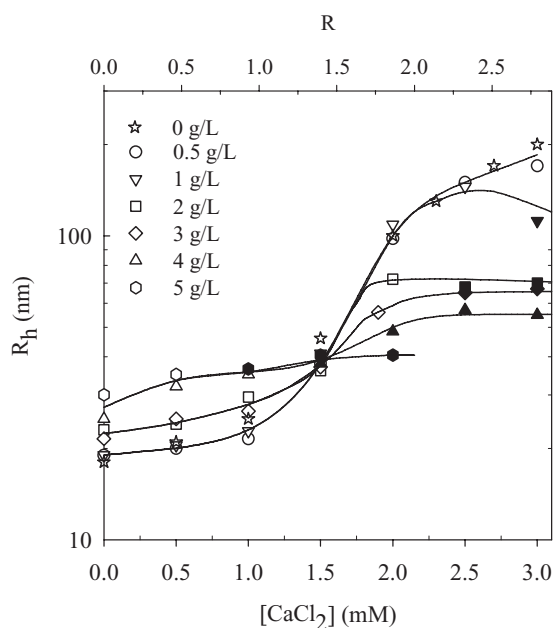


**Figure 7.** Dependence of the z-average hydrodynamic radius of the  $\beta$ -lg aggregates in the supernatant as a function of the  $\text{CaCl}_2$  concentration for mixtures (MBH) that were heated in the presence of different concentrations of  $\kappa$ -car indicated in the figure. Filled symbols indicate systems for which  $F_{ps} > 0.1$ .

### 3.6. Effect of varying the $\beta$ -lg concentration

The effect of varying the protein and polysaccharide concentrations on the structure is shown in figure 8 for mixtures (MAH) of  $\kappa$ -car and  $\beta$ -lg microgels. The microgels were formed by heating  $\beta$ -lg at  $40 \text{ g L}^{-1}$  at  $5.3 \text{ mM}$   $\text{CaCl}_2$  and had a hydrodynamic radius of  $240 \text{ nm}$ . Phase separation was observed when  $C_K > 0.5 \text{ g L}^{-1}$  independent of the  $\beta$ -lg concentration at least between  $C_b = 2 \text{ g L}^{-1}$  and  $40 \text{ g L}^{-1}$ . The number of protein rich domains increased with increasing protein concentration, as might be expected, but their diameter remained approximately the same. The number of protein rich domains also increased with increasing  $\kappa$ -car concentration, but again their diameter remained approximately the same. Similar results were obtained for larger ( $R_h = 320 \text{ nm}$ ) and smaller ( $130 \text{ nm}$ ) microgels (results not shown) the only difference being that the larger microgels already showed clear signs of phase separation at  $C_K = 0.5 \text{ g L}^{-1}$  and the smaller microgels started to phase separate at  $C_K = 2 \text{ g L}^{-1}$ . In all cases the domains agglomerated into large clusters except at very low protein concentrations.

The effect of  $\text{CaCl}_2$  on the structure of mixtures at other  $\beta$ -lg concentrations is similar to those shown above for  $C_b = 20 \text{ g L}^{-1}$  when they are compared at the same molar ratio of  $\text{CaCl}_2$  to  $\beta$ -lg. The reason is that, as was mentioned above, the transition between the formation of small strands and larger microgels occurs at a critical value of  $R$  independent of  $C_b$ . We illustrate this here for  $C_b = 40 \text{ g L}^{-1}$  for which twice as much  $\text{CaCl}_2$  is needed to induce the morphological transition than at  $C_b = 20 \text{ g L}^{-1}$ , see supplementary information. CLSM images of mixtures with  $C_K = 2 \text{ g L}^{-1}$  showed that protein rich domains were formed at  $[\text{CaCl}_2] \geq 4.0 \text{ mM}$  both when the

microgels are formed by heating native  $\beta$ -lg separately (MAH) and when they are formed by heating the mixtures (MBH), see figure 9. The microstructures of mixtures prepared by the two different methods were very similar, as was the case for  $C_b = 20 \text{ g L}^{-1}$ . Again coarser structures were found close to the critical concentration.

At  $C_b = 40 \text{ g L}^{-1}$  self supporting gels were formed when the protein were heated at  $[\text{CaCl}_2] > 6 \text{ mM}$  in the absence of  $\kappa$ -car. However, in the presence of  $2 \text{ g L}^{-1}$   $\kappa$ -car gels were formed already at  $[\text{CaCl}_2] = 3 \text{ mM}$ . Thus the systems formed by MBH shown in figure 9 are gels, but nevertheless, they have the same structure as the liquid systems formed by MAH. It appears that during heating micro-phase separation occurs first and subsequently the protein rich domains are permanently cross-linked. The effect of  $\text{CaCl}_2$  on the elastic modulus of these gels will be discussed elsewhere.

## 4. Discussion

We will first discuss the situation where protein aggregates were formed separately and subsequently mixed with the polysaccharides and then the situation where the aggregates were formed by heating native  $\beta$ -lg after mixing with  $\kappa$ -car.

### 4.1. Mixing after heating

The size of the protein aggregates increased when more  $\text{CaCl}_2$  was present during heating. The reason that phase separation was observed at lower  $\kappa$ -car concentrations when more  $\text{CaCl}_2$  was present is thus directly related to the increase of the average size of the aggregates. The results of the present study confirm earlier reports (Baussay *et al* 2006, Croguennoc *et al* 2001a) that phase separation occurs at increasingly lower  $\kappa$ -car concentrations when the aggregate size is larger. In these earlier studies the aggregates were formed by heating the proteins in the presence of  $\text{NaCl}$  at neutral pH. In that case, small strands are formed initially and larger aggregates are formed only by secondary aggregation of the strands at higher  $\beta$ -lg or  $\text{NaCl}$  concentrations. Larger aggregates formed by secondary aggregation have a fractal structure and have a broad size distribution of the aggregates. The  $\beta$ -lg microgels studied here have a much higher density and are more monodisperse. Both effects may explain why phase separation is induced at lower  $\kappa$ -car concentrations for microgels than for fractal aggregates with the same z-average hydrodynamic radius. The effective excluded volume of fractal aggregates is less than that of a homogeneous sphere of the same size so that there is less interaction with  $\kappa$ -car chains. At the same z-average hydrodynamic radius determined by light scattering, the number average hydrodynamic radius of the more polydisperse fractal aggregates is smaller than that of the more monodisperse microgels so that its mixing entropy is higher.

There are two possible driving forces for phase separation: thermodynamic incompatibility due to the different chemistry of proteins and polysaccharides and depletion of  $\kappa$ -car chains from between the protein aggregates. Depletion interaction

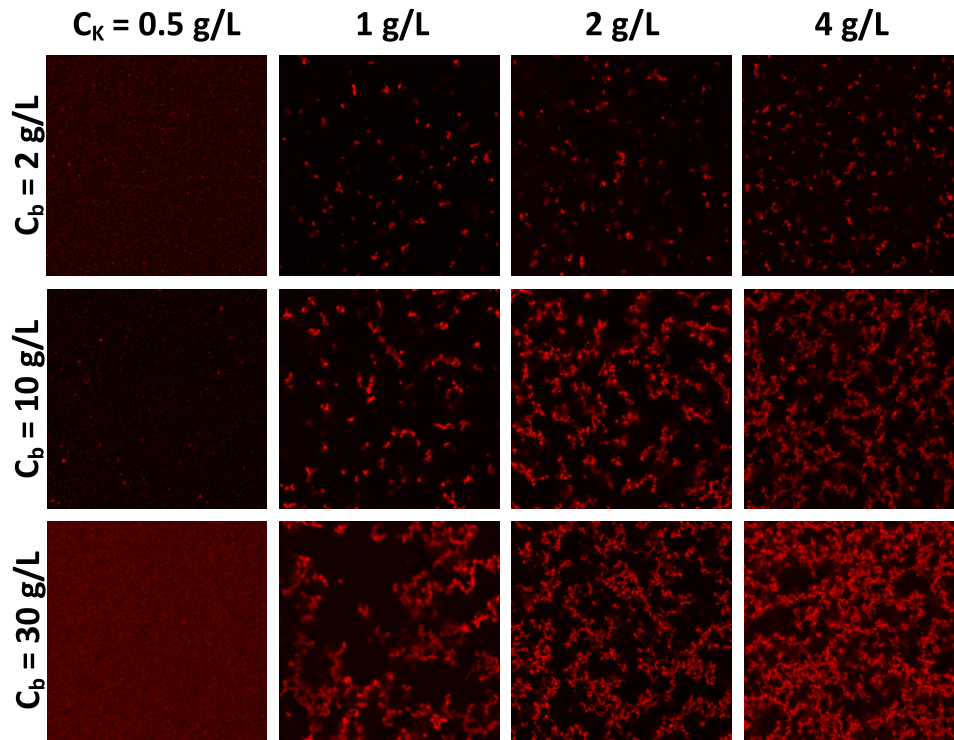


**Figure 8.** CLSM images of mixtures (MAH) of  $\kappa$ -car and partially labelled  $\beta$ -Ig microgels with  $R_h = 240$  nm at different  $\kappa$ -car and  $\beta$ -Ig concentrations. The images represent  $160 \times 160 \mu\text{m}^2$ .

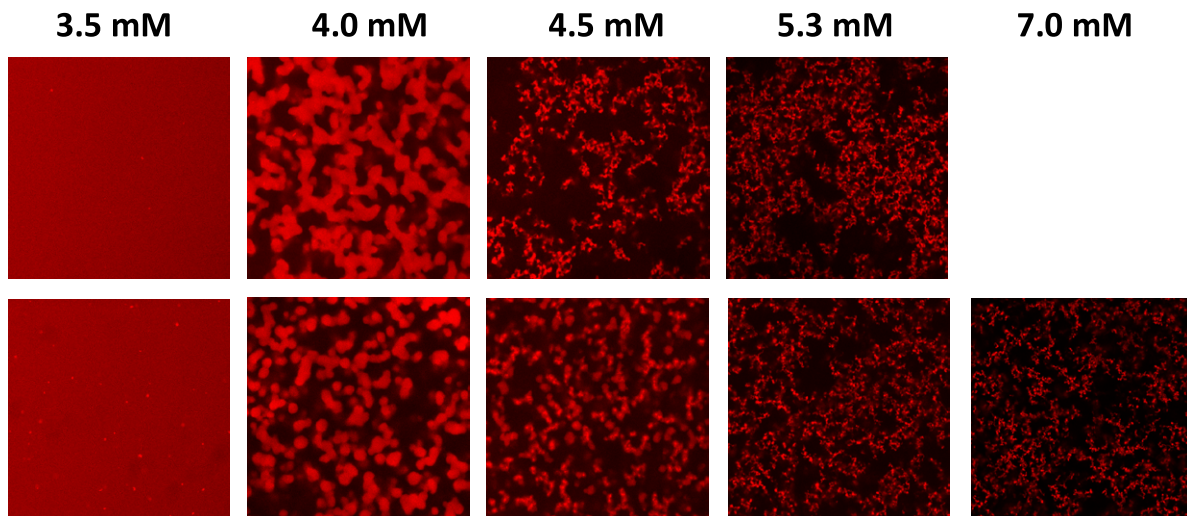


**Figure 9.** CLSM images of mixtures containing  $40 \text{ g L}^{-1}$  partially labelled  $\beta$ -Ig aggregates and  $2 \text{ g L}^{-1}$   $\kappa$ -car at different  $\text{CaCl}_2$  concentrations. The protein aggregates were formed by heating either after mixing (MAH) (top row) or before mixing (MBH) (bottom row). The images represent  $160 \times 160 \mu\text{m}^2$ .

was suggested to be the driving force for phase separation in mixtures of whey protein aggregates and polysaccharides (Tuinier *et al* 2003, Gaaloul *et al* 2010). However, we have two reasons to believe that depletion is not the principal driving force for phase separation in these mixtures. Firstly, we showed recently (Nguyen *et al* 2014) that phase separation was reduced at higher temperatures, which is expected in the case of thermodynamic incompatibility, but not for depletion interaction, which is purely entropic. Secondly, the  $\kappa$ -car

concentration is not strongly reduced within the protein rich domains.

A striking phenomenon is that the domains cease to grow when they have reached a certain size. The size of the domains at steady state decreased with increasing  $\text{CaCl}_2$  concentration i.e. when a larger fraction of the protein aggregates phase separated. Interestingly, the domains stick together into large clusters, but do not fuse completely even though partial fusion can be observed. A possible reason for this phenomenon is

that the microgels within the domains are bound together by bonds that are strong enough to resist fusion. However, these bonds are too weak to resist dilution in the case of MAH. Within this scenario, smaller protein rich domains are formed when phase separation is stronger, because they are sooner sufficiently strongly held together to inhibit fusion. Notice that the interfacial tension that drives fusion is very small in the case of two aqueous phases.

The extent of phase separation as a function of the  $\kappa$ -car concentration can be explained by considering the size distribution of the  $\beta$ -lg aggregates. Even though neither the strands nor the microgels are monodisperse, we may consider that the systems studied here contained two distinct populations of strands and microgels. At  $\kappa$ -car concentrations between 2 and 5 g L<sup>-1</sup>, practically none of the strands and all of the microgels phase separated. This explains why the extent of phase separation as a function of [CaCl<sub>2</sub>] closely mirrored the fraction of microgels as shown by the dashed line in figure 6(a). At  $C_K = 1$  g L<sup>-1</sup> the smallest microgels did not phase separate, which explains the shift to higher [CaCl<sub>2</sub>]. At  $C_K = 0.5$  g L<sup>-1</sup> even the largest microgels formed by heating at [CaCl<sub>2</sub>] = 3 mM did not phase separate.

#### 4.2. Mixing before heating

The main features observed for mixtures of  $\kappa$ -car and  $\beta$ -lg aggregates formed at different CaCl<sub>2</sub> are the same whether the proteins are heated before or after mixing. In both cases the critical  $\kappa$ -car concentration decreased strongly when the CaCl<sub>2</sub> was increased, because microgels were formed instead of small strands. The major difference was that phase separation in heated mixtures could not be reversed by dilution implying that the aggregates were rapidly strongly bound together within the domains. In addition, we found other more subtle differences.

The size of the strands increased when more than 1 g L<sup>-1</sup>  $\kappa$ -car was present during heating. A possible reason for the formation of larger strands is that the presence of  $\kappa$ -car influences the interaction between the growing  $\beta$ -lg aggregates. Notably, the incompatibility of the two polymers could modify locally the distribution of the growing aggregates in the solution even if it does not lead to phase separation. This could modify the growth mechanism of the strands. Increasing the size of the aggregates reduces the critical  $\kappa$ -car concentration needed to induce phase separation. This is why we observed weak phase separation at [CaCl<sub>2</sub>] = 1 mM for  $C_K = 5$  g L<sup>-1</sup> even when no microgels were formed. As a consequence, the effect of microgel formation on the evolution of the structure of the mixtures was not obvious at  $C_K = 5$  g L<sup>-1</sup>.

The evolution of  $F_{ps}$  was closest to that of the fraction of microgels for  $C_K = 4$  g L<sup>-1</sup> suggesting that in this case most of the strands remained in solution and most of the microgels phase separated. At  $C_K = 3$  g L<sup>-1</sup> and  $C_K = 2$  g L<sup>-1</sup>, the increase of  $F_{ps}$  started at larger [CaCl<sub>2</sub>] than for MAH, which implies that for a given [CaCl<sub>2</sub>] smaller or fewer microgels were formed when the systems were heated in the presence of  $\kappa$ -car. Indeed, figure 8 shows that in the presence of 2 and 3 g L<sup>-1</sup>  $\kappa$ -car smaller microgels were formed at [CaCl<sub>2</sub>] = 2 mM

than in the absence of  $\kappa$ -car. As we mentioned above, this is probably caused by the competition between  $\kappa$ -car and  $\beta$ -lg for the calcium ions so that amount of calcium available to the proteins is reduced.

We expect that the influence of CaCl<sub>2</sub> on the structure of the mixtures also influences the properties of gels that can be formed either by adding KCl or by using higher protein concentrations. In the first case  $\kappa$ -car gels upon cooling, while in the second case  $\beta$ -lg gels during heating. We will report elsewhere on the effect of CaCl<sub>2</sub> on the structure and rheology of gelled mixtures and we will discuss there the role of competition for calcium ions between  $\beta$ -lg and  $\kappa$ -car in more detail.

## 5. Conclusion

Addition of a small fraction of CaCl<sub>2</sub> has a major influence on the structure of heated mixtures of  $\beta$ -lg and  $\kappa$ -car. When more than about 1.5 calcium ions are present per protein, heating leads to the formation of microgels with  $R_h > 100$  nm rather than small strands with  $R_h < 20$  nm. In mixtures with  $\kappa$ -car,  $\beta$ -lg microgels phase separate at much lower  $\kappa$ -car concentrations than the small strands. Therefore the appearance and structure of heated mixtures is very sensitive to the addition of CaCl<sub>2</sub>. Phase separation leads to the formation of spherical protein rich domains with a diameter of a few microns. The concentration of  $\kappa$ -car is decreased by only about 30% in the protein rich domains. The protein rich domains cluster into large flocs that slowly sediment, but the precipitate can be easily dispersed by shaking. The structures of mixtures with the same composition are similar when separately formed  $\beta$ -lg microgels are mixed with  $\kappa$ -car at room temperature or when mixtures of native  $\beta$ -lg and  $\kappa$ -car are heated. However, in the former case phase separation can be reversed by dilution, while in the latter the proteins become strongly bound within the domains. Therefore, the domains persist after dilution in the latter case.

## Acknowledgments

BTN thanks the Ministry of Education and Training of Vietnam for financial support.

## References

- Baussay K, Nicolai T and Durand D 2006 Effect of the cluster size on the micro phase separation in mixtures of  $\beta$ -lactoglobulin clusters and  $\kappa$ -carrageenan *Biomacromolecules* **7** 304–9
- Berne B and Percora R 1976 *Dynamic Light Scattering* (New York: Wiley)
- Brownlow S, Cabral J H M, Cooper R, Flower D R, Yewdall S J, Polikarpov I, North A C and Sawyer L 1997 Bovine [beta]-lactoglobulin at 1.8 Å resolution—still an enigmatic lipocalin *Structure* **5** 481–95
- Bryant C M and McClements D J 1998 Molecular basis of protein functionality with special consideration of cold-set gels derived from heat-denatured whey *Trends Food Sci. Tech.* **9** 143–51
- Cakir E and Foegeding E A 2011 Combining protein micro-phase separation and protein–polysaccharide segregative phase



- separation to produce gel structures *Food Hydrocolloid* **25** 1538–46
- Capron I, Nicolai T and Smith C 1999 Effect of addition of kappa-carrageenan on the mechanical and structural properties of beta-lactoglobulin gels *Carbohydr. Polym.* **40** 233–8
- Clark A H 1999 *Functional Properties of Food Macromolecules* 2nd edn, ed S E Hill *et al* (Gaithersburg: Aspen Publishers) pp 77–142
- Croguennoc P, Durand D and Nicolai T 2001a Phase separation and association of globular protein aggregates in the presence of polysaccharides: 1. Mixtures of preheated  $\beta$ -lactoglobulin and  $\kappa$ -carrageenan at room temperature *Langmuir* **17** 4372–9
- Croguennoc P, Durand D and Nicolai T 2001b Phase separation and association of globular protein aggregates in the presence of polysaccharides: 2. Heated mixtures of native  $\beta$ -lactoglobulin and  $\kappa$ -carrageenan *Langmuir* **17** 4380–5
- de Jong S, Klok H J and van de Velde F 2009 The mechanism behind microstructure formation in mixed whey protein–polysaccharide cold-set gels *Food Hydrocolloid* **23** 755–64
- De Kruif C G and Tuinier R 2001 Polysaccharide protein interactions *Food Hydrocolloid* **15** 555–63
- De la Fuente M A, Singh H and Hemar Y 2002 Recent advances in the characterization of heat-induced aggregates and intermediates of whey proteins *Trends Food Sci. Tech.* **13** 262–74
- De Wit J N 1998 Nutritional and functional characteristics of whey proteins in food products *J. Dairy Sci.* **81** 597–608
- Donato L, Schmitt C, Bovetto L and Rouvet M 2009 Mechanism of formation of stable heat-induced beta-lactoglobulin microgels *Int. Dairy J.* **19** 295–306
- Durand D, Gimel J C and Nicolai T 2002 Aggregation, gelation and phase separation of heat denatured globular proteins *Physica A* **304** 253–65
- Eleya M M O and Turgeon S L 2000 Rheology of kappa-carrageenan and beta-lactoglobulin mixed gels *Food Hydrocolloid* **14** 29–40
- Fox P F 2003 *Advanced Dairy Chemistry: Proteins* vol 1 3rd edn, ed P F Fox and P L H McSweeney (London: Elsevier) pp 427–35
- Gaaloul S, Turgeon S L and Corredig M 2009 Influence of shearing on the physical characteristics and rheological behaviour of an aqueous whey protein isolate-kappa-carrageenan mixture *Food Hydrocolloid* **23** 1243–52
- Gaaloul S, Turgeon S L and Corredig M 2010 Phase behavior of whey protein aggregates/kappa-carrageenan mixtures: experiment and theory *Food Biophys.* **5** 103–13
- Gosal W S and Ross-Murphy S B 2000 Globular protein gelation *Curr. Opin. Colloid Interface Sci.* **5** 188–94
- Harrington J C, Foegeding E A, Mulvihill D M and Morris E R 2009 Segregative interactions and competitive binding of  $\text{Ca}^{2+}$  in gelling mixtures of whey protein isolate with  $\text{Na}^+$  kappa-carrageenan *Food Hydrocolloid* **23** 468–89
- Heilig A, Göggerle A and Hinrichs J 2009 Multiphase visualisation of fat containing  $\beta$ -lactoglobulin– $\kappa$ -carrageenan gels by confocal scanning laser microscopy, using a novel dye, V03-01136, for fat staining *LWT-Food Sci. Technol.* **42** 646–53
- Kinsella J E and Whitehead D M 1989 *Proteins in Whey: Chemical, Physical and Functional Properties* (San Diego: Academic) pp 343–437
- Meunier V, Nicolai T, Durand D and Parker A 1999 Light scattering and viscoelasticity of aggregating and gelling  $\kappa$ -carrageenan *Macromolecules* **32** 2610–6
- Mezzenga R and Fischer P 2013 The self-assembly, aggregation and phase transitions of food protein systems in one, two and three dimensions *Rep. Prog. Phys.* **76** 046601
- Morris V J 2007 *Understanding and Controlling the Microstructure of Complex Foods* ed D J McClements (Boca Raton, FL: CRC Press)
- Morris V J and Wilde P J 1997 Interactions of food biopolymers *Curr. Opin. Colloid Interface Sci.* **2** 567–72
- Nguyen B T, Phan-Xuan T, Benyahia L and Nicolai T 2014 Combined effects of temperature and elasticity on phase separation in mixtures of  $\kappa$ -carrageenan and  $\beta$ -lg aggregates *Food Hydrocolloid* **34** 138–44
- Nicolai T and Durand D 2013 Controlled food protein aggregation for new functionality *Curr. Opin. Colloid Interface Sci.* **18** 249–56
- Nicolai T, Britten M and Schmitt C 2011  $\beta$ -lactoglobulin and WPI aggregates: formation, structure and applications *Food Hydrocolloid* **25** 1945
- Nishinari K, Zhang W and Ikeda S 2000 Hydrocolloid gels of polysaccharides and proteins *Curr. Opin. Colloid Interface Sci.* **5** 195–201
- Phan-Xuan T, Durand D, Nicolai T, Donato L, Schmitt C and Bovetto L 2011 On the crucial importance of the pH for the formation and self-stabilization of protein microgels and strands *Langmuir* **27** 15092–101
- Phan-Xuan T, Durand D, Nicolai T, Donato L, Schmitt C and Bovetto L 2013 Tuning the structure of protein particles and gels with calcium or sodium ions *Biomacromolecules* **14** 1980–9
- Phan-Xuan T, Durand D, Nicolai T, Donato L, Schmitt C and Bovetto L 2014 Heat induced formation of beta-lactoglobulin microgels driven by addition of calcium ions *Food Hydrocolloid* **34** 227–35
- Piculell L 2006 *Food Polysaccharides and Their Applications* ed A M Stephen *et al* (Boca Raton, FL: CRC Press) p 239
- Roesch R, Cox S, Compton S, Happek U and Corredig M 2004 Kappa-carrageenan and beta-lactoglobulin interactions visualized by atomic force microscopy *Food Hydrocolloid* **18** 429–39
- Schmitt C, Bovay C, Vuillienet A M, Rouvet M, Bovetto L, Barbar R and Sanchez C 2009 Multiscale characterization of individualized beta-lactoglobulin microgels formed upon heat treatment under narrow pH range conditions *Langmuir* **25** 7899–909
- Schmitt C, Moitzi C, Bovay C, Rouvet M, Bovetto L, Donato L, Leser M E, Schurtenberger P and Stradner A 2010 Internal structure and colloidal behaviour of covalent whey protein microgels obtained by heat treatment *Soft Matter* **6** 4876–84
- Semenova M G, Dickinson E, Burlakova E B and Zaikov G E 2010 *Biopolymers in Food Colloids: Thermodynamics and Molecular Interactions* (Boca Raton, FL: Taylor and Francis)
- Totosaus A, Montejano J G, Salazar J A and Guerrero I 2002 A review of physical and chemical protein-gel induction *Int. J. Food Sci. Tech.* **37** 589–601
- Tuinier R, Rieger J and Kruif C G D 2003 Depletion-induced phase separation in colloid–polymer mixtures *Adv. Colloid Interface Sci.* **103** 1–31
- Turgeon S L, Beaulieu M, Schmitt C and Sanchez C 2003 Protein polysaccharide interactions: phase-ordering kinetics, thermodynamic and structural aspects *Curr. Opin. Colloid Interface Sci.* **8** 401–14

## **PAPER 4**





Contents lists available at ScienceDirect

## Colloids and Surfaces A: Physicochemical and Engineering Aspects

journal homepage: [www.elsevier.com/locate/colsurfa](http://www.elsevier.com/locate/colsurfa)



# The effect of the competition for calcium ions between $\kappa$ -carrageenan and $\beta$ -lactoglobulin on the rheology and the structure in mixed gels

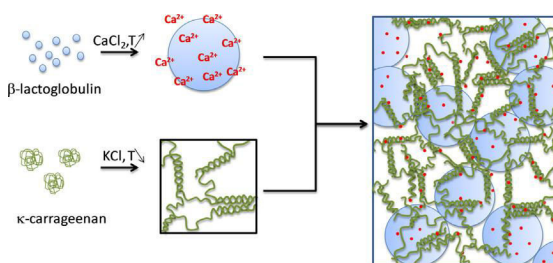
Bach T. Nguyen, Taco Nicolai\*, Lazhar Benyahia, Christophe Chassenieux

LUNAM Université, Laboratoire Polymères, Colloïdes et Interfaces, UMR CNRS 6283, Université du Maine, 72085 Le Mans cedex 9, France

### HIGHLIGHTS

- Microphase separation in heated  $\kappa$ -car/ $\beta$ -lg mixtures can be induced by addition of a small amount of  $\text{CaCl}_2$ .
- The elastic modulus of  $\kappa$ -car gels in the presence of  $\beta$ -lg is determined by the competition for  $\text{Ca}^{2+}$  between the two biopolymers.
- Interpenetrated  $\kappa$ -car and  $\beta$ -lg gels have approximately the same stiffness as the sum of individual gels.
- Heat-induced gelation of  $\beta$ -lg is favored by the presence of  $\kappa$ -car.

### GRAPHICAL ABSTRACT



### ARTICLE INFO

#### Article history:

Received 26 June 2014

Received in revised form 31 August 2014

Accepted 6 September 2014

Available online xxx

#### Keywords:

Protein  
Polysaccharide  
Lactoglobulin  
Carrageenan  
Gel  
Rheology

### ABSTRACT

Protein aggregates were formed by heating the globular protein  $\beta$ -lactoglobulin ( $\beta$ -lg) in aqueous solution in the presence of  $\text{CaCl}_2$  leading to small strands at low  $\text{CaCl}_2$  concentrations and larger spherical microgels at higher  $\text{CaCl}_2$  concentrations. The structure of mixtures of protein aggregates and the polysaccharide  $\kappa$ -carrageenan ( $\kappa$ -car) was investigated at pH 7 using confocal laser scanning microscopy. Microphase separation in the form of dense protein domains was observed for mixtures with microgels even at very low  $\kappa$ -car concentrations (0.5 g/L). Gelation of  $\kappa$ -car was induced by cooling in the presence of 10 mM KCl. Addition of microgels strongly increased the gelation rate and the elastic modulus of the  $\kappa$ -car gels, while the effect of adding native proteins or strands was small. The effect could be attributed to the presence of calcium ions used to form the microgels. However, the effect was smaller than in pure  $\kappa$ -car gels if the same amount of calcium ions was added in the form of  $\text{CaCl}_2$ . The effect is explained by the competition between  $\kappa$ -car and  $\beta$ -lg for calcium ions. A weaker effect was observed with native  $\beta$ -lg, which can be correlated with the weaker binding of  $\text{Ca}^{2+}$  by native  $\beta$ -lg compared to microgels. Gelation of  $\beta$ -lg in the presence of  $\kappa$ -car was induced by heating mixtures of  $\kappa$ -car and native  $\beta$ -lg. The presence of  $\kappa$ -car facilitated gelation of  $\beta$ -lg at lower  $\text{CaCl}_2$  concentrations.  $\kappa$ -car was gelled within the  $\beta$ -lg gel by cooling. It was found that the elastic modulus of the mixed gel was close to the sum of that of the  $\kappa$ -car gel with native  $\beta$ -lg and the  $\beta$ -lg gel with uncrosslinked  $\kappa$ -car coils.

© 2014 Elsevier B.V. All rights reserved.

## 1. Introduction

Globular proteins have a well-defined structure that is perturbed when they are heated in aqueous solution. This can lead to aggregation and gelation of the proteins, a process that is widely encountered in the manufacturing of food products [1]. Many food products contain polysaccharides as well as proteins.

\* Corresponding author. Tel.: +33 0243833139.

E-mail address: [Taco.Nicolai@univ-lemans.fr](mailto:Taco.Nicolai@univ-lemans.fr) (T. Nicolai).

Therefore it is important to understand how polysaccharides influence the aggregation process and how protein aggregates interact with polysaccharides. Here we report on an investigation of mixtures of the globular whey protein  $\beta$ -lactoglobulin ( $\beta$ -lg) and the polysaccharide  $\kappa$ -carrageenan ( $\kappa$ -car).

$\beta$ -lg aggregates irreversibly when heated in aqueous solution. It forms a gel above a critical gel concentration, but at lower concentrations a stable suspension of aggregates can be obtained [2]. Often whey protein isolate (WPI) is studied instead of pure  $\beta$ -lg. WPI contains mainly  $\beta$ -lg, but also other globular proteins such as  $\alpha$ -lactalbumin, and its behavior is similar to that of pure  $\beta$ -lg. The size and morphology of the aggregates depends on the pH, the type and concentration of salt, and the concentration of protein. At pH 7, a striking transition occurs in the morphology of the protein aggregates when  $\text{CaCl}_2$  is added [3]. When less than 1 calcium ion per protein is present, relatively small strand-like aggregates with a hydrodynamic radius ( $R_h$ ) of about 15 nm are formed, but at higher  $\text{CaCl}_2$  concentration a fraction of the proteins form spherical aggregates with  $R_h > 100$  nm. The fraction of proteins that form these so-called microgels increases rapidly with increasing  $\text{CaCl}_2$  concentration.

$\kappa$ -car is an anionic polysaccharide isolated from algae and is used as thickening or gelling agent in food products [4]. In aqueous solution it has a random coil conformation at high temperatures, but in the presence of salt it takes a helical conformation below a critical temperature ( $T_c$ ) that depends on the type and concentration of the cations.  $\kappa$ -car helices have a tendency to aggregate which can lead to the formation of a percolating network. Gelation of  $\kappa$ -car can be reversed by heating above another critical temperature that is generally higher than the gelling temperature.

At neutral pH, both  $\beta$ -lg and  $\kappa$ -car are negatively charged and native  $\beta$ -lg is compatible with  $\kappa$ -car over a wide range of biopolymer concentrations. However, when  $\beta$ -lg has formed aggregates, segregative phase separation can occur in mixtures with  $\kappa$ -car [5–7]. Most often phase separation leads to the formation of protein rich domains with a diameter of a few microns. These domains do not fuse spontaneously, but agglomerate into large clusters that slowly sediment under gravity. The critical  $\kappa$ -car concentration above which phase separation occurs, decreases with increasing size of the  $\beta$ -lg aggregates, but is only weakly dependent on the  $\beta$ -lg concentration. The effect of gelling of  $\kappa$ -car on microphase separation can be studied by cooling the solutions below  $T_c$  in the presence of salt. It was found that for weakly phase separated systems the domains redisperse when strong  $\kappa$ -car gels are formed [8,9].

Similar microphase separation also occurs when the  $\beta$ -lg aggregates are formed in mixtures with  $\kappa$ -car, e.g. heating a mixture of native  $\beta$ -lg and  $\kappa$ -car [6,10–17]. However, in this case the proteins in the dense domains are irreversibly crosslinked. Phase separation does not inhibit gelation of the proteins if their concentration is high enough, but it will lead to the formation of more heterogeneous gels. The formation of heterogeneous mixed gels has also been reported when gelation of homogeneous mixtures of  $\kappa$ -car with small  $\beta$ -lg aggregates was induced by reduction of the pH [18] or addition of salt [8].

Recently, we investigated the effect of the transition in the morphology of  $\beta$ -lg aggregates induced by adding  $\text{CaCl}_2$  [19] on phase separation in mixtures with  $\kappa$ -car.  $\beta$ -lg strands are much smaller than the microgels and are therefore compatible with  $\kappa$ -car at concentrations where mixtures with  $\beta$ -lg microgels show phase separation. As a consequence, when between 2 g/L and 5 g/L  $\kappa$ -car was mixed with both strands and microgels only the microgels phase separated. The same effect was found when the protein aggregates were formed in situ by heating mixtures of  $\kappa$ -car and native proteins. At lower  $\kappa$ -car concentrations, only the microgels phase separated while the strands remained homogeneously

distributed. For this reason the structure of heated mixtures changed from homogeneous at lower  $\text{CaCl}_2$  concentrations where only strands were formed to highly heterogeneous at higher  $\text{CaCl}_2$  concentrations where mainly microgels were formed. The transition occurred in a narrow range of the  $\text{CaCl}_2$  concentration, because the fraction of microgels that was formed during heating is very sensitive to the  $\text{CaCl}_2$  concentration.

The  $\text{CaCl}_2$  concentrations used in our earlier investigation were too low to induce the coil–helix transition of  $\kappa$ -car at room temperature. Furthermore, we did not investigate the rheology of the mixtures. The objective of the present investigation was to investigate the effect of  $\kappa$ -car gelation on the structure and the rheology of the mixtures. For this reason we have added a small amount of KCl, which induces  $\kappa$ -car gelation at 20 °C. We have investigated mixtures of  $\kappa$ -car with  $\beta$ -lg aggregates formed separately at different  $\text{CaCl}_2$  concentrations as well as heated mixtures of  $\kappa$ -car and native  $\beta$ -lg at different  $\text{CaCl}_2$  concentrations. We will show that the proteins gel in the heated mixtures and that subsequent cooling leads to the formation of an interpenetrated network of both biopolymers. We will compare the stiffness of the interpenetrated gels with the sum of the stiffness of the two individual biopolymer gels. The investigation presented here is closely related to that of Harrington et al. [14] who studied mixtures of  $\kappa$ -car with WPI in the presence of  $\text{CaCl}_2$ . These authors present a useful discussion of the older literature on mixtures of  $\kappa$ -car and WPI or  $\beta$ -lg in the presence of calcium ions. We will below discuss the results of their study in the context of the results obtained by our investigation.

## 2. Materials and methods

### 2.1. Materials

The  $\beta$ -lactoglobulin (Biopure, lot JE 001-8-415) used in this study was purchased from Davisco Foods International, Inc. (Le Sueur, MN, USA) and consisted of approximately equal quantities of variants A and B. The powder was dissolved by stirring in Milli-Q water with 200 ppm  $\text{NaN}_3$  added to prevent bacterial growth and the pH was adjusted to 7. The protein concentration ( $C_b$ ) was determined by UV absorption at 278 nm with a UV-Visible spectrometer Varian Cary-50 Bio (Les Ulis, France) using extinction coefficient  $0.96 \text{ L g}^{-1} \text{ cm}^{-1}$ . The sodium  $\kappa$ -carrageenan used for this study was a gift from Cargill (Baupre, France) and contained less than 5%  $\iota$ -carrageenan. The  $\kappa$ -car powder was dissolved in Milli-Q water with 200 ppm sodium azide while stirring for a few hours at 70 °C and the pH was adjusted to 7. The  $\kappa$ -car concentration ( $C_k$ ) was determined by measuring the refractive index using refractive index increment  $0.145 \text{ ml/g}$ . The molar mass ( $2.1 \times 10^5 \text{ g/mol}$ ) and the radius of gyration (52 nm) were determined by light scattering as described elsewhere [20].

Protein aggregates or gels were formed by heating  $\beta$ -lg solutions with or without  $\kappa$ -car in a waterbath thermostated at 85 °C. The pH and the salt concentration of all samples were set before heating. The samples were kept in the bath sufficiently long to ensure that steady state was reached, i.e. depending on the conditions between a few hours and overnight. Since the systems did not evolve further when steady state was reached the exact heating time is not important. As will be described below, either aggregates or gels were formed depending on the protein concentration and the concentrations of  $\kappa$ -car and salt.

### 2.2. Methods

Confocal Laser Scanning Microscopy (CLSM) was used in the fluorescence mode. Observations were made with a Leica TCS-SP2 (Leica Microsystems Heidelberg, Germany). A water immersion



objective lens was used HCxPL APO 63 $\times$  NA=1.2 with theoretical resolution of 0.3  $\mu$ m in the x–y plane.  $\beta$ -lg was physically labeled with the fluorochrome rhodamine B, by adding a small amount of a concentrated rhodamine solution (5 ppm) to the  $\beta$ -lg solutions. No effect of labeling was observed on the structure when the amount of labeling was varied unless a significantly larger amount of rhodamine was added. In addition the rheology was not found to be different for labeled and unlabelled samples.

Oscillatory shear measurements were done with a stress imposed rheometer (AR2000, TA Instruments) using a plate–plate geometry (diameter 40 mm, gap 700  $\mu$ m). The temperature was controlled by a Peltier system and the geometry was covered with paraffin oil to prevent water evaporation. The storage ( $G'$ ) and loss ( $G''$ ) moduli were determined in the linear response regime.

Light scattering measurements were done with a commercial apparatus (ALV-CGS3, ALV-Langen) operating with a vertically polarized He–Ne laser with wavelength  $\lambda$ =632 nm. The temperature was controlled at 20 °C with a thermostat bath to within  $\pm 0.2$  °C.

The calcium ion activity in solution was determined using a calcium-specific electrode (Fisher Scientific, USA). A calibration curve was obtained by measuring  $\text{CaCl}_2$  solutions in water at concentrations ranging from 0 to 25 mM. The concentration of free calcium ions was calculated by assuming that the activity of bound  $\text{Ca}^{2+}$  was zero and the activity of free  $\text{Ca}^{2+}$  was the same as in pure water.

### 3. Results

We will first discuss the effect of  $\kappa$ -car gelation on the structure of the mixtures and then the effect on the elastic modulus. We distinguish between mixtures of  $\kappa$ -car with  $\beta$ -lg aggregates prepared by heating native proteins separately and heated mixtures of  $\kappa$ -car and native  $\beta$ -lg.

#### 3.1. Structure

##### 3.1.1. Mixtures of protein aggregates and $\kappa$ -car

As it was mentioned in Section 1, aggregates with different sizes and shapes can be formed by  $\beta$ -lg when it is heated in aqueous solution at different  $\text{CaCl}_2$  concentrations. For the present investigation we have heated 40 g/L  $\beta$ -lg at pH 7 at different  $\text{CaCl}_2$  concentrations up to  $[\text{CaCl}_2]=5.3$  mM. At higher  $\text{CaCl}_2$  concentrations, secondary aggregation of the microgels occurred and at 7.0 mM a gel was formed. The hydrodynamic radius ( $R_h$ ) of the aggregates was measured using dynamic light scattering in same way as described elsewhere [3]. The results are shown as a function of  $[\text{CaCl}_2]$  in Fig. 1.  $R_h$  increased sharply for  $[\text{CaCl}_2]>2$  mM, because at a critical molar ratio of  $\text{CaCl}_2$  to  $\beta$ -lg ( $R$ ) of approximately 1.5 the morphology of the aggregates changed from relatively small strands to relatively large microgels.

Aggregates obtained at different  $\text{CaCl}_2$  concentrations were mixed with  $\kappa$ -car at 50 °C and subsequently observed with CLSM either directly at 20 °C or after cooling first to 5 °C, see Fig. 2. The mixtures contained 10 mM KCl, which induced slow gelation of  $\kappa$ -car at 20 °C and rapid gelation at 5 °C. Images that were taken immediately after cooling to 20 °C were the same as those taken after equilibrating for 1.5 h at this temperature. When cooled directly from 50 to 20 °C, microphase separation was observed for  $[\text{CaCl}_2]\geq 4.5$  mM ( $R_h\geq 200$  nm), but when the mixture was first cooled to 5 °C, microphase separation became apparent already for  $[\text{CaCl}_2]\geq 3.5$  mM ( $R_h\geq 75$  nm). The dependence on the temperature history was reversible, because when mixtures at  $[\text{CaCl}_2]=4.0$  mM were heated back to 50 °C and subsequently cooled to 20 °C they remained homogeneous. It appears that the critical aggregate size

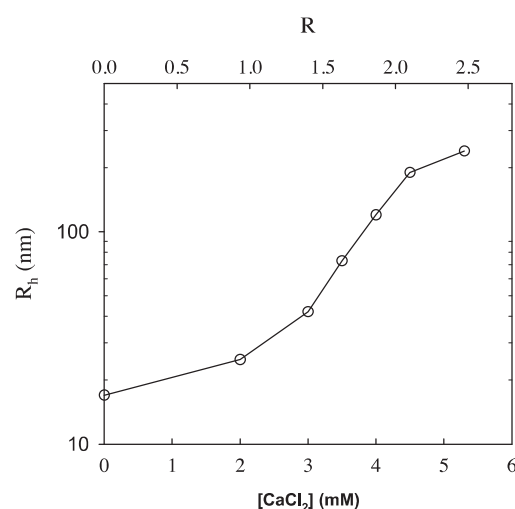


Fig. 1. Hydrodynamic radius of protein aggregates formed in solutions containing 40 g/L  $\beta$ -lg and different  $\text{CaCl}_2$  concentrations that were heated overnight at 85 °C.

required to induce microphase separation is smaller when the mixture is cooled to 5 °C.

We also investigated the effect of the  $\kappa$ -car concentration in the mixtures while keeping the concentration and size of the  $\beta$ -lg aggregates fixed. Fig. 3 shows CLSM images of mixtures that contained 40 g/L microgels formed at 5.3 mM  $\text{CaCl}_2$  with  $R_h=240$  nm and different  $\kappa$ -car concentrations. For this system phase separation was observed starting from 0.5 g/L  $\kappa$ -car. Relatively large protein rich domains were formed at  $C_k=0.5$  and 1 g/L, while small domains were formed for  $C_k\geq 2.0$  g/L. The small domains were randomly associated into large clusters. The effect of cooling to 5 °C led to the formation of more domains at  $C_k=0.5$  and 1 g/L and to coarsening of the structure at  $C_k=1.5$  g/L. We did not study here the distribution of  $\kappa$ -car between the two phases, but we showed in Ref. [19] that  $\kappa$ -car is only weakly phase separated. Indeed, even when the protein concentration was 6 times higher in the protein rich phase than in the protein poor phase, the concentration of  $\kappa$ -car was only about 25% lower in the protein rich phase than in the protein poor phase.

The dependence on the temperature history can be explained by the fact that phase separation is favored by lowering the temperature as was shown elsewhere [9]. This may appear in contradiction with the fact that the images were all taken at 20 °C, but in fact the enhanced phase separation during cooling to 5 °C is frozen-in by gelation of  $\kappa$ -car. An effect of cooling to 5 °C could still be seen in Fig. 2 for aggregates formed at 4.5 mM  $\text{CaCl}_2$ , but it was negligible for aggregates formed at 5.3 mM  $\text{CaCl}_2$ . Similarly, the effect of cooling to 5 °C disappeared for  $C_k\geq 2$  g/L in the mixtures with microgels shown in Fig. 3.

Gelation of  $\kappa$ -car also has an effect on the agglomeration of the protein rich domains. If the gelation of  $\kappa$ -car is fast, it can inhibit association of the protein domains into large clusters. We illustrate this for mixtures of 10 g/L microgels and different concentrations of  $\kappa$ -car. The solutions were mixed at 50 °C in the presence of 20 mM KCl in order to induce rapid gelation of  $\kappa$ -car at 20 °C. The mixtures were either cooled directly to 20 °C after mixing or they were kept during 15 min at 50 °C, i.e. above  $T_c$ , before cooling. CLSM images of mixtures containing 2 g/L or 4 g/L  $\kappa$ -car are shown in Fig. 4. When the systems were cooled immediately after mixing, the protein domains were much less agglomerated and more homogeneously distributed than when they were first kept for 15 min in the liquid state at 50 °C. The implication is that the protein rich domains

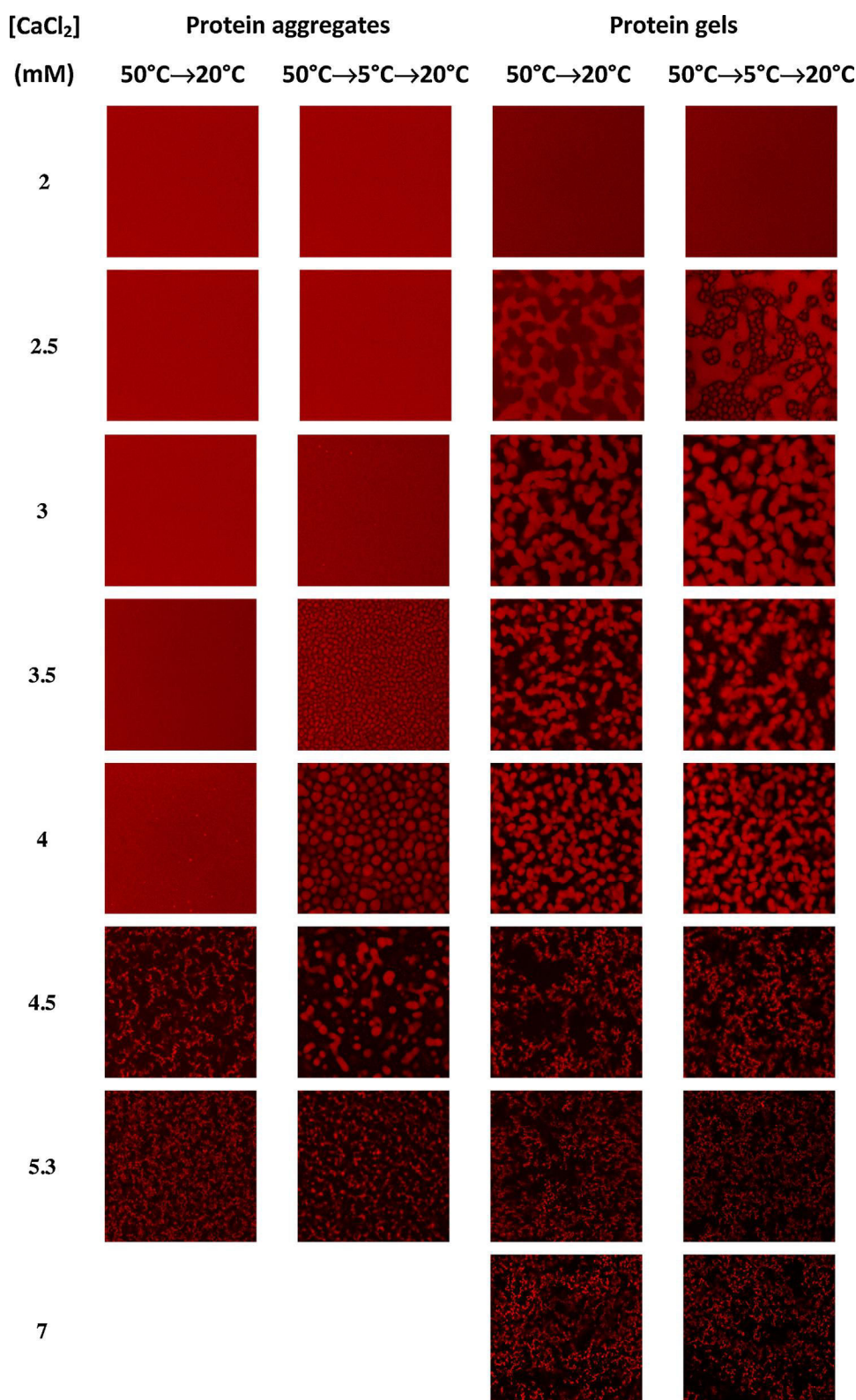


**Fig. 2.** CLSM images of mixtures containing 40 g/L partially labeled  $\beta$ -lg aggregates or gels and 2 g/L  $\kappa$ -car in the presence of 10 mM KCl. The protein aggregates were formed by heating  $\beta$ -lg solutions at 85 °C at different CaCl<sub>2</sub> concentrations as indicated in the figure. The protein gels were formed by heating mixtures of native  $\beta$ -lg with  $\kappa$ -car at 85 °C at different CaCl<sub>2</sub> concentrations as indicated in the figure. The images represent 160 × 160  $\mu$ m. The images were obtained at 20 °C after different temperature histories indicated in the figure, see text.



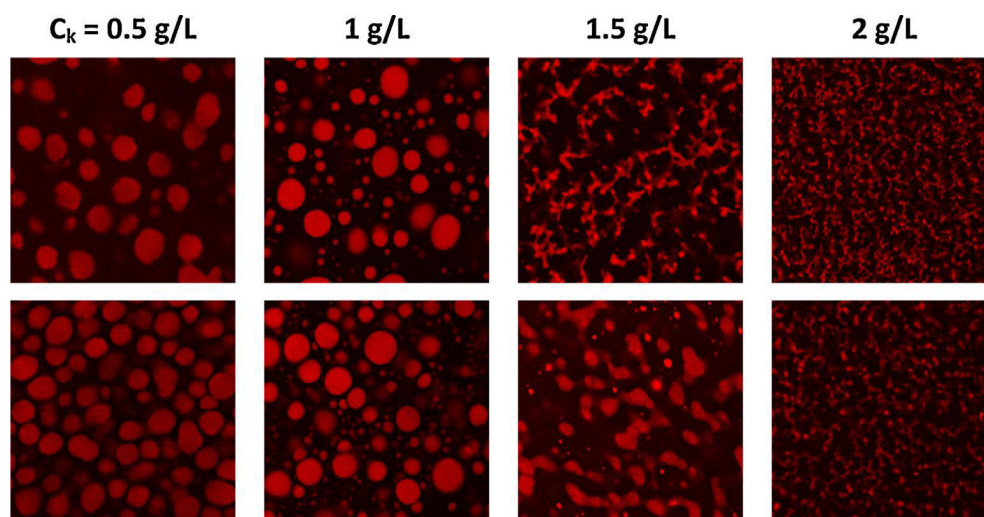


**Fig. 3.** CLSM images of mixtures containing 40 g/L partially labeled microgels ( $R_h = 240$  nm) and different  $\kappa$ -car concentrations in the presence of 10 mM KCl. The mixtures shown in the top row were directly cooled to 20 °C, while the images shown in the bottom row were first cooled to 5 °C and then measured at 20 °C. The images represent 160 × 160  $\mu$ m.

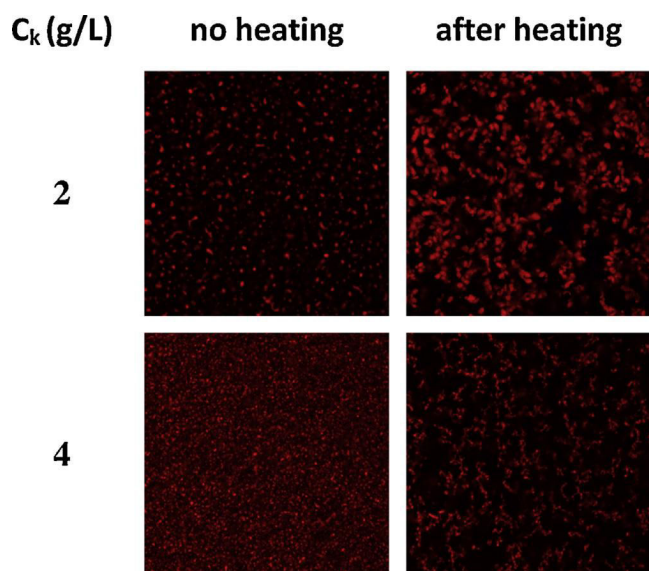


**Fig. 4.** CLSM images of mixtures containing 10 g/L partially labeled microgels ( $R_h = 240$  nm) and 2 or 4 g/L  $\kappa$ -car in the presence of 20 mM KCl. The mixtures were either cooled immediately to 20 °C after mixing at 50 °C (left column) or kept for 15 min at 50 °C before cooling (right column). The images represent 160 × 160  $\mu$ m.

are formed rapidly and that their agglomeration into large clusters takes some time and cannot occur if a strong  $\kappa$ -car gel is formed.

### 3.1.2. Mixtures of protein gels and $\kappa$ -car

Fig. 2 shows CLSM images of mixtures of 40 g/L native  $\beta$ -lg and 2 g/L  $\kappa$ -car that were heated at 85 °C in the presence of 10 mM KCl and various amounts of  $\text{CaCl}_2$ . They may be compared with images of mixtures with separately prepared protein aggregates that were discussed in the previous section. For the heated mixtures, phase separation became apparent at lower  $\text{CaCl}_2$  concentrations ( $[\text{CaCl}_2] \geq 2.5$  mM) than in the mixtures with separately prepared protein aggregates. The difference in the onset of phase separation is related to the fact that  $\beta$ -lg in the heated mixtures formed a gel even at low  $\text{CaCl}_2$  concentrations, see below.

For  $[\text{CaCl}_2] \geq 4.5$  mM the system consisted of agglomerated small protein rich domains and the structure was similar to that of mixtures of  $\kappa$ -car and  $\beta$ -lg aggregates at conditions where they

are strongly phase separated. At lower  $\text{CaCl}_2$  concentrations, the protein rich domains were larger and the distinction between the domains became less clear. At  $[\text{CaCl}_2] = 2.5$  mM the domains had fully merged into a continuous phase. For the heated mixtures, cooling to 5 °C did not have a strong influence on the structure, which can be understood from the fact that the proteins were covalently crosslinked into a network during heating. An exception is the system at 2.5 mM  $\text{CaCl}_2$  for which spherical protein rich domains appeared in the protein depleted phase when the system was cooled to 5 °C. The fact that cooling to 5 °C could induce secondary phase separation in the protein depleted phase implies that the protein aggregates in this phase were not connected to the covalently linked  $\beta$ -lg network.

From the fluorescence intensity we can deduce the protein concentration in the different phases. In this way we found at  $[\text{CaCl}_2] = 2.5$  mM for the system that was cooled to 20 °C,  $C_b = 56$  g/L in the dense phase and  $C_b = 30$  g/L in the depleted phase. After cooling to 5 °C we found  $C_b = 58$  g/L and  $C_b = 31$  g/L, respectively. Thus cooling to 5 °C did not influence the overall contrast between the dense and depleted phase in this case, probably because the proteins in the dense phase had formed a covalently crosslinked gel. However, within the protein depleted phase, dense domains with  $C_b = 43$  g/L were formed while the concentration outside these domains was  $C_b = 19$  g/L. With increasing  $\text{CaCl}_2$  concentration the ratio between the protein concentration in the dense and depleted phases increased rapidly from less than 2 at  $[\text{CaCl}_2] = 2.5$  mM to about 8 for  $[\text{CaCl}_2] > 4.0$  mM.

### 3.2. Rheology

#### 3.2.1. Mixtures of protein aggregates and $\kappa$ -car

The effect of the presence of  $\beta$ -lg aggregates on  $\kappa$ -car gelation at 10 mM KCl was studied for mixtures containing 2 g/L  $\kappa$ -car and microgels with  $R_h = 240$  nm at different concentrations between 5 and 40 g/L. The microgels were formed by heating 40 g/L  $\beta$ -lg at  $[\text{CaCl}_2] = 5.3$  mM and were subsequently mixed at different concentrations with  $\kappa$ -car at 50 °C. A CLSM image of the mixture at  $C_b = 40$  g/L is shown in Fig. 2. The structure at lower protein concentrations was similar except that it contained fewer domains as was shown by Nguyen et al. [19] for the same mixtures in the absence of KCl. No significant difference was observed between samples measured directly at 20 °C and those cooled first to 5 °C.

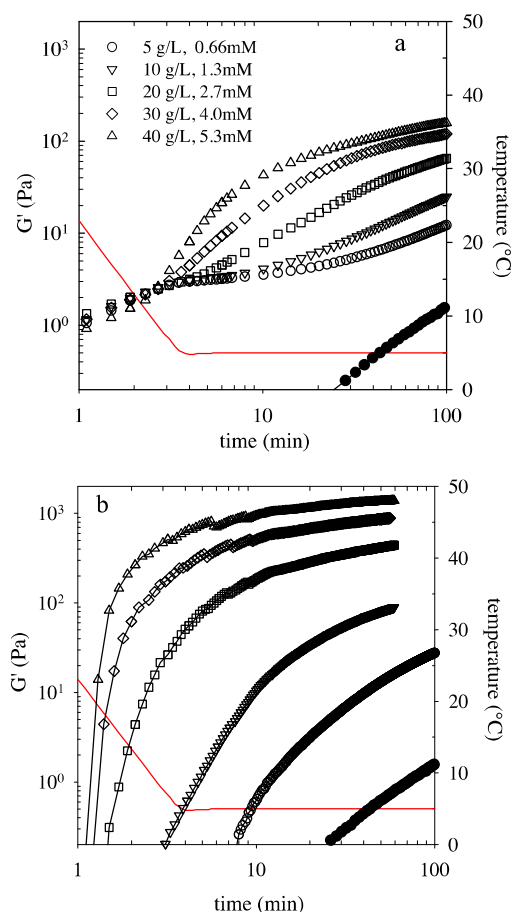


**Fig. 5.** (a) Evolution of  $G'$  at 0.1 Hz for mixtures of 2 g/L  $\kappa$ -car at 10 mM KCl and different concentrations of microgels with  $R_h = 240$  nm during and after rapid cooling from 50 °C to 5 °C. The evolution of the pure  $\kappa$ -car solution in 10 mM KCl is indicated by filled symbols. The microgels contained 2.5 calcium ions per protein. The solid line indicates the temperature as a function of time. (b) Evolution of  $G'$  at 0.1 Hz for 2 g/L  $\kappa$ -car at 10 mM KCl and different  $\text{CaCl}_2$  concentrations. The amount of calcium ions was chosen to be the same as for the mixtures shown in (a). Symbols for the different  $\text{CaCl}_2$  concentrations are the same as in (a).

Fig. 5a shows the evolution of the storage shear modulus at 0.1 Hz during and after rapid cooling from 50 °C to 5 °C. In the absence of microgels, gelation of  $\kappa$ -car was very slow and steady state was not yet reached even after 2 days (data not shown), but the rate of gelation increased strongly with increasing microgel concentration. Measurements of  $G'$  and  $G''$  as a function of the frequency showed that  $G'$  was much larger than  $G''$  and almost independent of the frequency between 1 and  $10^{-3}$  Hz (results not shown). It appears that the presence of protein microgels favors  $\kappa$ -car gelation. Measurements were also done in the presence of 40 g/L native  $\beta$ -lg or strands formed by heating in pure water (results not shown). For these mixtures the effect on the rate of  $\kappa$ -car gelation was weak, though it was slightly stronger in the presence of strands in which case it was comparable to that for mixtures with 5 g/L microgels.

It should be realized, however, that the microgels were formed in the presence of  $\text{CaCl}_2$ , which means that mixtures that contained more microgels also contained more  $\text{CaCl}_2$ . Elsewhere, we showed for pure  $\kappa$ -car solutions at 10 mM KCl that adding small amounts of  $\text{Ca}^{2+}$  strongly increases the gelation rate of  $\kappa$ -car and leads to stiffer gels [21] even though in the absence of KCl no gels were formed at low  $\text{CaCl}_2$  concentrations. Fig. 5b shows the evolution of  $G'$  for pure  $\kappa$ -car solutions containing the same amount of  $\text{CaCl}_2$  as in the mixtures with microgels. The effect of  $\text{Ca}^{2+}$  is even stronger

for the pure  $\kappa$ -car solutions than for the mixtures with microgels. It is likely, therefore, that the effect observed for the mixtures with microgels is caused by  $\text{Ca}^{2+}$  and not by the proteins. We note that in the presence of the microgels the shear modulus increased during cooling even before the  $\kappa$ -car gelled. This initial increase was not observed in pure  $\kappa$ -car solutions (Fig. 5b). A similar initial increase was also observed for mixtures with native proteins or strands, and even in pure protein solutions. We believe that it is caused by the adsorption of the proteins at the interface between the solution and the oil layer that was used to avoid evaporation. The proteins form an elastic layer at the interface with a modulus that increases with decreasing temperature.

Similar measurements were done for mixtures containing native  $\beta$ -lg instead of microgels with the same protein and  $\text{CaCl}_2$  composition. A reduction of the elastic modulus of  $\kappa$ -car gels in the presence of  $\text{CaCl}_2$  was also reported by Eleya et al. [12] and Harrington et al. [14]. For a given concentration of calcium ions the behavior of  $\kappa$ -car mixed with native proteins was intermediate between that of pure  $\kappa$ -car and mixtures with microgels. This is illustrated in Fig. 6a where we compare the elastic modulus of pure  $\kappa$ -car gels after aging for 100 min at 5 °C as a function of the  $\text{CaCl}_2$  with that of mixtures with native  $\beta$ -lg or microgels. As was suggested by Harrington et al. [14], the effect of  $\text{CaCl}_2$  on  $\kappa$ -car gelation is weaker in mixtures with proteins, because  $\text{Ca}^{2+}$  binds preferentially to  $\beta$ -lg. Therefore fewer  $\text{Ca}^{2+}$  ions are available to enhance  $\kappa$ -car gelation. Measurements of the activity of  $\text{Ca}^{2+}$  was much reduced in the presence of microgels, see Fig. 6b. It was somewhat less reduced by native  $\beta$ -lg, which explains why the effect of native  $\beta$ -lg on  $\kappa$ -car gelation was less important. For comparison we also show the binding capacity of  $\beta$ -lg strands formed by heating in pure water, which was intermediate. The elastic moduli in the mixtures with strands were close to those in mixtures with native proteins.

The competition between proteins and  $\kappa$ -car for  $\text{Ca}^{2+}$  can be clearly seen when one adds an increasing amount of native  $\beta$ -lg to a  $\kappa$ -car solution at a fixed  $\text{CaCl}_2$  concentration. We mixed 2 g/L  $\kappa$ -car, 10 mM KCl and 2.65 mM  $\text{CaCl}_2$  at 50 °C with native proteins at different concentrations. The gelation rate after cooling to 5 °C decreased with increasing protein concentration. The decrease of the elastic modulus with increasing  $\beta$ -lg concentration is clearly correlated to the decrease of the calcium activity, see Fig. 7. Notice that even in the absence of proteins the activity of the calcium ions is reduced by binding to  $\kappa$ -car.

Measurements were also done at higher  $\kappa$ -car concentrations, which led to stronger gels. The effect of adding proteins was similar, but at higher  $\kappa$ -car concentrations we often observed a decrease of the shear modulus during aging at 5 °C in mixtures containing higher microgel concentrations. The effect could not be reproduced quantitatively and we believe that it was an artifact caused by weak syneresis, which did not cause full slippage, but a reduction of the fraction of gel that remained in contact with the geometry. The effect was observed even with a serrated top plate.

### 3.2.2. Mixtures of $\beta$ -lg gels and $\kappa$ -car

When 40 g/L native  $\beta$ -lg was heated at 85 °C in the presence of 2 g/L  $\kappa$ -car aggregates were formed with  $R_h = 20$  nm at steady state, whereas in pure water the proteins formed aggregates with  $R_h = 17$  nm. When  $\text{CaCl}_2$  was added to the mixtures before heating,  $\beta$ -lg gels were formed for  $[\text{CaCl}_2] \geq 2$  mM, whereas in pure water gels were formed only for  $[\text{CaCl}_2] > 6$  mM [3]. In a separate set of experiments we added 10 mM KCl to the mixtures before heating, which induces gelation of  $\kappa$ -car by cooling mixtures after heating. In this case  $\beta$ -lg aggregates were formed with  $R_h = 30$  nm when no  $\text{CaCl}_2$  was added and  $\beta$ -lg gels were formed for  $[\text{CaCl}_2] \geq 2$  mM. It is clear that the presence of  $\kappa$ -car favors protein gelation induced by  $\text{CaCl}_2$ .

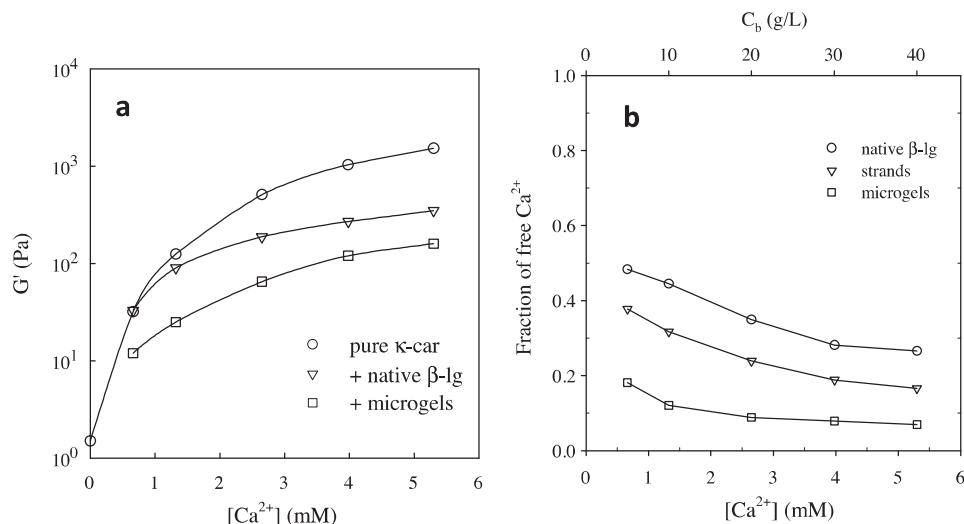


**Fig. 6.** (a) Elastic shear modulus of  $\kappa$ -car gels at 2 g/L after 100 min at 5 °C in the presence of 10 mM KCl as a function of the concentration of  $\text{Ca}^{2+}$ . The results for pure  $\kappa$ -car are compared with mixtures containing native  $\beta$ -lg or microgels. The molar ratio of calcium ions to proteins was 2.5. (b) The fraction of free calcium ions as a function of the total calcium ion concentration in pure protein solutions containing 2.5 calcium ions per protein.

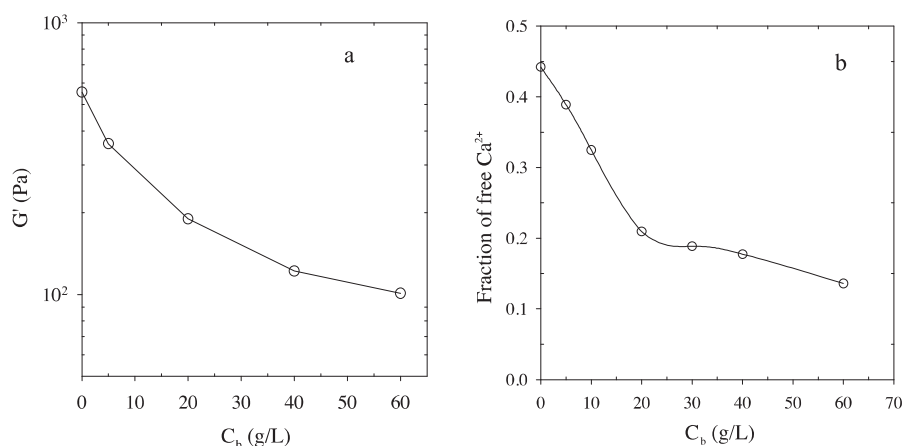


**Fig. 7.** (a) Dependence of the elastic modulus of  $\kappa$ -car gels after 100 min at 5 °C on the concentration of native  $\beta$ -lg. The systems contained 2 g/L  $\kappa$ -car, 10 mM KCl and 2.65 mM  $\text{CaCl}_2$ . (b) Concentration of free Calcium ions in the mixtures for which the elastic modulus is shown in (a).

Fig. 8 shows the evolution of  $G'$  at 0.1 Hz as a function of heating time at 85 °C for the different mixtures. The bottom plate reached 85 °C within 2 min. Measurements of the frequency dependence of  $G'$  and  $G''$  at the end of the heating process showed the commonly

observed behavior for whey protein gels, i.e. both moduli depended only weakly on the frequency and  $G' \gg G''$ . The presence of KCl led to stiffer gels at 2, 4 and 5.3 mM  $\text{CaCl}_2$ , but at higher  $\text{CaCl}_2$  concentrations the same gels were formed, see Fig. 8a. In fact, at 7 and

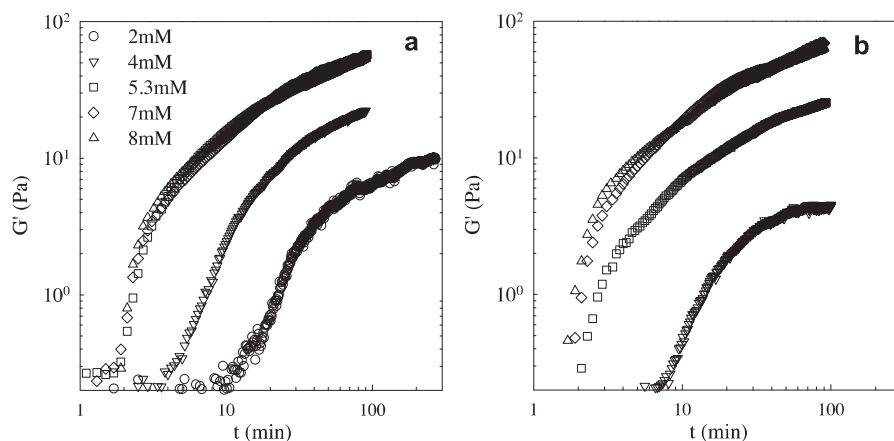


**Fig. 8.** Evolution of  $G'$  at 0.1 Hz during and after heating at 85 °C for solutions of 40 g/L  $\beta$ -lg and 2 g/L  $\kappa$ -car at different concentrations of  $\text{CaCl}_2$  with (a) and without (b) 10 mM KCl.



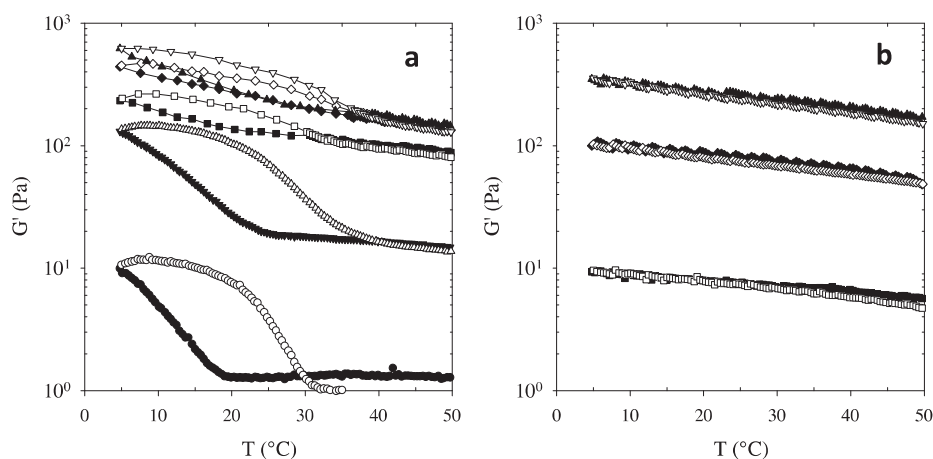


**Fig. 9.** Temperature dependence of  $G'$  at 0.1 Hz during cooling (closed symbols) and subsequent heating (open symbols) of  $\beta$ -lg gels (40 g/L) containing 2 g/L  $\kappa$ -car. The gels were formed at different concentrations of  $\text{CaCl}_2$  with (a) and without (b) 10 mM KCl. Symbols as in Fig. 8a.

8 mM  $\text{CaCl}_2$  the same  $\beta$ -lg gels were also formed in the absence of  $\kappa$ -car (results not shown).

CLSM images of the heated mixtures in the presence of 10 mM KCl are shown in Fig. 2. Corresponding images of mixtures heated in the absence of KCl are similar for  $[\text{CaCl}_2] \geq 4$  mM, but they are homogeneous at lower  $\text{CaCl}_2$  concentrations (results not shown). The structure of  $\beta$ -lg gels formed at  $[\text{CaCl}_2] \geq 7$  mM was the same with or without either  $\kappa$ -car or KCl. Clearly, at these higher  $\text{CaCl}_2$  concentrations the properties of the  $\beta$ -lg gels are dominated by the effect of  $\text{CaCl}_2$ .

The gels were subsequently cooled to 5 °C at a rate of 2 degrees/min while probing the shear moduli at 0.1 Hz, see Fig. 9. In the absence of KCl we find a weak progressive increase of  $G'$  with decreasing temperature that is well-known for whey protein gels, but in the presence of 10 mM KCl, we observed an additional increase of  $G'$  below a critical temperature of about 20 °C. This increase was caused by gelation of  $\kappa$ -car within the  $\beta$ -lg gel and was best observed when the latter was weak, i.e. at lower  $\text{CaCl}_2$  concentrations. When the mixtures were heated again to 85 °C, the modulus of the  $\beta$ -lg gel decreased without any hysteresis, but the  $\kappa$ -car gel melted at a higher critical temperature than at which it was formed during cooling. The critical temperatures for gelation and melting of  $\kappa$ -car was close to those found for the coil–helix and helix–coil transition of pure  $\kappa$ -car solutions with 10 mM KCl [22].

$\kappa$ -car gelation was relatively fast for these systems and the elastic moduli of the interpenetrated networks of  $\kappa$ -car and  $\beta$ -lg were determined 30 min after cooling to 5 °C, see Fig. 10. The results are compared with the elastic moduli of the  $\beta$ -lg gels that were obtained by extrapolation of the temperature dependence of  $G'$  at  $T > T_c$  to 5 °C. We also show in the same figure the elastic modulus of the  $\kappa$ -car gels obtained by cooling mixtures with native  $\beta$ -lg, but only up to  $[\text{CaCl}_2] = 5.3$  mM, because the stronger gels formed at 7 and 8 mM partially detached from the geometry rendering the results inaccurate. No such problems were encountered with the mixed gels, probably because of the protein gel. The single networks and the interpenetrated network all became stiffer with increasing  $\text{CaCl}_2$  concentration and the modulus of the interpenetrated network was close to the sum of the single networks.

#### 4. Discussion

Phase separation between  $\kappa$ -car and  $\beta$ -lg aggregates has already been studied in detail in the past [5–9]. We have shown elsewhere that the incompatibility between the two components increases with decreasing temperature and argued that therefore the driving

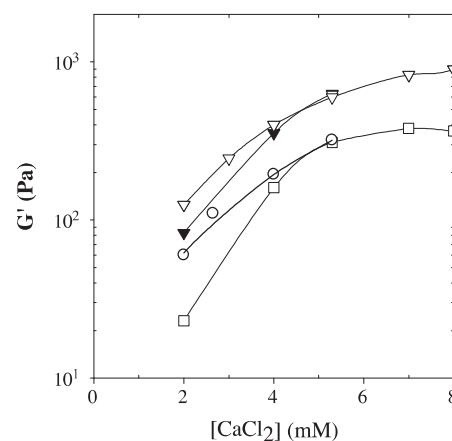


**Fig. 10.** Dependence on the  $\text{CaCl}_2$  concentration of the elastic modulus of interpenetrated  $\kappa$ -car (2 g/L) and  $\beta$ -lg gels (40 g/L) at 5 °C (triangles) in the presence of 10 mM KCl. For comparison we also show the elastic modulus of  $\kappa$ -car gels formed in the presence of native  $\beta$ -lg (circles) and the contribution to  $G'$  of the  $\beta$ -lg gel in mixed gels (squares). The sum of the  $\beta$ -lg and  $\kappa$ -car gels is shown as filled symbols. Solid lines are guides to the eye.

force for phase separation cannot solely be depletion [9]. It was also found that the formation of a strong  $\kappa$ -car gel can reverse phase separation close to the critical conditions [8,9,23]. Therefore when reduction of the temperature in the presence of salt causes  $\kappa$ -car to gel, both an increase and a decrease of the extent of phase separation can potentially be observed.

In the present study we observed increased phase separation upon cooling from 20 °C to 5 °C, when the mixture was close to the critical conditions. However, we did not observe decreased phase separation due to gelation of  $\kappa$ -car, probably because the gels were too weak. Interestingly, we observed secondary phase separation after cooling within the protein depleted phase (pores) of the covalently crosslinked  $\beta$ -lg gels near the critical conditions. Secondary phase separation was possible in this case even though the proteins had formed a gel, because the protein aggregates within the pores were not connected to the gel and their concentration was still relatively high.

When phase separation was induced by mixing the protein aggregates with  $\kappa$ -car at room temperature it could be reversed by dilution implying that interaction between the aggregates was not very strong [19]. Nevertheless, in most cases the protein rich domains did not fuse, but agglomerated into large flocs. The

implication is that the bonds between proteins within the domain were strong enough to inhibit fusion of the domains and macroscopic phase separation, but too weak to resist dilution. Phase separation that was induced by aggregation of native  $\beta$ -lg in the heated mixtures led to similar structures, but in this case the agglomerated protein dense domains were irreversibly crosslinked as was shown by Nguyen et al. [19].

The presence of proteins influenced  $\kappa$ -car gelation at low temperatures and, inversely, the presence of  $\kappa$ -car influenced  $\beta$ -lg gelation at high temperatures. In the following we will discuss first the effect of  $\beta$ -lg on  $\kappa$ -car gelation, then the effect of  $\kappa$ -car on  $\beta$ -lg gelation and finally the synergy between the two networks when both biopolymers are gelled. Addition of microgels led to an acceleration of the  $\kappa$ -car gelation and to stiffer gels. The effect was caused by the presence of  $\text{Ca}^{2+}$  that was added together with the proteins. It was shown elsewhere [21] that sodium and calcium ions cause acceleration of KCl-induced  $\kappa$ -car gelation and render the gels stiffer even if by themselves the concentrations of these ions are too weak to induce gelation. The effect is particularly strong for calcium ions, because they bind to  $\kappa$ -car as is shown by the reduced activity of  $\text{Ca}^{2+}$  in the presence of  $\kappa$ -car.  $\text{Ca}^{2+}$  also binds specifically to  $\beta$ -lg and even more strongly to the microgels than native proteins [3]. Therefore  $\kappa$ -car and  $\beta$ -lg compete for calcium ions in the mixtures and as a consequence the reinforcing effect of  $\text{Ca}^{2+}$  on the  $\kappa$ -car gels was less in the mixtures than in pure  $\kappa$ -car solutions. Nevertheless, the increase of the elastic modulus after adding microgels was still significant even though the fraction of free calcium ions in pure microgel solutions was very low. This means that a significant fraction of calcium ions that was bound to the microgels could be captured by the  $\kappa$ -car helices.

The competition for  $\text{Ca}^{2+}$  between  $\beta$ -lg and  $\kappa$ -car was corroborated by the slow-down of  $\kappa$ -car gelation in the presence of  $\text{CaCl}_2$  when increasing amounts of native  $\beta$ -lg was added. The same effect was already noted by Harrington et al. [14] for calcium induced gelation of  $\kappa$ -car in the presence of native WPI. They found that the elastic modulus of  $\kappa$ -car (5–30 g/L) at 8 mM  $\text{CaCl}_2$  was systematically an order of magnitude smaller when 100 g/L WPI was added. Here we find that the effect of adding proteins is stronger when they are aggregated than when they are in the native state. The stronger influence of microgels compared to native  $\beta$ -lg agrees with the stronger binding of  $\text{Ca}^{2+}$  to the microgels. Nevertheless, there might also be an effect of microphase separation that only occurred in mixtures with microgels. However, we believe that this effect is small, because the  $\kappa$ -car concentration is almost the same within the dense protein domains and in the protein depleted phase [19].

As it was mentioned above, heat-denatured  $\beta$ -lg forms a gel at 40 g/L in pure aqueous solution when  $[\text{CaCl}_2] > 6$  mM, but here we found that in the presence of 2 g/L  $\kappa$ -car  $\beta$ -lg gels were formed at lower  $\text{CaCl}_2$  concentrations. The influence of  $\kappa$ -car on  $\beta$ -lg gelation was already reported in the literature [11,12,14,16,17,24,25]. It has been shown that the presence of  $\kappa$ -car does not influence the denaturation rate of  $\beta$ -lg [24] or WPI [26]. Therefore, most likely  $\kappa$ -car influences the interaction between the growing aggregates, which in turn favors gelation. It has been found that with increasing  $\kappa$ -car concentration the elastic modulus of  $\beta$ -lg gels at a fixed protein concentration increases first, but then decreases at higher  $\kappa$ -car concentrations [11,14]. These effects have been attributed to micro phase separation. Weak phase separation at low  $\kappa$ -car content reinforces the connectivity between the proteins while strong phase separation leads to a coarser more disconnected network at higher  $\kappa$ -car concentrations. Notice, however, that in this study we found that gelation of  $\beta$ -lg was induced by the presence of  $\kappa$ -car even at 3 mM  $\text{CaCl}_2$  when the system remained homogeneous on microscopic length scales. Possibly weak depletion interactions or thermodynamic incompatibility plays a role in inducing stronger

aggregation of the protein aggregates without actually being strong enough to induce phase separation.

It is clear that  $\kappa$ -car can form a network within the  $\beta$ -lg gel as was already reported elsewhere [8,12,14]. We found that the elastic modulus of the mixed gels at 5 °C was close to the sum of the moduli of the  $\beta$ -lg gels in the presence of  $\kappa$ -car coils and the  $\kappa$ -car gels in the presence of native  $\beta$ -lg. It is perhaps not surprising that the stiffness of the rather rigid  $\beta$ -lg gel does not change much when  $\kappa$ -car gels during cooling, but one might expect that the modulus of the  $\kappa$ -car network formed in the microphase separated  $\beta$ -lg gels would be different from that in a solution of native proteins. It appears that this effect is not strong, perhaps because the concentration of the  $\kappa$ -car in the protein rich micro domains is only weakly lower than in the protein poor phase.

## 5. Conclusion

Addition of calcium ions renders  $\kappa$ -car gels formed with 10 mM KCl stiffer. In mixtures with  $\beta$ -lg the polysaccharide competes with the protein for the calcium ions which mitigates the effect of calcium on the  $\kappa$ -car gel.  $\beta$ -lg microgels compete more strongly for calcium ions than native  $\beta$ -lg so that the mitigating effect is stronger. Addition of microgels to a solution of  $\kappa$ -car coils leads to microphase separation already at very low  $\kappa$ -car concentrations (0.5 g/L). Micron sized protein rich domains are formed that remain well dispersed if  $\kappa$ -car gels soon after mixing, but when the mixture remains liquid the domains agglomerate into larger clusters. However, the agglomerated domains do not fuse even though they are liquid and redisperse upon dilution. The effect of microphase separation on the stiffness of  $\kappa$ -car gels is most likely small as the concentration of  $\kappa$ -car was only 25% lower in the protein rich than in the protein poor phase.

Heat-induced gelation of native  $\beta$ -lg is facilitated by the presence of  $\kappa$ -car probably because it favors contact between the growing  $\beta$ -lg aggregates. Above a critical amount of added  $\text{CaCl}_2$  microphase separation appears during heating and heterogeneous gels are formed. This effect of  $\text{CaCl}_2$  on the structure can be related to the transition between the formation of  $\beta$ -lg strands and microgels. Upon cooling,  $\kappa$ -car gels within the  $\beta$ -lg gel at a temperature close to that in the equivalent pure  $\kappa$ -car solutions. The  $\kappa$ -car gel melts again when heating, but the  $\beta$ -lg remains intact during cooling and reheating. The elastic modulus of the mixed gel is close to the sum of the  $\kappa$ -car gel in the presence of uncrosslinked  $\beta$ -lg and the  $\beta$ -lg gel in the presence of uncrosslinked  $\kappa$ -car, indicating that the structure of the  $\kappa$ -car network that is formed within the  $\beta$ -lg gel is close to that formed in the presence of native  $\beta$ -lg.

## Acknowledgement

BTN thanks the Ministry of Education and Training of Vietnam for financial support.

## References

- [1] R. Mezzenga, P. Fischer, The self-assembly, aggregation and phase transitions of food protein systems in one, two and three dimensions, *Rep. Prog. Phys.* 76 (2013) 046601.
- [2] T. Nicolai, M. Britten, C. Schmitt,  $\beta$ -Lactoglobulin and WPI aggregates: formation, structure and applications, *Food Hydrocoll.* 25 (2011) 1945.
- [3] T. Phan-Xuan, D. Durand, T. Nicolai, L.C.S. Donato, L. Bovetto, Heat induced formation of beta-lactoglobulin microgels driven by addition of calcium ions, *Food Hydrocoll.* 34 (2014) 227–235.
- [4] L. Piculell, Gelling carrageenans, in: A.M. Stephen, G.O. Philips, P.A. Williams (Eds.), *Food Polysaccharides and Their Applications*, CRC Press, Boca Raton, 2006, p. 239.
- [5] K. Baussay, T. Nicolai, D. Durand, Effect of the cluster size on the micro phase separation in mixtures of  $\beta$ -lactoglobulin clusters and  $\kappa$ -carrageenan, *Biomacromolecules* 7 (2006) 304–309.

- [6] P. Croguennoc, D. Durand, T. Nicolai, Phase separation and association of globular protein aggregates in the presence of polysaccharides: 1. Mixtures of preheated  $\beta$ -lactoglobulin and  $\kappa$ -carrageenan at room temperature, *Langmuir* 17 (2001) 4372–4379.
- [7] S. Gaaloul, S.L. Turgeon, M. Corredig, Phase behavior of whey protein aggregates/ $\kappa$ -carrageenan mixtures: experiment and theory, *Food Biophys.* 5 (2010) 103–113.
- [8] K. Ako, D. Durand, T. Nicolai, Phase separation driven by aggregation can be reversed by elasticity in gelling mixtures of polysaccharides and proteins, *Soft Matter* 7 (2011) 2507–2516.
- [9] B.T. Nguyen, T. Phan-Xuan, L. Benyahia, T. Nicolai, Combined effects of temperature and elasticity on phase separation in mixtures of  $\kappa$ -carrageenan and  $\beta$ -lg aggregates, *Food Hydrocoll.* 34 (2014) 138–144.
- [10] E. Cakir, E.A. Foegeding, Combining protein micro-phase separation and protein-polysaccharide segregative phase separation to produce gel structures, *Food Hydrocoll.* (2011).
- [11] I. Capron, T. Nicolai, C. Smith, Effect of addition of kappa-carrageenan on the mechanical and structural properties of beta-lactoglobulin gels, *Carbohydr. Polym.* 40 (1999) 233–238.
- [12] M.M.O. Eleya, S.L. Turgeon, Rheology of kappa-carrageenan and beta-lactoglobulin mixed gels, *Food Hydrocoll.* 14 (2000) 29–40.
- [13] S. Gaaloul, S.L. Turgeon, M. Corredig, Influence of shearing on the physical characteristics and rheological behaviour of an aqueous whey protein isolate-kappa-carrageenan mixture, *Food Hydrocoll.* 23 (2009) 1243–1252.
- [14] J.C. Harrington, E.A. Foegeding, D.M. Mulvihill, E.R. Morris, Segregative interactions and competitive binding of  $\text{Ca}^{2+}$  in gelling mixtures of whey protein isolate with  $\text{Na}^+$  kappa-carrageenan, *Food Hydrocoll.* 23 (2009) 468–489.
- [15] R. Roesch, S. Cox, S. Compton, U. Happek, M. Corredig, Kappa-carrageenan and beta-lactoglobulin interactions visualized by atomic force microscopy, *Food Hydrocoll.* 18 (2004) 429–439.
- [16] S.L. Turgeon, M. Beaulieu, Improvement and modification of whey protein gel texture using polysaccharides, *Food Hydrocoll.* 15 (2001) 583–591.
- [17] G. Zhang, E.A. Foegeding, Heat-induced phase behavior of  $\beta$ -lactoglobulin/polysaccharide mixtures, *Food Hydrocoll.* 17 (2003) 785–792.
- [18] S. de Jong, H.J. Klok, F. van de Velde, The mechanism behind microstructure formation in mixed whey protein-polysaccharide cold-set gels, *Food Hydrocoll.* 23 (2009) 755–764.
- [19] B.T. Nguyen, T. Nicolai, C. Chassenieux, L. Benyahia, The effect of the protein aggregate morphology on phase separation in mixtures with polysaccharides, *J. Phys. Cond. Mat.* (2014) [in press].
- [20] V. Meunier, T. Nicolai, D. Durand, A. Parker, Light scattering and viscoelasticity of aggregating and gelling  $\kappa$ -carrageenan, *Macromolecules* 32 (1999) 2610–2616.
- [21] B.T. Nguyen, T. Nicolai, C. Chassenieux, L. Benyahia, Synergistic effects of mixed salt on the gelation of  $\kappa$ -carrageenan, *Carbohydr. Polym.* 112 (2014) 10–15.
- [22] C. Rochas, M. Rinaudo, Activity coefficients of counterions and conformation in kappa-carrageenan systems, *Biopolymers* 19 (1980) 1675–1687.
- [23] K. Bausay, T. Nicolai, D. Durand, Coupling between polysaccharide gelation and micro-phase separation of globular protein clusters, *J. Coll. Int. Sci.* 304 (2006) 335–341.
- [24] I. Capron, T. Nicolai, D. Durand, Heat induced aggregation and gelation of  $\beta$ -lactoglobulin in the presence of  $\kappa$ -carrageenan, *Food Hydrocoll.* 13 (1999) 1–5.
- [25] P. Croguennoc, D. Durand, T. Nicolai, Phase separation and association of globular protein aggregates in the presence of polysaccharides: 2. Heated mixtures of native  $\beta$ -lactoglobulin and  $\kappa$ -carrageenan, *Langmuir* 17 (2001) 4380–4385.
- [26] M.A. de la Fuente, Y. Hemar, H. Singh, Influence of kappa-carrageenan on the aggregation behaviour of proteins in heated whey protein isolate solutions, *Food Chem.* 86 (2004) 1–9.



## **PAPER 5**

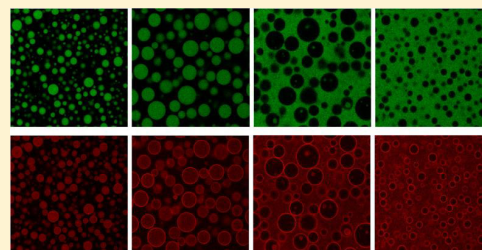


# Stabilization of Water-in-Water Emulsions by Addition of Protein Particles

Bach T. Nguyen, Taco Nicolai,\* and Lazhar Benyahia

LUNAM, Université du Maine, IMMM UMR CNRS 6283, PCI, 72085 Le Mans cedex 9, France

**ABSTRACT:** The effect of the addition of protein particles was investigated on the stability of water-in-water emulsions formed by mixing aqueous dextran and poly (ethylene oxide) solutions. Protein particles with hydrodynamic radii ranging from 15 to 320 nm were produced by heating globular proteins in controlled conditions. The structure of the emulsions was visualized with confocal laser scanning microscopy using different fluorescent probes to label the dextran phase and the protein particles. It is shown that contrary to native proteins, protein particles adsorb at the interface and can form a monolayer that inhibits fusion of emulsion droplets. In this way, water-in-water emulsions could be stabilized for a period of weeks. The effect of the polymer composition and the protein particle size and concentration was investigated.



## INTRODUCTION

When two incompatible liquids are mechanically mixed, generally an emulsion is formed of small droplets of one liquid embedded in the second liquid. At rest, the droplets will grow by fusion or Oswald ripening until finally two distinct macroscopic phases are formed. Emulsions can be stabilized by adding surfactants that adsorb to the interface and inhibit fusion of colliding droplets. Most often, surfactants are amphiphilic molecules or polymers, but it has been shown that solid particles adsorbed at the interfaces can be exceptionally efficient stabilizers forming so-called Pickering emulsions.<sup>1,2</sup> When a particle enters the interface, the free energy is reduced by an amount that depends on their radius ( $R$ ), the contact angle with the interface ( $\theta$ ), and the interfacial tension ( $\gamma$ ):

$$\Delta G = \pi R^2 \gamma (1 - \cos \theta)^2 \quad (1)$$

In the past, mainly oil-in-water Pickering emulsions have been studied and their stability can be understood by the fact that for  $R > 10$  nm particles, the binding energy is orders of magnitude larger than the kinetic energy.

Water-in-water emulsions can be produced by mixing aqueous solutions of incompatible polymers.<sup>3</sup> Such emulsions have been stabilized in the past by gelling one or both of the phases as they cannot be stabilized by molecular or polymeric surfactants. Recently, it was shown that submicrometer particles adsorb irreversibly to the interface of the two aqueous phases opening up the possibility to create stable water-in-water emulsions without gelling one of the phases.<sup>4–6</sup> A detailed quantitative investigation showed that also in this case, the adsorption of particles at the interface could be explained by the reduction of the free energy even though the interfacial tension between two aqueous polymer solutions is orders of magnitude smaller than between oil and water.<sup>7</sup> In that study, fusion of droplets was observed leading to expulsion of particles

from the interface and macroscopic phase separation, most likely because the mechanical forces during fusion were sufficient to drive the particles from the interface. However, for other systems, the adsorption of particles at the interface significantly stabilized the systems.<sup>4–6</sup>

The objective of the present investigation was to produce and characterize stable water-in-water emulsions using protein particles. Such types of emulsions could potentially be useful for applications, e.g., in cosmetics or food products, possibly as an alternative to oil-in-water emulsions or to deliver ingredients with preferred solubility in the dispersed phase. Model emulsions were formed by mixing dextran and poly(ethylene oxide) (PEO) for which the phase diagram and the interfacial tension have been reported elsewhere.<sup>7</sup> The protein particles were produced by heat-induced aggregation of the globular whey protein  $\beta$ -lactoglobulin ( $\beta$ -lg) under specific conditions, where the aggregation leads to the formation of stable suspensions of well-defined protein particles.<sup>8,9</sup> We will show that protein particles occupy the interface and can stabilize water-in-water emulsions for a period of weeks, whereas native proteins did not enter preferentially the interface. The effects of the polymer composition and thus the interfacial tension, and the protein particle concentration and size were investigated.

## MATERIALS AND METHODS

**Materials.** The dextran and PEO samples used for this investigation were purchased from Sigma-Aldrich. The nominal weight average molar mass was  $M_w = 5 \times 10^5$  g/mol for the dextran and  $M_w = 2 \times 10^5$  g/mol for the PEO. For this study rather high molar masses were chosen in order to delay creaming or sedimentation of the emulsion droplets. Dextran labeled with the fluorophore fluorescein isothiocyanate (FITC) ( $M_w = 5 \times 10^5$  g/mol) was purchased from

Received: June 5, 2013

Revised: July 29, 2013

Published: July 29, 2013

Sigma-Aldrich. Dextran was used without further purification, but the PEO sample contained a small amount of silica particles which were removed by filtration and centrifugation before use. Solutions of dextran and PEO were prepared by dissolving the powder in salt free water (Milli-Q) at neutral pH while mildly stirring. Concentrations are indicated as weight percentages.

$\beta$ -lactoglobulin (Biopure, lot JE 001-8-415) was purchased from Davisco Foods International, Inc. (Le Sueur, MN, U.S.). Stable suspensions of protein particles were prepared by heating aqueous solutions of  $\beta$ -lg at a concentration of 40g/L in pure water at pH 5.8 or at pH 7 with different amounts of  $\text{CaCl}_2$  (0–6 mM). The solutions were heated in airtight vials in a water bath at 85 °C for 10 h until the reaction was completed. The z-average hydrodynamic radius ( $R_h$ ) of the particles was determined by dynamic light scattering. In the absence of added salt, small strand-like  $\beta$ -lg aggregates were formed, while larger spherical particles were produced after adding controlled amounts of  $\text{CaCl}_2$ . A detailed description of the formation of the protein particles and their characterization using light scattering can be found in refs 8 and 9.

The emulsions were prepared by mixing aqueous solutions of PEO (0–8 wt %), dextran (0–14 wt %), and  $\beta$ -lg (0–1 wt %) at pH 7 in the required amounts using a mini shaker. Trials showed that the order of mixing or the speed of mixing did not significantly influence the structure of the emulsion. In fact, vigorous shaking by hand or using an Ultratorax with gave equivalent results.

**Methods.** The proteins and the dextran were visualized separately with a confocal laser scanning microscope (CLSM) by utilizing different fluorescent labeling. The proteins were labeled with the fluorochrome rhodamine B isothiocyanate, by adding 5 ppm rhodamine to the solutions. A small fraction of the dextran was labeled with Fluorescein isothiocyanate (FITC). CLSM observations were made with a Leica TCS-SP2 (Leica Microsystems Heidelberg, Germany). Images of  $512 \times 512$  pixels were produced at different zooms with two different water immersion objectives: HCX PL APO 63 $\times$  NA = 1.2 and 20 $\times$  NA = 0.7. The solutions were inserted between a concave slide and a coverslip and hermetically sealed. The incident light was emitted by a laser beam at 543 nm and/or at 488 nm. The fluorescence intensity was recorded between 560 and 700 nm. It was verified that the use of labeled dextran and proteins had no influence on the emulsions.

Care was taken not to saturate the fluorescence signal so that it was proportional to the concentration of the probes. It was furthermore verified that the rhodamine signal was proportional to the protein concentration. This allowed us to deduce the protein concentration in each phase from the rhodamine fluorescence signal. The proportionality between the fluorescence intensity and the concentration was calculated from the average intensity and the known average protein concentration.

The criterion for stability of the emulsions was taken as the absence of a visible layer of the pure dispersed phase. We considered the system unstable as soon as a thin (<1 mm) layer became noticeable. We stress that the formation of a layer of the pure continuous phase is not a sign of destabilization of the emulsion droplets, but of creaming or sedimentation of droplets of the dispersed phase.

## RESULTS AND DISCUSSION

The phase diagram of PEO/dextran mixtures used for this study has already been reported<sup>7</sup> and is reproduced in Figure 1. The two phases are practically pure semidilute PEO and dextran solutions except very close to the critical point situated at  $C_{\text{PEO}} = 1.0\%$  (w/w) and  $C_{\text{dex}} = 1.7\%$ . The dashed line in Figure 1 indicates the compositions where the phases occupy approximately the same volume fraction. The interfacial tension ( $\gamma$ ) increases with increasing polymer concentration, but remains orders of magnitude smaller than for oil-in-water emulsions even at the higher polymer concentrations studied here. For this system  $\gamma$  has the following power law dependence on the tie line length (TLL):<sup>7</sup>  $\gamma \approx 10^{-3} \cdot \text{TLL}^{3.9} \mu\text{N/m}^2$ . We

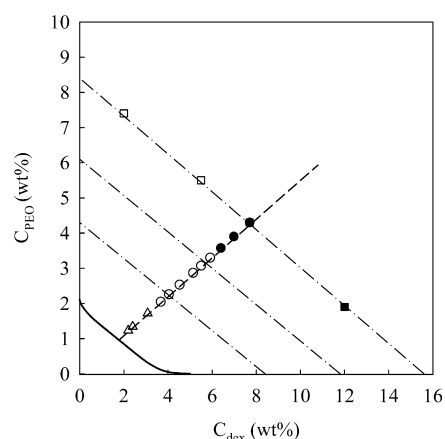


**Figure 1.** Phase diagram for aqueous mixtures of PEO and dextran. The solid line indicates the binodal. A few tie lines are drawn for illustration as dashed dotted lines. The dashed line indicates the compositions where the volume fraction of the two phases is equal. Open and filled squares indicate compositions leading to dextran droplets or PEO droplets, respectively. Circles indicate compositions at which protein particles ( $R_h = 150$  nm) adsorb to the interface of PEO droplets that remained stable for a period of at least one week (filled), or that showed signs of destabilization within that period (open). The triangles indicate compositions that led to phase separation without adsorption of protein particles at the interface.

verified that the phase diagram was not influenced by addition of protein particles up to at least  $C_{\text{pro}} = 1\%$ .

**Stability.** Pure mixtures of PEO and dextran completely phase separated within 1 h and formed a dextran-rich phase at the bottom and a PEO-rich phase at the top. Addition of native protein did not have a significant effect on the behavior of the mixtures. However, addition of protein particles led to stabilization of the emulsions, i.e., the droplets did not merge even though they creamed or sedimented at various rates, see below. This is illustrated in Figure 2a, where we show emulsions formed by mixing 3.3% PEO and 9.5% dextran in the presence of different concentrations of protein particles with hydrodynamic radius  $R_h = 150$  nm after having been left standing for one week. At this composition, PEO droplets are formed in the continuous dextran phase. For  $C_{\text{pro}} > 0.1\%$ , we

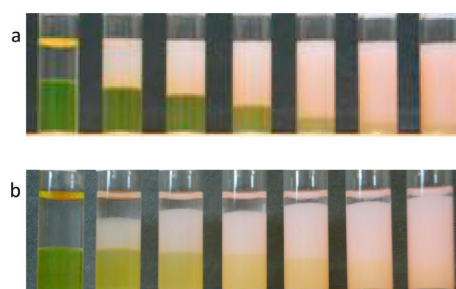


**Figure 2.** Emulsions of PEO/dextran mixtures in the presence of different concentrations of protein particles with  $R_h = 150$  nm ( $C_{\text{pro}} = 0, 0.1, 0.2, 0.3, 0.4, 0.5, 0.6\%$ , from left to right) after one week standing. (a)  $C_{\text{PEO}} = 3.3\%$  and  $C_{\text{dex}} = 9.5\%$ . (b)  $C_{\text{PEO}} = 3.3\%$  and  $C_{\text{dex}} = 5.5\%$ . Creaming of the PEO droplets gives rise to an opaque emulsion top layer, while destabilization causes a transparent PEO top layer. The dextran bottom phase is colored by the presence of labeled dextran. Excess protein particles render the dextran phase increasingly turbid with increasing protein concentrations.

did not visually observe destabilization of the PEO droplets for a period of at least a week. However, we did observe creaming of the droplets leading to an opaque top layer. The rate of creaming decreased with increasing protein concentration and will be discussed below. The increase of the turbidity of the bottom dextran layer was caused by the presence of excess protein particles that prefer to be situated in the dextran phase, see below.

At lower dextran concentrations ( $C_{\text{dex}} = 5.5\%$ ), the emulsions were not completely stable for a week. Destabilization of the PEO droplets manifested itself macroscopically by the appearance of a clear homogeneous PEO phase at the top, see Figure 2b. The stability decreased further with decreasing protein concentrations at low protein concentrations ( $C_{\text{pro}} < 0.2\%$ ). For  $C_{\text{pro}} = 0.05\%$ , the formation of a thin clear top layer signaling destabilization visually could be observed even at  $C_{\text{dex}} = 9.5\%$  after two days. A systematic study showed that at higher protein concentrations the stability of the emulsions was controlled by the interfacial tension and depended little on the composition. The duration for which the emulsions were stable at rest increased with increasing  $\gamma$  up to at least one week for  $\gamma > 30 \mu\text{N}$ .

The evolution with time of emulsions at different compositions on the same tie-line (maximum TLL in Figure 1,  $\gamma = 75 \mu\text{N}$ ) containing 0.5% protein particles with  $R_h = 150 \text{ nm}$  is shown in Figure 3. At this interfacial tension, the

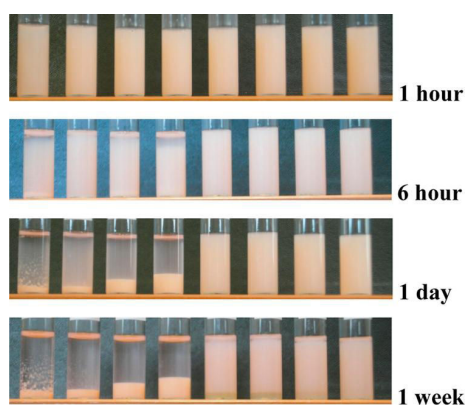


**Figure 3.** Evolution with waiting time of emulsions formed by dextran/PEO mixtures at different compositions on the same tie-line containing 0.5% protein particles with  $R_h = 150 \text{ nm}$ .  $C_{\text{PEO}}/C_{\text{dex}}$  (%) from left to right: 8/1; 7.4/2; 6.3/4; 5.5/5.5; 4.3/7.7; 3.3/9.5; 1.9/12; and 0.8/14. The 4 samples on the left formed dextran droplets in the continuous PEO phase and the 4 samples on the right formed PEO droplets in the continuous dextran phase.

emulsions were stable for at least one week at all compositions. CLSM images taken a few minutes after preparation of the suspensions showed that for  $C_{\text{PEO}} > 5\%$  droplets of the dextran phase formed in a continuous PEO phase, while at lower PEO concentrations, PEO droplets were formed in the continuous dextran phase, see Figure 4. Phase inversion occurred when the volume fraction ( $\phi$ ) of the dextran phase became larger than about 0.4. Creaming of PEO droplets was hardly visible after one week, while sedimentation of dextran droplets was complete after one day. The reason for the relatively rapid sedimentation of the dextran droplets is that they aggregated, which is also the reason why the front of the sedimenting emulsion is not very distinct. We do not know why the dextran

droplets aggregated, whereas the PEO droplets did not. In both cases, the droplets are covered with a layer of protein particles. Depletion interactions or attractive interactions between the protein layers would not be expected to differ much in the two situations. The principal difference is that the protein particles prefer to reside in the dextran phase, see below, but why that should induce aggregation of the dextran droplets is not obvious to us.

**Microscopic Structure.** Figure 4 shows CLSM images of emulsions formed at different compositions on the same tie-line ( $\gamma = 75 \mu\text{N}$ ) for which the evolution in time was shown in Figure 3. As was mentioned in the Materials and Methods section, the structure did not depend on the mixing procedure. We believe that the reason that the same structures are obtained is that in each case, the 3 components are much more finely dispersed during mixing. The droplets grow quickly by fusion until they have reached within minutes the metastable state size shown in the images. We could observe the latter stages of this ripening process with CLSM, but it was too quick for a systematic investigation with the methods at our disposal. At low dextran concentrations, droplets of the dextran phase were formed in a continuous PEO phase and vice versa for high dextran concentrations. It can be clearly seen that protein particles are adsorbed at the interface and that the excess protein prefers to reside in the dextran phase rather than the PEO phase.

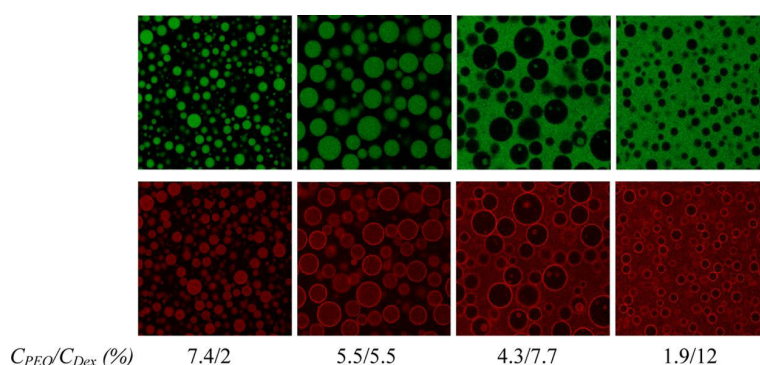
According to eq 1, the binding energy of protein particles at the interface depends on the interfacial tension that can be varied by varying the polymer composition. In order to test the effect of  $\gamma$  on the adsorption of protein particles at the interface, an emulsion prepared at  $C_{\text{PEO}} = 4.3\%$  and  $C_{\text{dex}} = 7.7\%$  with 0.4% protein particles was diluted progressively with water containing 0.4% protein toward the critical point.

Figure 5 shows CLSM images of the mixtures at different dilutions. Coverage of PEO droplets by protein particles was observed down to  $C_{\text{PEO}} = 2.05\%$  and  $C_{\text{dex}} = 3.7\%$  ( $\gamma \approx 4 \mu\text{N}/\text{m}^2$ ), but at  $C_{\text{PEO}} = 1.7\%$  and  $C_{\text{dex}} = 3.1\%$  ( $\gamma \approx 2 \mu\text{N}/\text{m}^2$ ) they no longer adsorbed at the interface. Unfortunately, we cannot quantify the reduction of the free energy for the present system, because the protein particles are polydisperse and we do not know the contact angle. Notice that the correlation length of the semidilute polymer phases is of the order a few nanometers so that the polymer solutions may be considered continuous on the length scale of the protein particles, but not on the length scale of native proteins.

The critical interfacial tension needed to drive adsorption of the protein particles at the interface did not depend significantly on the protein concentration nor on the polymer composition. However, the droplet size did depend on these parameters, see Figure 6. For a given composition the size of PEO droplets decreased with increasing protein concentration. The number average droplet radius ( $R$ ) was determined by manually measuring for several images the radii of the droplets that were in focus.

The results as a function of the protein concentration are shown in Figure 7 for two different compositions. For both compositions,  $R$  decreased with increasing  $C_{\text{pro}}$ , but the droplets were systematically smaller when the ratio  $C_{\text{PEO}}/C_{\text{dex}}$  was smaller. For Pickering emulsions, a decrease of the droplet size with increasing particle concentration is expected as incompletely covered small droplets will coalesce until the interface is fully stabilized. However, we do not find  $R^{-1} \propto C_{\text{pro}}$  as would be expected if the coverage at steady state was independent of the





**Figure 4.** CLSM images ( $160 \times 160 \mu\text{m}$ ) of the dextran signal (top) and the protein signal (bottom) for PEO/dextran mixtures in the presence of 0.5% protein particles ( $R_h = 150 \text{ nm}$ ) for different polymer compositions on the same tie-line indicated.

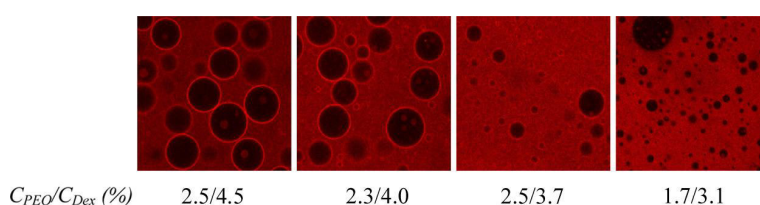


**Figure 5.** CLSM images ( $130 \times 130 \mu\text{m}$ ) of the protein signal for PEO/dextran mixtures in the presence of 0.4% protein particles with different polymer compositions.

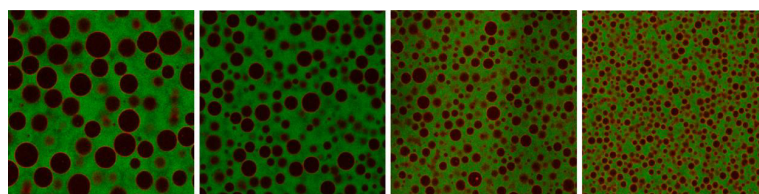


**Figure 6.** CLSM images of the dextran signal ( $500 \times 500 \mu\text{m}$ ) showing the effect of the protein particle ( $R_h = 150 \text{ nm}$ ) concentration on the droplet size for a mixture containing 3.3% PEO and 9.5% dextran: from left to right  $C_{\text{pro}} = 0.1, 0.15, 0.2$ , and  $0.4\%$ .

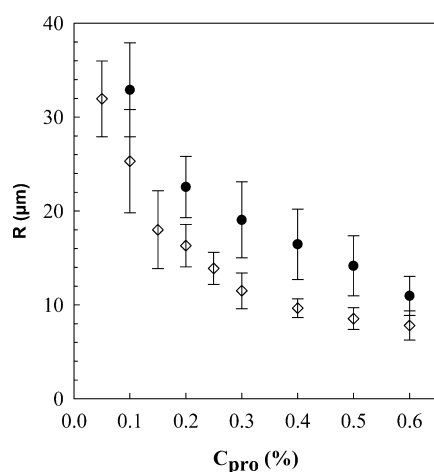


**Figure 7.** Dependence of the number average droplet radii on the protein concentration for two compositions:  $C_{\text{PEO}} = 3.3\%$  and  $C_{\text{dex}} = 5.5\%$  (closed symbols) or  $C_{\text{PEO}} = 3.3\%$  and  $C_{\text{dex}} = 9.5\%$  (open symbols). The error bars represent the standard deviation of the size distribution.

protein concentration,<sup>10</sup> see below. For a given protein concentration, the droplet size decreased for compositions

with a smaller volume fraction of the dispersed phase, which may also be explained by an increase of the ratio protein particles/interfacial area for a given droplet size.

The concentration of protein in the two phases was determined for mixtures containing 3.3% PEO and 9.5% dextran with different protein concentrations by measuring the fluorescence intensity of the two phases, see Figure 8a. The protein concentration was systematically higher in the dextran phase than in the PEO phase as can already be seen from the images taken with the protein signal shown in Figures 4 and 5. Knowing the volume fraction of each phase ( $\phi_{\text{dex}} = 59\%$  and  $\phi_{\text{PEO}} = 41\%$ ), we can calculate the amount of proteins in each phase and by comparing the sum with the total amount of proteins, we can deduce the amount of proteins at the interface per unit of volume ( $C_{\text{int}}$ ). The partitioning of the proteins between the two phases and the interface is shown in Figure 8b. The fraction of proteins at the interface was found to increase with  $C_{\text{pro}}$  from about 10% to 25% at  $C_{\text{pro}} = 0.3\%$  and then to weakly decrease at higher  $C_{\text{pro}}$ .

Using the average radius of the droplets, we can calculate the droplet surface area per unit of volume as follows:  $S = 3 \cdot \phi_{\text{PEO}} / R$ . The surface area occupied by an adsorbed spherical protein particle is  $\pi R_h^2$  and number of particles that is needed per unit of volume to form a dense monolayer is  $S / (\pi \cdot R_h^2)$ . The mass of a protein particle depends on the protein density within the

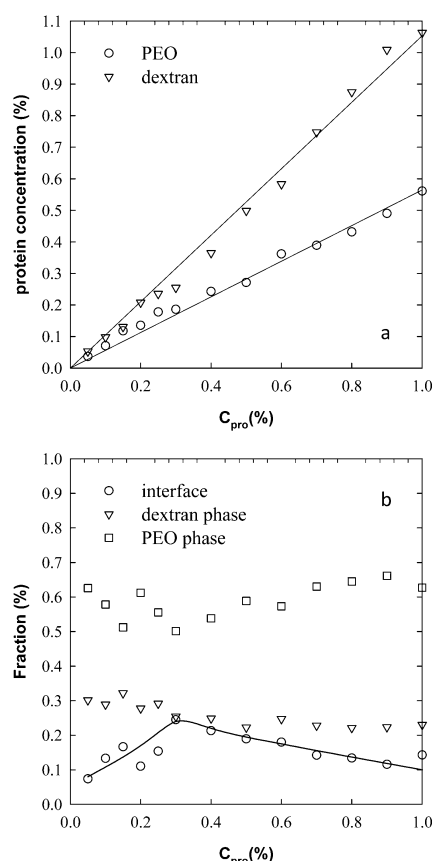


**Figure 8.** Part (a) shows the weight fraction of proteins in the dextran phase and the PEO phase for mixtures with  $C_{PEO} = 3.3\%$ ,  $C_{dex} = 9.5\%$  as a function of the total concentration of protein particles with  $R_h = 150$  nm. Part (b) shows the partitioning of protein particles between the dextran phase, the PEO phase and the interface for mixtures. The solid line is a guide to the eye.

particles ( $\rho \approx 15\%$ ):  $m_{pro} = \rho \cdot 4\pi R_h^3/3$ . Thus, the concentration of proteins that is needed to create a dense monolayer at the interface is equal to  $C_{int} = m_{pro} \cdot S / (\pi \cdot R_h^2)$ , i.e.,  $C_{int} = \rho \cdot R_h \cdot \phi_{PEO} \cdot 4/R$ .

The coverage of the interface is obtained by normalizing the experimentally observed amount of proteins at the interface with that expected for a dense monolayer, see Figure 9. The coverage increased at low protein concentrations until it stabilized for  $C_{pro} > 0.3\%$  at approximately 23%. Notice, however, that there is considerable uncertainty in the calculated value of the coverage for a dense monolayer because the protein particles and the droplets are polydisperse and the protein particles are not perfect spheres. Our use of the number average droplet radius and the z-average protein particle radius leads to an overestimation of  $C_{int}$  for a dense monolayer and thus an underestimation of the coverage. Therefore, it is difficult to draw firm conclusions about the packing of the proteins at the saturated interface, but it is highly unlikely that multilayers were formed.

**Droplet Creaming or Sedimentation.** PEO droplets creamed and dextran droplets sedimented, because in all cases, the dextran phase was denser than the PEO phase. For a given polymer composition, the creaming velocity ( $v$ ) of PEO droplets decreased rapidly with increasing protein particle concentration. The velocity of creaming or sedimentation was

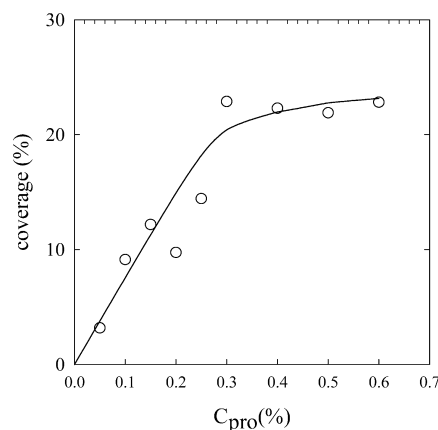


**Figure 9.** Percentage of the surface of the PEO droplets covered by protein particles with  $R_h = 150$  nm as function of the total protein concentration for mixtures with  $C_{PEO} = 3.3\%$  and  $C_{dex} = 9.5\%$ . The solid line is a guide to the eye.

quantified by measuring the height of the emulsion ( $h$ ) as a function of time. Figure 10a shows the results for creaming of PEO droplets in mixtures containing  $C_{PEO} = 3.3\%$ ,  $C_{dex} = 9.5\%$ , and different concentrations of protein particles. The height of

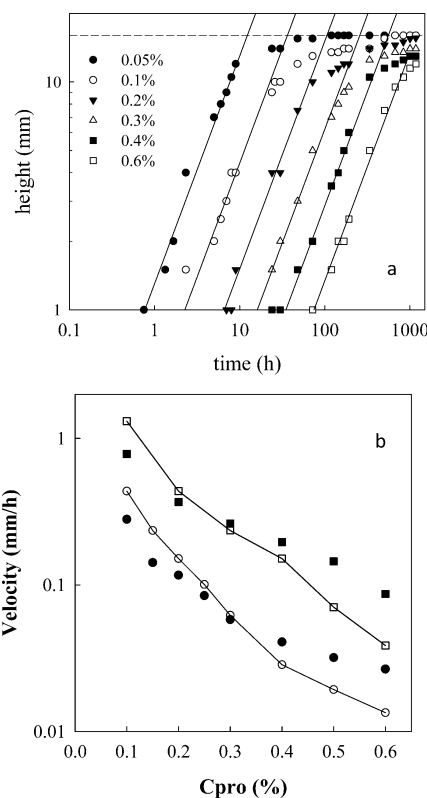


**Figure 10.** (a) Evolution of the height of the emulsion layer with time during standing for mixtures with  $C_{PEO} = 3.3\%$ ,  $C_{dex} = 9.5\%$ , and different concentrations of protein particles with  $R_h = 150$  nm. The straight lines have a slope of one. (b) Creaming velocity as a function of the protein particle concentration for mixtures with  $C_{PEO} = 3.3\%$ ,  $C_{dex} = 9.5\%$  (circles) and  $C_{PEO} = 3.3\%$ , and  $C_{dex} = 5.5\%$  (squares). Velocities calculated from the measured droplet sizes are shown as filled symbols.

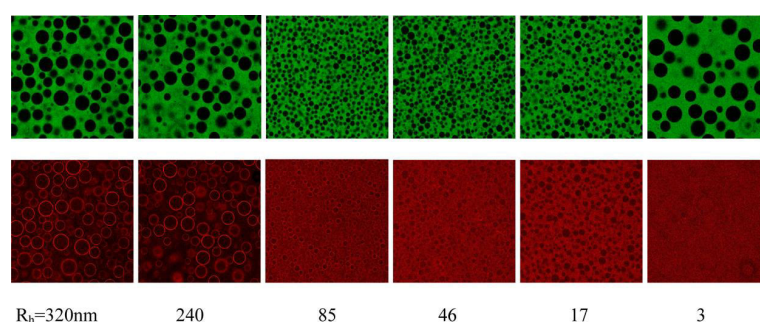


**Figure 11.** CLSM images of the dextran signal (top) and the protein particles with different sizes indicated in the figure (bottom) taken within a few minutes after preparation. The emulsions contained 3.3% PEO, 9.5% dextran, and 0.2% protein.

the emulsion layer decreased initially approximately linearly with time implying that the emulsion creamed with constant velocity:  $h(0) - h(t) = v \cdot t$ . The velocity strongly decreased with increasing protein concentration, see Figure 10b.

The velocity of a droplet under gravity is a function of the viscosity of the continuous phase ( $\eta$ ), the density difference between the two phases ( $\Delta\rho$ ), and the radius of the droplet:

$$v = g \cdot \Delta\rho \cdot 2 \cdot R^2 / (9 \cdot \eta) \quad (2)$$

$\Delta\rho$  was calculated from the polymer concentrations in each phase using the specific volumes of PEO (0.831 mL/g) and dextran (0.626 mL/g)<sup>11</sup> yielding  $\Delta\rho = 50 \text{ kg/m}^3$ . The viscosity of the continuous dextran medium was determined as 0.09 Pa·s and was not significantly different when 1% protein particles were added. The velocities calculated using the measured droplet sizes are compared with the observed velocities in Figure 10b. The agreement is reasonable considering the uncertainty in the measured droplet sizes. Similar experiments done at a lower dextran concentration (5.5%) showed faster creaming, because the viscosity of the continuous dextran medium was lower (0.04 Pa·s), but also because the average droplet size was slightly larger.

The thickness of the creamed emulsion layer at steady state was close to that of the pure PEO phase layer obtained in the absence of proteins, implying that the PEO droplets pack densely, leaving little space for the continuous dextran phase. The volume fraction of randomly closed packed monodisperse spherical droplets is about 0.63, but for polydisperse and deformable droplets it can be closer to unity.

Sedimentation of dextran droplets was much faster than predicted from their size. The reason is that these droplets stick together and form large flocs that can even be observed macroscopically. Creamed PEO droplets could be easily dispersed by gently shaking, but sedimented dextran droplet required strong shaking to redisperse.

#### Effect of the Size and Nature of the Protein Particles.

The PEO droplet size in the emulsions depended on the size of the protein particles. This is illustrated in Figure 11 for mixtures at  $C_{\text{PEO}} = 3.3\%$  and  $C_{\text{dex}} = 9.5\%$  containing 0.2% proteins. The droplet size decreased with decreasing size of the protein particles down to  $R_h = 85 \text{ nm}$ . It was similar for  $R_h = 46 \text{ nm}$  and  $R_h = 85 \text{ nm}$ , but increased for  $R_h = 17 \text{ nm}$  and  $R_h = 3 \text{ nm}$  (native proteins). We note that the particles with  $R_h = 17 \text{ nm}$  are not spherical, but curved strands with a length of about 50 nm and a diameter of about 5 nm.<sup>12</sup> Down to  $R_h = 46 \text{ nm}$ , a protein layer adsorbed at the interface could be clearly seen, but for  $R_h = 17 \text{ nm}$ , it was not obvious. Native proteins could not be detected at the interface and did not show a marked

preference for the dextran phase. The decrease of the droplet size with decreasing particle size can be explained by the fact that at the same weight concentration of protein, the number of particles increases with decreasing size. The smallest protein particles did not effectively inhibit fusion of PEO droplets, which explains why the droplet size was larger.

The macroscopic evolution of the samples as a function of time showed that the emulsions were not stabilized by native proteins and phase separated at approximately the same rate as protein free mixtures. Systems containing small strands with  $R_h = 17 \text{ nm}$  phase separated slightly slower indicating that the particles did adsorb at the interface, but did not effectively inhibit fusion of the droplets. Particles with  $R_h = 46 \text{ nm}$  stabilized the emulsion for up to 7 h, but after one day clear signs of destabilization were observed. It should be noted, however, that this system is in fact a mixture of smaller strand-like particles and larger spherical particles as explained in refs 8 and 9. The larger spherical protein particles ( $R_h \geq 85 \text{ nm}$ ) stabilized the emulsions for a period of up to about a week. For these mixtures, the velocity at which the PEO droplets creamed increased with increasing particle size, which can be explained by the increase of the droplet size.

The protein particles we have used in this study were produced by heating. However, milk naturally contains protein particles with similar size and density that are called casein micelles. It might be of interest to know if these particles can also be used to stabilize water-in-water emulsions. Casein micelles are approximately spherical complexes of different types of casein proteins with an average radius of about 150 nm held together by colloidal calcium phosphate.<sup>13</sup> We have done preliminary measurements on emulsions in the presence of casein micelles and found that casein micelles do adsorb to the interface, but that the emulsions destabilized within a few hours.

It is clear that in order to effectively stabilize water-in-water emulsions with protein particles, one needs to use particles with a radius larger than 50 nm. However, the particles should not be too large in order to maximize the number of particles at a given protein concentration. The shape and composition of the particles may also be important, as already indicated by the preliminary tests with casein micelles. Here we have used relatively dense spherical particles, but it would be interesting to test the stabilization capacity of protein particles with different morphologies.

## CONCLUSIONS

Water-in-water emulsions formed by mixing dextran and PEO solutions could be stabilized by addition of protein particles,



while keeping both phases in the liquid state. The stability of the emulsions increased with increasing interfacial tension and particle size and the time during which no visible layer of the dispersed phase was formed could last for a period of weeks, which may be useful for applications.

The emulsions were stabilized by the formation of a monolayer of protein particles at the water–water interface that was driven by the reduction of the free energy when particles adsorb to the interface. Native proteins did not adsorb to the interface, because they were too small and therefore could not stabilize water-in-water emulsions via this so-called Pickering effect even though they are excellent stabilizers of oil-in-water emulsions. The droplet size of the dispersed phase was found to decrease with increasing protein concentration and when the difference between the volume fractions of the two phases was larger. With increasing protein concentration, the surface coverage increased initially, but saturated when it reached about 30%. Best results were obtained with protein particles with a radius of around 100 nm, but the structure and the composition of the particles may also be important to consider.

Gravity caused creaming of PEO droplets in the continuous dextran medium and sedimentation of dextran droplets in the continuous PEO phase. In the former case the rate of creaming was determined by the droplet size and the viscosity of the continuous medium and could be extremely slow; less than 1 mm per week. Sedimentation of dextran droplets in the continuous PEO phase was relatively rapid at all conditions due to aggregation of the droplets.

## AUTHOR INFORMATION

### Corresponding Author

\*E-mail: Taco.Nicolai@univ-lemans.fr.

### Notes

The authors declare no competing financial interest.

## REFERENCES

- (1) Binks, B. P.; Horozov, T. S. *Colloidal Particles at Liquid Interfaces*; Cambridge Univ Press: Cambridge, 2006.
- (2) Aveyard, R.; Binks, B. P.; Clint, J. H. Emulsions stabilised solely by colloidal particles. *Adv. Colloid Interface Sci.* **2003**, *100*, 503–546.
- (3) Frith, W. J. Mixed biopolymer aqueous solutions—Phase behaviour and rheology. *Adv. Colloid Interface Sci.* **2010**, *161* (1–2), 48–60.
- (4) Firoozmand, H.; Murray, B. S.; Dickinson, E. Interfacial structuring in a phase-separating mixed biopolymer solution containing colloidal particles. *Langmuir* **2009**, *25* (3), 1300–1305.
- (5) Poortinga, A. T. Microcapsules from self-assembled colloidal particles using aqueous phase-separated polymer solutions. *Langmuir* **2008**, *24* (5), 1644–1647.
- (6) Hanazawa, T.; Murray, B. S. The influence of oil droplets on the phase separation of protein-polysaccharide mixtures. *Food Hydrocolloids*, <http://dx.doi.org/10.1016/j.foodhyd.2012.11.025>.
- (7) Balakrishnan, G.; Nicolai, T.; Benyahia, L.; Durand, D. Particles trapped at the droplet interface in water-in-water emulsions. *Langmuir* **2012**, *28* (14), 5921–5926.
- (8) Phan-Xuan, T.; Durand, D.; Nicolai, T.; Donato, L.; Schmitt, C.; Bovetto, L. On the crucial importance of the pH for the formation and self-stabilization of protein microgels and strands. *Langmuir* **2011**, *27* (24), 15092–15101.
- (9) Phan-Xuan, T.; Durand, D.; Nicolai, T.; Donato, L.; Schmitt, C.; Bovetto, L. Heat induced formation of beta-lactoglobulin microgels driven by addition of calcium ions. *Food Hydrocolloids* <http://dx.doi.org/10.1016/j.foodhyd.2012.09.008>.

(10) Arditty, S.; Whitby, C. P.; Binks, B. P.; Schmitt, V.; Leal-Calderon, F. Some general features of limited coalescence in solid-stabilized emulsions. *Eur. Phys. J. E* **2003**, *11* (3), 273–281.

(11) Kang, C.; Sandler, S. Phase behavior of aqueous two-polymer systems. *Fluid Phase Equilib.* **1987**, *38* (3), 245–272.

(12) Jung, J. M.; Savin, G.; Pouzot, M.; Schmitt, C.; Mezzenga, R. Structure of heat-induced  $\beta$ -lactoglobulin aggregates and their complexes with sodium-dodecyl sulfate. *Biomacromolecules* **2008**, *9* (9), 2477–2486.

(13) Fox, P. F. Milk proteins: General and historical aspects. In *Advanced Dairy Chemistry Vol 1: Proteins 3rd Editions*; Fox, P.F., McSweeney, P.L.H., Eds.; 2003; Vol. 42, pp 427–435.



# Thèse de Doctorat

Trong Bach NGUYEN

## Structure and rheology of mixtures of the protein $\beta$ -lactoglobulin and the polysaccharide $\kappa$ -carrageenan

### Résumé

Les protéines et les polysaccharides constituent avec les lipides les principaux ingrédients de l'alimentation et lui confèrent à la fois ses propriétés de nutrition et de texture. Une tendance actuelle de l'industrie agroalimentaire est d'élaborer des aliments plus sains c'est-à-dire moins gras et moins salés. A ce titre, les polysaccharides sont des agents de texturation efficaces lorsqu'ils sont utilisés seuls ou en combinaison avec des protéines. Le développement de nouveaux produits alimentaires nécessite donc de rationaliser et mieux comprendre les propriétés physico-chimiques des solutions et des gels mixtes à base de protéines et de polysaccharides.

Au cours de ce travail de thèse, nous avons étudié des mélanges de protéines globulaires (la  $\beta$ -lactoglobuline:  $\beta$ -lac) et de polysaccharide (le  $\kappa$ -carraghénane:  $\kappa$ -carr). Ce dernier provient d'algues et, en solution, il conduit à des gels au dessous d'une température critique qui dépend de la nature du sel ajouté. Le  $\kappa$ -carr est un additif important dans l'industrie alimentaire et plus particulièrement comme texturants des produits laitiers. Il est donc essentiel de comprendre les interactions qu'il développe avec les protéines du lait comme la  $\beta$ -lac.

L'objectif de ce travail est d'étudier la structure et les propriétés mécaniques d'agrégats ou de gels de  $\beta$ -lac mélangés avec du  $\kappa$ -carr et d'étudier leur influence sur la gélification de ce dernier. Nous nous sommes plus particulièrement intéressés à la sensibilité des mélanges aux ions calcium. Des agrégats protéiques ont été formés soit indépendamment puis mélangés au  $\kappa$ -carr soit directement in situ en dénaturant thermiquement des mélanges  $\kappa$ -carr/ $\beta$ -lac native. Les deux méthodes de préparation ont été comparées pour des compositions constantes des mélanges. La diffusion de la lumière, la rhéologie et la microscopie laser confocale ont été mises en œuvre pour étudier la texture des mélanges.

La taille et la morphologie des agrégats protéiques dépendent fortement de la concentration en ions calcium ajoutés qui se lient spécifiquement aux protéines. Nous avons montré que les très grands agrégats protéiques formés en présence de calcium conduisent à une microséparation de phase quand ils sont mélangés avec du  $\kappa$ -carr même à très faible concentration. Ainsi, la structure des systèmes mixtes est très sensible à la quantité de calcium en présence. Les agrégats protéiques renforcent les gels de  $\kappa$ -carr formés en présence de potassium tout comme l'ajout de calcium. Ce renforcement dans le cas des agrégats protéiques est dû au transfert des ions calcium de la  $\beta$ -lac vers le  $\kappa$ -carr. De plus, nous avons montré que la gélification du  $\beta$ -carr induite par des ions potassium continuait à avoir lieu en refroidissant des mélanges  $\kappa$ -carr/ $\beta$ -lac où cette dernière est dénaturée in situ. Cela conduit à des réseaux interpénétrés qui sont plus forts mécaniquement que la somme des deux réseaux pris individuellement. En conclusion, nous avons montré que la compétition entre la  $\beta$ -lac et le  $\kappa$ -carr pour les ions calcium était le paramètre de contrôle des propriétés texturales des gels mixtes.

**Mots clés** structure, rhéologie,  $\beta$ -lactoglobuline,  $\kappa$ -carraghénane, calcium

### Abstract

Protein and polysaccharide are together with lipids the main ingredients of food and procure both nutrition and texture. A recent tendency in the food industry is to develop more healthy products that contain less fat and salt. The addition of polysaccharides is recognized as a good way to control the texture of food products. The texture of many food products is determined by gelation of either the proteins or the polysaccharides, or both. When both are present, gelation of the protein or the polysaccharide will be influenced by the presence of the other type. Understanding of the physical chemical properties of aqueous solutions and gels containing protein and polysaccharides by themselves and in mixtures is needed for a rational development of novel food products.

This thesis describes an investigation of mixtures of the globular protein  $\beta$ -lactoglobulin ( $\beta$ -lg) and the polysaccharide  $\kappa$ -carrageenan ( $\kappa$ -car).  $\kappa$ -car is a polysaccharide isolated from algae that is often used as an additive in food industry. In solution it forms a gel below a critical temperature that depends on the amount and the type of salt. Addition of  $\kappa$ -car can improve the smoothness, creaminess, and body of food products and is often used to modify the texture of dairy products. Therefore it is important to understand the interaction of  $\kappa$ -car with milk proteins such as  $\beta$ -lg, which is the main protein component of whey.

The objective of the present investigation was to study the structure and the mechanical properties of  $\beta$ -lg aggregates or gels when mixed with  $\kappa$ -car and to study the influence of the former on the gelation of  $\kappa$ -car. The focus was on the sensitivity of the system to calcium ions. Protein particles were either formed separately and subsequently mixed with  $\kappa$ -car or formed directly in mixtures of  $\kappa$ -car and native  $\beta$ -lg by heating. The two different methods of preparation were compared with the same composition of polymers. The research presented in this thesis is essentially experimental using scattering techniques and confocal laser scanning microscopy to study the structure and shear rheology to study the dynamic mechanical properties.

The size and morphology of protein aggregates formed by heating  $\beta$ -lg is strongly dependent on the concentration of  $\text{Ca}^{2+}$  that binds specifically to the proteins. It is shown that larger aggregates formed in the presence of  $\text{Ca}^{2+}$  micro-phase separate already at low  $\kappa$ -car concentrations. Therefore the structure of mixed systems is extremely sensitive to the amount of  $\text{Ca}^{2+}$  present in the system. The presence of protein aggregates was found to reinforce potassium induced  $\kappa$ -car gels, but it was also found that addition of  $\text{CaCl}_2$  strengthens potassium induced pure  $\kappa$ -car gels. We show that the reinforcement by addition of protein aggregates is caused by the transfer of a fraction of  $\text{Ca}^{2+}$  from  $\beta$ -lg to  $\kappa$ -car. It was shown that potassium induced gelation of  $\kappa$ -car also occurs during cooling heat-set  $\beta$ -lg gels formed in mixtures at higher protein concentrations leading to interpenetrated networks that are stronger than the sum of the individual networks. The main conclusion of the investigation reported here is that the competition of  $\kappa$ -car and  $\beta$ -lg for calcium ions determines both the structure and the mechanical properties of the mixed systems.

**Key Words** structure, rheology,  $\beta$ -lactoglobulin,  $\kappa$ -carrageenan, calcium